# ASSESSING THE IMPACTS OF LAND USE CHANGE FROM COTTON (*GOSSYPIUM HIRSUTUM* L.) TO CELLULOSIC BIOENERGY CROPS ON WATERSHED HYDROLOGY AND WATER QUALITY IN THE TEXAS HIGH PLAINS

A Dissertation

by

YONG CHEN

Submitted to the Office of Graduate and Professional Studies of
Texas A&M University
in partial fulfillment of the requirements for the degree of

DOCTOR OF PHILOSOPHY

| | |
|---|---|
| Chair of Committee, | Nithya Rajan |
| Co-Chair of Committee, | Srinivasulu Ale |
| Committee Members, | Cristine L. S. Morgan |
| | Clyde Munster |
| Head of Department, | David D. Baltensperger |

December 2016

Major Subject: Agronomy

## ABSTRACT

The semi-arid Texas High Plains (THP) is one of the intensively managed agricultural regions in the United States (US) where cotton (*Gossypium hirsutum* L.) is a major crop. The THP region produces about a quarter of the US cotton. About 97% of the groundwater from the underlying Ogallala Aquifer is used for irrigating row crops including cotton in this semi-arid region. However, groundwater levels/quality in this region are experiencing a continuous decline/deterioration. This region also experiences recurring droughts and climate change studies predict warmer and drier summers in the future. These challenges may induce change in land use in the THP from high-water-demanding crops such as cotton to high water- and nitrogen-use-efficient cellulosic bioenergy crops such as perennial grasses and biomass sorghum [*Sorghum bicolor* (L.) Moench]. The region also holds enormous potential for the biofuel production according to the United States Department of Agriculture (USDA). The overall goal of this study is to assess the impacts of biofuel-induced land use change and climate change on hydrology, water quality and biomass production in the Double Mountain Fork Brazos watershed in the THP using the Soil and Water Assessment Tool (SWAT), Agricultural Policy/Environmental eXtender (APEX) and an integrated APEX-SWAT models.

Switchgrass (*Panicum virgatum* L.) and *Miscanthus* × *giganteus* were found to be ideal bioenergy crops to replace cotton under the irrigated and dryland conditions, respectively. About 18 and 19 Mg $ha^{-1}$ $yr^{-1}$ of biomass could potentially be produced under the irrigated switchgrass and dryland *Miscanthus* scenarios. The land use change

from cotton to perennial grasses decreased average annual (1994-2009) surface runoff, total nitrogen (TN) load through surface runoff and $NO_3$-N leaching to groundwater by 88%, 86% and 100%, respectively and increased percolation by 28%. The climate change analysis indicated that the simulated annual irrigation water use and TN load under the future perennial grass land uses reduced by 60% and 30%, respectively, when compared to future cotton land use. However, under future climate scenarios, irrigated switchgrass yields were projected to reduce by 16-28% and dryland *Miscanthus* yields were simulated to increase by 32-38% when compared to the historic yields.

## DEDICATION

To Xiaoxiao

A hardworking lady, a wonderful cook and a great wife.

## ACKNOWLEDGEMENTS

Many people have made invaluable contributions, both directly and indirectly to my research. I would like to express my warmest gratitude to Drs. Srinivasulu Ale and Nithya Rajan, my supervisors, for his and her instructive suggestions and valuable comments on the writing of this dissertation and all the papers. Without their invaluable help and generous encouragement, the present dissertation would not have been accomplished. At the same time, I am also grateful to Dr. Cristine L. S. Morgan and Dr. Clyde Munster for providing me with valuable advice and suggestions on my dissertation and papers.

I also wish to thank my friend Dr. Jongyoon Park, who taught me a lot of knowledge about the hydrologic models and offered me a lot of help. In addition, I would like to thank my friend Partson Mubvumba for his kindly help for my research and life. What's more, I gratefully thank the anonymous reviewers for their valuable suggestions for improving my papers, which made me keep moving.

Finally, I greatly appreciate the support and endless love of my wife and parents. They have always been helping me out of difficulties and supporting without a word of complaint. My heart swells with gratitude to all the people who helped me.

This is the last section I compose for my dissertation. This is also the beginning of my new research trip.

## CONTRIBUTORS AND FUNDING SOURCES

This work was supported by a dissertation committee consisting of Professors Nithya Rajan [advisor] of the Department of Soil and Crop Sciences, Srinivasulu Ale [co-advisor] of the Texas A&M AgriLife Research Center at Vernon, Cristine L. S. Morgan of the Department of Soil and Crop Sciences and Professor Clyde Munster of the Department of Biological and Agricultural Engineering. All work for the dissertation was completed independently by the student.

This material is based upon work that is supported by the National Institute of Food and Agriculture, U.S. Department of Agriculture, under award number NIFA-2012-67009-19595. Any opinions, findings, conclusions, or recommendations expressed in this publication are those of the author(s) and do not necessarily reflect the view of the U.S. Department of Agriculture. We gratefully thank the help from Dr. Raghavan Srinivasan, Texas A&M University, College Station, TX; Dr. Jongyoon Park, Texas A&M AgriLife Research, Vernon, TX; and Nancy Sammons, USDA-ARS Lab, Temple, TX.

# TABLE OF CONTENTS

Page

## LIST OF FIGURES

Page

# LIST OF TABLES

Page

# 1. INTRODUCTION

The semi-arid Texas High Plains (THP) in the United States is one of the most intensive agricultural regions in the world. Irrigated agriculture in the THP depends primarily on groundwater availability in the vast underlying Ogallala Aquifer. About 97% of water drawn from the Ogallala Aquifer is used for crop irrigation in the region (Maupin and Barber, 2005). However, groundwater levels in this region are experiencing a continuous decline and groundwater quality has been deteriorating due to the intensive agricultural activities (Chaudhuri and Ale, 2014a; Rajan et al., 2015). A majority of producers in this region are facing water shortages due to lower groundwater availability and higher pumping costs (Nair et al., 2013). Many climate change studies for this region predict warmer and drier summers in the future (Modala et al., 2016), which necessitate larger groundwater withdrawals. In order to extend the life of the Ogallala Aquifer and to insure that at least a certain percentage (varies with the water district) of currently available groundwater will still be available in 2060, Groundwater Conservation Districts (GCDs), which are the primary regulatory agencies in the region imposed new rules to limit the allowable annual groundwater pumping for irrigation.

Cotton (*Gossypium hirsutum* L.) is a major crop grown in the THP region, which produced approximately 25% of U.S. cotton in 2013 (NASS, 2014). The new restrictions on groundwater pumping in the THP are expected to result in a change in land use from high-water-demanding crops, such as cotton and corn (*Zea mays* L.), to relatively less water-demanding crops in the near future (Rajan et al., 2014). The agricultural land in

the THP region has the potential to grow cellulosic bioenergy crops such as perennial grasses and biomass sorghum [*Sorghum bicolor* (L.) Moench] (United States Department of Agriculture; USDA, 2010), which have higher water and nitrogen use efficiencies compared to cotton, and they can provide many water quality and economic benefits (Rooney et al., 2007; Sarkar et al., 2011; Kiniry et al., 2013; Sarkar and Miller, 2014). The USDA has also estimated that about 11.4% of existing croplands and pastures in the Southeastern U.S. region, which includes the THP, will be required for fuel use to meet the 2022 U.S. cellulosic biofuel target (USDA, 2010).

A potential land use change from croplands to cellulosic bioenergy crops may significantly affect the regional hydrologic cycle and water quality. Evaluation of the detailed hydrologic and water quality impacts of biofuel-induced land use change from cotton to cellulosic bioenergy crops in the semi-arid THP is therefore necessary to assess the feasibility of proposed land use change. In this study, *Miscanthus* × *giganteus*, Alamo switchgrass (*Panicum virgatum* L.), big bluestem (*Andropogon gerardii*) and biomass sorghum were selected to hypothetically replace the existing cotton land use (considered as the "baseline" scenario).

Several models are available for simulating the hydrological and water quality impacts of land use change, such as the Soil and Water Assessment Tool (SWAT; Arnold et al., 1998) model, Agricultural Policy/Environmental Extender (APEX) model (Williams, 1995), European Hydrological System Model MIKE SHE (Refsgaard and Storm, 1995), DRAINMOD (Youssef et al., 2005; Skaggs et al., 2012) and the Agricultural Drainage and Pesticide Transport (ADAPT) model (Gowda et al., 2012).

Among these, the SWAT and APEX models have been used widely across the world, and they demonstrated the potential to satisfactorily predict long-term impacts of land use change on hydrologic processes and water quality in complex watersheds (Williams 1995; Ko et al., 2009; Ghaffari et al., 2010; Gassman et al., 2010; Srinivasan et al., 2010; Tuppad et al., 2010; Powers et al., 2011; Wu and Liu, 2012; Zatta et al., 2014). The SWAT and APEX models were therefore used in this study. An integrated version of the SWAT and APEX models was also developed as a part of this study in order to utilize the relative advantages of these models in simulating certain crops/processes. More details about the rationale behind this study and the research approach are discussed in detail in the following sections.

## 1.1 Background

### *1.1.1 Texas High Plains and the Study Watershed*

The THP, which encompasses 41 counties in the northwest Texas (Figure 1.1), is a treeless, windswept and semi-arid region within the Great Plains (Webb, 1931). The region has a flat terrain with the elevation ranging from 900 to 1300 m. The THP region is characterized by slow to moderate drainage conditions with the presence of many small shallow lakes called as playas. The long-term average (1981-2010) annual precipitation in this region was about 508 mm (NOAA-NCDC, 2014). The annual frost-free period during the above period varied from 180 to 220 days, and the long-term daily average maximum and minimum temperatures were 24$^{\circ}$C and 9$^{\circ}$C, respectively. The major soil types are Acuff sandy clay loam (fine-loamy, mixed, superactive, thermic

Aridic Paleustolls), Amarillo sandy loam (fine-loamy, mixed, superactive, thermic Aridic Paleustalfs) and Pullman clay loam (fine, mixed, superactive, thermic Torrertic Paleustoll) (Soil Survey Staff, 2010). The natural vegetation of the THP consists primarily of short grasses, and the northern portion of the region is one of the most distinctive short grass regions of the US. The predominant agriculture land use is cotton in the THP, which accounted for about 37% of entire U.S. cotton harvest acres in 2015 (NASS, 2016). The THP has been under cotton production for more than 100 years (Bruton et al., 2007).

Availability of a good quality measured data over a longer period of time for calibrating and validating hydrologic and water quality models is a key for successful application of these models. Only a limited number of United States Geological Survey (USGS) gauges are available in the THP region and they recorded very low streamflow in most parts of the year, which posed some challenges for the SWAT model calibration in this study. The Double Mountain Fork Brazos watershed, located in the southern part of the THP, was selected for this study because of the existence of cotton land use in about 30% of the watershed and availability of sufficient streamflow and water quality data for evaluation of the SWAT model (Figure 1.1). Two USGS gauges exist in this watershed, and one of them is located at the watershed outlet. While daily streamflow data has been recorded at both the USGS gauges, limited data on total nitrogen (TN) concentration is available at the downstream USGS gauge (watershed outlet). The delineated watershed area is about 6000 $km^2$, and the topography is flat. The major land uses are cotton (30%), range grass (21%) and range brush (31%). The major soil types

are Acuff sandy clay loam (fine-loamy, mixed, superactive, thermic Aridic Paleustolls), Amarillo sandy loam (fine-loamy, mixed, superactive, thermic Aridic Paleustalfs) and Olton clay loam (fine, mixed, superactive, thermic Aridic Paleustolls) (Soil Survey Staff, 2010).

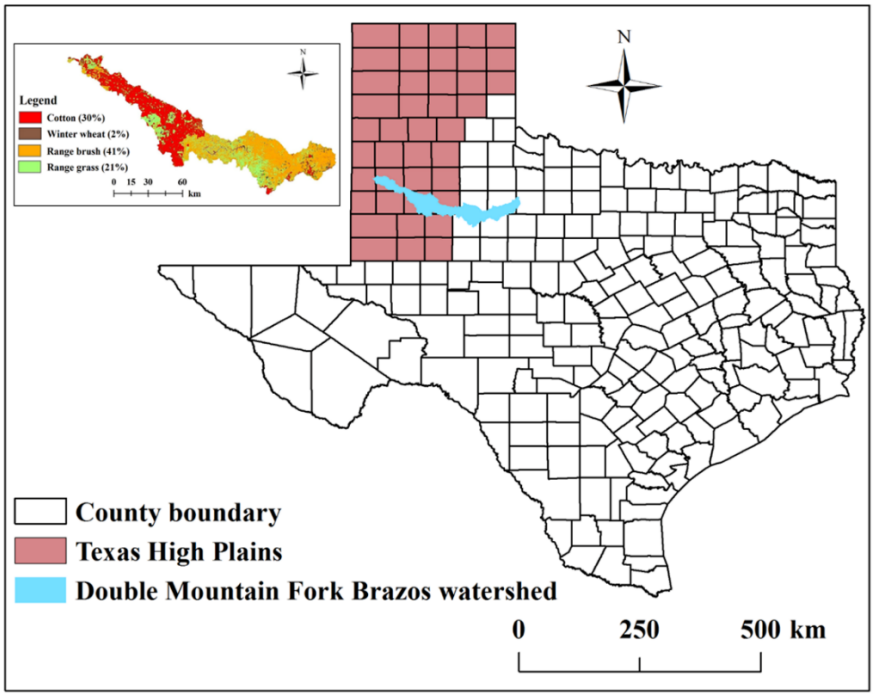


**Figure 1.1 Location of the study watershed in the Texas High Plains**

*1.1.2 Groundwater Depletion and Deterioration in the Texas High Plains*

The discovery of the vast underground Ogallala Aquifer in the early 20th century made the Ogallala groundwater available for irrigated agriculture in the THP (Hornbeck and Keskin, 2012). Development of improved center pivot irrigation technology further contributed to rapid expansion of irrigated agriculture in this region. About 97% of water drawn from the Ogallala Aquifer is used for intensive agricultural production in the THP

(Maupin and Barber, 2005). However, due to extensive groundwater pumping that far exceeds the recharge over the last eight decades, many producers in this region are facing water shortages due to lower groundwater availability (Nair et al., 2013). Chaudhuri and Ale (2014a), for example, reported that the mean groundwater level in the THP region has declined significantly ($p < 0.05$) from about 19 m in the 1930s to 52 m in the 2000s due to extensive pumping for meeting agricultural irrigation demand. Projected future changes in climate in this region are expected to further contribute to this problem. Recently, Modala et al. (2016) predicted an apparent increase in daily temperature (1.9 to 3.2 ºC) and a decrease in precipitation (30 to 127 mm) in the future in the THP region, which indicate that the groundwater availability could reduce substantially in the future. Using the Hydrologic Unit Model for the United States (HUMUS), Rosenberg et al. (1999) also predicted a further reduction in the recharge to the Ogallala Aquifer under the future climate change scenarios because of the increase in evapotranspiration (ET) due to elevated temperatures, and such trends would further reduce groundwater availability in this region.

In addition to groundwater depletion, groundwater quality in the THP region has also deteriorated over time due to both natural and anthropogenic factors (Chaudhuri and Ale, 2014b). Most importantly, nitrate concentrations in groundwater increased with time, especially in the southern part of the THP where intensive agricultural activities take place. For example, the percentage of groundwater quality observations from the shallow wells that exceeded the United States Environmental Protection Agency's Maximum Contaminant Level (MCL) for nitrate ($NO_3$) (44 mg $L^{-1}$) increased from 3%

in the 1960s (1960-1969) to 32% in the 2000s (2000-2010) (Chaudhuri and Ale, 2014b). Agricultural activities, mainly application of large quantities of inorganic fertilizers on croplands together with shallow depth of the aquifer were some of the important reasons for high nitrate concentrations in groundwater.

In order to extend the life of the Ogallala Aquifer and to insure that at least a certain percentage of currently available groundwater will still be available in 2060, Groundwater Conservation Districts (GCDs), which are the primary regulatory agencies in the region imposed new rules to limit the allowable annual groundwater pumping for irrigation. For example, the High Plains Underground Water Conservation District (HPUWCD) (http://www.hpwd.org/) set the annual groundwater pumping limit for 2015 and 2016 at 18 inches (457 mm) (HPUWCD, 2016). Decline of groundwater levels and the restrictions on groundwater pumping may induce changes in land use and cause a shift from irrigated to dryland cultivation in the THP in the future. However, studies focusing on such land use changes on hydrology and water quality of the THP watersheds are lacking.

### *1.1.3 Potential Changes in Land Use and the Associated Environmental Impacts*

A potential land use change from croplands to cellulosic bioenergy crops may significantly affect the regional hydrologic cycle and water quality. For example, using the SWAT model, Schilling et al. (2008) predicted that a land cover change from cropland to switchgrass in the Raccoon River watershed in west-central Iowa would increase ET by about 9% and decrease water yield (sum of surface runoff and subsurface

runoff) by about 28%. VanLoocke et al. (2010) also predicted that the land use change from corn to perennial bioenergy grass would increase ET within a range of 50 to 150 mm $yr^{-1}$ and decrease subsurface drainage within a range of 50 to 250 mm $yr^{-1}$ in the Corn Belt of the Midwest U.S., and they used the Integrated Biosphere Simulator - agricultural version (Agro-IBIS) model in their study. Another SWAT modeling study by Ng et al. (2010) estimated that a 10% land use change from cropland to *Miscanthus* × *giganteus* would lead to a reduction in nitrate-nitrogen ($NO_3$-N) load by about 6.4% at the outlet of the Salt Creek watershed in Illinois. A majority of these biofuel-induced land use change studies focused on the humid regions of the U.S. such as the Upper Mississippi River Basin of the Corn Belt region (Srinivasan et al., 2010; Demissie et al., 2012; Zhuang et al., 2013). Such detailed assessments on hydrology and water quality impacts of biofuel-induced change in land use are very limited for the arid/semi-arid regions such as the THP. In addition, no comprehensive assessment of hydrologic responses and water quality impacts of land use change from major row crops such as cotton to cellulosic bioenergy crops under the changing climate are documented (Sarkar and Miller, 2014). Evaluating the environmental impacts of land use change from cotton to cellulosic bioenergy crops in the semi-arid THP under the historic as well as future climatic conditions is, therefore, necessary to assess the feasibility of proposed land use change.

### 1.2 Ideal Bioenergy Crops and Their Potential for Biofuel Production

The potential for growing cellulosic crops such as Alamo switchgrass, *Miscanthus* × *giganteus*, big bluestem and biomass sorghum as bioenergy crops was studied by several researchers in different parts of the world through field experimentation (Heaton et al., 2008; Zatta et al., 2014; Yimam et al., 2014, 2015; Oikawa et al., 2015; Zhang et al., 2015a) and hydrologic and water quality modeling (Wright, 2007; Jain et al., 2010; Qin et al., 2011; Zhuang et al., 2013; Qin et al., 2015). Alamo switchgrass is a perennial C4 warm-season bunch grass native to North America, and it is found in low, moist areas and prairies of north-central Texas (Diggs et al., 1999). *Miscanthus* × *giganteus* is also a C4 warm-season perennial grass (Heaton et al., 2004, 2008) that is native to Southeast Asia (Ohwi, 1964) and Africa (Adati and Shiotani, 1962). Big bluestem is a C4 warm-season perennial native grass that comprises as much as 80% of the plant biomass in prairies in the Midwestern grasslands of North America (Gould and Shaw, 1983; Knapp et al., 1998). Biomass sorghum is an annual photoperiod sensitive C4 type cellulosic crop that adapts to the subtropical and temperate climates (Rooney et al., 2007). Several field studies that evaluate the feasibility of growing these bioenergy crops/grasses are in progress in the THP. However, evaluation of long-term effects of growing cellulosic bioenergy crops would be necessary before adopting them on a large-scale, and hydrologic and water quality models are very useful for such purposes.

Cellulosic biomass can be converted into biofuel through various biochemical processes, which include pretreatment, enzymatic hydrolysis and fermentation

(Christakopoulos et al., 1993). Bioethanol production from cellulosic biomass is considered as a viable option because it does not compete with human food production. According to the US Department of Energy (http://www.afdc.energy.gov/fuels/ethanol_feedstocks.html), the estimated ethanol production from cotton gin trash, rice/wheat straw, hardwood sawdust, switchgrass/*Miscanthus* and biomass sorghum is about 215, 416, 382, 366 and 428 liters $Mg^{-1}$ dry biomass, respectively (Table 1.1).

**Table 1.1 Theoretical ethanol yields of the selected feedstocks**

| Feedstock | Theoretical ethanol yield (Liter per dry Mg of feedstock) |
|---|---|
| Corn grain | 470.9 |
| Corn/sorghum stover | 427.8 |
| Rice/wheat straw | 416 |
| Cotton gin trash | 215 |
| Forest thinnings | 308.5 |
| Hardwood sawdust | 381.6 |
| Bagasse | 422.1 |
| Mixed paper | 439.9 |
| Switchgrass | 366 |

*280 for switchgrass whole plant
Source: U.S. Department of Energy Biomass Program, Theoretical Ethanol Yield Calculator and Biomass Feedstock Composition and Property Database

## 1.3 Objectives and Hypotheses

The overall goal of this study is to assess the impacts of land use change from cotton to cellulosic bioenergy crops on hydrology and water quality of the Double

Mountain Fork Brazos watershed in the THP under the current and future climate scenarios using the SWAT, APEX and Integrated APEX-SWAT models. Specific objectives of the study were to:

1. evaluate the impacts of land use change from cotton to bioenergy crops such as switchgrass, *Miscanthus*, big bluestem and biomass sorghum, on water balances at the field and watershed scales
2. quantify the biomass and biofuel production potential of above cellulosic bioenergy crops, and identify ideal bioenergy crops for the THP region
3. identify marginal cotton-growing areas in the watershed for potential replacement with switchgrass, and evaluate associated land use change impacts on water use efficiency and hydrologic fluxes
4. compare and contrast the hydrologic and water quality impacts of the proposed land use change under irrigated and dryland agricultural systems
5. assess the combined impacts of climate change and proposed land use change on hydrologic fluxes, water quality and crop yield

**Hypothesis 1:**

Perennial bioenergy crops such as switchgrass, *Miscanthus* and big bluestem are ideal for water conservation when compared to cotton.

This hypothesis was tested on the Double Mountain Fork Brazos watershed in the THP using the calibrated SWAT model for streamflow and cotton lint yield. Results showed that the average annual (1994-2009) surface runoff from the entire watershed

under the perennial grass scenarios decreased by 6% to 8% relative to the baseline cotton scenario. Perennial grass land use change scenarios also suggested an increase in average annual percolation within a range of 3% to 22% and maintenance of higher soil water content during August to April compared to the baseline cotton scenario. Therefore, the perennial bioenergy crops were found to conserve water better when compared to cotton.

**Hypothesis 2:**

Switchgrass and *Miscanthus* are ideal cellulosic bioenergy crops for the irrigated and dryland conditions in the THP.

This hypothesis was also verified using the calibrated SWAT model. Results showed that *Miscanthus* and switchgrass were found to be ideal bioenergy crops for the dryland and irrigated conditions, respectively, in the study watershed due to their higher water use efficiency, better water conservation effects, greater biomass and biofuel production potential, and minimum crop management requirements compared to the big bluestem and biomass sorghum.

**Hypothesis 3:**

Perennial grasses reduce nutrient loads to surface and groundwater when compared to cotton.

This hypothesis was tested by using the Integrated APEX-SWAT model. The Integrated APEX-SWAT model was calibrated against the observed streamflow, cotton lint yield and TN load in streamflow. The nitrogen balances of cotton were also analyzed

to verify the model performance. Results showed that the $NO_3$-N and organic-N loads in surface runoff and $NO_3$-N leaching to groundwater reduced significantly by 86%, 98% and 100%, respectively, under the perennial grass scenarios relative to the baseline cotton scenario.

**Hypothesis 4:**

a) The biomass yields of perennial bioenergy crops will decrease under the future climate scenarios when compared to the historic period.
b) Cotton is more sensitive to future climate change impacts when compared to bioenergy crops.

These hypotheses were also examined on the Double Mountain Fork Brazos watershed in the THP using the calibrated SWAT model and projected Coupled Model Intercomparison Project Phase 5 (CMIP5) climate data from 19 General Circulation Models (GCMs). Two Representative Concentration Pathway (RCP) emission scenarios of RCP4.5 (moderate) and RCP8.5 (severe) for the middle of the 21$^{st}$ century (2040 to 2069) and end of the 21$^{st}$ century (2070 to 2099) were used. Results indicated that cotton is more sensitive to future climate change when compared to perennial grasses. While irrigated and dryland cotton yields increased within the ranges of 69% to 91% and 100% to 129%, respectively, the irrigated switchgrass biomass yield decreased within a range of 16% to 28%, and the dryland *Miscanthus* biomass yield increased within a range of 32% to 38% under the future climate change scenarios when compared to the historic period.

## 1.4 Organization of Dissertation

This dissertation consists of seven sections. Section 1 is devoted to a general introduction, science questions and the objectives & hypotheses of the study. Section 2 addresses the first and second objectives. It describes the methodology adopted for SWAT model setup, parameterization and calibration for the study watershed. It also provides a detailed analysis of the impacts of land use change from cotton to cellulosic bioenergy crops on hydrology and identification of ideal cellulosic bioenergy crops for the irrigated and dryland conditions in the THP. Section 3 addresses third objective and it discusses about the hydrologic impacts of replacing cotton on marginal lands in the study watershed with switchgrass using the APEX model. In addition to identifying marginal cotton growing subareas in the watershed for potential replacement with switchgrass, this section also discusses the spatial variability in water use efficiency and hydrologic fluxes under the baseline cotton and hypothetical switchgrass replacement scenarios. Section 4 addresses the objective 4. In this section, the APEX model was integrated with the SWAT model to enable assessment of water quality effects of proposed land use change from the watershed. This section also describes the impacts of land use change on $NO_3$-N leaching to groundwater, which is a major concern in the THP. Section 5 addresses the objective 5. It discusses the impacts of land use change from cotton to perennial grasses on hydrology, water quality and crop yield under current and future climate change scenarios. It uses the CMIP5 climate projections from 19 GCMs under two emission scenarios of RCP4.5 and RCP8.5 during two 30-year periods of middle (2040-2069) and end (2070-2099) of the 21$^{st}$ century. Section 6 also

addresses objective 1 and it describes field-scale calibration of the SWAT model using eddy covariance data and assessment of water balances. The one hydrologic response unit (HRU) method, which is a very flexible and time-saving method, was used to calibrate the SWAT model against the field observations of ET and aboveground biomass. Section 7 summarizes the study, draws some appropriate conclusions and makes several recommendations for the future work.

# 2. HYDROLOGICAL RESPONSES OF LAND USE CHANGE FROM COTTON (*GOSSYPIUM HIRSUTUM* L.) TO CELLULOSIC BIOENERGY CROPS IN THE SOUTHERN HIGH PLAINS OF TEXAS, USA*

## 2.1 Synopsis

The Southern High Plains (SHP) region of Texas in the United States, where cotton is grown in a vast acreage, has the potential to grow cellulosic bioenergy crops such as perennial grasses and biomass sorghum (*Sorghum bicolor*). Evaluation of hydrological responses and biofuel production potential of hypothetical land use change from cotton (*Gossypium hirsutum* L.) to cellulosic bioenergy crops enables better understanding of the associated key agroecosystem processes and provides for the feasibility assessment of the targeted land use change in the SHP. The Soil and Water Assessment Tool (SWAT) was used to assess the impacts of replacing cotton with perennial Alamo switchgrass (*Panicum virgatum* L.), *Miscanthus* × *giganteus* (*Miscanthus sinensis* Anderss. [Poaceae]), big bluestem (*Andropogon gerardii*) and annual biomass sorghum on water balances, water use efficiency and biofuel production potential in the Double Mountain Fork Brazos watershed. Under perennial grass scenarios, the average (1994-2009) annual surface runoff from the entire watershed decreased by 6% to 8% relative to the baseline cotton scenario. In contrast, surface runoff increased by about 5% under the biomass sorghum scenario. Perennial grass land

* The following material in this section is used with permission from John Wiley & Sons, Inc. It has been published as a peer-reviewed research paper in the journal of *Global Change Biology Bioenergy*. 2016. 8: 981-999.

use change scenarios suggested an increase in average annual percolation within a range of 3% to 22% and maintenance of a higher soil water content during August to April compared to the baseline cotton scenario. About 19.1, 11.1, 3.2 and 8.8 Mg $ha^{-1}$ of biomass could potentially be produced if cotton area in the watershed would hypothetically be replaced by *Miscanthus*, switchgrass, big bluestem and biomass sorghum, respectively. Finally, *Miscanthus* and switchgrass were found to be ideal bioenergy crops for the dryland and irrigated systems, respectively, in the study watershed due to their higher water use efficiency, better water conservation effects, greater biomass and biofuel production potential, and minimum crop management requirements.

## 2.2 Introduction

The semi-arid Southern High Plains (SHP) of Texas in the United States is one of the most agriculturally intensive regions in the world. Irrigated agriculture in the SHP depends primarily on groundwater availability in the underlying vast Ogallala Aquifer. About 97% of water withdrawn from the Ogallala Aquifer is used for crop irrigation in the SHP (Maupin and Barber, 2005). However, groundwater levels in this region are experiencing a continuous decline due to much higher rates of groundwater extraction compared to recharge (Chaudhuri and Ale, 2014a; Rajan et al., 2015b). Many producers in this region are facing water shortages due to lower groundwater availability and higher pumping costs (Nair et al., 2013). In order to extend the life of the Ogallala Aquifer and to insure that at least certain percentage (varies with the water district) of

currently available groundwater will still be available in 2060, the primary regulatory agencies in the region imposed new rules to limit the allowable annual groundwater pumping for irrigation. For example, the High Plains Underground Water Conservation District (http://www.hpwd.org/) set the pumping limit for 2015 at 46 cm (HPUWCD, 2015).

The major crop grown in the SHP region is cotton, and this region produced approximately 13% of U.S. cotton in 2013 (NASS, 2013). The new restrictions on groundwater pumping in the SHP are expected to result in a change in land use from high-water-demanding crops such as cotton and corn to relatively less water demanding crops in the near future (Rajan et al., 2015a). The agricultural land in the SHP region has the potential to grow cellulosic bioenergy crops such as perennial grasses and biomass sorghum (*Sorghum bicolor*) (USDA, 2010), which have higher water use efficiency compared to cotton, and can provide water quality and economic benefits (Rooney et al., 2007; Sarkar et al., 2011; Kiniry et al., 2013; Sarkar and Miller, 2014). The United States Department of Agriculture (USDA) has also estimated that about 11.4% of existing croplands and pastures in the Southeastern U.S. region, which includes the SHP, will be required for fuel use for meeting the 2022 national cellulosic biofuel target (USDA, 2010).

A potential land use change from croplands to cellulosic bioenergy crops in the SHP may significantly affect regional hydrologic cycle by altering proportions of surface runoff, water yield (the net amount of water that generates from a landscape and contributes to streamflow during a given time interval), evapotranspiration (ET), soil

water content and percolation (the amount of water that percolates below the root zone during a given time). For example, Schilling et al. (2008) found that the land use/land cover change from cropland to cellulosic bioenergy crop of switchgrass in the Raccoon River watershed in west-central Iowa would increase ET by about 9% and decrease water yield by about 28%. VanLoocke et al. (2010) also reported that the land use conversion from corn (*Zea mays* L.) to perennial biofuel grasses would increase ET within a range of 50 to 150 mm year$^{-1}$ and decrease the drainage within a range of 50 to 250 mm year$^{-1}$ in the Corn Belt of Midwest U.S. Majority of these biofuel-induced land use change studies focused on the humid regions of the U.S. such as the Upper Mississippi River Basin of the Corn Belt region (Srinivasan et al., 2010; Demissie et al., 2012; Zhuang et al., 2013). Such detailed assessments of hydrological impacts of biofuel-induced land use change are lacking for the arid/semi-arid regions such as the SHP. In addition, no comprehensive assessment of hydrological responses and biofuel production potential of land use change from major row crops such as cotton to various cellulosic bioenergy crops are documented (Sarkar and Miller, 2014). Evaluating the hydrologic impacts of land use change from cotton to cellulosic bioenergy crops in the semi-arid SHP is therefore necessary to assess the feasibility of the proposed land use change.

The potential for the use of cellulosic crops such as Alamo switchgrass (*Panicum virgatum* L.), *Miscanthus* × *giganteus* (*Miscanthus sinensis* Anderss. [Poaceae]), big bluestem (*Andropogon gerardii*) and biomass sorghum as bioenergy crops was studied by several researchers in different parts of the world through field experimentation and

modeling (Wright, 2007; Heaton et al., 2008; Jain et al., 2010; Qin et al., 2011; Qin et al., 2015; Zhuang et al., 2013; Oikawa et al., 2014; Zatta et al., 2014; Yimam et al., 2014, 2015; Zhang et al., 2015a). Alamo switchgrass is a perennial C4 warm-season bunch grass native to North America and it is found in low, moist areas and prairies of north-central Texas (Diggs et al., 1999). *Miscanthus* × *giganteus* is a C4 cool-season grass (Heaton et al., 2004, 2008) that is native to Southeast Asia (Ohwi, 1964) and Africa (Adati and Shiotani, 1962). Big bluestem is a C4 warm-season perennial native grass that comprises as much as 80% of the plant biomass in prairies in the Midwestern grasslands of North America (Gould and Shaw, 1983; Knapp et al., 1998). Biomass sorghum is a photoperiod sensitive C4 type lignocellulosic biomass crop that remains in a vegetative growth stage for most of the growing season in subtropical and temperate climates (Rooney et al., 2007). In this study, *Miscanthus* × *giganteus*, Alamo switchgrass, big bluestem and biomass sorghum were selected to hypothetically replace the existing cotton land use (baseline). Alamo switchgrass has higher radiation use efficiency and water use efficiency than Kanlow and other switchgrass varieties (Blackwell, Cave-in-Rock, and Shawnee) in the Southern Great Plains (Kiniry et al., 2013), and hence Alamo switchgrass was selected in this study.

Several hydrologic models are available for simulating the hydrological impacts of land use change, such as the Soil and Water Assessment Tool (SWAT; Arnold et al., 1998), Agricultural Policy/Environmental Extender (APEX) model (Williams, 1995), European Hydrological System Model MIKE SHE (Refsgaard and Storm, 1995), DRAINMOD (Youssef et al., 2005; Skaggs et al., 2012) and the Agricultural Drainage

and Pesticide Transport (ADAPT) model (Gowda et al., 2012). Among these models, the SWAT model has been used widely across the world and it demonstrated potential to satisfactorily predict long-term impacts of land use change on hydrologic processes in complex watersheds (Ghaffari et al., 2010; Srinivasan et al., 2010; Wu and Liu, 2012; Zatta et al., 2014), and hence the same model was used in this study. The availability of good quality observed streamflow data is vital for developing a well-calibrated SWAT model for the study watershed. There are only a limited number of USGS gauges in the SHP region and they recorded very low streamflow in most parts of the year, which posed some challenges for the SWAT model calibration. Several recent studies used crop yield as an auxiliary data for model calibration, as crop yield is directly proportional to ET component of the water balance (Akhavan et al., 2010; Srinivasan et al., 2010; Zhang et al., 2013; Mittelstet et al., 2015; Zhang et al., 2015b). This additional step in model calibration gives more confidence on the partitioning of water between soil storage, ET and aquifer recharge (Faramarzi et al., 2009, 2010; Akhavan et al., 2010). Therefore, the SWAT model was calibrated against reported county-level cotton lint yield data in addition to streamflow.

The overall goal of this study was to evaluate the hydrological responses and biofuel production potential of hypothetical land use change from cotton to cellulosic bioenergy crops including two native perennial grasses, switchgrass and big bluestem; one non-native perennial grass, *Miscanthus*; and an annual, high potential biofuel crop of biomass sorghum in the Double Mountain Fork Brazos watershed in the SHP using the SWAT model. In the SWAT crop database, big bluestem and biomass sorghum are

included as generic crops, and hence we modeled these two crops as generic crops instead of specific varieties. Specific objectives of the study were to: (1) assess the impacts of hypothetical land use change from cotton to bioenergy crops such as switchgrass, *Miscanthus*, big bluestem and biomass sorghum, on water balances; (2) quantify the potential amount of biofuel production from these cellulosic bioenergy crops, and identify appropriate bioenergy crops for the SHP region; and (3) compare and contrast the hydrologic impacts and biofuel production potential of the proposed hypothetical land use changes under irrigated and dryland agricultural systems.

## 2.3 Materials and Methods

### *2.3.1 Watershed Description*

The Double Mountain Fork Brazos watershed (HUC # 12050004) in the SHP has a total delineated area of about 6,000 $km^2$. Larger parts of the watershed are located in the counties of Hockey, Lynn, Garza, Scurry, Kent and Stonewall, and some smaller portions in Terry, Lubbock, Dawson, Borden, Fisher and Haskell Counties (Figure 1.1). The long term (1981-2010) average annual precipitation across the watershed varies between 457 and 559 mm, and the long term average annual maximum and minimum temperatures are about 23°C to 25°C and 8°C to 10°C, respectively. The topography of the watershed is flat, and there is a long history of cotton and winter wheat (*Triticum aestivum*) cultivation in this watershed. The primary soil types in the watershed are Amarillo sandy loam (fine-loamy, mixed, superactive, thermic Aridic Paleustalfs), Acuff sandy clay loam (fine-loamy, mixed, superactive, thermic Aridic Paleustolls) and Olton

clay loam (fine, mixed, superactive, thermic Aridic Paleustolls) (Soil Survey Staff, 2010).

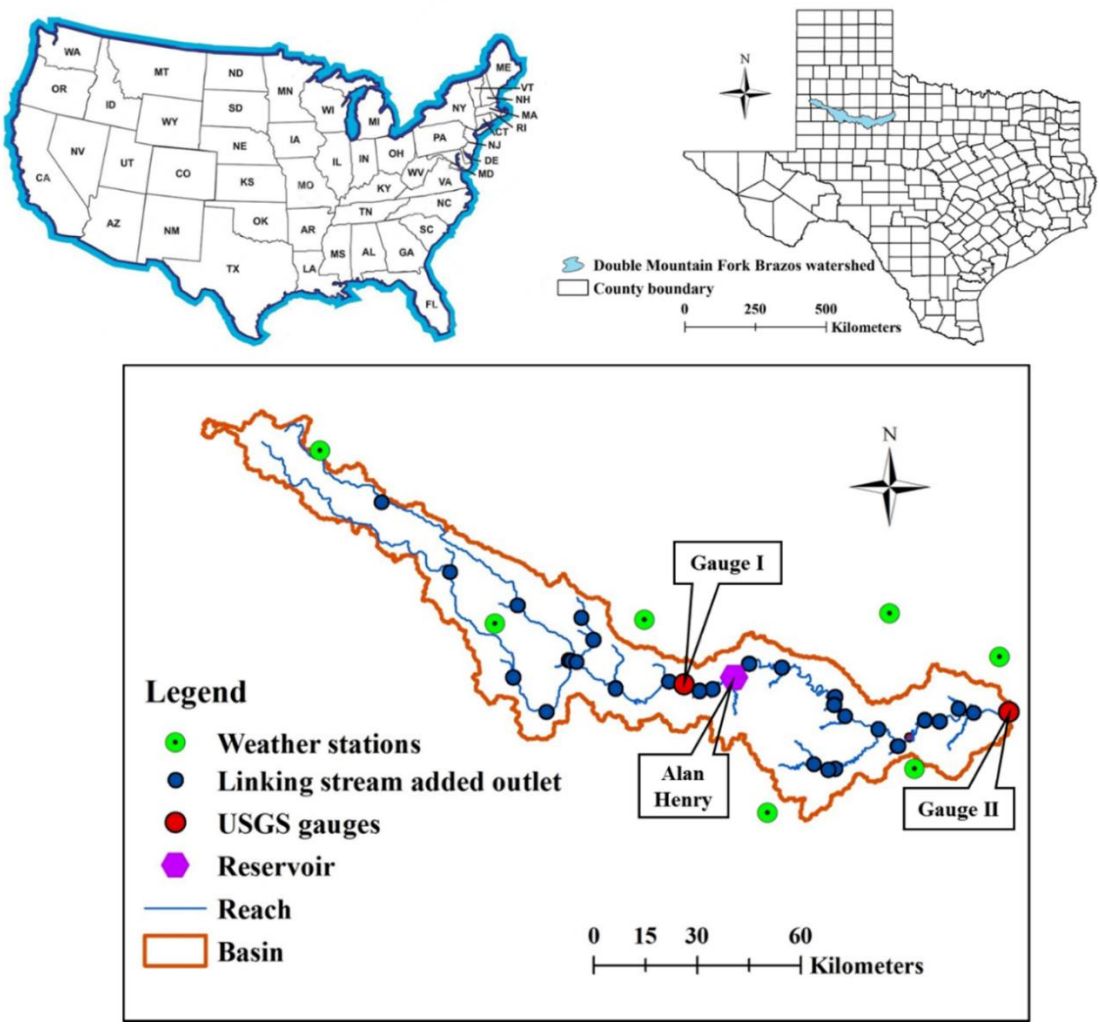


**Figure 2.1 Location of the study watershed.**

Seven weather stations with daily precipitation, and minimum and maximum temperature data exist inside or within a closer distance of the watershed. Although three USGS gauges are located in this watershed, the streamflow data from only two gauges (08079600, which is denoted as Gauge I and 08080500, which is at the watershed outlet

and denoted as Gauge II) was used in this study (Figure 1.1). Data from the remaining gauge was not used to calibrate the SWAT model as only limited streamflow data pertaining to 1949-1951 period was available for that gauge (08080000).

### *2.3.2 SWAT Model Description*

The SWAT model is a continuous-time, semi-distributed, process-based, river basin scale model (Arnold et al., 2012). Large number of input parameters are needed for SWAT to evaluate the effects of land use change on hydrology and water quality. SWAT is operated on a daily time step and is widely proven as a feasible tool to predict the impact of land use and management on water, sediment and agricultural chemical yields in many watersheds (Gassman et al., 2014). The primary model components in SWAT include the pesticide, hydrology and crop growth (Knisel, 1980; Leonard et al., 1987; Williams et al., 2008; Wang et al., 2011). Major model inputs are related to hydrography, terrain, land use, soil, tile, weather and management practices (Srinivasan et al., 2010).

In this study, ArcSWAT (Version 2012.10_2.16 released on 9/9/14) for ArcGIS 10.2.2 platform was used. The SWAT Calibration and Uncertainty Procedures (SWAT-CUP) (Abbaspour et al., 2007), a program that has been frequently used for sensitivity analysis, calibration, validation and uncertainty analysis of SWAT models (Chandra et al., 2014; Vaghefi et al., 2014), was used in this study. Currently, SWAT-CUP 2012 can link Generalized Likelihood Uncertainty Estimation (GLUE; Beven and Binley, 1992), Parameter Solution (van Griensven and Meixner, 2006), Sequential Uncertainty Fitting version-2 (SUFI-2; Abbaspour et al., 2007) and Markov chain Monte Carlo procedures

(Marshall et al., 2004) to SWAT. In this study, SWAT-CUP 2012 SUFI-2 procedure was used to accomplish the model sensitivity analysis, calibration and validation, and estimation of various SWAT parameters related to streamflow.

### *2.3.3 SWAT Model Setup*

#### 2.3.3.1 Digital Elevation Model (DEM)

The DEM of the watershed, with a horizontal resolution of $30 \times 30$ m was downloaded from the U.S. Geological Survey (http://viewer.nationalmap.gov/viewer/#) and input to the SWAT model. The DEM was used for estimation of watershed topography related parameters for the study watershed.

#### 2.3.3.2 Land Use, Soils and Slope

The 2008 National Agricultural Statistics Service (NASS) Cropland Data layer (CDL) (http://nassgeodata.gmu.edu/CropScape/) was used as a land use input to the model to appropriately represent the land use condition of the simulated period from 1994 to 2009. The dominant agricultural land uses in the watershed in 2008 were cotton and winter wheat, which occupied about 30% and 2% of the watershed area (Figure 2). About 41% and 21% of the watershed area was covered by range brush and range grass, respectively. The finer-scale soils data from the Soil Survey Geographic Database (SSURGO) (SSURGO, 2014), which was compatible to ArcSWAT 2012, was used. The watershed was classified into four groups according to soil slope: $\leq 1\%$, 1%-3%, 3%-5% and $> 5\%$.

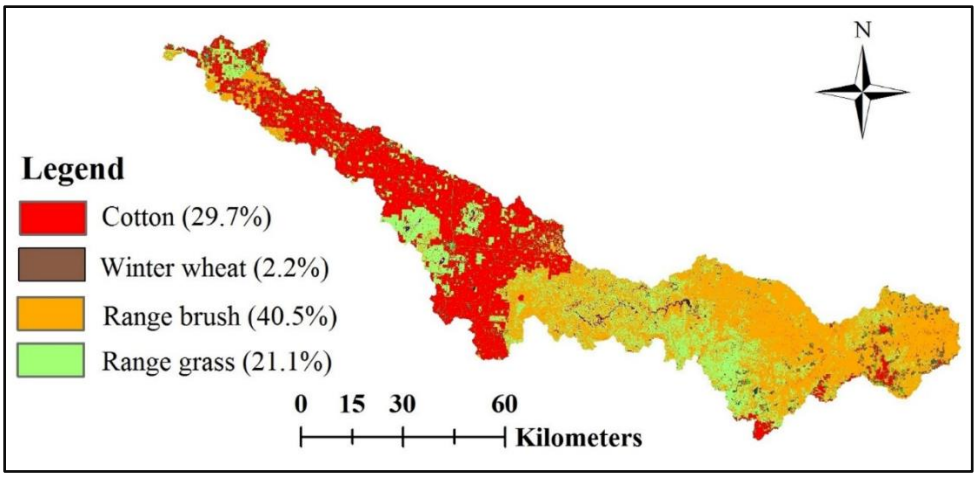


**Figure 2.2 Major land uses in the study watershed.**

#### 2.3.3.3 Hydrologic Response Units (HRUs)

The Hydrologic Response Units (HRUs) are the basic building blocks of the SWAT model, from which all landscape processes are computed. The HRUs consist of homogeneous land use, soil characteristics and soil slope. For the HRU definition, thresholds of 5%, 5% and 10% were used for land use, soil type and slope, respectively. The number of subbasins and HRUs identified for this watershed were 60 and 2160, respectively.

#### 2.3.3.4 Weather

Daily weather data was obtained from the National Climatic Data Center (NCDC) for the period from 1992 to 2009 (NOAA-NCDC, 2014) and used in this study. Data from a total of seven weather stations, which were located either inside or within a closer distance of the study watershed, was used (Figure 2.1). These weather stations were very well distributed spatially across the watershed. The missing precipitation,

maximum temperature and minimum temperature data for a weather station was manually filled with the average value of weather parameter for two adjacent weather stations (Ale et al., 2009).

#### 2.3.3.5 Management Practices of Crops

Crop management related parameters for two dominant row crops, cotton and winter wheat, were set at appropriate values observed in the study area based on published reports, local expertise, and web resources. The management parameters for other land uses were mostly kept at their default values. In this study, management practices in the SWAT model were scheduled by date. Generic spring plowing and generic fall plowing, which were widely adopted tillage practices in this watershed, were used in cotton and winter wheat growing areas, respectively (Table 2.1). About 300 and 150 kg $ha^{-1}$ of urea was applied to the irrigated and dryland cotton HRUs, respectively. About 108 kg $ha^{-1}$ of urea was used for the winter wheat, which was grown under dryland systems. According to the published county-wise cotton acreage estimates over the period from 1994 to 2009 (NASS, 2014), about 39% of the cotton acreage in the watershed was irrigated. In this study, auto-irrigation was therefore simulated in an appropriate number of cotton HRUs so that about 39% of cotton acres in the watershed were irrigated. The auto-irrigation operation applied water whenever 10% reduction in plant growth occurred due to water stress (Table 2.1). Shallow aquifer was assigned as the source of irrigation water for the irrigated subbasins.

**Table 2.1 Simulated management practices for cotton and winter wheat in SWAT**

| No. | Operations | Description | Input data |
|---|---|---|---|
| Irrigated cotton | | | |
| 1 | Tillage Parameters (Tillage on April 1) | | |
| | TILL_ID | Tillage ID | Generic Spring Plowing[#] |
| 2 | Fertilizer Application Parameters (May 1) | | |
| | FERT_ID | Fertilizer ID | Urea |
| | FRT_KG | Amount of fertilizer applied to HRU | 300.7 (kg $ha^{-1}$)[#] |
| 3 | Begin Growing Season Parameters ( Planting on May 15) | | Default |
| | Heat units to maturity | | 2354℃-day ξ |
| 4* | Auto-irrigation Parameters (Start date: May 15; End date: October 31) | | |
| | WSTRS_ID | Water stress identifier | Plant Water Demand |
| | IRR_SCA | Irrigation source | Shallow Aquifer |
| | AUTO_WSTRS | Water stress threshold | 0.9 |
| | IRR_EFF | Irrigation efficiency | 0.80[#] |
| 5 | Harvest and Kill Parameters (Kill on October 31) | | Default |
| Dryland cotton | | | |
| 1 | Tillage Parameters (Tillage on April 1) | | |
| | TILL_ID | Tillage ID | Generic Spring Plowing[#] |
| 2 | Fertilizer Application Parameters (May 1) | | |
| | FERT_ID | Fertilizer ID | Urea |
| | FRT_KG | Amount of fertilizer applied to HRU | 150 (kg $ha^{-1}$)[#] |
| 3 | Begin Growing Season Parameters (Planting on May 15) | | Default |
| | Heat units to maturity | | 2354℃-day ξ |
| 4 | Harvest and Kill Parameters (Kill on October 31) | | Default |
| Winter wheat | | | |
| 1 | Tillage Parameters (Tillage on October 8) | | |
| | TILL_ID | Tillage ID | Generic Fall Plowing[#] |
| 2 | Fertilizer Application Parameters (October 8) | | |
| | FERT_ID | Fertilizer ID | Urea |
| | FRT_KG | Amount of fertilizer applied to HRU | 108 (kg $ha^{-1}$)[#] |
| 3 | Begin Growing Season Parameters (Planting on October 15) | | Default |
| | Heat units to maturity | | 1518℃-day ξ |
| 4 | Harvest and Kill Parameters (Kill on July 1) | | Default |

*Auto-irrigation was simulated in appropriate proportion of cotton area based on County cotton irrigation acreage summary reports

[#]The management methods and parameters were based on published reports and local expertise

ξ Heat units to maturity for cotton and winter wheat were estimated using the SWAT-PHU program (http://swat.tamu.edu/software/potential-heat-unit-program/)

### 2.3.3.6 Reservoir

Alan Henry, a big reservoir, exists in the study watershed, and operation parameters for this reservoir were obtained from the Texas Water Development Board's report on Volumetric Survey of Alan Henry reservoir (2005). The reservoir surface area when the reservoir was filled to the emergency and principal spillways was about 1215

and 1109 ha, respectively. Volume of water needed to fill the reservoir to the emergency and principal spillways was estimated as $12688.3 \times 10^4$ and $11694.4 \times 10^4$ $m^3$, respectively. Average value of initial reservoir volume was taken as $4882.1 \times 10^4$ $m^3$, which was calculated based on the reservoir storage level records of the USGS gauge 08079700. Although the reservoir was operated from 1994, continuous daily reservoir release data was available only from 1997 to 2003. A relationship between the reservoir releases and annual rainfall was established based on the observed data for the 1997-2003 period, and the developed relationship was used to fill the missing reservoir release data for the 1994-1996 and 2004-2009 periods. Finally, the "Measured Daily Outflow" method available in the SWAT model was used to estimate the reservoir discharge based on the reservoir storage levels recorded by the USGS gauge.

### *2.3.4 Observed Streamflow and Cotton Lint Yield*

Observed daily streamflow data recorded at Gauges I and II over the time period from 1994 to 2009 was obtained from the USGS National Water Information System (http://waterdata.usgs.gov/nwis/sw). The observed cotton lint yield data (under both dryland and irrigated systems) for the period from 1994 to 2009 for the Lynn County in the study watershed, in which the highest cotton acreage was reported, was obtained from the National Agricultural Statistics Service (NASS) reports (http://quickstats.nass.usda.gov/). However, the SWAT model simulates whole cotton yield (seed cotton yield), which comprises of both cotton seed and lint. In order to

compare with the observed cotton lint yield data obtained from the NASS, the simulated seed cotton yield was converted to lint yield using the following equation:

$$Y_{lint} = 0.39 \times Y_{whole} \quad (1)$$

where $Y_{lint}$ is the simulated lint yield (Mg $ha^{-1}$) and $Y_{whole}$ is the simulated seed cotton yield (Mg $ha^{-1}$). The conversion factor of 0.39 was obtained from the relationship: about 340 kg cotton seed is equivalent to 218 kg lint (Wanjura et al., 2014).

### *2.3.5 SWAT Model Calibration*

The streamflow data was divided into two parts, and the data for the 1994-2001 and 2002-2009 periods was used for model calibration and validation, respectively. The SWAT model calibration was performed in three steps. First of all, the sensitive model parameters were identified by performing sensitivity analysis using the SWAT-CUP (Abbaspour et al., 2007; Veith et al., 2010; Arnold et al., 2012). In the second step, auto-calibration was performed using the SUFI-2 procedure available in the SWAT-CUP. During this step, sensitive model parameters were adjusted within ±10% range to obtain calibrated parameters for the study watershed. Finally, the calibrated parameters were slightly adjusted manually to achieve the best calibrated SWAT model for the watershed. The model was initially calibrated against the observed streamflow data recorded at Gauge I by adjusting the parameters in all subbasins that contributed flow to Gauge I. The model was then validated against the remaining streamflow data recorded at Gauge I. After achieving a satisfactory calibration of the model for Gauge I, the model was calibrated against the streamflow data recorded at Gauge II. To start with, the calibrated

parameter values that were obtained from model calibration for Gauge I were used in all subbasins between Gauge I and Gauge II, and later they were adjusted as needed to obtain a better match between the simulated and observed streamflow at Gauge II. The model was finally validated based on the remaining streamflow data recorded at Gauge II.

The highly sensitive curve number (CN2) was decreased by 6.5% for all of the subbasins that discharged to Gauge I and it was decreased by 9% for other subbasins in order to reduce the surface runoff and thereby obtain a good match between the simulated and observed streamflow in the watershed (Table 2.2). The available soil water capacity (SOL_AWC) was increased by 10% for all subbasins in order to further improve the match between the simulated and observed streamflow. The soil evaporation compensation factor (ESCO) was decreased from a default value of 0.95 to 0.855 in order to increase the soil evaporation and adjust crop yield prediction. A base flow recession constant (ALPHA_BF) of 0.0765, which was obtained from the baseflow filter method (Arnold et al., 1995; Arnold and Allen, 1999), was used.

**Table 2.2 Default and calibrated values of some important hydrologic and crop parameters in SWAT**

| No. | Parameter | Description | Default value | Calibrated value | Reference |
|---|---|---|---|---|---|
| Hydrologic parameters | | | | | |
| 1 | ESCO | Soil evaporation compensation factor | 0.95 | 0.855 | -- |
| 2 | SOL_AWC | Available soil water capacity (mm $H_2O$ $mm^{-1}$ soil) | 0.1-0.17 | Increased by 10% | -- |
| 3 | CN2 | Curve number for moisture condition II | 39-84 | Decreased by 6.5% or 9%* | -- |
| 4 | ALPHA_BF | Base flow recession constant | 0.048 | 0.0765# | -- |
| Dryland cotton parameters | | | | | |
| 5 | BIO_E | Biomass/energy ratio [(kg $ha^{-1}$)/(MJ $m^{-2}$)] | 15 | 16.8 | (Sarkar et al., 2011) |
| 6 | HVSTI | Harvest index [(kg $ha^{-1}$)/(kg $ha^{-1}$)] | 0.5 | 0.49 | (Wanjura et al., 2014) |
| 7 | BLAI | Max leaf area index ($m^2/m^2$) | 4 | 4.5 | (Sarkar et al., 2011) |
| Irrigated cotton parameters | | | | | |
| 8 | BIO_E | Biomass/energy ratio [(kg $ha^{-1}$)/(MJ $m^{-2}$)] | 15 | 19.95 | (Sarkar et al., 2011) |
| 9 | BLAI | Max leaf area index ($m^2/m^2$) | 4 | 5.98 | (Sarkar et al., 2011) |
| 10 | EXT_COEF | Light extinction coefficient | 0.65 | 0.78 | (Sarkar et al., 2011) |

* Curve number decreased by 6.5% all of the subbasins that discharged to Gauge I and decreased by 9% for other subbasins

# Obtained from baseflow filter method

After achieving a satisfactory streamflow calibration, the model was further calibrated for prediction of cotton lint yield under both irrigated and dryland systems in order to obtain a good match between the simulated and reported cotton lint yields. Previous SWAT modeling studies that performed crop yield calibration (Hu et al., 2007; Nair et al., 2011; Sarkar et al., 2011; Ávila-Carrasco et al., 2012) suggested adjusting the biomass/energy ratio (BIO_E) and maximum leaf area index (BLAI) to calibrate the SWAT model for crop yield prediction. Among these studies, Sarkar et al. (2011) compared observed and simulated cotton lint yields, and they suggested the parameter

ranges of BIO_E (10-20), BLAI (2-6), and light extinction coefficient (EXT_COEF; 0.5-0.8) for calibrating cotton lint yield. Following the procedure of Sarkar et al. (2011), the parameters BIO_E, BLAI, and EXT_COEF were adjusted within their reported ranges in this study. For the dryland cotton, BIO_E and BLAI of the crop database were increased from default values of 15 and 4 to 16.8 and 4.5, respectively (Table 2.2). The harvest index (HVSTI) was decreased from 0.5 to 0.49 based on the reported HVSTI value for the dryland cotton production systems in this region (Wanjura et al., 2014). The BIO_E and BLAI were increased to 19.95 and 5.98, respectively, and EXT_COEF was changed from 0.65 to 0.78 for the irrigated cotton production systems (Table 2.2). Finally, after achieving a good crop yield calibration, the model performance in streamflow prediction was re-evaluated and necessary minor adjustments to initially calibrated streamflow related parameters were made.

### *2.3.6 Evaluating the Performance of the SWAT Model*

The SWAT model performance in streamflow prediction during calibration and validation periods was evaluated using four different statistical measures: square of Pearson's product- moment correlation coefficient ($R^2$) (Legates and McCabe, 1999), Nash-Sutcliffe efficiency (*NSE*) (Nash and Sutcliffe, 1970), index of agreement (*d*) (Willmott, 1981) and percent bias (*PBIAS*). The model performance in cotton lint yield prediction was assessed using the *PBIAS* only.

The $R^2$ represents the proportion of total variance in the observed data that can be explained by the model. The $R^2$ ranges from 0 to 1 with higher values denoting better

model performance. The *NSE* indicates how well the plot of observed vs. simulated values fits on the 1:1 line. It ranges from -∞ to 1, and the *NSE* values closer to 1 indicate the better model performance. The *d* varies from 0 (no correlation) to 1 (perfect fit), and it overcomes the insensitivity of $R^2$ and *NSE* to differences in the observed and simulated means and variances (Willmott, 1981). The *PBIAS* varies between -100 and ∞, with smaller absolute values closer to 0 indicating better agreement. In this study, we aimed to achieve *NSE*, $R^2$, *d* and *PBIAS* of > 0.6, > 0.65, > 0.9 and within ±15%, respectively, during the model calibration and validation periods.

### *2.3.7 Water Use Efficiency*

The Water Use Efficiency (WUE; kg $ha^{-1}$ $mm^{-1}$) of both dryland and irrigated bioenergy crops was estimated and compared over the model simulation period. The WUE of the dryland systems was estimated as (Musick et al., 1994; Howell, 2001):

$$WUE = \frac{B_d}{ET} \quad (2a)$$

where $B_d$ is the biomass yield (kg $ha^{-1}$ $year^{-1}$) under dryland systems, and ET is the evapotranspiration (mm $year^{-1}$).

The WUE of irrigated systems (IWUE; kg $ha^{-1}$ $mm^{-1}$) was estimated using the following relationship:

$$IWUE = \frac{B_i - B_d}{I} \quad (2b)$$

where $B_i$ is the biomass yield (kg $ha^{-1}$ $year^{-1}$) under irrigated systems, and I is the amount of irrigation water application in millimeter per year (Bos, 1980).

### *2.3.8 Scenario Analysis*

For the scenario analysis, four promising cellulosic bioenergy crops, switchgrass, *Miscanthus*, big bluestem and biomass sorghum were selected to hypothetically replace cotton. The impacts of these land use changes on water balances over the period from 1994 to 2009 were evaluated. The impacts were assessed both at the watershed scale and only among the HRUs where cotton was grown under baseline condition (hereafter referred as "baseline cotton HRUs"). In addition, the land use change impacts under both irrigated and dryland systems were compared and contrasted.

In the scenario analysis, perennial grasses were planted on May 15, 1992 and harvested on November 15$^{th}$ of each year in order to maximize biomass potential (Griffith et al., 2014; Hudiburg et al., 2015). The annual biomass sorghum was planted on June 1$^{st}$ and harvested on October 31$^{st}$ of each year (Hao et al., 2014) (Table 2.3). In the baseline cotton HRUs where irrigated cotton was simulated, cellulosic bioenergy crops were also assigned the same irrigation management practices as cotton. For switchgrass and big bluestem, about 270 and 180 kg ha$^{-1}$ of urea was applied on irrigated and dryland systems, respectively (Yimam et al., 2014). About 320 and 214 kg ha$^{-1}$ of urea was applied under irrigated and dryland *Miscanthus* scenarios, respectively (Lewandowski and Schmidt, 2006; Danalatos et al., 2007). Approximately 360 and 240 kg ha$^{-1}$ of urea was applied on irrigated and dryland biomass sorghum, respectively (Yimam et al., 2014; Hao et al., 2014) (Table 2.3).

**Table 2.3 Simulated management practices for cellulosic bioenergy crops in SWAT**

| No. | Operations | Description | Input data |
|---|---|---|---|
| Irrigated switchgrass and big bluestem (Yimam et al., 2014) | | | |
| 1 | Fertilizer Application Parameters (May 1) | | |
| | FERT_ID | Fertilizer ID | Urea |
| | FRT_KG | Amount of fertilizer applied to HRU | 270 (kg $ha^{-1}$) |
| 2 | Begin Growing Season Parameters ( Planting on May 15) | | Default |
| 3 | Auto-irrigation Parameters (Start date: May 15; End date: November 15) | | |
| | WSTRS_ID | Water stress identifier | Plant Water Demand |
| | IRR_SCA | Irrigation source | Shallow Aquifer |
| | AUTO_WSTRS | Water stress threshold | 0.9 |
| 4 | Harvest (only) Parameters (Harvest on November 15) | | Default |
| Dryland switchgrass and big bluestem (Yimam et al., 2014) | | | |
| 1 | Fertilizer Application Parameters (May 1) | | |
| | FERT_ID | Fertilizer ID | Urea |
| | FRT_KG | Amount of fertilizer applied to HRU | 180 (kg $ha^{-1}$) |
| 2 | Begin Growing Season Parameters (Planting on May 15) | | Default |
| 3 | Harvest (only) Parameters (Harvest on November 15) | | Default |
| Irrigated *Miscanthus* (Lewandowski and Schmidt, 2006; Danalatos et al., 2007) | | | |
| 1 | Fertilizer Application Parameters (May 1) | | |
| | FERT_ID | Fertilizer ID | Urea |
| | FRT_KG | Amount of fertilizer applied to HRU | 320 (kg $ha^{-1}$) |
| 2 | Begin Growing Season Parameters ( Planting on May 15) | | Default |
| 3 | Auto-irrigation Parameters (Start date: May 15; End date: November 15) | | |
| | WSTRS_ID | Water stress identifier | Plant Water Demand |
| | IRR_SCA | Irrigation source | Shallow Aquifer |
| | AUTO_WSTRS | Water stress threshold | 0.9 |
| 4 | Harvest (only) Parameters (Harvest on November 15) | | Default |
| Dryland *Miscanthus* (Lewandowski and Schmidt, 2006; Danalatos et al., 2007) | | | |
| 1 | Fertilizer Application Parameters (May 1) | | |
| | FERT_ID | Fertilizer ID | Urea |
| | FRT_KG | Amount of fertilizer applied to HRU | 214 (kg $ha^{-1}$) |
| 2 | Begin Growing Season Parameters (Planting on May 15) | | Default |
| 3 | Harvest (only) Parameters (Harvest on November 15) | | Default |
| Irrigated biomass sorghum (Yimam et al., 2014; Hao et al., 2014) | | | |
| 1 | Fertilizer Application Parameters (May 15) | | |
| | FERT_ID | Fertilizer ID | Urea |
| | FRT_KG | Amount of fertilizer applied to HRU | 360 (kg $ha^{-1}$) |
| 2 | Begin Growing Season Parameters ( Planting on Jun 1) | | Default |
| 3 | Auto-irrigation Parameters (Start date: Jun 1; End date: October 31) | | |
| | WSTRS_ID | Water stress identifier | Plant Water Demand |
| | IRR_SCA | Irrigation source | Shallow Aquifer |
| | AUTO_WSTRS | Water stress threshold | 0.9 |
| 4 | Harvest and Kill Parameters (Kill on October 31) | | Default |
| Dryland biomass sorghum (Yimam et al., 2014; Hao et al., 2014) | | | |
| 1 | Fertilizer Application Parameters (May 15) | | |
| | FERT_ID | Fertilizer ID | Urea |
| | FRT_KG | Amount of fertilizer applied to HRU | 240 (kg $ha^{-1}$) |
| 2 | Begin Growing Season Parameters (Planting on Jun 1) | | Default |
| 3 | Harvest and Kill Parameters (Kill on October 31) | | Default |

In all hypothetical land use change scenarios, tillage was not simulated. Heat units to maturity for cotton, winter wheat, and the cellulosic bioenergy crops were estimated by using the SWAT Potential Heat Unit (SWAT-PHU) program (http://swat.tamu.edu/software/potential-heat-unit-program/). The values of heat units to maturity of these crops are shown in Table 2.1 and Table 2.4.

*Miscanthus* is an emerging commercial bioenergy crop, and crop growth parameters for this crop are lacking in the SWAT crop database. We therefore adopted the *Miscanthus* growth parameters from Trybula et al. (2015) field study at the Purdue University Water Quality Field Station in northwestern Indiana. The harvest efficiency of *Miscanthus* was taken as 0.7 based on Trybula et al. (2015) study. The harvest efficiency of 0.75 reported by Trybula et al. (2015) for Shawnee switchgrass was used for Alamo switchgrass and big bluestem in this study. Based on the similarities in physiological characteristics of *Miscanthus* and switchgrass, *Miscanthus* was assigned the same Soil Conservation Service (SCS) runoff curve numbers as that of switchgrass (Love and Nejadhashemi, 2011; Trybula et al., 2015). The default curve number values for the selected bioenergy crops were modified by the same percentage as those for cotton crop (baseline) during the model calibration. The detailed crop growth parameters for the selected cellulosic bioenergy crops are included in Table 2.4.

**Table 2.4 Crop growth parameters for all the selected cellulosic bioenergy crops**

| Parameter | Acronym | Unit | *Miscanthus* × *giganteus** | Alamo switchgrass# | Big bluestem# | Biomass sorghum# |
|---|---|---|---|---|---|---|
| Biomass/energy ratio | BIO_E | (kg ha$^{-1}$)/(MJ m$^{-2}$) | 41 | 47 | 14 | 33.5 |
| Harvest index | HVSTI | (kg ha$^{-1}$)/(kg ha$^{-1}$) | 1 | 0.9 | 0.9 | 0.9 |
| Harvest efficiency | HE | NA | 0.70 | 0.75ξ | 0.75ξ | - - |
| Heat units to maturity | - - | ℃-day | 1800‡ | 1800‡ | 1800‡ | 1295‡ |
| Maximum leaf area index | BLAI | m$^2$/m$^2$ | 11 | 6 | 3 | 4 |
| Fraction of growing season coinciding with LAIMX1 | FRGRW1 | NA | 0.1 | 0.1 | 0.05 | 0.15 |
| First point fraction of BLAI for optimum growth curve | LAIMX1 | NA | 0.1 | 0.2 | 0.1 | 0.05 |
| Max. canopy height | CHTMX | m | 3.5 | 2.5 | 1 | 1.5 |
| Max root depth | RDMX | m | 3 | 2.2 | 2 | 2 |
| Fraction of growing season coinciding with LAIMX2 | FRGRW2 | NA | 0.45 | 0.2 | 0.25 | 0.5 |
| Second point fraction of BLAI for optimum growth curve | LAIMX2 | NA | 0.85 | 0.95 | 0.7 | 0.95 |
| Fraction of growing season when leaf area starts declining | DLAI | NA | 1.1 | 0.7 | 0.35 | 0.64 |
| Optimal temperature | T_OPT | °C | 25 | 25 | 25 | 30 |
| Min temperature | T_BASE | °C | 8 | 12 | 12 | 11 |
| Fraction of nitrogen in harvested biomass | CNYLD | (Kg N)/(Kg yield) | 0.0035 | 0.016 | 0.016 | 0.0199 |
| Fraction of phosphorus in harvested biomass | CPYLD | (Kg P)/(Kg yield) | 0.0003 | 0.0022 | 0.0022 | 0.0032 |
| Fraction of nitrogen in plant at emergence | BN1 | (Kg N)/(Kg biomass) | 0.01 | 0.035 | 0.02 | 0.044 |
| Fraction of nitrogen in plant at 0.5 maturity | BN2 | (Kg N)/(Kg biomass) | 0.0065 | 0.015 | 0.012 | 0.0164 |
| Fraction of nitrogen in plant at maturity | BN3 | (Kg N)/(Kg biomass) | 0.0057 | 0.0038 | 0.005 | 0.0128 |
| Fraction of phosphorus in plant at emergence | BP1 | (Kg P)/(Kg biomass) | 0.0016 | 0.0014 | 0.0014 | 0.006 |

**Table 2.4 Continued**

| Parameter | Acronym | Unit | *Miscanthus* × *giganteus** | Alamo switchgrass[#] | Big bluestem[#] | Biomass sorghum[#] |
|---|---|---|---|---|---|---|
| Fraction of phosphorus in plant at 0.5 maturity | BP2 | (Kg P)/(Kg biomass) | 0.0012 | 0.001 | 0.001 | 0.0022 |
| Fraction of phosphorus in plant at maturity | BP3 | (Kg P)/(Kg biomass) | 0.0009 | 0.0007 | 0.0007 | 0.0018 |
| Lower limit of harvest index | WSYF | (kg $ha^{-1}$)/(kg $ha^{-1}$) | 1 | 0.9 | 0.9 | 0.9 |
| Min crop factor for water erosion | USLE_C | NA | 0.003 | 0.003 | 0.003 | 0.2 |
| Max stomatal conductance | GSI | m/s | 0.005 | 0.005 | 0.005 | 0.005 |
| Vapor pressure deficit | VPDFR | kPa | 4 | 4 | 4 | 4 |
| GSI fraction corresponding to the second point on the stomatal conductance curve | FRGMAX | NA | 0.75 | 0.75 | 0.75 | 0.75 |
| Rate of decline in RUE due to increase in vapor pressure deficit | WAVP | NA | 8.5 | 8.5 | 10 | 8.5 |
| Biomass-energy ratio corresponding to the 2nd point on the radiation use efficiency curve | BIOEHI | NA | 54 (existing Alamo switchgrass value)** | 54 | 39 | 36 |
| Minimum LAI for plant during dormant period | ALAI_MIN | $m^2/m^2$ | 0 | 0 | 0 | 0 |
| Light extinction coefficient | EXT_COEF | NA | 0.55 | 0.33 | 0.36 | 0.65 |
| Root fraction at emergence | RFR1C | NA | 0.87 | 0.4 | 0.4 | 0.4 |
| Root fraction at maturity | RFR2C | NA | 0.18 | 0.2 | 0.2 | 0.2 |
| SCS runoff curve numbers | A, B, C, D | NA | 31, 59, 72, 79 (existing Alamo switchgrass value)** | 31, 59, 72, 79 | 31, 59, 72, 79 | 67, 77, 83, 87 |

* Crop parameters obtained from Trybula et al. (2015) field study

[#] The default values in the SWAT 2012 crop database or management files

**We used the existing Alamo switchgrass parameters for *Miscanthus* × *giganteus*

ξ We used the harvest efficiency value of Shawnee switchgrass obtained from Trybula et al. (2015) field study for the Alamo switchgrass and big bluestem

‡ Heat units to maturity for *Miscanthus* × *giganteus*, Alamo switchgrass, big bluestem, and biomass sorghum were estimated using the SWAT-PHU program (http://swat.tamu.edu/software/potential-heat-unit-program/)

## 2.4 Results

### *2.4.1 SWAT Calibration and Validation*

The simulated monthly streamflow at two USGS gauges during the calibration (1994-2001) and validation (2002-2009) periods closely matched with the observed streamflow (Figures 2.3 and 2.4). The *NSE*, $R^2$, *d* and *PBIAS* values for monthly predictions of streamflow at Gauge I were 0.78, 0.87, 0.95 and -6.3%, respectively and those at Gauge II were 0.66, 0.66, 0.88, and -4.1%, respectively during the model calibration period, demonstrating a "very good" to "good" agreement between the simulated and observed streamflow according to Moriasi et al. (2007) criteria (Table 2.5). The model performance in predicting streamflow during the validation period was also in the range of "good" (based on the *NSE* and *PBIAS* of 0.66 and 10.8% for Gauge II) to "satisfactory" (based on the *NSE* and *PBIAS* of 0.59 and -6.4% for Gauge I) according to Moriasi et al. (2007) criteria.

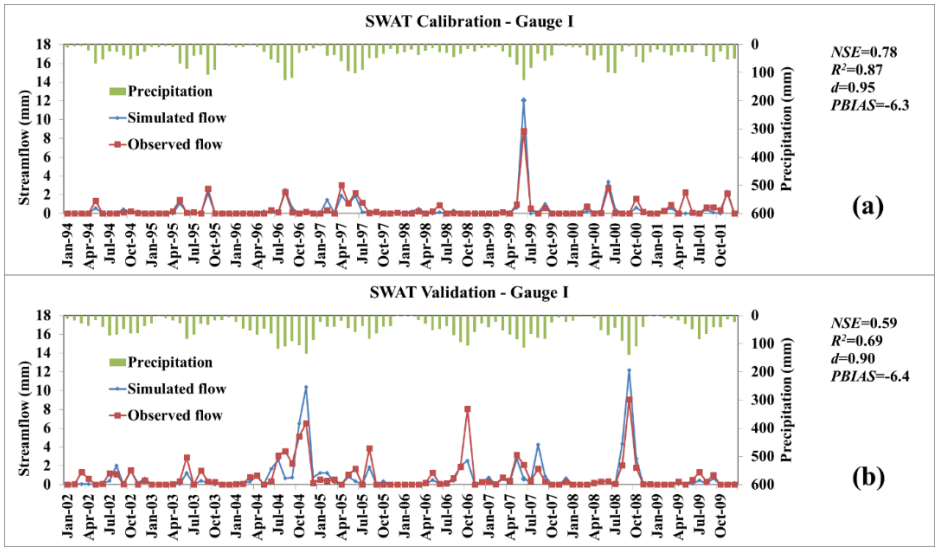


**Figure 2.3 Comparison of observed and simulated monthly streamflow at Gauge I during the model a) calibration and b) validation periods.**

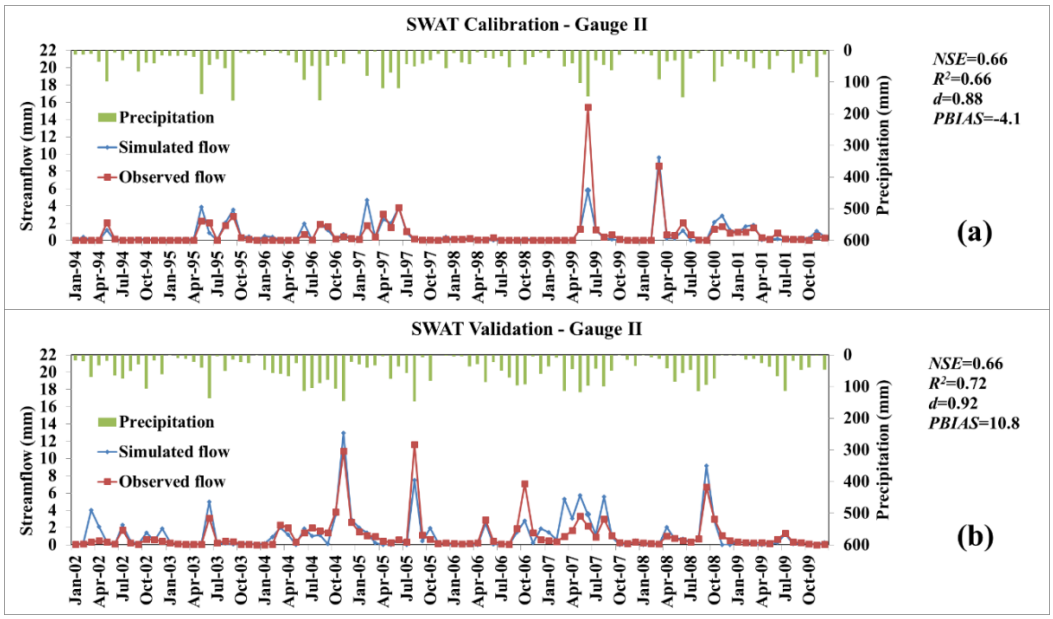


**Figure 2.4 Comparison of observed and simulated monthly streamflow at Gauge II during the model a) calibration and b) validation periods.**

**Table 2.5 Monthly statistical parameters for the model streamflow calibration and validation on two USGS gauges**

| Time scale | Gauge I | | Gauge II | |
|---|---|---|---|---|
| | Calibration (1994-2001) | Validation (2002-2009) | Calibration (1994-2001) | Validation (2002-2009) |
| Nash-Sutcliffe efficiency | 0.78 (Very good*) | 0.59 (Satisfactory) | 0.66 (Good) | 0.66 (Good) |
| $R^2$ | 0.87 | 0.69 | 0.66 | 0.72 |
| Index of agreement | 0.95 | 0.90 | 0.88 | 0.92 |
| Percent bias (%) | -6.3 (Very good) | -6.4 (Very good) | -4.1 (Very good) | 10.8 (Good) |

* General model performance ratings suggested by Moriasi et al. (2007) for monthly predictions of streamflow

Lower *NSE* value for the Gauge I during the validation period was mainly due to an over-prediction of streamflow in November 2004 and an under-prediction in October 2006 (Figure 2.3b). Accurate prediction of streamflow by the SWAT model during wet

(high rainfall) periods such as those in November 2004 in this study was particularly challenging due to the use of the SCS runoff curve number method, and this limitation of the model (Garen and Moore, 2005; White et al., 2009; Rathjens et al., 2014) might have caused the poor predictions in that month at Gauge I. The under prediction of streamflow in October 2006 at Gauge I was most probably due to differences in precipitation data input to the model and the actual precipitation that occurred within the catchment of Gauge I (Figure 2.3b). Although the precipitation recorded at three rain gauges within the area of influence of the Gauge I on October 15 and 16, 2006 was less than 30 mm, the observed streamflow on the above dates was 76 and 50 mm, respectively, indicating potential errors in precipitation input.

### *2.4.2 Cotton Lint Yield Comparison*

After calibrating for streamflow prediction, the SWAT model was calibrated for cotton lint yield prediction in the Lynn County. Results showed that the average *PBIAS* in predicting dryland cotton lint yield over the calibration and validation periods was -2.6% and 2.4%, respectively, and the *PBIAS* over the entire time period (1994-2009) was 0.4%, indicating a good match between the simulated and observed cotton lint yields (Table 2.6). In case of irrigated cotton, the average *PBIAS* in yield prediction was 12.7% and -14.5% during the calibration and validation periods, respectively, representing a satisfactory agreement between the simulated and observed cotton lint yields. However, the model hugely over-predicted cotton lint yield under irrigated systems in 1998, which was an extremely dry year (annual rainfall about 300 mm). The auto-irrigation option

used in this study, which did not consider actual availability of irrigation water in a dry year, led to this over-prediction of cotton lint yield under irrigated systems.

**Table 2.6 Comparison of cotton lint yield for Lynn County (Mg ha$^{-1}$)**

| Years | Simulated lint yield | Observed lint yield | *PBIAS* (%) |
|---|---|---|---|
| Dryland cotton | | | |
| 1994 | 0.27 | 0.25 | 8 |
| 1995 | 0.09 | 0.18 | -51 |
| 1996 | 0.32 | 0.39 | -20 |
| 1997 | 0.22 | 0.32 | -33 |
| 1998 | 0.37 | 0.37 | 1 |
| 1999 | 0.45 | 0.38 | 20 |
| 2000 | 0.36 | 0.23 | 58 |
| 2001 | 0.19 | 0.20 | -8 |
| Average for calibration period | 0.28 | 0.29 | -2.6 |
| 2002 | 0.28 | 0.27 | 5 |
| 2003 | 0.27 | 0.26 | 2 |
| 2004 | 0.47 | 0.58 | -18 |
| 2005 | 0.71 | 0.70 | 1 |
| 2006 | 0.57 | 0.33 | 75 |
| 2007 | 0.61 | 0.65 | -6 |
| 2008 | 0.24 | 0.31 | -22 |
| 2009 | 0.43 | 0.40 | 6 |
| Average for validation period | 0.45 | 0.44 | 2.4 |
| Overall (1994-2009) | 0.37 | 0.36 | 0.4 |
| Irrigated cotton | | | |
| 1994 | 0.72 | 0.71 | 2 |
| 1995 | 0.32 | 0.53 | -39 |
| 1996 | 0.56 | 0.62 | -9 |
| 1997 | 0.33 | 0.55 | -41 |
| 1998 | 1.37 | 0.64 | 115 |
| 1999 | 0.66 | 0.55 | 18 |
| 2000 | 0.69 | 0.50 | 40 |
| 2001 | 0.63 | 0.60 | 6 |
| Average for calibration period | 0.66 | 0.59 | 12.7 |
| 2002 | 0.77 | 0.74 | 3 |
| 2003 | 0.67 | 0.67 | 1 |
| 2004 | 0.80 | 0.88 | -8 |
| 2005 | 1.11 | 1.05 | 6 |
| 2006 | 1.30 | 0.92 | 42 |
| 2007 | 0.34 | 0.96 | -64 |
| 2008 | 0.52 | 0.88 | -41 |
| 2009 | 0.48 | 0.92 | -47 |
| Average for validation period | 0.75 | 0.88 | -14.5 |
| Overall (1994-2009) | 0.71 | 0.73 | -3.6 |

### *2.4.3 Simulated Water Balances under Baseline and Hypothetical Land Use Change Scenarios*

At the watershed scale, on an average (1994-2009), results showed that about 94% of the input water (precipitation + irrigation) was lost due to ET (Table 2.7a). The changes in ET with reference to the baseline cotton scenario were within ±3% under all hypothetical land use change scenarios. Under perennial grass scenarios, the average annual surface runoff and water yield decreased by about 6% to 8% and 3% to 4%, respectively, when compared to the baseline cotton scenario (Table 2.7a). However, when cotton was replaced by biomass sorghum, the average annual surface runoff and water yield increased by about 5% and 3%, respectively. Under the hypothetical perennial grass land use change scenarios, average annual percolation increased within a range of 3% to 22%, as compared to the baseline cotton scenario.

The monthly water balance analysis showed that the peak ET occurred in June or July under all land use change scenarios (Figure 2.5). The monthly surface runoff apparently decreased under perennial grass scenarios during high rainfall months (June, August and September) when compared to the baseline cotton and biomass sorghum scenarios (Figure 2.6). The reduction in surface runoff under perennial grass scenarios and the decrease in ET during August to October under cellulosic bioenergy crop scenarios as compared to the baseline cotton scenario resulted in a higher soil water content under cellulosic bioenergy crop scenarios from August to April (Figure 2.7).

**Table 2.7 Comparison of the average (1994-2009) annual water balance parameters under baseline and hypothetical land use change scenarios in the entire watershed and baseline cotton HRUs**

| Unit (mm) | Cotton | Switchgrass | *Miscanthus* | Big bluestem | Biomass sorghum |
|---|---|---|---|---|---|
| a) Entire watershed | | | | | |
| Precipitation | 520.1 | 520.1 | 520.1 | 520.1 | 520.1 |
| Irrigation | 25.7 | 26.5 (3.0*) | 34.0 (17.5) | 16.7 (-35.3) | 11.9 (-53.8) |
| Evapotranspiration | 515.7 | 516.4 (0.1) | 518.3 (0.5) | 507.1 (-1.7) | 501.0 (-2.9) |
| Surface runoff | 11.2 | 10.4 (-7.3) | 10.5 (-6.3) | 10.4 (-7.8) | 11.8 (4.9) |
| Percolation | 10.5 | 11.4 (8.7) | 12.8 (22.2) | 10.8 (2.8) | 10.6 (0.9) |
| Water yield | 21.1 | 20.3 (-3.6) | 20.5 (-2.6) | 20.2 (-4.0) | 21.6 (2.6) |
| b) Baseline cotton HRUs (irrigated and dryland combined) | | | | | |
| Precipitation | 497.2 | 497.2 | 497.2 | 497.2 | 497.2 |
| Irrigation | 82.9 | 85.4 (3.0) | 97.4 (17.5) | 53.6 (-35.3) | 38.2 (-53.8) |
| Evapotranspiration | 575.3 | 577.5 (0.4) | 583.7 (1.5) | 547.7 (-4.8) | 528.0 (-8.2) |
| Surface runoff | 3.0 | 0.4 (-88) | 0.7 (-77) | 0.20 (-93) | 4.8 (59) |
| Percolation | 0.003 | 2.9 | 7.5 | 1.0 | 0.30 |
| Water yield | 3.7 | 1.3 (-65) | 1.9 (-47) | 0.9 (-75) | 5.4 (48) |
| c) Baseline irrigated cotton HRUs | | | | | |
| Precipitation | 483.7 | 483.7 | 483.7 | 483.7 | 483.7 |
| Irrigation | 276.0 | 284.3 (3.0) | 324.3 (17.5) | 178.5 (-35.3) | 127.1 (-53.8) |
| Evapotranspiration | 754.0 | 759.9 (0.8) | 790.6 (4.9) | 658.2 (-12.7) | 602.2 (-20.1) |
| Surface runoff | 3.4 | 0.55 (-84) | 0.9 (-74) | 0.2 (-94) | 5.8 (70) |
| Percolation | 0.001 | 6.7 | 14.6 | 2.1 | 0.59 |
| Water yield | 4.6 | 2.2 (-52) | 3.1 (-32) | 1.4 (-70) | 6.8 (47) |
| d) Baseline dryland cotton HRUs | | | | | |
| Precipitation | 502.9 | 502.9 | 502.9 | 502.9 | 502.9 |
| Evapotranspiration | 498.5 | 499.1 (0.1) | 494.9 (-0.7) | 500.2 (0.3) | 496.1 (-0.5) |
| Surface runoff | 2.81 | 0.27 (-90) | 0.62 (-78) | 0.20 (-93) | 4.3 (54) |
| Percolation | 0.004 | 1.3 | 4.5 | 0.5 | 0.17 |
| Water yield | 3.3 | 0.9 (-74) | 1.4 (-57) | 0.7 (-78) | 4.8 (48) |

*The number in the parentheses is the percent change with each cellulosic bioenergy crop scenario relative to baseline cotton scenario

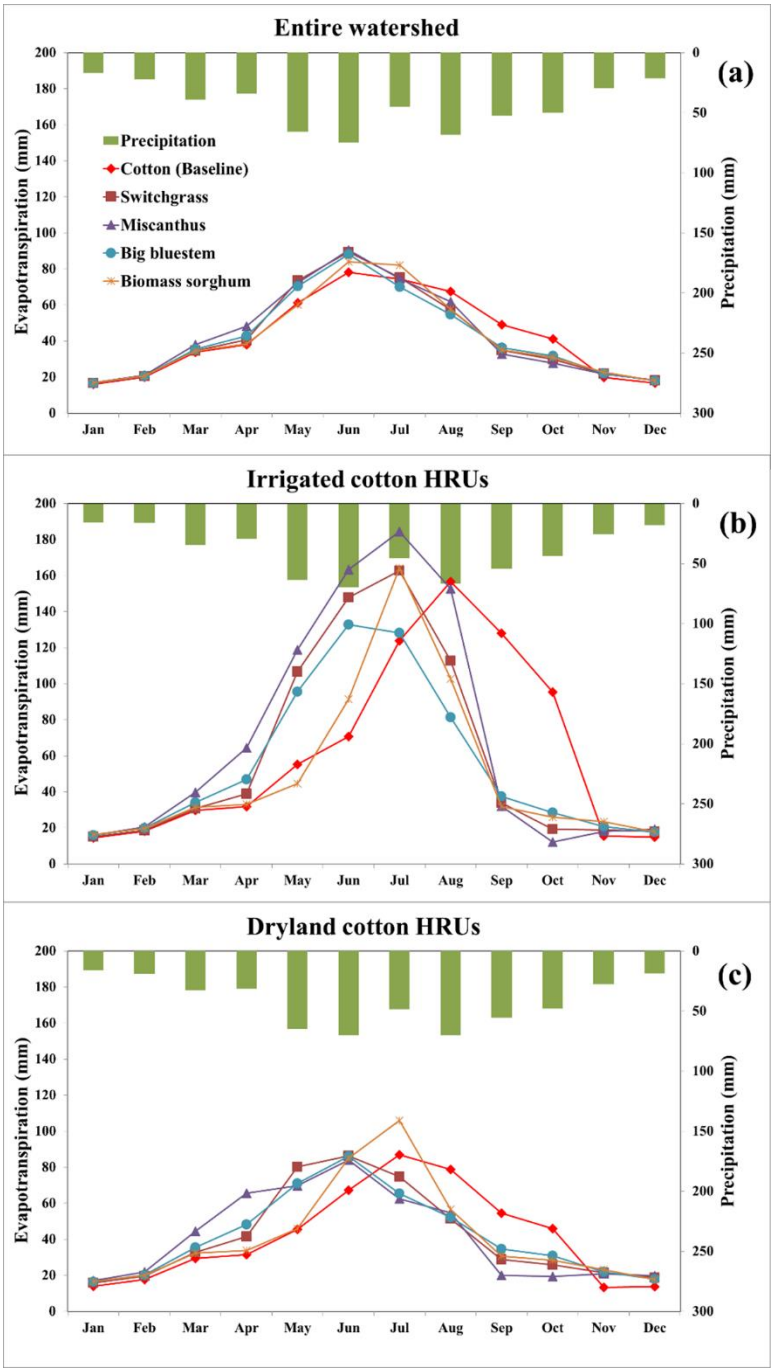


**Figure 2.5 Average (1994-2009) monthly variability of evapotranspiration under entire watershed and irrigated and dryland baseline cotton Hydrologic Response Units (HRUs).**

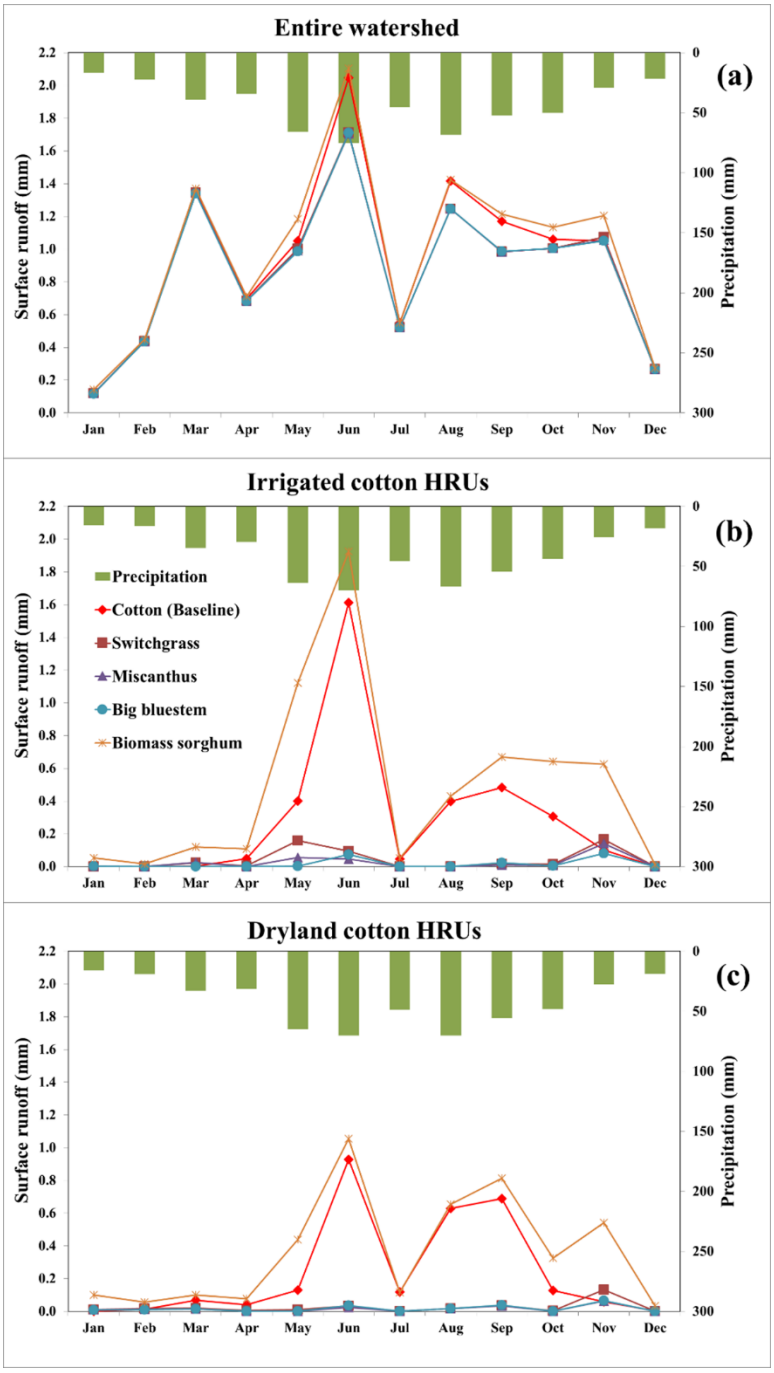


**Figure 2.6 Average (1994-2009) monthly variability of surface runoff under entire watershed and irrigated and dryland baseline cotton Hydrologic Response Units (HRUs).**

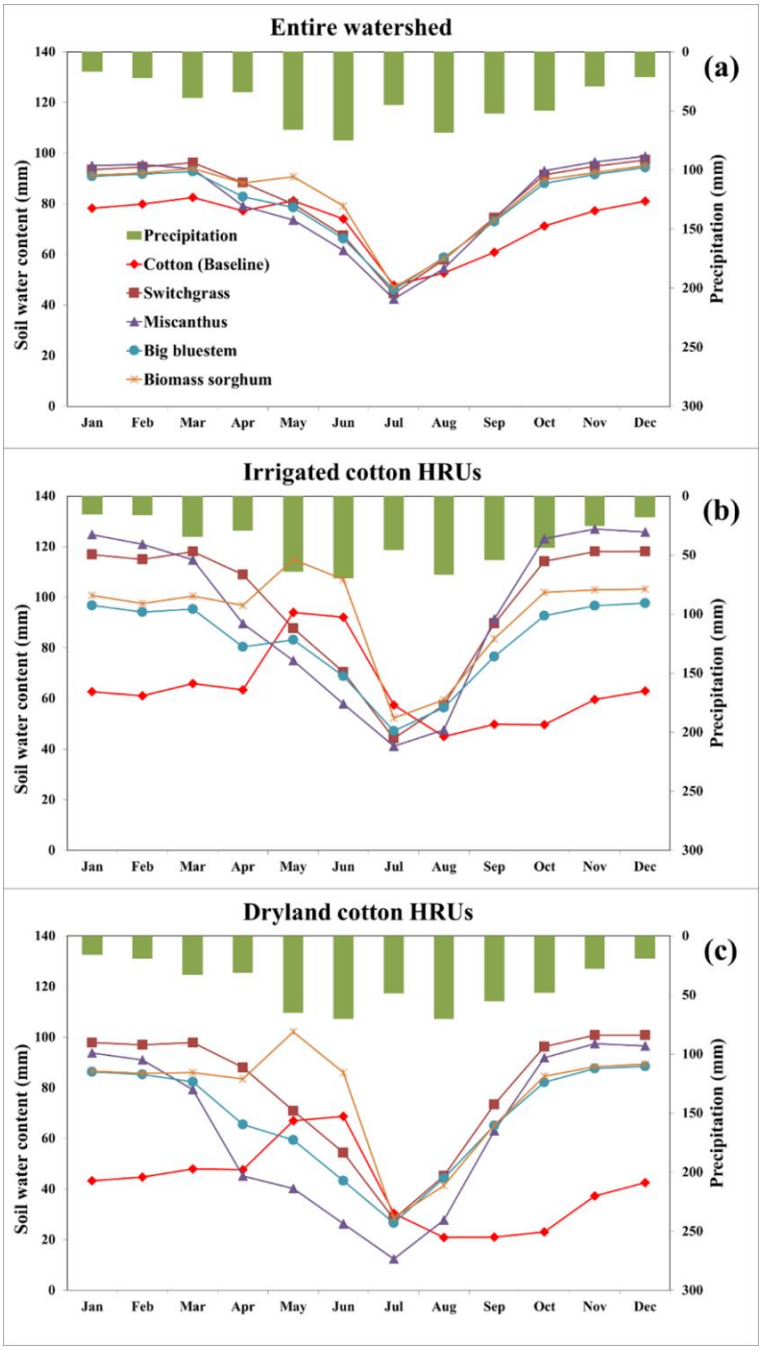


**Figure 2.7 Average (1994-2009) monthly variability of soil water content under entire watershed and irrigated and dryland baseline cotton Hydrologic Response Units (HRUs).**

Among the baseline cotton HRUs, the percent changes in all water balance parameters, except ET, under hypothetical land use change scenarios increased substantially (Table 2.7b). For example, average (1994-2009) annual surface runoff under perennial grass scenarios decreased within a range of 77% to 93% compared to the baseline cotton scenario. In the irrigated baseline cotton HRUs, auto-irrigation was used to optimally meet the crop water needs, which highlighted the differences in water requirements of the studied crops. Results showed that *Miscanthus* required the highest amount of irrigation water among all crops (Table 2.7c). However, the percent changes in water balances for the irrigated baseline cotton HRUs could be somewhat misleading as the amount of irrigation water applied for the simulated crops was not the same as that applied to cotton under the baseline scenario due to implementation of auto-irrigation (Table 2.7b, c).

The water balance assessments within the dryland baseline cotton HRUs (Table 2.7d) represented appropriate comparison of scenarios as precipitation, which was the same for all scenarios, was the only source of input water. The average (1994-2009) annual ET within the dryland baseline cotton HRUs was nearly the same under all scenarios (Table 2.7d). The average annual surface runoff was almost negligible under perennial grass scenarios, but it increased from 2.8 mm under the baseline cotton scenario to 4.3 mm under the biomass sorghum scenario (a 54% increase). When compared to the baseline cotton scenario, there is a considerable increase in average annual percolation and average monthly soil water content during August to April under different cellulosic bioenergy crop scenarios (Table 2.7d; Figure 2.7c). This is a very

important finding from this study in view of depleting groundwater levels in the Ogallala Aquifer. It is expected that most of the currently irrigated lands in the SHP could eventually be converted into drylands in the future, and replacing cotton with bioenergy crops under those circumstances could therefore not only improve soil water content, but also contribute to groundwater recharge.

The simulated emergence of perennial grasses in the study watershed began around April. This is in consistence with Yimam et al. (2015), who reported that the emergence of switchgrass occurred between mid-March and mid-April in a field experiment at Stillwater in Oklahoma. Vanloocke et al. (2010) also reported that perennial crops emergence in mid- to late April in the Midwest U.S., about a month earlier than most annual crops. Monthly water balance analysis in the dryland baseline cotton HRUs indicated that the peak ET occurred one month early under the perennial grass scenarios when compared to the baseline cotton and biomass sorghum scenarios (Figure 2.5c). The ET in irrigated baseline cotton HRUs during June to August was almost twice of that in the dryland baseline cotton HRUs (Figure 2.5b and c). There was a negligible generation of surface runoff under perennial grass scenarios (Figure 2.6b and c). The lowest soil water content under perennial grass scenarios was simulated one month earlier when compared to the baseline cotton scenario (Figure 2.7b and c). This was associated with the early occurrence of peak ET under perennial grass scenarios by one month relative to the baseline cotton scenario. Clearly, higher soil water storage was simulated in the irrigated baseline cotton HRUs during the whole year when compared to the dryland baseline cotton HRUs due to the application of irrigation water (Figure 2.7).

### *2.4.4 Biomass and Biofuel Production Potential and Water Use Efficiency*

The simulated average (1994-2009) annual harvestable biomass under *Miscanthus*, switchgrass, big bluestem and biomass sorghum scenarios was 19.1, 11.1, 3.2, and 8.8 Mg $ha^{-1}$, respectively, when both irrigated and dryland baseline cotton HRUs were combined (Table 2.8). It is worth noting that the simulated biomass production under the irrigated systems was higher by about 50% to 111% when compared to the dryland systems (Table 2.8). Based on current biofuel conversion efficiency of 282 liter ethanol $Mg^{-1}$ biomass (Lynd et al., 2008; Fargione et al., 2010), *Miscanthus* and switchgrass exhibited superior ethanol production potential compared to biomass sorghum and big bluestem under both irrigated and dryland systems (Table 2.8). The estimated average annual quantity of ethanol that could be produced with the simulated biomass of *Miscanthus,* switchgrass, big bluestem and biomass sorghum was 7,548, 4,931, 1,170 and 3,271 liter $ha^{-1}$, respectively, under the irrigated systems, and 4,398, 2,347, 778 and 2,143 liter $ha^{-1}$, respectively, under the dryland systems (Table 2.8). The simulated WUEs under the dryland *Miscanthus*, switchgrass, big bluestem, and biomass sorghum scenarios were 32, 17, 6, and 15 kg $ha^{-1}$ $mm^{-1}$, respectively (Table 2.8). The simulated IWUEs ranged from 8 to 36 kg $ha^{-1}$ $mm^{-1}$ with the highest IWUE simulated under *Miscanthus* scenario (36 kg $ha^{-1}$ $mm^{-1}$), followed by switchgrass scenario (32 kg $ha^{-1}$ $mm^{-1}$).

**Table 2.8 Average (1994-2009) annual biomass and biofuel production, and water use efficiency of switchgrass, *Miscanthus*, big bluestem and biomass sorghum under hypothetical land use change scenarios**

| Average value | Switchgrass | *Miscanthus* | Big bluestem | Biomass sorghum |
|---|---|---|---|---|
| Baseline cotton HRUs (irrigated and dryland combined) | | | | |
| Biomass production (Mg $ha^{-1}$) | 11.1 | 19.1 | 3.2 | 8.8 |
| Biofuel production* (liter ethanol $ha^{-1}$) | 3,123 | 5,374 | 896 | 2,482 |
| Baseline irrigated cotton HRUs | | | | |
| Biomass production (Mg $ha^{-1}$) | 17.5 | 27.1 | 4.2 | 11.6 |
| Biofuel production (liter ethanol $ha^{-1}$) | 4,931 | 7,548 | 1,170 | 3,271 |
| Irrigated water use efficiency (kg $ha^{-1}$ $mm^{-1}$) | 32.2 | 35.5 | 7.8 | 31.5 |
| Baseline dryland cotton HRUs | | | | |
| Biomass production (Mg $ha^{-1}$) | 8.3 | 15.6 | 2.8 | 7.6 |
| Biofuel production (liter ethanol $ha^{-1}$) | 2,347 | 4,398 | 778 | 2,143 |
| Water use efficiency (kg $ha^{-1}$ $mm^{-1}$) | 16.7 | 31.5 | 5.5 | 15.3 |

*Based on current biofuel conversion efficiency of 282 liter ethanol $Mg^{-1}$ biomass (Lynd et al., 2008; Fargione et al., 2010)

## 2.5 Discussion

### *2.5.1 Evaluation of SWAT Model Performance*

For the hydrologic model evaluations performed on a monthly time step, Moriasi et al. (2007) proposed that *NSE* values should exceed 0.5, 0.65 and 0.75, and *PBIAS* should be within ±25%, ±15% and ±10% in order for model performance to be judged as "satisfactory", "good" and "very good", respectively. According to this criteria, the model performance in this study was between "very good" and "good" during the calibration period and was between "satisfactory" and "good" during the validation period (Table 2.5). Harmel et al. (2014) recommended considering the model's intended use while evaluating the model performance. Since this study mainly focused on

assessing the influence of land use change on watershed hydrology on a monthly or annual basis, achieving good model performance on a monthly time step was considered as acceptable to use the calibrated SWAT model for scenario analysis. Comparison of the predicted cotton lint yields with the NASS-reported county-wise yields within the study watershed under both dryland and irrigated systems indicated that they both matched well (Table 2.6), and this additional evaluation further enhanced confidence in the calibrated model.

In this study, high inter-annual variability in *PBIAS* in cotton lint yield prediction existed in some years (Table 2.6). The long-term observed cotton lint yields used in this study were available at the county level (NASS). However, the SWAT model simulated cotton lint yields at the subbasin/HRU level, and hence simulated yields might not have spatially represented the observed county-wise yields very well. Also, the SWAT model was setup with 2008 NASS-CDL land use in this study and it was assumed that the cotton planting area was the same during the whole simulation period. The crop growth algorithm of the SWAT model is also not capable of taking into account the genetic improvements of crops in the long-term predictions. In addition, the use of auto-irrigation option provided more timely and adequate water for cotton growth, but in reality, water limiting conditions might have existed for cotton production in the study watershed. For example, the year 1998 was a very dry year with an annual precipitation of 300 mm, and hence observed cotton lint yield was about 0.64 Mg $ha^{-1}$. However, because of auto-irrigation and non-water-limiting conditions, more irrigation water was applied in that year, which has resulted in a very high simulated yield of 1.37 Mg $ha^{-1}$,

and a huge *PBIAS* of 115%. Several of the aforementioned reasons might have led to high inter-annual variability in *PBIAS* in this study.

### *2.5.2 Hydrological Responses of Hypothetical Land Use Change Scenarios*

An important factor for environmental evaluation of land use change is the assessment of associated hydrological responses. In this study, changes in hydrological fluxes of ET, surface runoff, soil water content, percolation and water yield under various hypothetical land use change scenarios were studied. The dominant component of the water balance in the study watershed is the water lost through ET, which accounted for about 94% of the input water (precipitation + irrigation). This is comparable with the ET losses from biomass sorghum production systems in the Texas High Plains reported in Hao et al. (2014), which stated that more than 90% of the growing season precipitation was lost as growing season ET. The crop available water in this semi-arid study watershed is very limited because of low annual precipitation (520 mm). In general, crop ET under the irrigated systems was higher than that under the dryland systems because of the much higher annual potential ET of 1700 mm (as estimated by the SWAT model) than the highest total input water in this region (e.g. 808 mm under irrigated *Miscanthus* scenario). For example, the ET of *Miscanthus* under the irrigated systems was higher by about 60% when compared to *Miscanthus* under the dryland systems (Table 2.7c, d). *Miscanthus* requires more irrigation water than cotton (16-year average irrigation amount of 324 mm (*Miscanthus*) vs. 276 mm (cotton)). Higher water requirement and larger biomass production potential of *Miscanthus*

(Heaton et al., 2004) explained the apparent increase in ET under the irrigated *Miscanthus* scenario when compared to the irrigated baseline cotton scenario (Table 2.7c). However, the irrigation water requirement of switchgrass, big bluestem and biomass sorghum were similar to or less than that of cotton (baseline scenario) (Table 2.7c). Therefore, there is a potential for maintaining or reducing groundwater withdrawals from the Ogallala Aquifer when irrigated cotton is replaced by switchgrass, big bluestem and biomass sorghum.

Assessment of water balances among the dryland baseline cotton HRUs represents a more appropriate comparison of scenarios as it eliminates differential amounts of irrigation water simulated for the studied crops due to implementation of auto-irrigation. Within the dryland baseline cotton HRUs, crop ET values of all simulated bioenergy crops were almost the same as that of cotton, and it accounted for about 98% of annual rainfall (Table 2.7; Figure 2.5c). The surface runoff and water yield were apparently reduced within a range of 78% to 93% and 57% to 78%, respectively, under perennial grass scenarios compared to the baseline cotton scenario (Table 2.7d). More importantly, the peak surface runoff in high rainfall months of May, June, August and September decreased by a huge proportion under the perennial grasses scenarios (Figure 2.6). In contrast, the surface runoff and water yield increased by about 54% and 48%, respectively, under the biomass sorghum scenario when compared to the baseline cotton scenario (Table 2.7d). The higher biomass density and lower surface runoff potential (average calibrated curve number of 54.4) of the perennial grasses as compared to cotton (average calibrated curve number of 71.0) contributed to the reduction in

surface runoff and water yield. Le et al. (2011) also found that land use change from maize to *Miscanthus* and switchgrass decreased the surface runoff by 24 and 6 mm, respectively, in the Midwestern United States. In the case of biomass sorghum scenario, shorter growing period and lesser ground cover after harvest compared to cotton contributed to higher surface runoff (16-year average surface runoff of 4.3 mm (biomass sorghum) vs. 2.8 mm (cotton), a 54% increase) and water yield (16-year average water yield of 4.8 mm (biomass sorghum) vs. 3.3 mm (cotton), a 48% increase).

Results have also showed that the average annual percolation increased considerably under the perennial grass land use change scenarios relative to the baseline cotton scenario (Table 2.7d). The monthly soil water content was higher under perennial grass scenarios compared to the baseline cotton scenario during August to April (Figure 2.7c). Reduction in surface runoff was the dominant factor responsible for the increase in soil water content and percolation under perennial grass scenarios. However, the simulated monthly soil water content under the dryland *Miscanthus* scenarios was lesser than that under the dryland baseline cotton scenario during the period from May to July (Figure 2.7c). Some published studies from the Midwest U.S. have also reported reductions in soil water content under *Miscanthus* due to the higher simulated ET when compared to corn (VanLoocke et al., 2010; Le et al., 2011).

### *2.5.3 Biomass Production Potential of Selected Cellulosic Bioenergy Crops*

The simulated average (1994-2009) annual biomass yield was the highest (27.1 Mg $ha^{-1}$) under the irrigated *Miscanthus* scenario, followed by the irrigated switchgrass

scenario (17.5 Mg $ha^{-1}$) (Figure 2.8; Table 2.8). The simulated *Miscanthus* biomass yields from this study (27.1 and 15.6 Mg $ha^{-1}$ under the irrigated and dryland systems, respectively; Table 2.8) were within the range of reported yields in the literature (5 to 44 Mg $ha^{-1}$) (Lewandowski et al., 2000; Powelson et al., 2005; Kindred et al., 2008). More specifically, the predicted average annual *Miscanthus* biomass yield under the dryland systems in this study was also within the range of reported *Miscanthus* biomass yield (9.8 to 17.8 Mg $ha^{-1}$) in the dryland production systems in United Kingdom (U.K.) (Christian, 2008). In addition, the simulated *Miscanthus* biomass yield under the irrigated systems was consistent with the irrigated *Miscanthus* biomass yield reported from the field experiments conducted in Portugal (26.9 Mg $ha^{-1}$; Clifton-Brown et al., 2001) and Italy (27.1 Mg $ha^{-1}$; Cosentino et al., 2007).

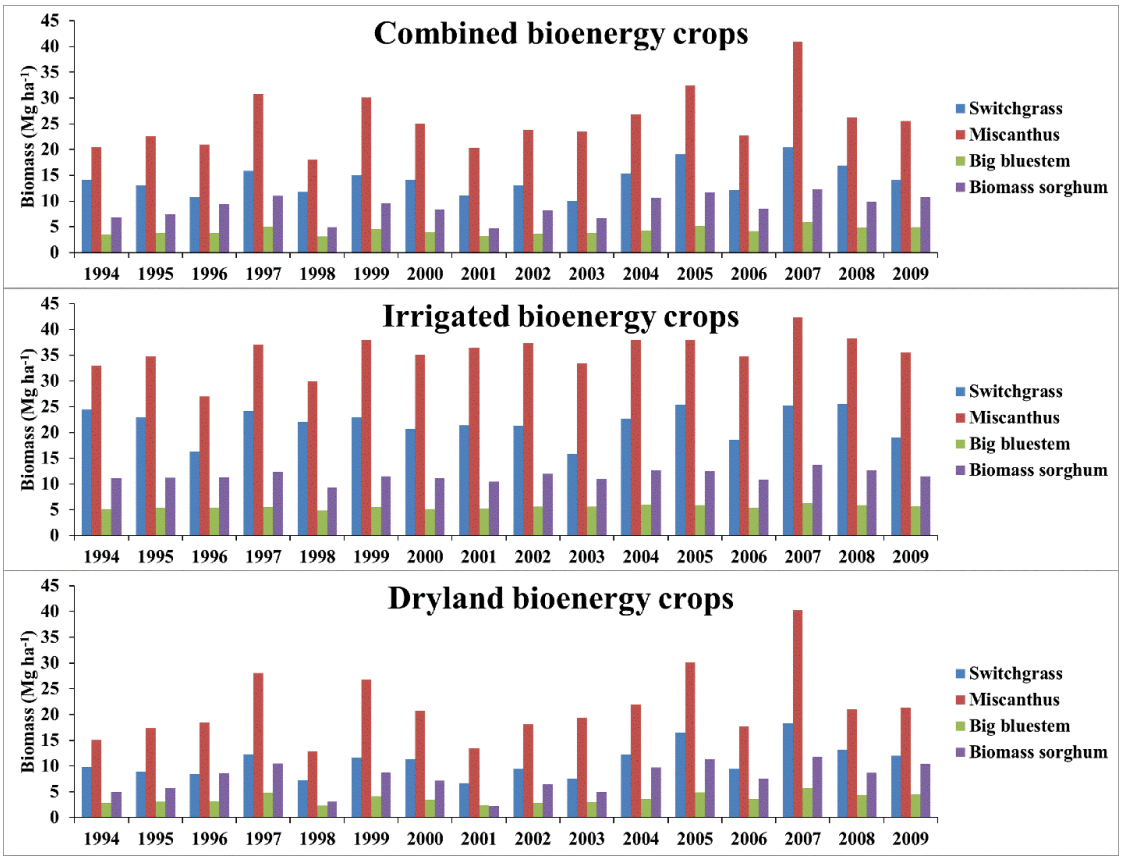


**Figure 2.8 Simulated average (1994-2009) annual biomass production from switchgrass, *Miscanthus*, big bluestem and biomass sorghum in combined, irrigated, and dryland baseline cotton Hydrologic Response Units (HRUs).**

The predicted switchgrass biomass yields in this study were 17.5 and 8.3 Mg ha$^{-1}$ under the irrigated and dryland systems, respectively. The simulated dryland switchgrass biomass yield in this study was within the range of measured biomass yields of 8.1 to 16.5 Mg ha$^{-1}$ reported by McLaughlin and Adams (2005) for Dallas, College Station, and Stephenville in Texas during the period from 1995 to 2000. The differences in dryland switchgrass biomass yield between this study and that of McLaughlin and Adams (2005) were most probably be due to the differences in average annual

precipitation. The study watershed receives much smaller annual precipitation compared to Dallas, College Station, and Stephenville. Ocumpaugh et al. (1998) reported that a single mid-season irrigation event may double switchgrass yields in dry years in Texas. The results from the McLaughlin and Adams (2005) study also suggested that switchgrass yields could increase substantially in arid areas by low frequency irrigation.

Among the simulated bioenergy crops, biomass sorghum generated more surface runoff than others (Table 2.7). In addition, biomass sorghum requires more management efforts for replanting it every year, and for meeting additional transportation and harvesting requirements (Turhollow et al., 2010). On the other hand, biomass production potential of big bluestem was much lower compared to that of *Miscanthus* and switchgrass (Figure 2.8; Table 2.8). It was interesting to note that the simulated biomass yield under dryland *Miscanthus* was nearly the same as that of irrigated switchgrass. In addition, *Miscanthus* showed the highest WUE among all rainfed land use change scenarios. This indicated that *Miscanthus* is a good bioenergy crop choice for large areas of dryland crop production systems in the study region. On the other hand, switchgrass recorded the second highest IWUE under the irrigated land use change scenarios. Furthermore, irrigated switchgrass demonstrated greater potential for effective water conservation when compared to the irrigated *Miscanthus*. Due to higher WUE/IWUE, better potential for water conservation, greater biomass and biofuel production potential, and minimum crop management, *Miscanthus* and switchgrass were therefore found to be ideal bioenergy crops for the dryland and irrigated systems in the study watershed, respectively.

# 3. SPATIAL VARIABILITY OF BIOFUEL PRODUCTION POTENTIAL AND HYDROLOGIC FLUXES OF LAND USE CHANGE FROM COTTON (*GOSSYPIUM HIRSUTUM* L.) TO ALAMO SWITCHGRASS (*PANICUM VIRGATUM* L.) IN THE TEXAS HIGH PLAINS*

## 3.1 Synopsis

Bioenergy crop production has the potential to protect marginal crop lands that generate high surface runoff and produce poor crop yields. Long term evaluation of the impacts of such land use change on hydrologic fluxes and biofuel production potential is necessary before adopting such strategies on a large-scale. In this study, the hydrologic impacts of replacing cotton (*Gossypium hirsutum* L.) on marginal lands in an intensive agricultural watershed in the Texas High Plains with Alamo switchgrass (*Panicum virgatum* L.) as a bioenergy crop were evaluated using the Agricultural Policy/Environmental eXtender (APEX) model. The surface runoff to cotton yield ratio was used as a criterion to identify marginal cotton subareas (homogenous spatial units delineated by APEX) in the study watershed, and three replacement scenarios (low (9%), medium (33%) and high (57%) extents of cotton acreage replaced by switchgrass) were implemented in the scenario analysis. The average (1994-2009) annual surface runoff decreased by about 84% and 66%, and the percolation increased by 106% and 57% in the irrigated and dryland subareas, respectively, when cotton was replaced by

* The following material in this section is used with permission from Springer. It has been published as a peer-reviewed research paper in the journal of *BioEnergy Research*. 2016, doi: 10.1007/s12155-016-9758-7

switchgrass under the high replacement scenario. Spatial analysis showed that switchgrass was a feasible bioenergy crop for replacing cotton, especially in the western part of the study watershed, due to its higher water use efficiency and better water conservation effects compared to cotton. It is estimated that 193 and 381 million liters of ethanol could be produced from the dryland and irrigated subareas of the study watershed, respectively under the high replacement scenario.

## 3.2 Introduction

Concerns about the projections of reduced fossil fuel availability, energy security, and global warming have led to an increased interest in expanding renewable bioenergy production. In the United States, bioenergy crops have been promoted to fulfill the mandated 2022 national biofuel target of 79 million $m^3$ (Energy Independence and Security Act; EISA, 2007). However, there are growing concerns for food security if the first generation bioenergy crops (grain-based crops) such as corn (*Zea mays* L.), wheat (*Triticum aestivum* L.) and grain sorghum (*Sorghum bicolor L.*) are used for bioenergy production (Ayre, 2007; Tenenbaum, 2008). In addition, the existing limited arable land and water resources present another constraint for grain-based bioenergy crop production. More attention, therefore, has been given to using marginal lands for the production of second generation cellulosic bioenergy crops such as Alamo switchgrass (*Panicum virgatum* L.) (Hill et al., 2006; Campbell et al., 2008; Searchinger et al., 2008; Qin et al., 2011; Qin et al., 2015). A number of studies have used a variety of definitions for identifying marginal lands. For example, Cai et al. (2011) defined marginal lands as

lands that are susceptible to degradation and have low crop productivity. The lands having severe to very severe limitations for production of crops were considered as marginal lands by Graham (1994). In this study, we considered lands with low crop yield potential and high surface runoff risk as marginal lands.

Historically, cotton (*Gossypium hirsutum* L.) has been produced in large acreage in the Texas High Plains (THP). In this region, groundwater from the Ogallala Aquifer is the major source of irrigation water. However, groundwater levels in this region have been experiencing a continuous decline due to intensive agricultural activities, and much less recharge compared to groundwater withdrawals (Chaudhuri and Ale, 2014a; Rajan et al., 2015b). Using the Hydrologic Unit Model for the United States (HUMUS), Rosenberg et al. (1999) predicted a further reduction in the recharge to the Ogallala Aquifer under future climate change scenarios because of the increase in evapotranspiration (ET) due to elevated temperatures. Such trends will further reduce groundwater availability in this region. Recently, Modala et al. (2016) also predicted an apparent increase in daily temperature (1.9 to 3.2 ºC) and decrease in precipitation (30 to 127 mm) in the future in the Texas High Plains and Rolling Plains regions, indicating that the groundwater availability could be reduced substantially.

Reductions in groundwater availability for irrigation and the demand for bioenergy production from this region (USDA, 2010) are expected to result in a shift in land use from high-water-demanding cotton to high water use efficient perennial bioenergy crops such as Alamo switchgrass (Kiniry et al., 2008; Kiniry et al., 2013; Chen et al., 2016a). Alamo switchgrass was originally collected from the north bank of

the Frio River in Live Oak County in Texas (Behrman et al., 2014). Alamo switchgrass (lowland cultivar) exhibited higher radiation and water use efficiency than Kanlow (lowland cultivar) and other upland switchgrass varieties such as Blackwell, Cave-in-Rock and Shawnee in the Southern Great Plains (Kiniry et al., 2012; Kiniry et al., 2013). Measured Alamo switchgrass yields in Texas were much higher than those in Arkansas, Oklahoma and Missouri (Behrman et al., 2014). Based on an economic and greenhouse gas efficiency analysis, Wang et al. (2014b) also concluded that dryland switchgrass is superior to other feedstocks such as irrigated or dryland sweet sorghum and mesquite (*Prosopis glandulosa*). Using the SWAT model, Chen et al. (2016a) simulated that the surface runoff was higher by 7% and percolation was less by 9% under current cotton land use when compared to the switchgrass scenario in the Double Mountain Fork Brazos watershed in the Texas High Plains. The ET was almost the same under both cotton and switchgrass scenarios, however. Alamo switchgrass was therefore selected to replace cotton in this study. An assessment of potential impacts of such hypothetical land use change from cotton to switchgrass on hydrologic fluxes and biofuel production potential would enable better understanding of relative advantages and disadvantages of proposed land use change in the THP.

A majority of the studies that evaluated switchgrass biomass production potential and corresponding hydrological responses in the U.S. focused on corn producing regions of the Midwest (Sarkar and Miller, 2014). For example, using the Soil and Water Assessment Tool (SWAT), Schilling et al. (2008) predicted that a land cover change from cropland to switchgrass in the Raccoon River watershed in west-central Iowa would

increase ET by about 9% and decrease water yield by about 28%. Using the APEX model, Feng et al. (2015) found a significant ($p$<0.05) decrease in water yield (27%) when corn/soybean was replaced by switchgrass from the marginal lands of the St. Joseph River watershed in Indiana. In another APEX simulation study, Powers et al. (2011) predicted that a land use change from corn to switchgrass reduced total nitrogen load by about 65% in eastern Iowa. Wu and Liu (2012) concluded from a SWAT modeling study in the Iowa River Basin that switchgrass was a more promising bioenergy crop in dry areas than corn and *Miscanthus* based on its less water requirement, fertilizer use, and nitrate nitrogen ($NO_3$-N) load. Recently, Chen et al. (2016a) also used the SWAT model in a biofuel-induced land use change study, and assessed the impacts of replacing the entire cotton acreage in the Double Mountain Fork Brazos watershed of the THP (about 30% of the watershed area) with switchgrass and three other cellulosic bioenergy crops on hydrologic processes. However, to our knowledge, none of the previous studies focused on assessing biofuel production potential and the associated hydrologic impacts of replacing cotton in marginal lands with switchgrass.

The Agricultural Policy Environmental eXtender (APEX), which includes detailed cotton growth parameters, was used in this study. The APEX model has a separate crop database for cotton. It provides cotton seed and lint yields separately. The APEX model also allows the users to adjust plant population, and specify disease/pest infestation severity, wind erosion of plant residue, etc. In addition, APEX satisfactorily simulates the impacts of land use change and best management practices (BMPs) on

watershed hydrology and crop yields in intensively managed agricultural watersheds with large extents of irrigated areas (Saleh and Gallego, 2007; Ko et al., 2009; Gassman et al., 2010; Tuppad et al., 2010; Powers et al., 2011; Wang et al., 2011; Jung et al., 2014; Wang et al., 2014a). For example, Powers et al. (2011) used APEX in a watershed study in eastern Iowa and found that the land use change from continuous corn to switchgrass would yield much higher biomass and provide water quality benefits such as reduced total nitrogen and total phosphorus loads. Ko et al. (2009) achieved a good agreement between the simulated and measured irrigated cotton and maize yields in South Texas by using EPIC, a field-scale version of APEX.

The overall goal of this study was to evaluate effects of biofuel-induced land use change from cotton to switchgrass on water balances in the upstream subwatershed of the Double Mountain Fork Brazos watershed in the THP under three replacement scenarios: low, medium and high extents of cotton acreage replaced by switchgrass. Specific objectives were to: (1) identify marginal cotton growing subareas in the watershed for potential replacement with switchgrass; (2) estimate the biofuel production potential, and land and irrigation water requirement for biomass production under the proposed switchgrass replacement scenarios; and (3) compare spatial variability in water use efficiency and hydrologic fluxes of ET, surface runoff, percolation and soil water content in both irrigated and dryland subareas under the baseline cotton and hypothetical switchgrass replacement scenarios.

## 3.3 Materials and Methods

### *3.3.1 Study Watershed*

The upstream subwatershed of the Double Mountain Fork Brazos watershed, which spans over the Cochran, Hockley, Lynn, Garza and Borden counties in the THP, was selected for this study (Figure 3.1). The delineated watershed area is about 3297 $km^2$. The surface elevation of the watershed ranges from 679 to 1152 m. Cotton is the major crop in this watershed, grown on 52% of the land area. The predominant soil types in the watershed are Amarillo sandy loam and Acuff sandy clay loam (Soil Survey Staff, 2010). The long term (1981-2010) daily average air temperature in the region ranged from 9°C in the winter to 24°C in the summer, with an average annual precipitation of 508 mm (NOAA-NCDC, 2014).

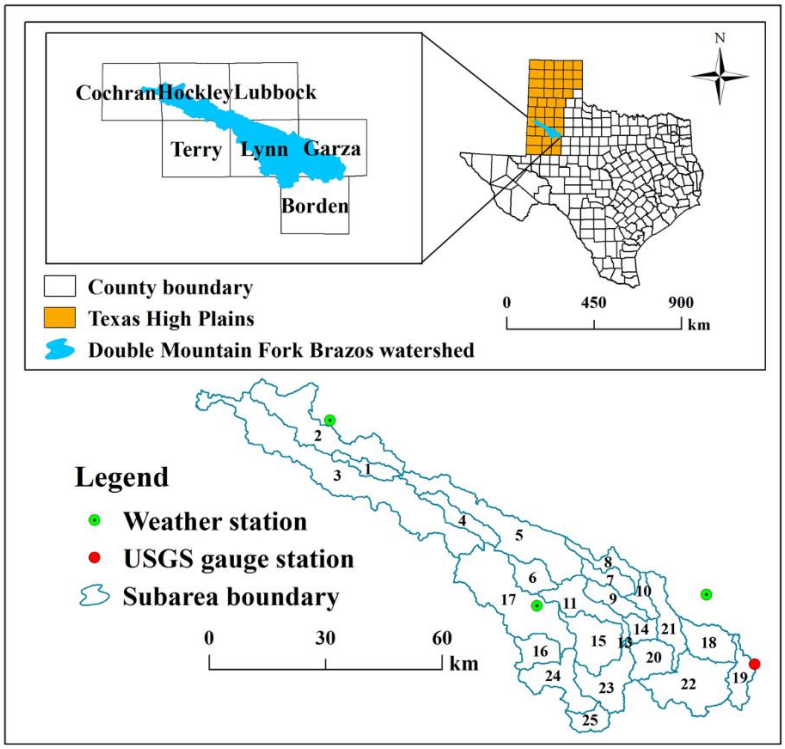


**Figure 3.1 Locations of weather stations and the USGS gauge station in the Double Mountain Fork Brazos watershed in the Texas High Plains.**

### *3.3.2 APEX Model*

The APEX model is a flexible and dynamic tool that is capable of simulating land management and land use change impacts on hydrology and water quality of whole farms and small watersheds (Williams 1995; Williams et al., 2008). The model consists of 12 major components: climate, hydrology, crop growth, pesticide fate, nutrient cycling, erosion-sedimentation, carbon cycling, management practices, soil temperature, plant environment control, economic budgets, and subarea/routing (Golmohammadi et al., 2014). More details about the APEX model components can be found in Williams (1995), Tuppad et al. (2009) and Wang et al. (2012). The ArcAPEX model (Version 0806.10_2.1 Beta4 released on 12/19/14), which is interfaced with the ArcGIS 10.2.2 platform, was used in this study.

APEX delineates a watershed into a number of subareas, which are the basic building blocks of the model. Three options are available for defining a subarea in APEX: (1) the dominant land use, dominant soil and dominant slope for each of the three landscape characteristics; (2) the dominant land use/soil/slope combination, which represents the most dominant unique combination of the three landscape characteristics; and (3) user defined, which allows the users to define each subarea separately by using either option (1) or option (2). The option (1) was used in this study. A threshold area of 5000 ha, which was calculated from the digital elevation model (DEM) of the watershed, was used for defining flow direction and accumulation. This criterion has resulted in 25 subareas.

In APEX, surface runoff can be computed by using the modified USDA Natural Resources Conservation Service (NRCS) runoff curve number (RCN) technique (Williams, 1995; USDA-NRCS, 2004) or the Green and Ampt infiltration equation (Green and Ampt, 1911). The former method was used in this study. The peak runoff rate is estimated in the APEX model for each storm event, and it is used for calculating erosion loss. The peak runoff rate can be estimated by either using the modified Rational Formula (Williams, 1995) or the USDA-NRCS Technical Release 55 (TR-55) method (USDA-NRCS, 1986). The latter method was used in this study. Five methods are provided in APEX for estimating potential ET. They are Hargreaves (Hargreaves and Samani, 1985), Penman (Penman, 1948), Priestley-Taylor (Priestley and Taylor, 1972), Penman-Monteith (Monteith, 1965) and Baier-Robertson (Baier and Robertson, 1965) methods. The "Penman-Monteith" method was used in this study.

The crop growth module in the APEX model is based on the EPIC model (Williams et al., 1989). About 100 crop growth related parameters have been included the APEX model. The APEX model is capable of simulating growth of both annual (e.g. cotton) and perennial (e.g. Alamo switchgrass) crops. Annual crops grow from planting to harvest or until the accumulated heat units of the crops equal their potential heat units. Perennial crops maintain their root systems during the entire year, even though they become dormant after frost. They start to regrow when the mean daily air temperature exceeds their minimum needed temperature. More detailed descriptions of the APEX model concepts and methodology are given in Williams and Izaurralde (2006) and Gassman et al. (2010).

*3.3.3 APEX Model Setup*

### 3.3.3.1 Topography, Land Use, Soil, and Slope

The DEM of the watershed, with a horizontal resolution of 30 m, was downloaded from the USGS (http://viewer.nationalmap.gov/viewer/#) and input to the APEX model. The 2008 National Agricultural Statistics Service (NASS) Cropland Data layer (CDL) was used as a land use input to the model to appropriately represent the land use conditions in the watershed over the simulated period from 1994 to 2009. The dominant agricultural land use in the study watershed in 2008 was cotton, which occupied 52% of the watershed area (Figure 3.2). Thirty nine percent of the watershed area was covered by range brush and range grass. The finer-scale soils data from the Soil Survey Geographic Database (SSURGO) was used in this study (Soil Survey Staff, 2015). Based on studies by Mednick (2010) and Zhang et al. (2014), the higher resolution soil data provides greater accuracy in predicting hydrologic fluxes. In order to accurately simulate runoff potential, four slope classes were considered in this study: ≤ 1%, 1%-3%, 3%-5%, and > 5%.

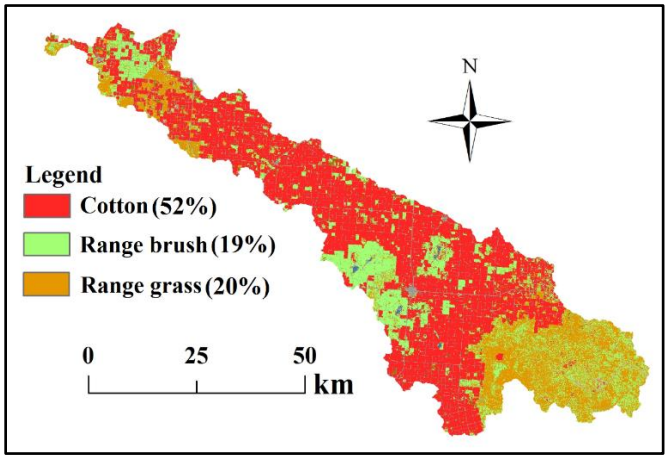


**Figure 3.2 Major land uses of the study watershed in 2008 (Source: National Agricultural Statistics Service (NASS) Cropland Data layer).**

#### 3.3.3.2 Weather Data Input

Weather data from three National Climatic Data Center (NCDC) weather stations that are situated inside or within a close distance to the study watershed were used in this study (Figure 3.1). Daily weather data including rainfall, and minimum and maximum temperature for the period from 1992 to 2009 (NOAA-NCDC, 2014) was used. Missing rainfall and temperature data for a weather station was filled with the average value of weather parameter from two adjacent weather stations (Ale et al., 2009).

#### 3.3.3.3 Operation Schedules of Cotton

Cotton operation schedules were set as practiced in the study area. The operation schedules for range brush and grass were kept at their default values. Chisel plow, which is widely used for tillage operation in this watershed, was used in all cotton growing subareas (Table 3.1). About 300 and 150 kg $ha^{-1}$ of urea was applied to the irrigated and dryland cotton, respectively. The commonly used center pivot irrigation method was selected to apply irrigation water to cotton. According to the published county-wise cotton acreage estimates over the period of 1994 to 2009, 39% of the cotton growing areas in the watershed were under irrigation. In this study, automatic irrigation was therefore implemented in 5 out of 25 subareas in such a way that a total of 39% of simulated cotton growing areas were irrigated.

**Table 3.1 Simulated management practices for dryland and irrigated cotton in APEX**

| No. | Operations | Description | Input data |
|---|---|---|---|
| Irrigated cotton | | | |
| 1 | Plow, cultivate, other (Tillage on April 1) | | |
| | JX4 | Tillage ID | Chisel plow[#] |
| 2 | Fertilize (May 1) | | |
| | JX7 | Fertilizer ID | Urea (46-00-00) |
| | OPV1 | Fertilizer application rate | 300.7 (kg $ha^{-1}$)[#] |
| 3 | Plant in rows ( Planting on May 15) | | Default |
| 4* | Irrigate (automatic irrigation) (Start date: May 15; End date: October 31) | | |
| | IRR | Irrigation Code | Sprinkler irrigation |
| | BIR | Plant water stress factor to trigger automatic irrigation | 0.9 |
| 5 | Harvest without kill (Harvest on October 31) | | Default |
| 6 | Kill crop (Kill on October 31) | | Default |
| Dryland cotton | | | |
| 1 | Plow, cultivate, other (Tillage on April 1) | | |
| | JX4 | Tillage ID | Chisel plow[#] |
| 2 | Fertilizer Application Parameters (May 1) | | |
| | JX7 | Fertilizer ID | Urea(46-00-00) |
| | OPV1 | Fertilizer application rate | 150 (kg $ha^{-1}$)[#] |
| 3 | Plant in rows (Planting on May 15) | | Default |
| 4 | Harvest without kill (Harvest on October 31) | | Default |
| 5 | Kill crop (Kill on October 31) | | Default |

*Auto-irrigation was simulated in 39% of cotton acreage based on County cotton irrigated acreage summary reports

[#]The parameter values related to management practices were based on local expertise

### *3.3.4 Observed Streamflow and Cotton Lint Yield Data*

The observed daily streamflow data recorded at the USGS gauge 08079600, which was delineated as the watershed outlet, over the time period from 1994 to 2009 were obtained from the USGS National Water Information System (http://waterdata.usgs.gov/nwis/sw). The observed cotton lint yield data for the period from 1994 to 2009 from dryland and irrigated areas in the Lynn County, in which the highest cotton planting acreage was documented in the study watershed, was obtained from the NASS reports (http://www.nass.usda.gov/Quick_Stats/). The simulated data was compared with this observed data during the APEX model calibration for the study watershed.

### *3.3.5 APEX Calibration and Validation*

APEX was run for 1992 to 2009. The first two years were considered as the model warm-up period (Daggupati et al., 2015). The periods from 1994 to 2001 and 2002 to 2009 were considered as the model calibration and validation periods, respectively. Four sensitive hydrologic parameters including "CN retention parameter coefficient", "runoff CN initial abstraction", "soil evaporation coefficient", and "evaporation plant cover factor" were adjusted during the APEX hydrology calibration (Table 3.2). Several recent studies emphasized using crop yield as auxiliary data for further improving model calibration as crop yield has a direct relationship with ET (Faramarzi et al., 2009; Akhavan et al., 2010; Faramarzi et al., 2010; Zhang et al., 2013; Chen et al., 2016a; Mittelstet et al., 2015; Zhang et al., 2015b). After achieving a satisfactory streamflow prediction, the model was calibrated for cotton lint yield prediction under irrigated and dryland conditions. Based on the literature values (Sarkar et al., 2011; Wanjura et al., 2014), crop parameters such as the harvest index (HI), maximum potential leaf area index (DMLA), and biomass-energy ratio (WA) of the crop database were adjusted while calibrating the model for cotton lint yield prediction (Table 3.2). Finally, after obtaining a satisfactory cotton lint yield calibration, the model performance was re-evaluated for streamflow prediction, and necessary finer adjustments to calibrated hydrologic parameters were made.

**Table 3.2 Initial and calibrated values of some major hydrologic and crop parameters in the APEX model**

| No. | Parameter | Description | Initial value | Calibrated value | Source |
|---|---|---|---|---|---|
| Hydrology calibration | | | | | |
| 1 | Parm92 | Curve number retention parameter coefficient | 1.0 | 1.31 | -- |
| 2 | Parm20 | Runoff curve number initial abstraction | 0.2 | 0.336 | -- |
| 3 | Parm12 | Soil evaporation coefficient | 2.5 | 2.44 | -- |
| 4 | Parm17 | Evaporation plant cover factor | 1.0 | 0.921 | -- |
| Cotton yield calibration | | | | | |
| 5 | WA | Biomass Energy Ratio ($CO_2$=330 ppm) | 25 | 15.48 (Dryland)<br>16.0 (Irrigated) | Sarkar et al. (2011) |
| 6 | HI | Harvest index | 0.6 | 0.49 (Dryland)<br>0.48 (Irrigated) | Wanjura et al. (2014) |
| 7 | DMLA | Maximum potential leaf area index | 6.0 | 4.0 | Sarkar et al. (2011) |

### *3.3.6 Model Performance Assessment*

APEX performance during the calibration and validation periods was evaluated using three statistical measures: i) square of Pearson's product- moment correlation coefficient ($R^2$) (Legates and McCabe Jr, 1999), ii) Nash-Sutcliffe efficiency (*NSE*) (Nash and Sutcliffe, 1970), and iii) percent bias (*PBIAS*). The $R^2$ indicates the proportion of total variance of the observed data that can be explained by the simulation result. The $R^2$ ranges from 0 to 1 with higher values representing better model performance. The *NSE* denotes how well the plot of observed versus simulated results matches with the 1:1 line. The *NSE* ranges from -∞ to 1, and the value of *NSE* closer to 1 indicates the better model performance. The *PBIAS* varies between -100 and ∞, with smaller absolute values closer to 0 demonstrating better agreement.

### *3.3.7 Water Use Efficiency*

Average annual (1994-2009) water use efficiency of switchgrass/cotton under the dryland conditions (DWUE; kg $ha^{-1}$ $mm^{-1}$) was determined as the ratio of dryland switchgrass/cotton biomass yield per unit area (kg $ha^{-1}$) to its ET (mm) (Musick et al., 1994; Howell, 2001). The average annual irrigated water use efficiency (IWUE; kg $ha^{-1}$ $mm^{-1}$) of switchgrass/cotton was calculated as the ratio of difference in irrigated and dryland switchgrass/cotton biomass (kg $ha^{-1}$) to the amount of irrigation water applied (mm) (Bos, 1980; Chen et al., 2016a). In this study, 90% of aboveground switchgrass biomass was considered as the biomass yield to calculate the DWUE and IWUE based on the suggested HI value of 0.90 by Kiniry et al. (1996). In order to maintain consistency, the same percentage of aboveground biomass was considered as biomass yield in estimation of cotton DWUE and IWUE.

### *3.3.8 Scenario Development and Analysis*

Scenarios simulated in this study focused on evaluating the hydrologic impacts of land use change from cotton to switchgrass in marginal lands of the watershed. Cotton lint yield production and surface runoff generation potential were considered as two major factors in identifying marginal croplands where switchgrass replacement scenarios could be implemented. The ratio of surface runoff to cotton lint yield was estimated for each of the cotton subareas of the watershed and then marginal subareas were identified. Interestingly, the runoff/yield ratio increased abruptly between two intervals, once between 11 and 88 $m^3$ $Mg^{-1}$ $yr^{-1}$, and then between 121 and 439 $m^3$ $Mg^{-1}$ $yr^{-1}$ (Figure

3.3). The cotton subareas with the runoff/yield ratios ≥ 88 $m^3$ $Mg^{-1}$ $yr^{-1}$ were considered as the marginal lands (subareas).

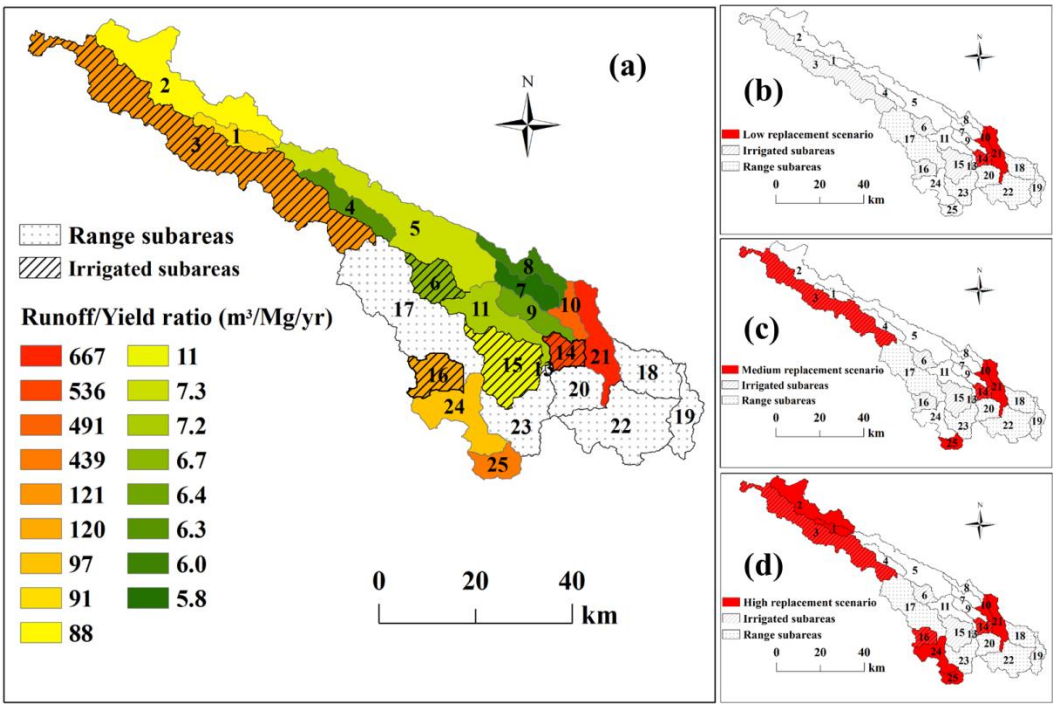


**Figure 3.3 a) Spatial distribution of surface runoff to cotton lint yield ratio in the study watershed, and (b-d) the switchgrass replacement scenarios simulated.**

After sorting the subareas according to runoff/yield ratio (from the highest to the lowest), three scenarios were considered to hypothetically replace cotton (baseline) with switchgrass. In the first scenario, which is denoted as the "low replacement scenario", three subareas with high runoff/yield ratio (10, 14, and 21), which constituted about 9% of cotton acreage in the watershed were considered for replacement by switchgrass (Figure 3.3). Interestingly, all these subareas are located in the eastern part of the watershed. In the second scenario, in addition to the above three subareas, two subareas (25 and 3) with next highest runoff/yield ratio were considered. The second scenario was

designated as the “medium replacement scenario” and the cotton acreage considered for replacement under this scenario represented 33% of the total cotton area in the watershed. In the third scenario, which was denoted as the “high replacement scenario”, 57% of cotton acreage was considered for replacement by switchgrass by including four additional subareas 1, 2, 16 and 24. This classification was made in such a way that at least one additional irrigated and one dryland subarea were added to each higher replacement scenario.

Switchgrass was planted on May 15 of 1992 and harvested (without kill) on November 15 of each subsequent year (Chen et al., 2016a). If cotton in the irrigated subareas was replaced by switchgrass, switchgrass was assigned the same irrigation management practices as cotton. About 270 and 180 kg $ha^{-1}$ of urea (N-P-K: 46-00-00) was applied on irrigated and dryland switchgrass, respectively (Yimam et al., 2014). “No tillage” practice was implemented under the hypothetical switchgrass replacement scenarios.

## 3.4 Results and Discussion

### *3.4.1 APEX Model Performance during Calibration and Validation*

#### 3.4.1.1 Prediction of Streamflow

The simulated monthly streamflow at the watershed outlet during the calibration and validation periods matched well with the observed streamflow (Figure 3.4). The *NSE*, $R^2$, and *PBIAS* for monthly predictions of streamflow during the model calibration and validation periods were 0.65 and 0.59, 0.76 and 0.69, and -1.8% and -14.4%,

respectively, representing a satisfactory agreement between the simulated and observed streamflow according to Wang et al. (2012) and Moriasi et al. (2007) criteria (Table 3.3). Harmel et al. (2014) emphasized that the project goal and the intended use of the calibrated model should be taken into account while deciding the time-step for evaluating the model performance. This study focused on assessing the impacts of proposed land use change on the seasonal and annual water balances. Hence obtaining a satisfactory model performance on a monthly time step was considered as making APEX acceptable to use for scenario analysis.

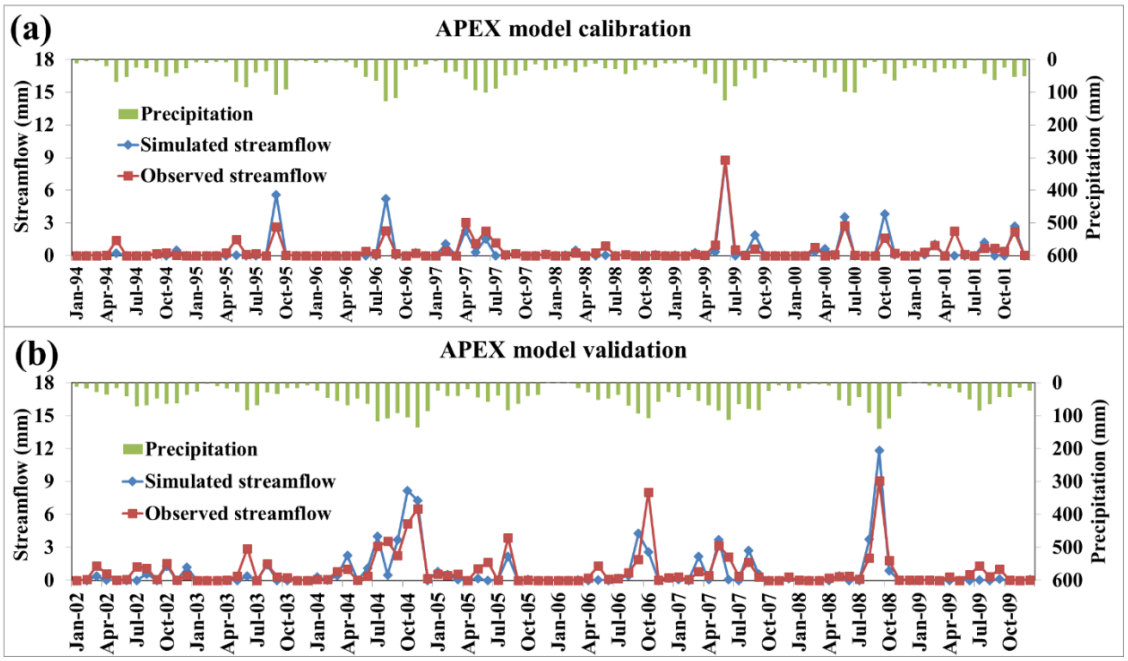


**Figure 3.4 Comparison of observed and simulated monthly streamflow at the watershed outlet during the model a) calibration and b) validation periods.**

**Table 3.3 Monthly statistical parameters for the model streamflow calibration and validation**

| Statistical parameters | Calibration (1994-2001) | Validation (2002-2009) |
|---|---|---|
| Nash-Sutcliffe efficiency (*NSE*) | 0.65 (Good*) | 0.59 (Satisfactory) |
| $R^2$ | 0.76 | 0.69 |
| Percent bias (*PBIAS*) (%) | -1.8 (Very good) | -14.4 (Good) |

* General model performance ratings suggested by Wang et al. (2012) and Moriasi et al. (2007) for predictions of streamflow

### 3.4.1.2 Prediction of Cotton Lint Yield

After obtaining a satisfactory model calibration for streamflow prediction, APEX was calibrated for cotton lint yield prediction under both irrigated and dryland subareas. This additional step enhanced our confidence on the partitioning of water between ET, soil water content and percolation (Faramarzi et al., 2009; Akhavan et al., 2010; Faramarzi et al., 2010). Results showed that the $R^2$ and average *PBIAS* in predicting cotton lint yield in the dryland cotton subareas over the entire simulation period (1994-2009) were 0.36 and 0.1%, respectively (Figure 3.5). For the irrigated cotton subareas, the $R^2$ and average *PBIAS* in cotton lint yield prediction were 0.14 and 0.7%, respectively.

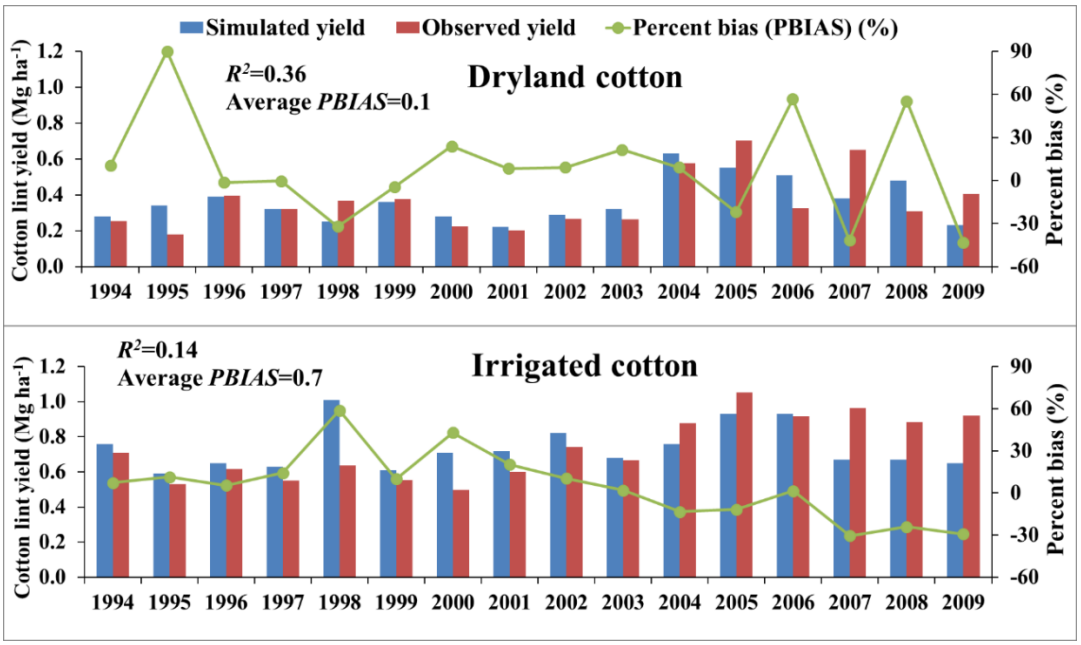


**Figure 3.5 Comparison of simulated and observed cotton lint yield in Lynn County under dryland and irrigated conditions.**

High bias between the simulated and observed cotton lint yield was found in some years (Figure 3.5). For example, the simulated cotton lint yield in the irrigated subareas in 1998, which was an extremely dry year (annual rainfall of 300 mm), was clearly overestimated (60%). The automatic irrigation option, which did not consider the actual water availability for crop irrigation under severe dry conditions, was used in this study. It led to an optimistic over-prediction of cotton lint yield in 1998. Another potential reason for this mismatch could be due to differences in the procedure used for estimation of simulated and observed yields. While the long-term measured cotton lint yields from NASS were available at the county level, the APEX model simulated cotton lint yields at the subarea level. The simulated yields might, therefore, have not adequately represented the measured county-level yields well. Using EPIC, Ko et al. (2009) also found that the simulated cotton lint yield matched well with the measured

yield from small field experiments ($R^2$=0.74 and *PBIAS*=-7.6%) in South Texas, but the agreement weakened when simulated cotton lint yield was compared with the NASS county-wide observed yield ($R^2$=0.05 and *PBIAS*=-2.0%). Overall, model predictions of cotton lint yield were better under dryland conditions than under irrigated conditions (Figure 3.5). Using SWAT, Mittelstet et al. (2015) similarly reported that the prediction accuracies of cotton lint yield under the dryland conditions were better than those under the irrigated conditions in the North Fork River Basin of the Southwestern Oklahoma and the Texas Panhandle.

### *3.4.2 Land Replacement, Biomass Production, Irrigation Water Use and Biofuel Production Potential under Three Switchgrass Replacement Scenarios*

Marginal cotton lands in the dryland subareas that were replaced by switchgrass under the low, medium and high replacement scenarios were 14800, 18100 and 64100 ha, respectively (Figure 3.6). Corresponding marginal cotton lands in the irrigated subareas that were replaced by switchgrass under the low, medium and high replacement scenarios were 4500, 55400 and 63100 ha, respectively. Among all switchgrass replacement scenarios studied, the highest average (1994-2009) annual total biomass production of 1042 million kg was simulated from the irrigated subareas of the watershed under the high replacement scenario, followed by the irrigated subareas under the medium replacement scenario (927 million kg) (Figure 3.6). Simulated average annual total switchgrass biomass yield in the dryland subareas varied within a range of 111 to 526 million kg among the three replacement scenarios (Figure 3.6).

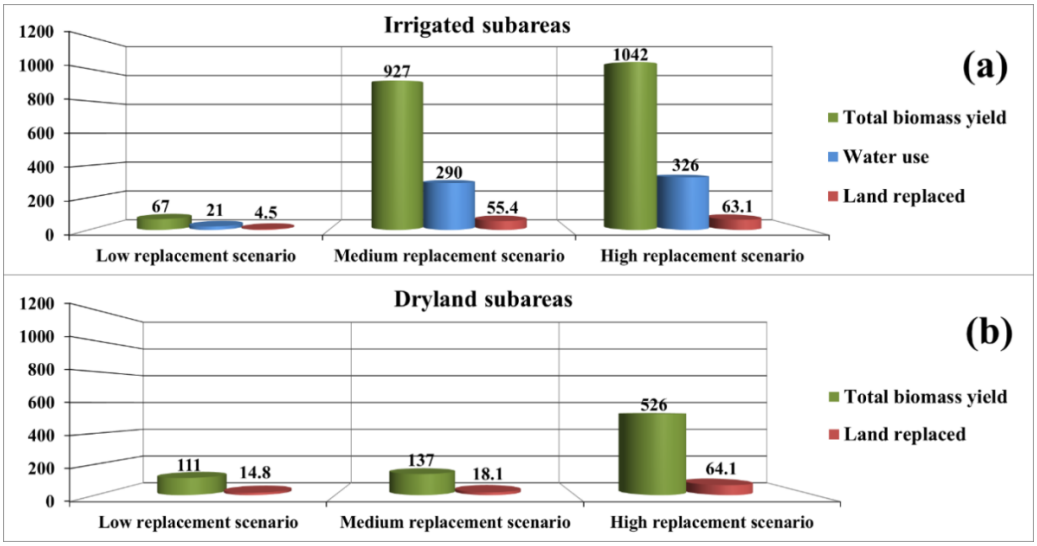


**Figure 3.6 Biomass production potential, land replaced and water use under three replacement scenarios. Units are million kg for biomass, million $m^3$ for irrigation water consumption and 1000 ha for land requirements.**

About 21, 290 and 327 million $m^3$ of irrigation water was used under the low, medium and high replacement scenarios, respectively (Figure 3.6). The estimated switchgrass biomass yield per unit area under irrigated medium and high replacement scenarios (17 and 16.5 Mg $ha^{-1}$, respectively) was slightly higher than that under the low replacement scenario (15 Mg $ha^{-1}$). A similar trend was found in case of dryland subareas (8.2, 7.7 and 7.7 Mg $ha^{-1}$ under the high, medium and low replacement scenarios, respectively). The estimated biomass yield per unit of water used was the highest (2013 Mg $mm^{-1}$) under the high replacement scenario and the lowest under the low replacement scenario (144 Mg $mm^{-1}$). Based on the theoretical ethanol yield of switchgrass biomass of 366 liters $Mg^{-1}$, the average annual volume of ethanol that could be produced from the irrigated subareas in the study watershed was estimated as 25, 339 and 381 million liters under the low, medium and high replacement scenarios, respectively. The estimated ethanol production from the dryland subareas of the

watershed was 41, 50 and 193 million liters under the low, medium and high replacement scenarios, respectively.

Spatial variability in cotton lint yield under baseline scenario, and switchgrass biomass yield and biofuel production potential under high replacement scenario are depicted in Figure 3.7. The predicted cotton lint yield under baseline scenario ranged from 0.31 to 0.44 Mg $ha^{-1}$ and from 0.77 to 1.02 Mg $ha^{-1}$ in the dryland and irrigated high replacement subareas, respectively (Figure 3.7a). The simulated switchgrass biomass yield under the high replacement scenario ranged from 7.1 to 9.1 Mg $ha^{-1}$ and from 14.7 to 16.9 Mg $ha^{-1}$ in the dryland and irrigated subareas, respectively (Figure 3.7b). APEX-predicted switchgrass biomass yields in this study were similar to those simulated by SWAT (17.5 and 8.3 Mg $ha^{-1}$ under the irrigated and dryland systems, respectively) for this watershed (Chen et al., 2016a). In addition, the predicted switchgrass biomass yields from dryland subareas in this study were comparable to measured switchgrass biomass yields reported in McLaughlin and Adams (2005) for Dallas, Stephenville and College Station in Texas, which ranged from 8.1 to 16.5 Mg $ha^{-1}$. Relatively lower dryland switchgrass biomass yields simulated in this study as compared to those reported in McLaughlin and Adams (2005) were most probably due to the lower average annual precipitation received in the study watershed when compared to Dallas, Stephenville and College Station. The estimated biofuel that could be produced with the simulated switchgrass biomass under the high replacement scenario ranged from 2602 to 3313 liters $ha^{-1}$ and from 5385 to 6194 liters $ha^{-1}$ in dryland and irrigated subareas, respectively (Figure 3.7c).

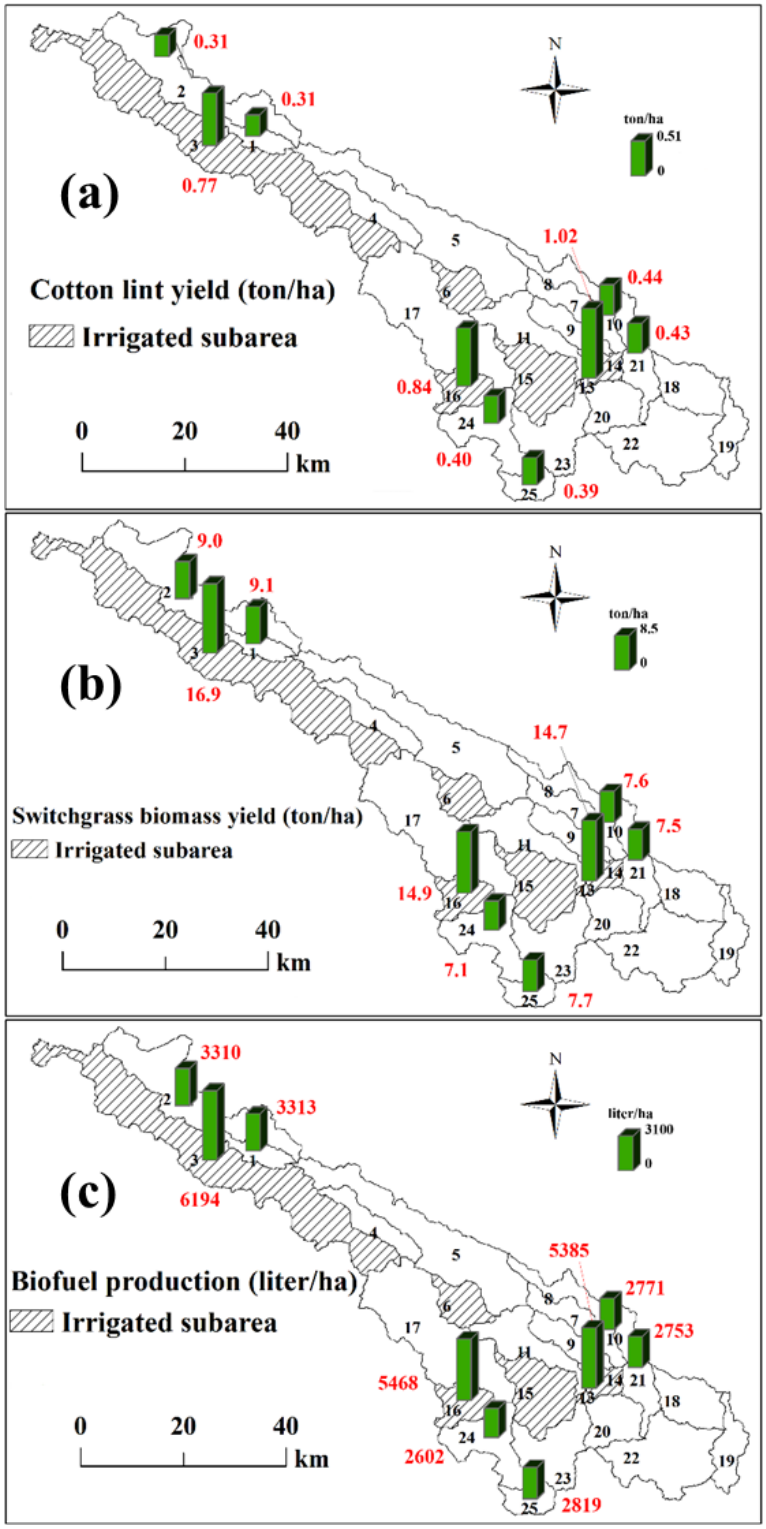


**Figure 3.7 The spatial distribution of cotton lint yield under baseline scenario, and switchgrass biomass yield and biofuel production potential in the study watershed under high replacement scenario.**

### *3.4.3 Hydrologic Fluxes under the Switchgrass Replacement Scenarios*

#### 3.4.3.1 Average Annual Hydrologic Fluxes

Changes in fluxes of ET, surface runoff, percolation, and soil water content were evaluated under the three hypothetical switchgrass replacement scenarios considered in this study. The dominant component of water balances in the study watershed is the water lost through ET. Scenario analysis results showed that for 1994-2009, 84% and 91% of the input water (precipitation + irrigation) was lost due to ET in the irrigated and dryland subareas, respectively, under the baseline scenario (Table 3.4). When compared to the baseline scenario, average annual ET decreased within ranges of 2%-3% and 1%-4% in the irrigated and dryland subareas, respectively, under the hypothetical replacement scenarios. The irrigation water requirement under the low replacement scenario was 2% lower than that under the baseline scenario (Table 3.4). In contrast, the irrigation water requirement under the medium and high replacement scenarios was 4% and 5% higher, respectively, when compared to the baseline scenario (Table 3.4).

**Table 3.4 Comparison of the average (1994-2009) annual water balance parameters under baseline and hypothetical land use change scenarios in the irrigated and dryland subareas**

| Scenario/Parameter | All cotton subareas (mm) | Irrigated cotton subareas (mm) | Dryland cotton subareas (mm) |
|---|---|---|---|
| Baseline scenario | | | |
| Rainfall | 490.4 | 481.2 | 496.3 |
| Irrigation | 185.9 | 479.5 | 0.0 |
| Evapotranspiration | 620.3 | 856.5 | 470.7 |
| Soil water content | 1163.7 | 1854.9 | 726.0 |
| Percolation | 49.1 | 95.0 | 20.0 |
| Surface runoff | 6.0 | 7.9 | 4.8 |
| Low replacement scenario [9%][#] | 10, 14, 21ξ | 14 | 10, 21 |
| Irrigation | 182.8 (-1.7)* | 471.4 (-1.7) | 0.0 |
| Evapotranspiration | 612.9 (-1.2) | 843.4 (-1.5) | 467.0 (-0.8) |
| Soil water content | 1208.6 (3.9) | 1897.7 (2.3) | 772.2 (6.4) |
| Percolation | 55.0 (12.0) | 101.9 (7.2) | 25.3 (26.4) |
| Surface runoff | 4.5 (-25.5) | 6.8 (-14.3) | 3.0 (-37.2) |
| Medium replacement scenario [33%] | 3, 10, 14, 21, 25 | 3, 14 | 10, 21, 25 |
| Irrigation | 192.7 (3.6) | 497.0 (3.6) | 0.0 |
| Evapotranspiration | 606.4 (-2.2) | 828.2 (-3.3) | 466.0 (-1.0) |
| Soil water content | 1317.3 (13.2) | 2156.6 (16.3) | 785.8 (8.2) |
| Percolation | 73.1 (49.0) | 146.7 (54.5) | 26.5 (32.5) |
| Surface runoff | 2.5 (-59.3) | 2.0 (-74.9) | 2.7 (-43.0) |
| High replacement scenario [57%] | 1, 2, 3, 10, 14, 16, 21, 24, 25 | 3, 14, 16 | 1, 2, 10, 21, 24, 25 |
| Irrigation | 195.8 (5.3) | 504.8 (5.3) | 0.0 |
| Evapotranspiration | 601.0 (-3.1) | 834.4 (-2.6) | 453.1 (-3.7) |
| Soil water content | 1393.5 (20.2) | 2134.0 (15.0) | 932.7 (28.5) |
| Percolation | 83.0 (69.1) | 149.1 (56.9) | 41.2 (105.9) |
| Surface runoff | 1.5 (-75.6) | 1.2 (-84.4) | 1.6 (-66.3) |

*Numbers in parentheses indicate the percent change under each scenario relative to baseline scenario

[#]Numbers in square bracket indicate the percent cotton area replaced by switchgrass

ξ These numbers represent the subarea identification numbers

Average annual surface runoff under the replacement scenarios decreased within the ranges of 14% to 84% and 37% to 66% in the irrigated and dryland subareas, respectively, when compared to the baseline scenarios (Table 3.4). Average annual

percolation in the irrigated subareas increased by 7%, 55% and 57% under the low, medium and high replacement scenarios, respectively, as compared to the baseline scenario. In the dryland subareas, average annual percolation increased by 26%, 33% and 106% under the low, medium and high replacement scenarios, respectively, relative to the baseline scenario (Table 3.4). The reduction in ET and surface runoff were key factors for the increased percolation under the switchgrass replacement scenarios. The higher percolation under switchgrass replacement scenarios when compared to cotton indicates the potential for higher groundwater recharge to the underlying Ogallala Aquifer, which is desirable under the current situation of rapidly declining groundwater levels in the THP (Chaudhuri and Ale, 2014a and 2014b). Soil water storage apparently increased under all switchgrass replacement scenarios. For example, under the high replacement scenario, average annual soil water content in irrigated and dryland subareas increased by 15% and 29%, respectively, when compared to the baseline scenario (Table 3.4). This simulated trend is different from other biofuel-induced land use change studies in the Midwest U.S. in which maize was replaced by switchgrass. They predicted reductions in soil water storage under switchgrass scenarios due to the higher simulated ET of switchgrass compared to maize (VanLoocke et al., 2010; Le et al., 2011). When compared to maize, cotton needs longer to mature (Agricultural Resources and Environmental Indicators, 1996-97) as it is a perennial shrub that is cultivated as an annual economic crop (Ton, 2004). Cotton, therefore, has a higher ET requirement compared to that of maize.

#### 3.4.3.2 Average Monthly and Seasonal Hydrological Fluxes

In general, hydrological fluxes did not change much on a monthly basis under the low replacement scenario when compared to the baseline scenario because only 9% of cotton area was replaced with switchgrass. Under the medium and high replacement scenarios, the peak ET in the irrigated subareas occurred about a month early when compared to the baseline scenario (Figure 3.8a). A similar trend was found under the high replacement scenario in the dryland subareas (Figure 3.8b). The main reason for this trend is because the simulated emergence of switchgrass began in late March/early April while cotton was planted in mid-May. Using the Integrated Biosphere Simulator - agricultural version (Agro-IBIS) model, Vanloocke et al. (2010) also predicted that the emergence of perennial crops occurred in mid- to late April in the Midwest U.S., about a month earlier than most annual crops. Yimam et al. (2015) also observed that the switchgrass emergence occurred between mid-March and mid-April in a field experiment at Stillwater in Oklahoma. About 85% and 94% of the average annual ET was simulated during the cotton (baseline) growing season from May to October in the dryland and irrigated subareas, respectively. During the same period, a slightly higher percent of the average annual ET (88% and 97% in the dryland and irrigated subareas, respectively) was simulated under the high replacement scenario.

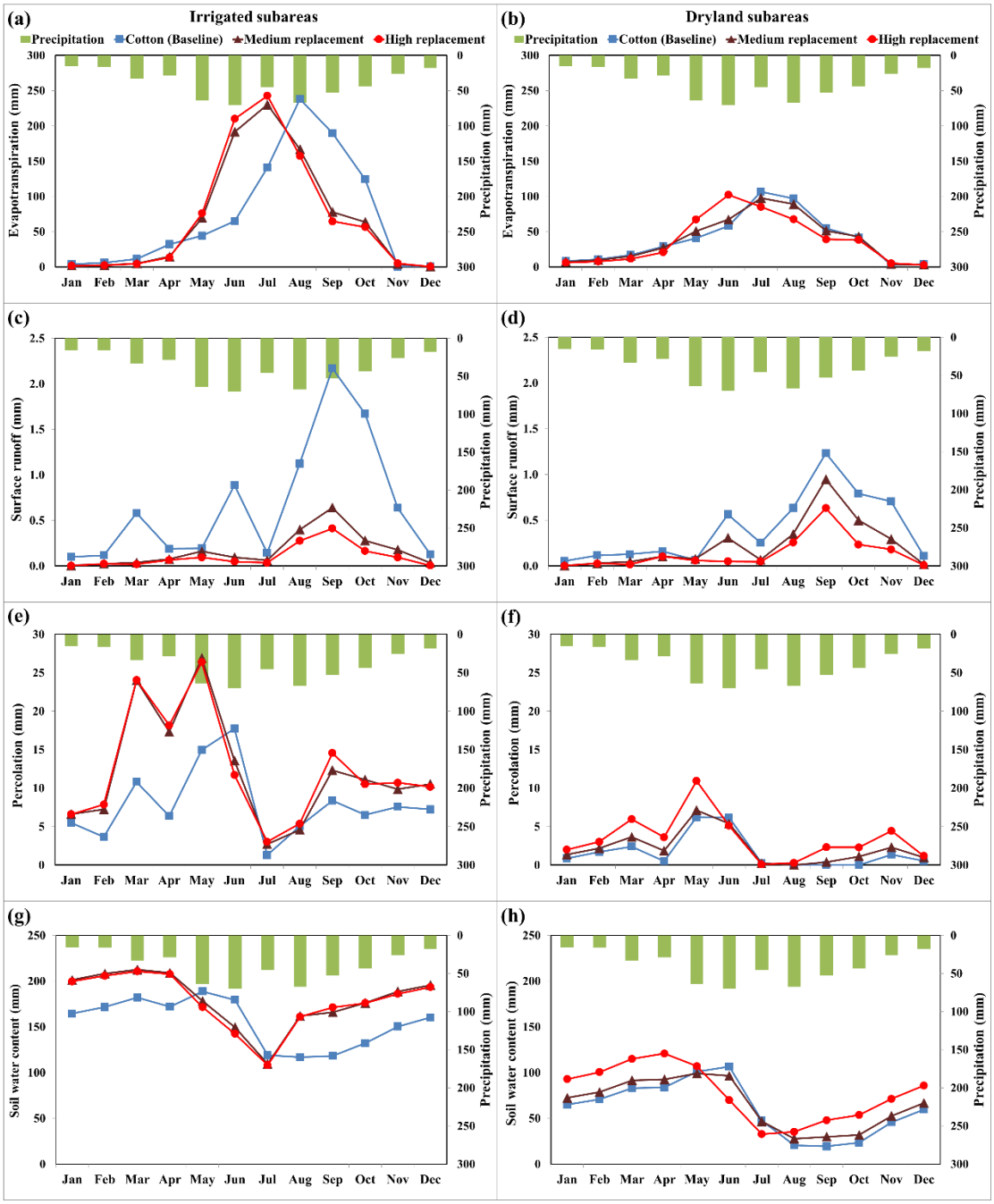


**Figure 3.8 Average (1994-2009) monthly water fluxes in irrigated and dryland subareas under the baseline, and the medium and high switchgrass replacement scenarios.**

Simulated average monthly surface runoff decreased throughout the year under the medium and high replacement scenarios relative to the baseline scenario (Figure 3.8c and d). The higher biomass density/ground cover and longer growing period of switchgrass compared to cotton resulted in this substantial reduction in the surface runoff. The effect of replacement of cotton by switchgrass on reduction in surface runoff was much higher in the irrigated subareas when compared to the dryland subareas (Figure 3.8d). The reduction in surface runoff was higher under the high replacement scenario when compared to the low and medium scenarios. More than 73% and 78% of annual surface runoff was generated during May to October in the dryland and irrigated subareas, respectively, under both baseline and hypothetical replacement scenarios.

Simulated average monthly percolation in the irrigated subareas was substantially higher under the medium and high replacement scenarios relative to the baseline scenario during September to May (Figure 3.8e). A similar trend was predicted in case of the dryland subareas (Figure 3.8f). A lower simulated monthly percolation in July and August in both dryland and irrigated subareas among all scenarios was because of the higher ET demand in these months. Simulated average monthly percolation under the baseline scenario during November to April (cotton non-growing season) was about 37% and 43% of the annual percolation in the dryland and irrigated subareas, respectively. In contrast, during the same period, the simulated average monthly percolation under the high replacement scenario was 49% and 52% of the total percolation in the dryland and irrigated subareas, respectively. These results indicated that providing appropriate

ground cover during the cotton non-growing season could increase percolation and thereby enhance groundwater recharge.

Simulated soil water content during August to April in irrigated subareas was substantially higher under the medium and high replacement scenarios when compared to the baseline scenario (Figure 3.8g). During the same period, simulated soil water content in the dryland subareas was higher under the high replacement scenario than the medium replacement and baseline scenarios (Figure 3.8h). Higher soil water content during August to April under the high replacement scenario when compared to the baseline scenario in both dryland and irrigated subareas can be attributed to higher reduction in ET and surface runoff under the high replacement scenario.

### *3.4.4 Spatial Variability in Irrigation Water Use, Water Use Efficiency and Hydrologic Fluxes under the Baseline and Switchgrass Replacement Scenarios*

Based on the average (1994-2009) annual precipitation, subareas in the study watershed can be categorized into three groups (Figure 3.9a). Subareas which received low precipitation (average annual precipitation of 464 mm) are located in the western part of the study watershed. Subareas with medium and high precipitation (average annual precipitation of 503 and 528 mm, respectively) are situated in the southcentral and northeastern parts of the watershed, respectively (Figure 3.9a). Simulated average annual irrigation water requirement for cotton (baseline) of 480 mm (18.9 inches) mm was close to the annual allowable groundwater pumping limit for irrigation of 457 mm (18 inches) set up by the High Plains Water District in order to prolong the usable

lifetime of the underlying Ogallala Aquifer in the Southern High Plains region (HPUWCD, 2015). Simulated irrigation water use of switchgrass under the high replacement scenario was higher by 9% and 4% relative to that of cotton (baseline) in the western subareas (with low precipitation) and southcentral subareas (with medium precipitation), respectively. In contrast, simulated irrigation water use of switchgrass decreased by 5% when compared to the baseline scenario in the northeastern subareas that received high precipitation (Figure 3.9b).

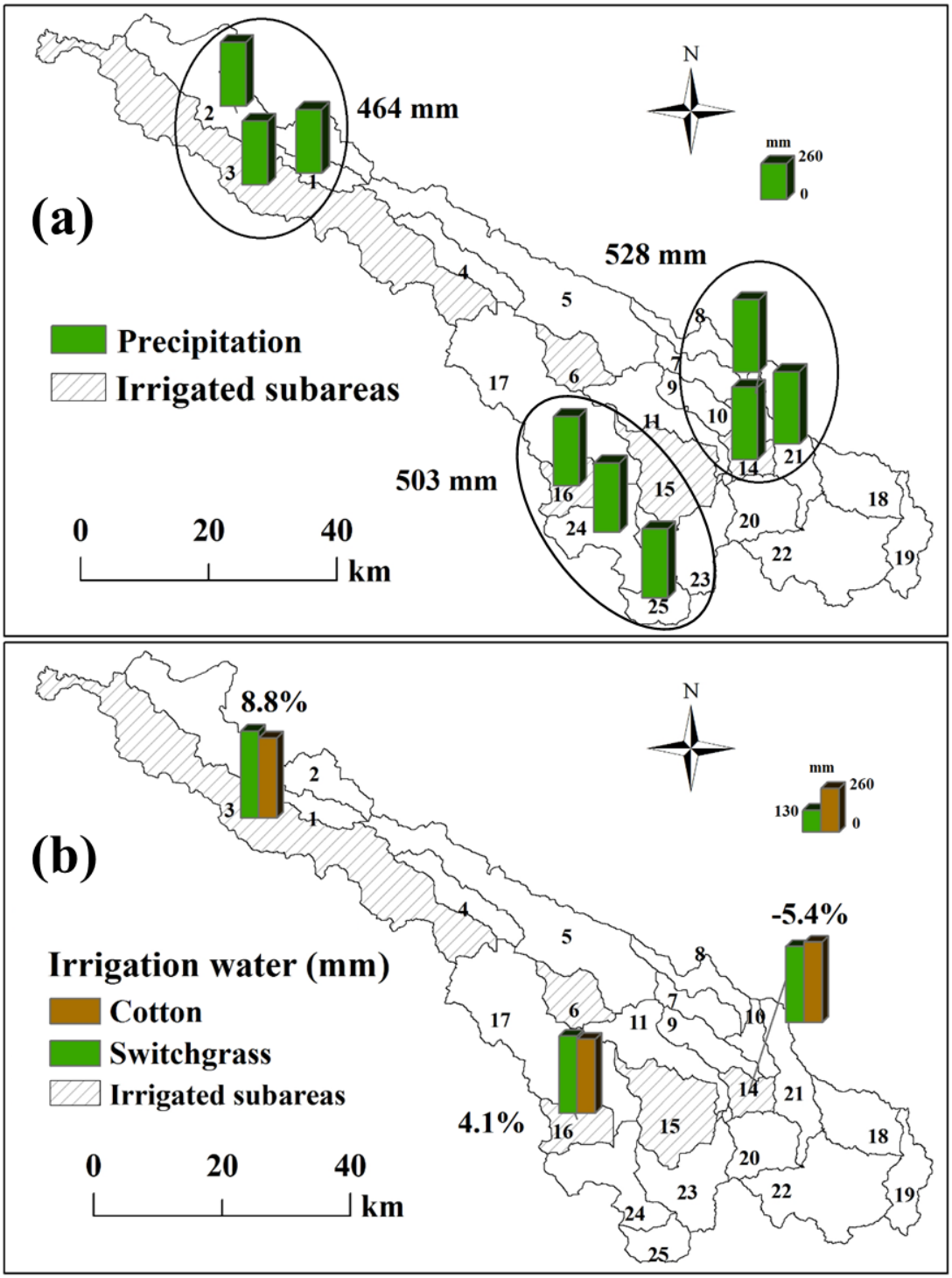


**Figure 3.9 Spatial distribution of average (1994-2009) annual precipitation across the watershed and comparison of average annual irrigation water use under the baseline and proposed high replacement switchgrass scenarios.**

Simulated DWUE of switchgrass (range between 16.4 and 21.5 kg $ha^{-1}$ $mm^{-1}$) was higher than that of cotton (6.2 to 7.7 kg $ha^{-1}$ $mm^{-1}$) in all dryland subareas across the study watershed (Figure 3.10a). Simulated DWUE of switchgrass was 242% higher than that of cotton in the western subareas of the study watershed, which received lower average annual precipitation. In the eastern subareas which received higher precipitation, the simulated DWUE of switchgrass was higher within a range of 117% to 139% when compared to baseline (cotton) scenario. Simulated IWUE of switchgrass (14.0 to 16.5 kg $ha^{-1}$ $mm^{-1}$) was also higher than that of cotton (8.0 to 9.5 kg $ha^{-1}$ $mm^{-1}$) in all irrigated subareas, especially in the westernmost subarea 3 (107% higher) (Figure 3.10b). These are important results in view of the projected reductions in irrigation water availability for agriculture in the THP. Limited groundwater resources in the future can therefore be used more efficiently for switchgrass production than for cotton. Interestingly, the IWUE of cotton was higher than its DWUE while this trend was reversed in the case of switchgrass (DWUE > IWUE) (Figure 3.10a and b).

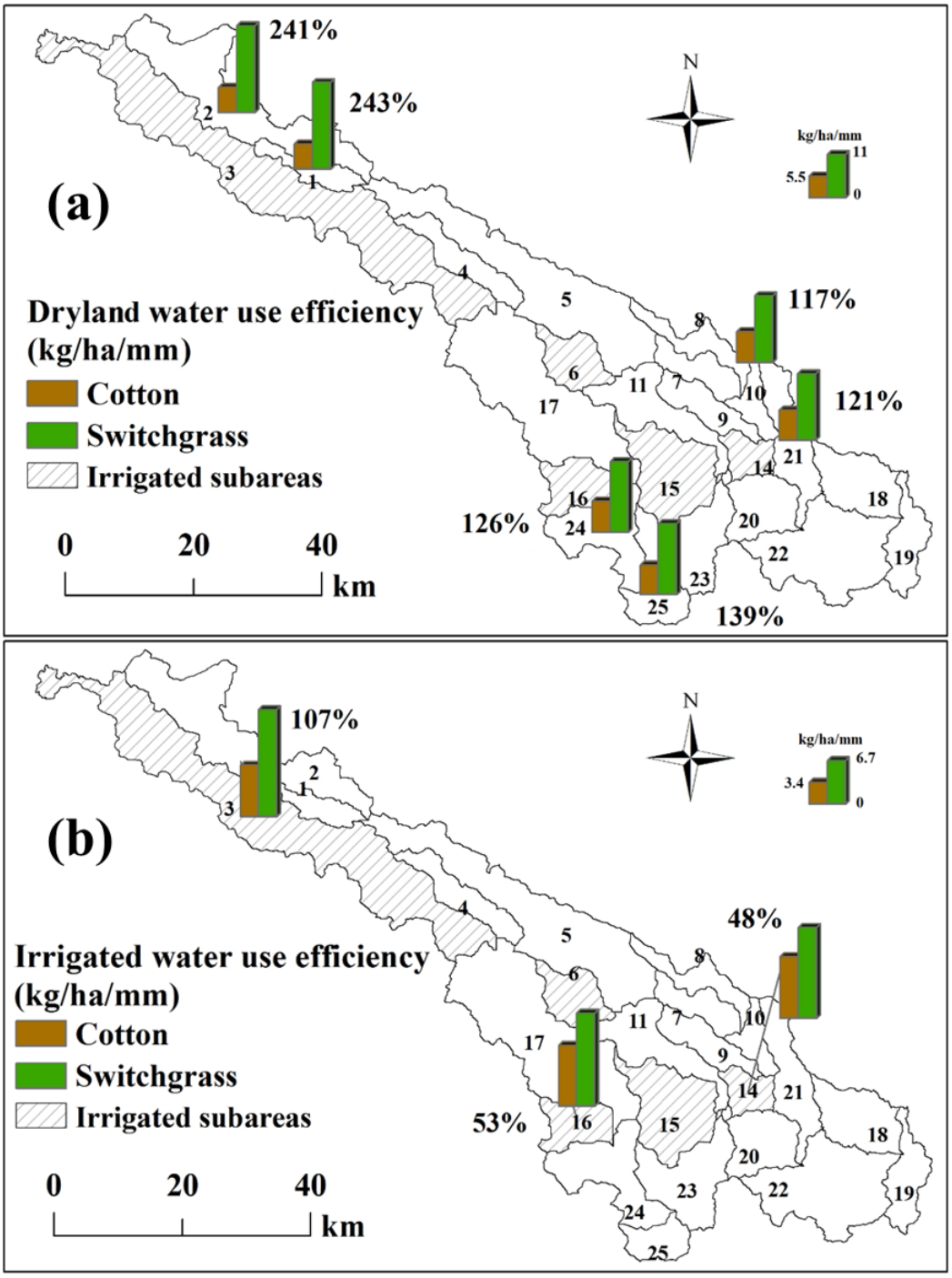


**Figure 3.10 Comparison of average (1994-2009) annual water use efficiency and irrigation water use efficiency under the baseline and proposed high replacement switchgrass scenarios.**

Average (1994-2009) annual ET decreased 3% to 11% under the high replacement scenario relative to the baseline scenario across the watershed (Figure 3.11a). Average annual surface runoff was also reduced by about 59% to 98% under the high replacement scenario relative to the baseline scenario (Figure 3.11b). Percent reduction in surface runoff was higher in subareas 1, 2 and 3 in the western part of the study watershed, which received lower annual rainfall and have sandy soil characteristics (Hydrologic soil group B; Figure 3.12). Nelson et al. (2006) predicted a 99% reduction in the SWAT-simulated surface runoff in the Delaware basin in northeast Kansas when land use was changed from the traditional corn-soybean cropping rotation to switchgrass.

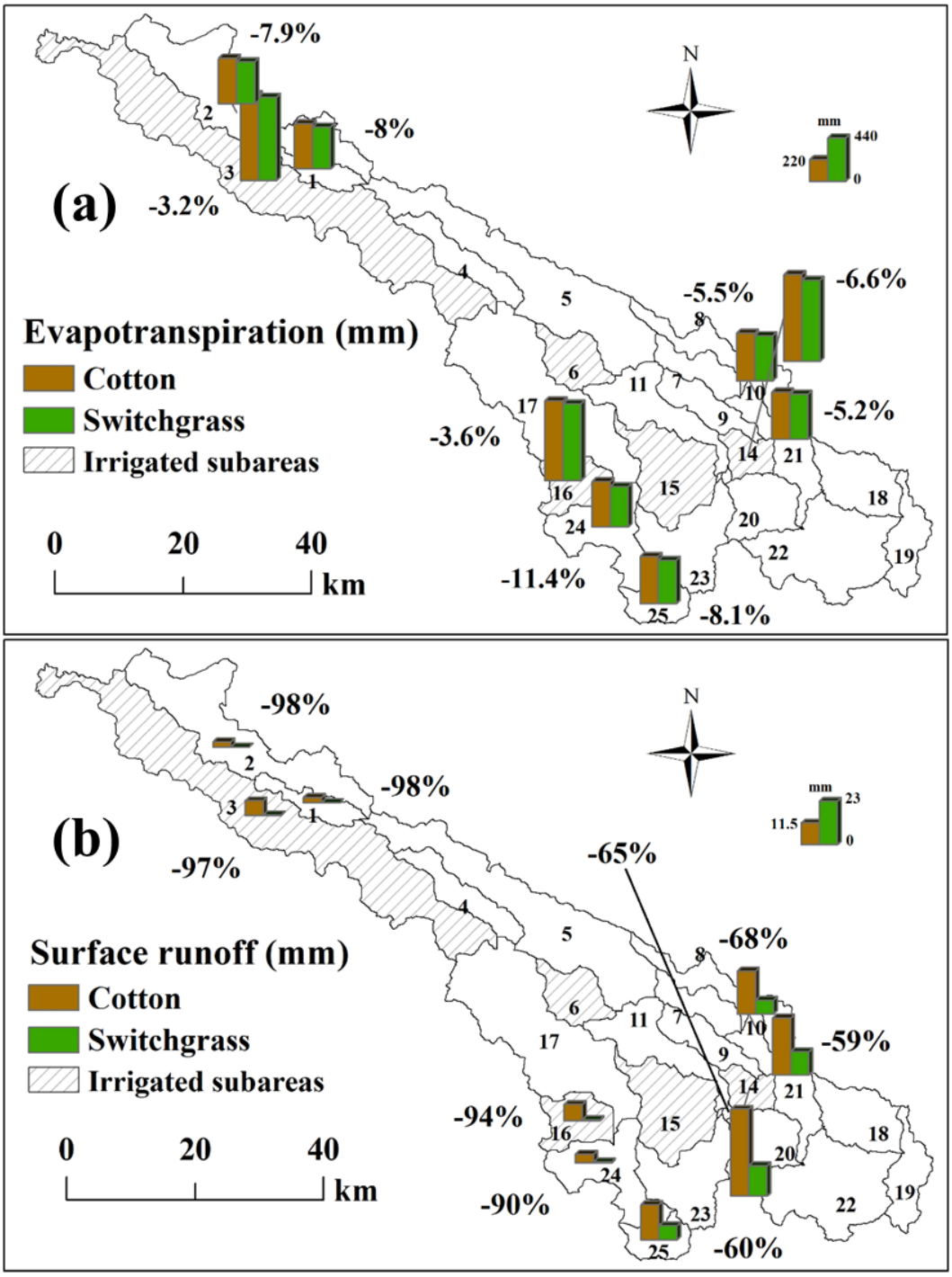


**Figure 3.11 Comparison of average (1994-2009) annual evapotranspiration loss and surface runoff generation under the baseline and proposed high replacement switchgrass scenarios.**

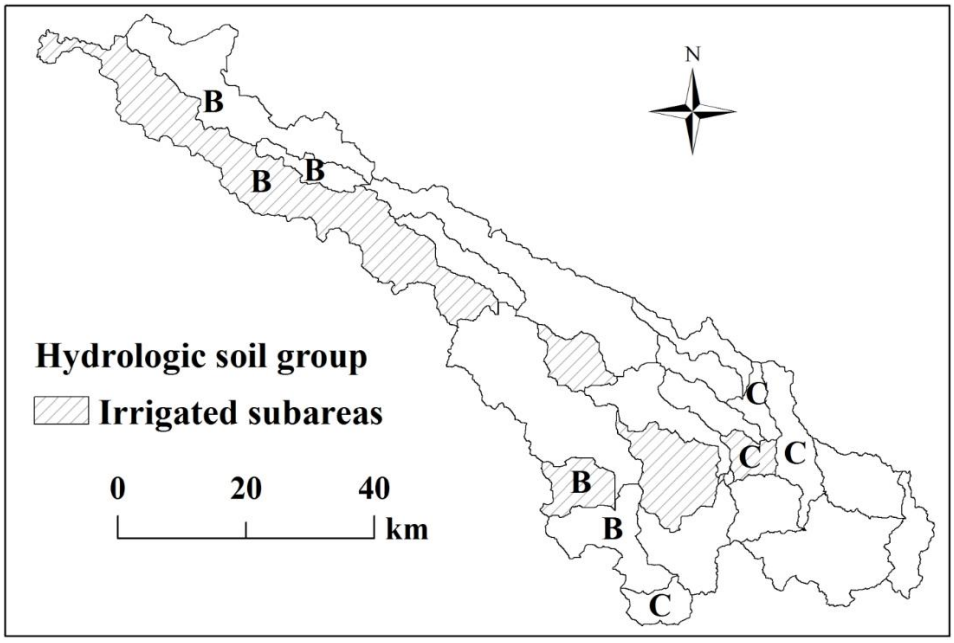


**Figure 3.12 The spatial distribution of hydrologic soil groups in the study watershed.**

Simulated average annual percolation across the watershed was higher (increased by 44% (from 135.6 to 195 mm in subarea 16) to 3595% (from 1.2 to 42.9 mm in subarea 1)) under the high replacement scenario relative to the baseline scenario (Figure 3.13a). The trend was more obvious in the dryland subareas in the western part of the study watershed where simulated percolation was negligible under cotton. The percent increase in percolation was substantially higher under the dryland subareas when compared to the irrigated subareas. Using the SWAT model, Cibin et al. (2016) also reported that the land use change from corn/soybean to switchgrass in Wildcat Creek and St. Joseph River watersheds in Indiana would increase percolation due to the presence of surface cover of switchgrass for a longer period when compared to corn/soybean. Presence of larger amounts of switchgrass residue as compared to that of cotton could also have contributed to higher percolation under switchgrass scenario in our study. The

soil water content increased 3% to 74% under the high replacement scenario when compared to the baseline scenario across the study watershed (Figure 3.13b).

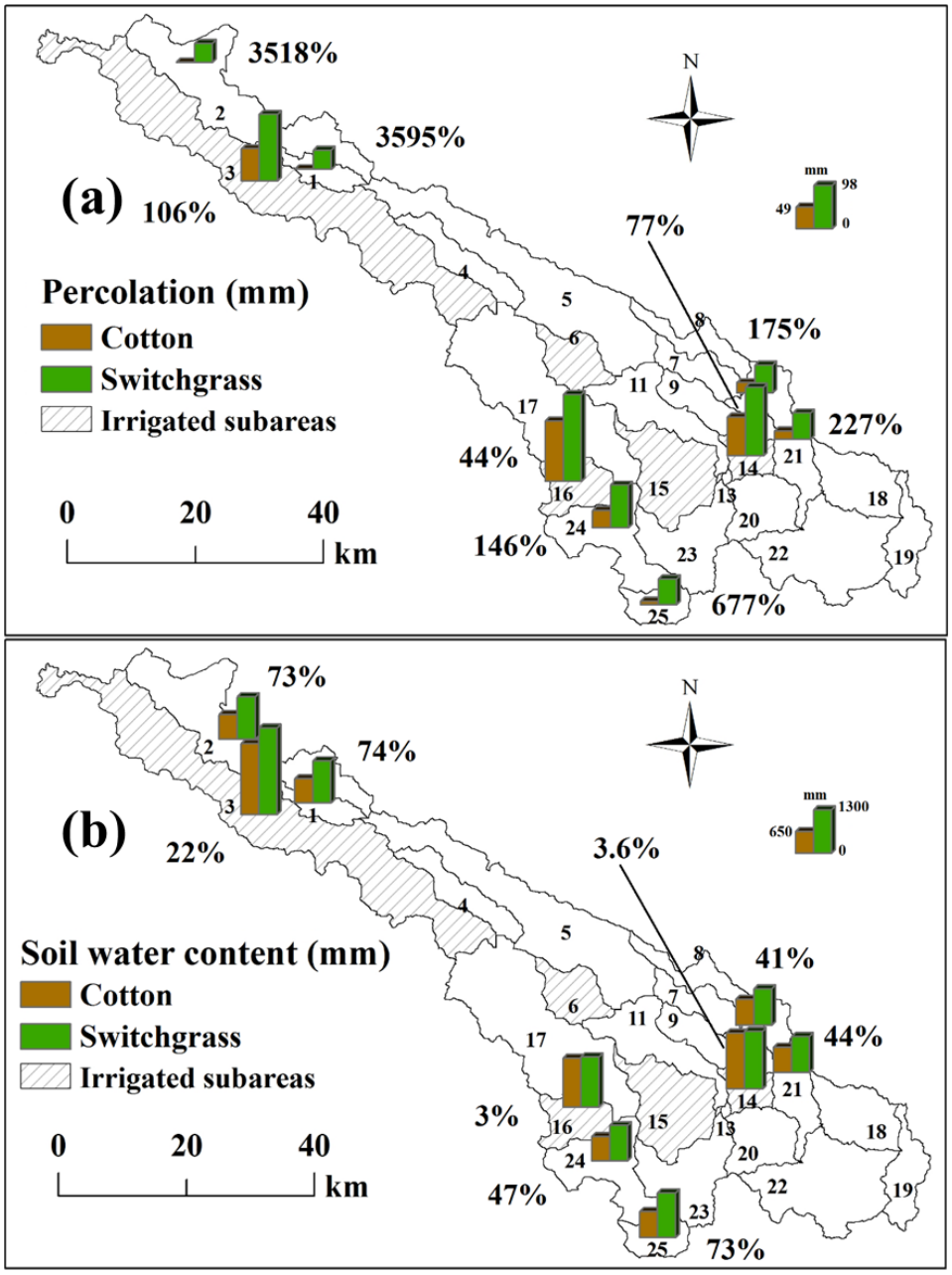


**Figure 3.13 Comparison of average (1994-2009) annual soil water content and percolation under the baseline and proposed high replacement switchgrass scenarios**

Overall, results from water balance analysis of baseline and switchgrass scenarios demonstrated potential advantages of proposed land use change from cotton to switchgrass such as higher DWUE/IWUE, and increased percolation and soil water content. These findings are useful to producers and land/water managers in this region and will enable them to better plan agricultural activities in the future in view of decreasing groundwater levels in the Ogallala Aquifer. It is expected that a majority of the current irrigated lands in the THP could gradually be converted into drylands in the future. Under those circumstances, replacing cotton with switchgrass will not only improve the water use efficiency, but also increase the soil water content and groundwater recharge.

## 3.5 Conclusions

The impact of potential land use change from cotton to switchgrass in the marginal cotton growing areas in an intensively managed agricultural watershed in the Texas High Plains on water balances and biofuel production potential was evaluated using APEX. Three scenarios with low (9%), medium (33%) and high (57%) extents of cotton growing areas replaced by switchgrass, were studied. When compared to the baseline scenario, the average (1994-2009) annual irrigation water use under the switchgrass replacement scenarios was 4% to 9% higher in the western subareas that received lower annual precipitation, and 5% lower in the eastern subareas with higher annual precipitation. The average annual surface runoff reduced by 84% and 66% under the irrigated and dryland high replacement scenarios, respectively when compared to the

baseline scenario. The simulations also showed a higher average monthly soil water content during August to April and larger percolation during September to May under the high replacement scenario relative to the baseline scenario. The spatial analysis indicated greater soil water storage, and higher percolation and DWUE/IWUE under switchgrass scenarios in the western subareas when compared to the eastern subareas. Based on the simulated total biomass, 381 and 193 million liters of biofuel can be produced from the irrigated and dryland subareas of the study watershed under the high replacement scenario. Switchgrass was, therefore, found to be a feasible bioenergy crop for replacing cotton in the Texas High Plains.

# 4. ASSESSING THE HYDROLOGIC AND WATER QUALITY IMPACTS OF BIOFUEL-INDUCED CHANGES IN LAND USE AND MANAGEMENT*

## 4.1 Synopsis

The Southern High Plains (SHP) of Texas, where cotton (*Gossypium hirsutum* L.) is grown in vast acreage, and the Texas Rolling Plains (TRP), which is dominated by an invasive brush, honey mesquite (*Prosopis glandulosa*) have the potential for biofuel production for meeting the U.S. bioenergy target of 2022. However, a shift in land use from cotton to perennial grasses and a change in land management such as the harvesting of mesquite for biofuel production can significantly affect regional hydrology and water quality. In this study, APEX and SWAT models were integrated to assess the impacts of replacing cotton with Alamo switchgrass (*Panicum virgatum* L.) and *Miscanthus* × *giganteus* in the upstream subwatershed, and harvesting mesquite in the downstream subwatershed on water and nitrogen balances in the Double Mountain Fork Brazos watershed in the SHP and TRP regions. The simulated average (1994-2009) annual surface runoff decreased significantly ($p$<0.05) by 88%, and percolation increased by 28% under the perennial grasses scenario compared to the baseline cotton scenario. The soil water content enhanced significantly under the irrigated switchgrass scenario compared to the baseline irrigated cotton scenario from January to April and August to October. However, the soil water content was depleted significantly under the dryland *Miscanthus* scenario from April to July relative to the baseline dryland cotton scenario. The nitrate-nitrogen ($NO_3$-N) and organic-N loads in surface runoff and $NO_3$-N

* This section is under review in the journal of *Global Change Biology Bioenergy*. 2016.

leaching to groundwater reduced significantly by 86%, 98% and 100%, respectively, under the perennial grasses scenario relative to the baseline cotton scenario. Perennial grasses exhibited superior ethanol production potential compared to mesquite. However, mesquite is an appropriate supplementary bioenergy source in the TRP region because of its standing biomass and rapid regrowth characteristics.

## 4.2 Introduction

The U.S. agriculture is facing an unprecedented challenge in securing the nation's energy future in addition to meeting the traditional goal of food security. According to the current Renewable Fuels Standard Program (RFS2), the volume of renewable fuel required to be blended into transportation fuel will be 136 million $m^3$ by 2022 (U.S. Department of Agriculture; USDA, 2010). As one of the world's largest food producer, exporter and donor, the U.S. plays a vital role in addressing these challenges. Further increase of crop production or change in land use will be needed for meeting these challenges in the coming years. Since the industrial revolution, human actions (including agriculture) have become a major driving factor for global environmental change, land and water degradation, and biodiversity loss (Foley et al., 2011; Rockström et al., 2009). As a result, agriculture must address its environmental consequences as it seeks to meet the aforementioned food security and renewable fuels challenges.

There are two general types of renewable biofuels. First generation biofuels are usually produced through intensive agricultural activities, which are similar to those used in growing primary food crops such as maize (*Zea mays* L.) and grain sorghum

(*Sorghum bicolor*). Production of first generation biofuels potentially competes with the production of food. Thus, if the production of first generation biofuels rises to certain levels, there can be detrimental social consequences in the form of reduced food supplies and associated increases in commodity prices that can be passed on to consumers. Since intensive agricultural activities typically utilize more resources (prime farmland, irrigation water, fertilizers and pesticides, and fuel for farming operations), there can be increased negative environmental effects associated with the production of first generation biofuels. To address these concerns, the USDA recommended that, out of the targeted production of 136 million $m^3$ of biofuels by 2022, 76 million $m^3$ should be produced from cellulosic and other advanced biofuel feedstocks (USDA, 2010). Cellulosic biofuels, which are also called second generation biofuels, are primarily made from the byproducts of intensive agricultural activities or from less-intensive agricultural activities performed on non-food croplands using substantially reduced resource inputs.

The Southern High Plains (SHP) of Texas in the U.S. is one of the most intensively managed cotton growing regions in the world. The cotton planting area in the SHP accounted for approximately 31% of the entire U.S. cotton acreage in 2015 (National Agricultural Statistics Service; NASS, 2015). The Ogallala Aquifer is the primary source of irrigation water for this region. Intensive agricultural production in the SHP since 1950s has resulted in a continuous decline of groundwater levels and deterioration of groundwater quality, mainly due to high concentrations of nitrate-nitrogen ($NO_3$-N) (Chaudhuri and Ale, 2014a and b; Rajan et al., 2015b). The land use change from high water and N consuming crops such as cotton to more water- and

nitrogen-use-efficient perennial grasses such as Alamo switchgrass (*Panicum virgatum* L.) and *Miscanthus* × *giganteus*, may benefit this region by prolonging the availability of groundwater and improving groundwater quality. Using the Soil and Water Assessment Tool (SWAT), Cibin et al. (2016) simulated a reduction in annual surface runoff by about 12% and 15% under the *Miscanthus* and switchgrass land use scenarios, respectively, compared to the baseline corn/soybean land use in the Wildcat Creek watershed in Indiana. In another SWAT simulation study, Ng et al. (2010) showed that a 10% change in land use from cropland to *Miscanthus* would decrease the $NO_3$-N load in streamflow by about 6.4% at the outlet of the Salt Creek watershed in Illinois. Sarkar and Miller (2014) also predicted from a SWAT modeling study that the loss of N to surface runoff from switchgrass systems was approximately 73% lower than that from cotton systems in the Black Creek watershed in South Carolina. Through a GIS-based approach, Rao and Yang (2010) predicted that the increase in the extent of grassland could significantly increase groundwater recharge and thereby decrease the groundwater level decline rates, especially in the environmentally sensitive Texas High Plains (THP) region.

Honey mesquite (*Prosopis glandulosa*) is a polymorphic woody legume that invaded grasslands and rangelands in the Southwestern U.S., and it is spread over 21 million ha in Texas alone (SCS, 1988; Asner et al., 2003). It has been recognized as a bioenergy feedstock (Padron and Navarro, 2004; Singh et al., 2007; Ansley et al., 2010; Wang et al., 2014b) and it is grown under a vast acreage in the Texas Rolling Plains (TRP), which is adjacent to the SHP. The invasion of honey mesquite on grasslands of

the TRP caused several negative impacts such as increasing the extent of bare ground and thereby increasing erosion potential, and reducing herbaceous production, which is harmful to the livestock industry and grassland ecosystems (Teague and Dowhower, 2003; Ansley et al., 2010; Wang et al., 2014b). Mesquite harvest may not only supply feedstock for biofuel production, but also help in the recovery of grassland functions. Park et al. (2012) also reported that honey mesquite has the potential for use as bioenergy feedstock given its high density and presence in large extent of area in the TRP.

The SWAT model (Arnold et al., 1998) and the Agricultural Policy/Environmental Extender (APEX) model (Williams, 1995), which are widely used across the world, have demonstrated potential to satisfactorily predict long-term impacts of land use change and land management practices on hydrologic processes and water quality in complex watersheds (Ko et al., 2009; Ghaffari et al., 2010; Gassman et al., 2010; Srinivasan et al., 2010; Tuppad et al., 2010; Powers et al., 2011; Wu and Liu, 2012). Specifically, the APEX model has the capability to accurately predict hydrology and water quality in intensively managed agricultural watersheds with large extents of irrigated areas (Saleh and Gallego, 2007; Wang et al., 2011; Jung et al., 2014). The auto-irrigation function included in the APEX model simulates irrigation water as the precipitation, which results in a realistic simulation of percolation during the irrigation process. In contrast, auto-irrigation feature in the SWAT model applies irrigation water until the soil moisture content reaches the field capacity level and hence the model, in general, simulates negligible percolation during irrigation events. In addition, the APEX

model includes detailed cotton growth parameters, which are very useful for accurate prediction of cotton growth. Furthermore, APEX outputs both cotton lint and seed yields, and it permits specifying disease severity and plant population. As for the SWAT model, it provides reasonable crop management functions for satisfactorily simulating range grass and honey mesquite land uses. For example, the SWAT model allows users to input initial biomass for honey mesquite (tree crop in the crop database), which eliminates the need to grow honey mesquite from seed at the beginning of the simulation. The SWAT model also includes four methods for accurately simulating the reservoir releases. Therefore, the APEX and SWAT models were integrated in this study (hereafter referred as "Integrated APEX-SWAT model") to make use of the strengths of both models.

A majority of the published biofuel-induced water quantity and quality studies were conducted in the watersheds located in the humid regions of the U.S. such as the Upper Mississippi River Basin (Daloğlu et al., 2012; Demissie et al., 2012; Scherer et al., 2015). However, such assessments are limited in the semi-arid SHP and TRP regions. The objectives of this study were to: (1) assess the impacts of biofuel-induced land use change from cotton to perennial bioenergy crops such as switchgrass and *Miscanthus*, and the harvest of mesquite for biofuel use on hydrology and water quality in the semi-arid Double Mountain Fork Brazos watershed that spans across the SHP and TRP regions using the Integrated APEX-SWAT model; (2) estimate the biomass and biofuel production potential of three bioenergy crops considered in this study; and (3)

compare and contrast the effects of the proposed changes in land use on water and N balances under irrigated and dryland conditions.

## 4.3 Materials and Methods

### *4.3.1 Study Watershed*

The delineated area of the Double Mountain Fork Brazos watershed is about 6,000 $km^2$ (Figure 4.1). The areas of the upstream subwatershed (upstream of Gauge I) and the downstream subwatershed (downstream of Gauge I and upstream of Gauge II) are about 3,297 and 2,703 $km^2$, respectively. The upstream subwatershed is located in the Hockley, Lynn and Garza Counties (Figure 4.1), where cotton is the dominant land use (Figure 4.2). The downstream subwatershed, which is primarily composed of rangelands (Figure 4.2), is situated in Scurry, Kent and Stonewall Counties. The long-term (1981-2010) average annual rainfall across the watershed varies between 457 and 559 mm, and the long-term average annual maximum and minimum temperatures are about 24°C and 9°C, respectively. The topography of the watershed is relatively flat. The major soil types in the watershed are classified as Amarillo sandy loam, Acuff sandy clay loam and Olton clay loam (Soil Survey Staff, 2010).

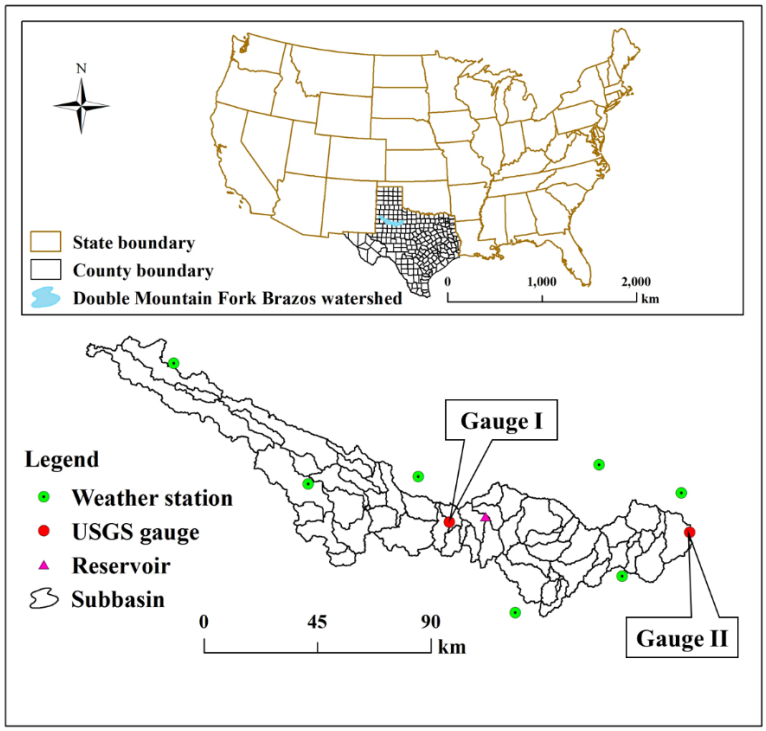


**Figure 4.1 Location of the study watershed, weather stations and USGS gauging stations.**

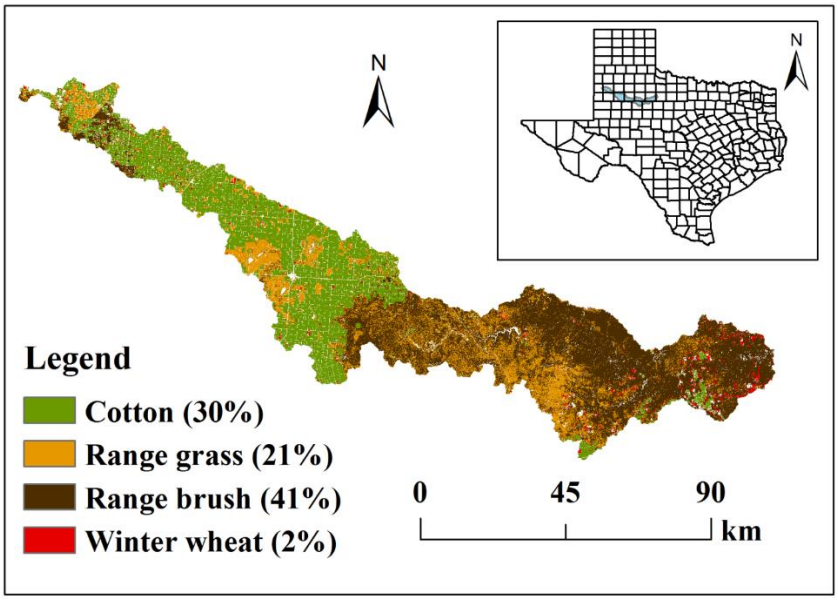


**Figure 4.2 Major land uses in the study watershed according to the 2008 National Agricultural Statistics Service (NASS) Cropland Data Layer (CDL).**

### *4.3.2 SWAT and APEX Models' Setup and Integration*

The DEM (30×30 m) of the study watershed was downloaded from the U.S. Geological Survey (http://viewer.nationalmap.gov/viewer/#) and input to the Integrated APEX-SWAT model. The 2008 NASS Cropland Data layer (CDL) (http://nassgeodata.gmu.edu/CropScape/) was used to represent the prevalent land use conditions during the period of model simulations (1994 to 2009). The dominant agricultural land use in the watershed in 2008 was cotton, which occupied about 30% of the entire watershed area, and about 52% of the upstream subwatershed (Figure 4.2). About 41% and 21% of the entire watershed area was covered by range brush and range grass, respectively. The soil data was obtained from the Soil Survey Geographic Database (SSURGO) (Soil Survey Staff, 2014), which was compatible with the Integrated APEX-SWAT model. Four soil slopes were considered: ≤ 1%, 1%-3%, 3%-5% and > 5%. Daily weather data from a total of seven weather stations for the period from 1992 to 2009 was obtained from the National Climatic Data Center (NCDC) and used in this study (Fig. S1) (NOAA-NCDC, 2014). The missing weather data for a weather station was filled with the average value of weather parameter for two adjacent weather stations (Ale et al., 2009). More detailed information for the model setup can be found in Chen et al. (2016a and b). For the HRU and subarea definitions, thresholds of 5%, 5% and 10% were used for land use, soil type and slope, respectively. A total of 25 APEX subareas were delineated in the upstream subwatershed, and 35 SWAT subbasins and 1,417 HRUs were identified in the downstream subwatershed.

The Alan Henry Reservoir (storage capacity: $4882 \times 10^4$ $m^3$) exists in the downstream subwatershed. The SWAT parameters related to the operation of this reservoir were obtained from the Texas Water Development Board's report on "Volumetric Survey of Alan Henry Reservoir" (Texas Water Development Board, 2005). The "Measured Daily Outflow" method available in the SWAT model was used to estimate the reservoir discharge based on the reservoir storage levels recorded by the USGS gauge. More details about the parameters used for reservoir simulation are provided in Chen et al. (2016a).

The APEX model is capable of simulating croplands better when compared to the SWAT model, and on the other hand, SWAT performs better in simulating noncroplands and transport of flow, sediment and nutrients through detailed in-stream channel and reservoir processes (Santhi et al., 2014). In order to take advantage of the strengths of APEX and SWAT models, the APEX model was integrated with SWAT model in this study. Initially, the APEX model was set up for the upstream subwatershed (Figure 4.3), where cotton was the dominant land use. The SWAT model was then setup for the entire watershed, and the upstream subwatershed was simulated as one subbasin in the SWAT model. The APEX-simulated net flows, and sediment and nutrient loads were then input as a point source to the SWAT model at Gauge I (outlet of the upstream subwatershed). The downstream subwatershed, which is dominated by the range land use and contains the Alan Henry Reservoir, was therefore essentially modeled using the SWAT model. Also, this coupling of two models enabled assessment of water quality effects of proposed land use change and mesquite harvest from the entire 6000 $km^2$

watershed as the measured surface water N concentration data was available at Gauge II only.

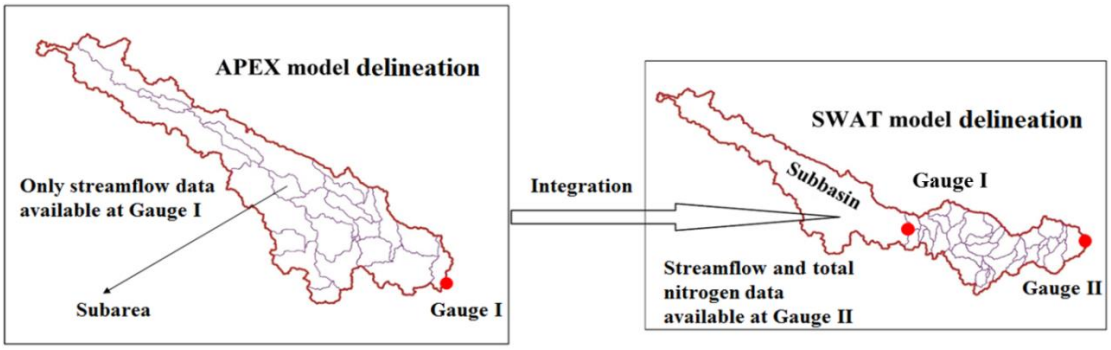


**Figure 4.3 Illustration showing the APEX model integration with the SWAT model.**

The management related parameters for cotton were specified based on the locally followed practices. Spring tillage was implemented for cotton (Table 4.1). About 138 and 69 kg N $ha^{-1}$ was applied to the irrigated and dryland cotton, respectively. According to the NASS county-wise cotton acreage estimates over the period from 1994 to 2009 (NASS, 2014), about 39% of the cotton acreage in the watershed was irrigated. Auto-irrigation was therefore simulated in about 39% of cotton planting area in the watershed based on plant water stress.

The land uses of range grass and range brush were simulated as Southwestern U.S. range and honey mesquite, respectively. The most commonly adopted heavy continuous grazing management practice was simulated on the range grassland (Park et al., 2016). The detailed management related parameters for the range grass were set up according to Park et al. (2016) (Table 4.1). Biomass of honey mesquite at the beginning

of the simulation was assumed as 19.4 Mg $ha^{-1}$ (Whisenant and Burzlaff, 1978) (Table 4.1).

**Table 4.1 Simulated management practices of cotton, winter wheat, Southwestern U.S. range and honey mesquite in APEX and SWAT models**

| No. | Management operations | Input data |
|---|---|---|
| Irrigated cotton | | |
| 1 | Tillage (Tillage on April 1) | |
| | Tillage ID | Chisel plow# |
| 2 | Fertilization (May 1) | |
| | Fertilizer ID | Urea (46-00-00) |
| | Fertilizer application rate | 300.7 (kg $ha^{-1}$)# |
| 3 | Planting ( Planting on May 15) | Default |
| | Heat units to maturity | 2354℃-day ξ |
| 4* | Irrigation (automatic irrigation) (Start date: May 15; End date: October 31) | |
| | Water stress identifier | Plant water demand |
| | Water stress threshold | 0.9 |
| 5 | Harvest and kill (Kill on October 31) | Default |
| Dryland cotton | | |
| 1 | Tillage (Tillage on April 1) | |
| | Tillage ID | Chisel plow # |
| 2 | Fertilization (May 1) | |
| | Fertilizer ID | Urea(46-00-00) |
| | Fertilizer application rate | 150 (kg $ha^{-1}$)# |
| 3 | Planting (Planting on May 15) | Default |
| | Heat units to maturity | 2354℃-day ξ |
| 4 | Harvest and kill (Kill on October 31) | Default |
| Winter wheat | | |
| 1 | Tillage (Tillage on October 8) | |
| | Tillage ID | Generic Fall Plowing# |
| 2 | Fertilization (October 8) | |
| | Fertilizer ID | Urea |
| | Amount of fertilizer applied to HRU | 108 (kg $ha^{-1}$)# |
| 3 | Planting (Planting on October 15) | Default |
| | Heat units to maturity | 1518℃-day ξ |
| 4 | Harvest and Kill (Kill on July 1) | Default |

**Table 4.1 Continued**

| No. | Management operations | Input data |
|---|---|---|
| Southwestern U.S. range** | | |
| 1 | Planting (Planting on March 20) | |
| | Heat units to maturity | 1800℃-day ξ |
| 2 | Grazing operation (start on January 1) | |
| | Manure ID | Sheep fresh manure |
| | Grazing days | 365 |
| | Biomass consumed | 0.33 (kg $ha^{-1}$ $day^{-1}$) |
| | Biomass trampled | 0.03 (kg $ha^{-1}$ $day^{-1}$) |
| | Manure deposited | 0.012 (kg $ha^{-1}$ $day^{-1}$) |
| 3 | Grazing operation (start on January 1) | |
| | Manure ID | Beef fresh manure |
| | Grazing days | 365 |
| | Biomass consumed | 3.14 (kg $ha^{-1}$ $day^{-1}$) |
| | Biomass trampled | 3.14 (kg $ha^{-1}$ $day^{-1}$) |
| | Manure deposited | 1.03 (kg $ha^{-1}$ $day^{-1}$) |
| 4 | Grazing operation (start on January 1) | |
| | Manure ID | Goat fresh manure |
| | Grazing days | 365 |
| | Biomass consumed | 0.06 (kg $ha^{-1}$ $day^{-1}$) |
| | Biomass trampled | 0.06 (kg $ha^{-1}$ $day^{-1}$) |
| | Manure deposited | 0.0019 (kg $ha^{-1}$ $day^{-1}$) |
| 5 | Grazing operation (start on January 1) | |
| | Manure ID | Horse fresh manure |
| | Grazing days | 365 |
| | Biomass consumed | 0.86 (kg $ha^{-1}$ $day^{-1}$) |
| | Biomass trampled | 0.86 (kg $ha^{-1}$ $day^{-1}$) |
| | Manure deposited | 0.64 (kg $ha^{-1}$ $day^{-1}$) |
| Honey mesquite | | |
| 1 | Initial land cover | Honey mesquite |
| | Initial biomass | 19400 (kg $ha^{-1}$) *** |
| 2 | Planting (Planting on January 1) | |
| | Heat units to maturity | 1800℃-day ξ |
| 3 | Harvest only without kill (Harvest on December 31) | Default |

* Auto-irrigation was simulated in 39% of cotton acreage based on NASS County-level cotton irrigated acreage summary reports

# The parameters related to management methods were based on published reports, local expertise, and web resources

ξ Heat units to maturity for cotton, winter wheat, Southwestern U.S. range and honey mesquite were estimated using the SWAT-PHU program (http://swat.tamu.edu/software/potential-heat-unit-program/)

** Data were obtained from NASS and analyzed based on Park et al. (2016) grazing management study

*** Data were obtained from Whisenant and Burzlaff (1978) honey mesquite field study

### *4.3.3 Observed Streamflow, Cotton Lint Yield and Water Quality Data Used for Model Calibration*

Observed daily streamflow recorded at Gauges I and II during the period from 1994 to 2009 was obtained from the USGS National Water Information System

(http://waterdata.usgs.gov/nwis/sw). The observed dryland and irrigated cotton lint yield data over the period from 1994 to 2009 for Lynn County, the county with the highest cotton acreage in the study area, was obtained from the NASS reports (http://quickstats.nass.usda.gov/). The daily total nitrogen (TN) concentration data (39 samples) measured at the watershed outlet at Gauge II (Figure 4.4) were used for model water quality calibration. These concentrations were used to estimate continuous daily TN loads by using the USGS Load Estimator (LOADEST) regression model (Runkel et al., 2004). A detailed description of LOADEST can be found in Jha et al. (2007). The estimated daily TN load data were distributed over 1995-2000 period.

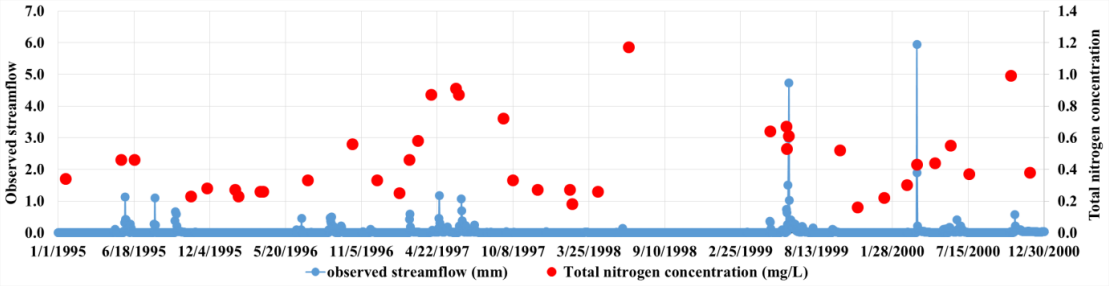


**Figure 4.4 Illustration showing the patterns of water quality sampling under various flow conditions.**

### *4.3.4 Integrated APEX-SWAT Model Calibration*

The APEX model was initially calibrated against observed streamflow and cotton lint yield data for the upstream subwatershed (Chen et al., 2016b). Since the observed N load data was not available for this upstream subwatershed, the APEX model was integrated with the SWAT model and the net flow, and sediment and nutrient loads from the upstream subwatershed were input as a point source to the downstream subwatershed

at Gauge I (Figure 4.3). The Integrated APEX-SWAT model was then calibrated against the observed streamflow data at Gauge II by solely adjusting SWAT model parameters in the downstream subwatershed. The calibration and validation periods considered for streamflow prediction were 1994-2001 and 2002-2009, respectively. After achieving a satisfactory streamflow calibration, the Integrated APEX-SWAT model was calibrated for the TN load prediction by changing the water quality parameters of both APEX (in the upstream subwatershed) and the SWAT (in the downstream subwatershed) models. Based on the available data, 1995-1997 and 1998-2000 periods were considered as the calibration and validation periods for TN, respectively. The calibrated Integrated APEX-SWAT model was then used to simulate the impacts of land use change from cotton to perennial grasses, and mesquite harvest on water and N balances. The values of calibrated parameters related to hydrology, crop growth and water quality are shown in Table 4.2.

The performance of the Integrated APEX-SWAT model in predicting streamflow and water quality during the calibration and validation periods was evaluated using three different statistical measures: square of Pearson's product-moment correlation coefficient ($R^2$) (Legates and McCabe Jr, 1999), Nash-Sutcliffe efficiency (*NSE*) (Nash and Sutcliffe, 1970) and percent bias (*PBIAS*). The goal of calibration for monthly streamflow and water quality predictions was to achieve all three objective functions: minimize *PBIAS*, maximize *NSE* and maximize $R^2$. We aimed to achieve $NSE \geq 0.60$, $R^2 \geq 0.65$ and *PBIAS* within ±15% in monthly streamflow, and $NSE \geq 0.60$, $R^2 \geq 0.65$ and *PBIAS* within ±40% in monthly TN load.

**Table 4.2 Default and calibrated values of some major hydrology, crop growth and water quality related parameters in APEX and SWAT models**

| No. | Parameter | Description | Default value | Calibrated value | Reference |
|---|---|---|---|---|---|
| APEX hydrology parameters (for upstream subwatershed above Gauge I) | | | | | |
| 1 | Parm92 | Curve number retention parameter coefficient | 1.0 | 1.31 | -- |
| 2 | Parm20 | Runoff curve number initial abstraction | 0.2 | 0.336 | -- |
| 3 | Parm12 | Soil evaporation coefficient | 2.5 | 2.44 | -- |
| 4 | Parm17 | Evaporation plant cover factor | 1.0 | 0.921 | -- |
| APEX cotton parameters | | | | | |
| 5 | WA | Biomass Energy Ratio ($CO_2$=330 ppm) | 25 | 15.48 (Dryland) 16.0 (Irrigated) | Sarkar et al. (2011) |
| 6 | HI | Harvest index | 0.60 | 0.49 (Dryland) 0.48 (Irrigated) | Wanjura et al. (2014) |
| 7 | DMLA | Maximum potential leaf area index | 6.0 | 4.0 | Sarkar et al. (2011) |
| SWAT hydrology parameters (for downstream subwatershed (between Gauges I and II) | | | | | |
| 8 | ESCO | Soil evaporation compensation factor | 0.95 | 0.75 | -- |
| 9 | SOL_AWC | Available soil water capacity (mm $H_2O$ $mm^{-1}$ soil) | 0.1-0.17 | Increased by 10% | -- |
| 10 | CN2 | Curve number for moisture condition II | 39-84 | Decreased by 1% to 12% | -- |
| 11 | ALPHA_BF | Base flow recession constant | 0.048 | 0.0765 | -- |
| 12 | GW_REVAP | Groundwater "revap" coefficient | 0.02 | 0.2 | |
| SWAT honey mesquite parameters | | | | | |
| 13 | PLTNFR(1) | Nitrogen uptake parameter #1: normal fraction of nitrogen in plant biomass at emergence | 0.02 | 0.01 | 0.006-0.02* |
| 14 | PLTNFR(2) | Nitrogen uptake parameter #2: normal fraction of nitrogen in plant biomass at 50% maturity | 0.01 | 0.005 | 0.002-0.012* |
| 15 | PLTNFR(3) | Nitrogen uptake parameter #3: normal fraction of nitrogen in plant biomass at maturity | 0.008 | 0.005 | 0.0015-0.005* |
| 16[#] | BIO_LEAF | Fraction of tree biomass accumulated each year that is converted to residue during dormancy | 0.3 | 0.05 | Ansley et al. (2010); Wang et al. (2014b) |
| 17 | MAT_YRS | Number of years required for tree species to reach full development (years) | 10 | 14 | Ansley et al. (2010) |
| 18 | BMX_TREES | Maximum biomass for a forest (ton/ha) | 50 | 70 | Ansley et al. (2010) |

**Table 4.2 Continued**

| No. | Parameter | Description | Default value | Calibrated value | Reference |
|---|---|---|---|---|---|
| APEX water quality parameters for upstream watershed (before Gauge I) | | | | | |
| 19 | Parm29 | Biological mixing efficiency | 0.4 | 0.5 | -- |
| 20 | Parm72 | Volatilization/nitrification partitioning coefficient | 0.3 | 0.05 | -- |
| 21 | Parm47 | RUSLE c factor coefficient in exponential crop height function in biomass factor | 0.1 | 3 | -- |
| SWAT water quality parameters for downstream watershed (between Gauge I and Gauge II) | | | | | |
| 22 | CDN | Denitrification exponential rate coefficient | 1.4 | 0.5 | -- |
| 23 | SDNCO | Denitrification threshold water content | 1.1 | 0.0 | Akhavan et al. (2010) |
| 24 | NPERCO | Nitrogen percolation coefficient | 0.2 | 0.55 | -- |
| 25 | ERORGN | Organic N enrichment ratio | 0 | 4.9 | -- |
| 26 | RS4 | Rate coefficient for organic N settling in the reach at 20 ℃ ($day^{-1}$) | 0.05 | 0.01 | -- |
| 27 | N_UPDIS | Nitrogen uptake distribution parameter | 20 | 15 | -- |
| 28 | BC1 | Rate constant for biological oxidation of $NH_4$ to $NO_2$ in the reach at 20 ℃ in the well-aerated conditions ($day^{-1}$) | 0.55 | 1 | -- |
| 29 | BC2 | Rate constant for biological oxidation of $NO_2$ to $NO_3$ in the reach at 20 ℃ in the well-aerated conditions ($day^{-1}$) | 1.1 | 2 | -- |
| 30 | BC3 | Rate constant for hydrolysis of organic N to $NH_4$ in the reach at 20 ℃ ($day^{-1}$) | 0.21 | 0.4 | -- |
| 31 | SOL_NO3 | Initial $NO_3$ concentration in the soil layer (mg/kg) | 0 | 13 | -- |

* The range of the parameters were plant types between tree and range brush (perennial)
# The parameter was adjusted based on the annual regrowth rate reported by Ansley et al. (2010) and Wang et al. (2014b)

The model performance in cotton lint yield prediction was assessed using $R^2$ and *PBIAS* only and we aimed to achieve a *PBIAS* within ±10% in average annual cotton lint yield under both irrigated and dryland conditions. Statistical analyses of the scenario analysis results were carried out using the Statistical Package for Social Science (SPSS

19.0). Analysis of variance (ANOVA) was used to test the difference with significance levels set at $p<0.05$ or $p<0.1$. Microsoft Excel 2013 was used for other data analysis.

### *4.3.5 Scenario Analysis*

In this study, switchgrass and *Miscanthus*, which were identified as ideal bioenergy grasses for this study region (Chen et al., 2016a), were selected to hypothetically replace irrigated and dryland cotton areas, respectively. Honey mesquite, which was dominant in the range brush areas, was also considered as the bioenergy crop. Although honey mesquite harvest was recommended at a ten-year interval (Wang et al., 2014b), a nine-year harvest interval was assumed in this study so that it could be harvested twice (in 2000 and 2009) over the total simulation period of 18 years. In addition, standing honey mesquite biomass of 19.4 Mg $ha^{-1}$ was harvested in 1992, at the beginning of the simulation period.

The Integrated APEX-SWAT model simulations were run from 1992 to 2009, and the 1992-1993 period was considered as the model warm-up period. The impacts of hypothetical biofuel-induced land use change and mesquite harvest on hydrology and water quality under simulated scenarios were evaluated over the remaining simulation period from 1994 to 2009. The land use change effects under both irrigated and dryland conditions were compared and contrasted.

Perennial grasses were planted on May 15$^{th}$, 1992 and harvested once every year on November 15$^{th}$ (Table 4.3). Irrigated switchgrass was assigned the same irrigation management practices as irrigated cotton. A recommended fertilization application rate

of about 124 kg N $ha^{-1}$ was applied for irrigated switchgrass (Yimam et al., 2014). About 98 kg N $ha^{-1}$ was applied to dryland *Miscanthus* (Lewandowski and Schmidt, 2006; Danalatos et al., 2007) (Table 4.3). No fertilizer was applied to honey mesquite. Tillage was not simulated under any of these hypothetical scenarios. Heat units to maturity of all simulated crops were estimated by using the SWAT Potential Heat Unit (SWAT-PHU) program (http://swat.tamu.edu/software/potential-heat-unit-program/) (Tables 4.1 and 4.3). Since crop growth parameter values for *Miscanthus* were not available in the models' crop database, the values from Trybula et al. (2015) field study were adopted.

**Table 4.3 Simulated management practices for irrigated switchgrass and dryland *Miscanthus* in the APEX model**

| No. | Management operations | Input data |
|---|---|---|
| Irrigated switchgrass | | |
| 1 | Fertilizer Application Parameters (May 1) | |
| | Fertilizer ID | Urea |
| | Fertilizer application rate | 270 (kg $ha^{-1}$) (Yimam et al., 2014) |
| 2 | Planting ( Planting on May 15 in 1992) | Default |
| | Heat units to maturity | 1800℃-day ξ |
| 3 | Irrigation (automatic irrigation) (Start date: | May 15; End date: November 15) |
| | Water stress identifier | Plant Water Demand |
| | Water stress threshold | 0.9 |
| 4 | Harvest only without kill (Harvest on November 15) | Default |
| Dryland *Miscanthus* | | |
| 1 | Fertilizer Application Parameters (May 1) | |
| | Fertilizer ID | Urea |
| | Fertilizer application rate | 214 (kg $ha^{-1}$) (Lewandowski and Schmidt, 2006; Danalatos et al. 2007) |
| 2 | Planting (Planting on May 15 in 1992) | Default |
| | Heat units to maturity | 1800℃-day ξ |
| 3 | Harvest only without kill (Harvest on November 15) | Default |

ξ Heat units to maturity for cotton and winter wheat were estimated using the SWAT-PHU program (http://swat.tamu.edu/software/potential-heat-unit-program/)

## 4.4 Results

### *4.4.1 Integrated APEX-SWAT Model Calibration and Validation Results*

The simulated monthly streamflow at the watershed outlet (Gauge II) during the calibration (1994-2001) and validation (2002-2009) periods closely matched with the observed streamflow (Figure 4.5). The *NSE*, $R^2$ and *PBIAS* values for monthly predictions of streamflow were 0.64, 0.67 and 10.7%, respectively, during the calibration period and they were 0.60, 0.65 and -9.3%, respectively, during the validation period. These values demonstrate a "satisfactory" agreement between the simulated and observed streamflow according to the Moriasi et al. (2007) criteria.

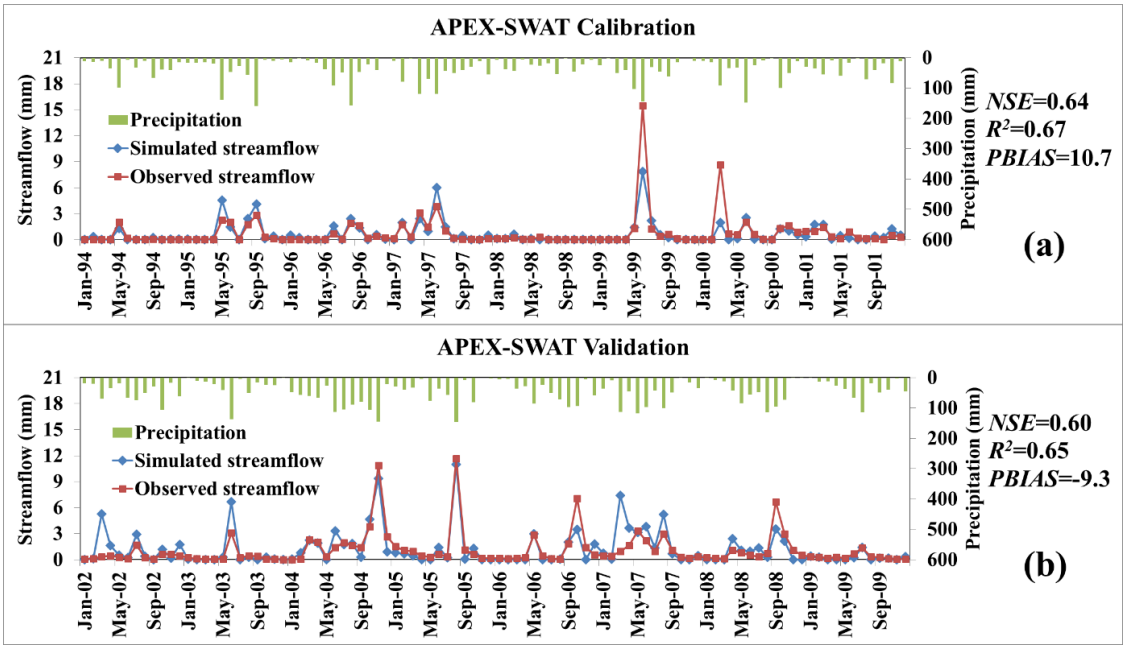


**Figure 4.5 Comparison of observed and simulated monthly streamflow at watershed outlet during the model a) calibration (1994-2001) and b) validation (2002-2009) periods.**

The simulated monthly TN load and the LOADEST estimated load during the calibration (1995-1997) and validation (1998-2000) periods also matched well as shown

in Figure 4.6. The *NSE* for monthly TN load prediction was 0.70 and 0.65 during the calibration and validation periods, respectively. The *PBIAS* in predicting TN load was -20.4% and 34.8% for the calibration and validation periods, respectively. The model performance ratings for the monthly TN load predictions were considered as "satisfactory" for both the calibration and validation periods based on the *NSE* and *PBIAS* values, according to Moriasi et al. (2007) and Wang et al. (2012) criteria.

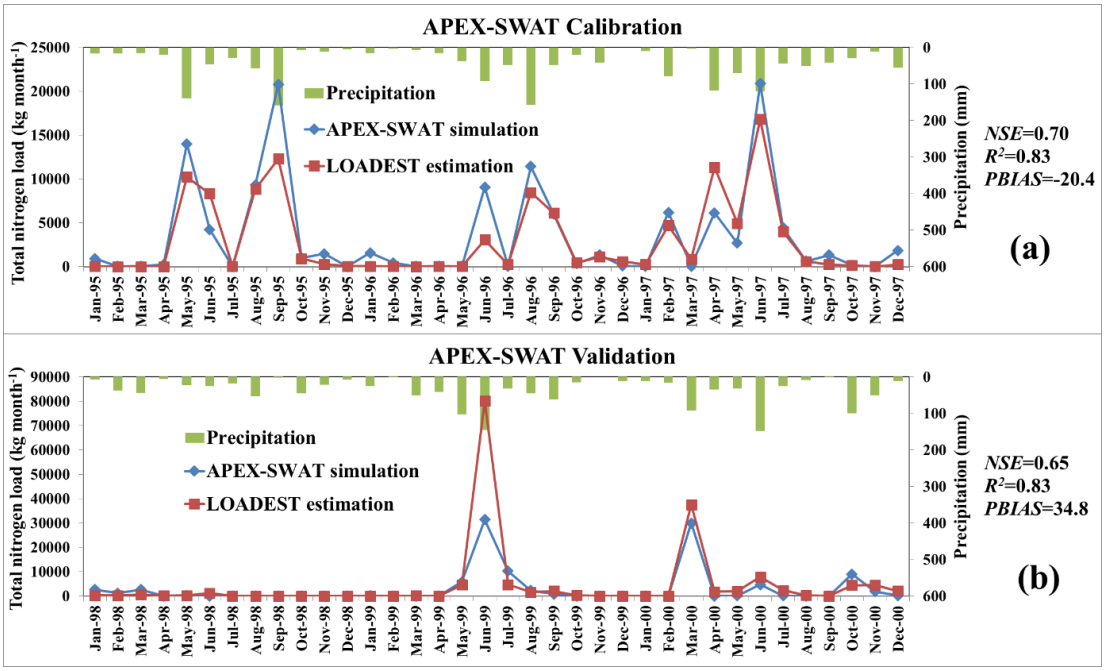


**Figure 4.6 Comparison of observed and simulated monthly total nitrogen load in streamflow at watershed outlet during the model a) calibration (1995-1997) and b) validation (1998-2000) periods.**

*4.4.2 Simulated Water and N Mass Balances in the Upstream Subwatershed under the Baseline Cotton Scenario*

The primary component of water balance in the upstream subwatershed, which is dominated by cropland, is the evapotranspiration (ET). Results showed that approximately 89% and 95% of the average annual (1994-2009) input water

(precipitation + irrigation) was lost due to ET in the irrigated and dryland conditions, respectively, under the baseline cotton scenario (Table 4.4).

**Table 4.4 Hydrologic and water quality impacts of land use change from irrigated cotton to irrigated switchgrass, and dryland cotton to dryland *Miscanthus* in the upstream subwatershed**

| Irrigated and dryland combined | Cotton (baseline) | Perennial grasses | Change percentage (%) |
|---|---|---|---|
| Precipitation (mm) | 490.4 | 490.4 | -- |
| ET (mm) | 624.1 | 626.0 | 0.3 |
| Surface runoff (mm) | 6.1 | 0.7 | -88.1* |
| Percolation (mm) | 47.0 | 60.3 | 28.1 |
| $NO_3$-N load in surface runoff (kg $ha^{-1}$) | 0.11 | 0.01 | -86.3* |
| Organic-N load in surface runoff (kg $ha^{-1}$) | 0.21 | 0.003 | -98.4* |
| $NO_3$-N leaching (kg $ha^{-1}$) | 9.43 | 0.05 | -99.5* |
| Irrigated conditions | Irrigated cotton | Irrigated switchgrass | Change percentage (%) |
| Precipitation (mm) | 481.2 | 481.2 | -- |
| Irrigation (mm) | 484.5 | 509.9 | 5.2 |
| ET (mm) | 863.7 | 841.3 | -2.6 |
| Surface runoff (mm) | 8.2 | 1.0 | -87.3* |
| Percolation (mm) | 92.3 | 147.6 | 59.9** |
| $NO_3$-N load in surface runoff (kg $ha^{-1}$) | 0.16 | 0.04 | -77.5* |
| Organic-N load in surface runoff (kg $ha^{-1}$) | 0.26 | 0.001 | -99.5* |
| $NO_3$-N leaching (kg $ha^{-1}$) | 21.03 | 0.12 | -99.4* |
| Dryland conditions | Dryland cotton | Dryland *Miscanthus* | Change percentage (%) |
| Precipitation (mm) | 496.3 | 496.3 | -- |
| ET (mm) | 472.5 | 489.6 | 3.6 |
| Surface runoff (mm) | 4.7 | 0.5 | -88.9* |
| Percolation (mm) | 18.4 | 4.9 | -73.1 |
| $NO_3$-N load in surface runoff (kg $ha^{-1}$) | 0.08 | 0.002 | -97.7* |
| Organic-N load in surface runoff (kg $ha^{-1}$) | 0.18 | 0.005 | -97.4* |
| $NO_3$-N leaching (kg $ha^{-1}$) | 2.08 | 0.01 | -99.7** |

* indicates a significant difference at $p<0.05$; ** indicates a significant difference at $p<0.1$

Less than 1% of the input water yielded as surface runoff under the baseline cotton scenario in both the irrigated and dryland conditions (Table 4.4). Average annual percolation accounted for approximately 10% and 4% of the total water input under the baseline cotton scenario in the irrigated and dryland conditions, respectively (Table 4.4).

The simulated N mass balance under the baseline cotton scenario is shown in Table 4.5. On average, approximately 48% of the N inputs remained in soil under the baseline irrigated cotton scenario with 27% of N inputs taken up by the harvested portion of cotton and 13% leached to groundwater. Bronson et al. (2004) reported that the total nitrogen content of surface soil (0 to 10 cm) in some fields within our study watershed in 2001 was about 479 kg $ha^{-1}$ under the long-term irrigated cotton land use. At the same sampling locations, Zobeck et al. (2007) further documented that the soil total nitrogen content in 0 to 10 cm soil profile in 2003 was about 590 kg $ha^{-1}$ under the long-term irrigated cotton land use. They found that about 56 kg $ha^{-1}$ total nitrogen was accumulated in the soil each year under the irrigated cotton production. The simulated annual soil total nitrogen accumulation under the baseline irrigated cotton scenario in our study (about 68 kg $ha^{-1}$; Table 4.5) was comparable to the value reported in the above studies. The simulated average annual total N uptake by the irrigated cotton in our study (about 189 kg $ha^{-1}$; Table 4.5) was also comparable to the measured N uptake of 168 kg $ha^{-1}$ by cotton, which was irrigated at 75% ET replacement in a field study by Li and Lascano (2011) in the SHP. Under the baseline dryland cotton scenario, approximately 64%, 25% and 3% of N inputs were accumulated in soil, taken up by the harvested portion of cotton and leached to groundwater, respectively (Table 4.5). The

simulated total N uptake during the period of simulation (1994-2009) ranged from 56 to 152 kg $ha^{-1}$ under the baseline dryland cotton scenario. Mullins and Burmester (1990) also documented that the total N uptake by dryland cotton ranged from 127 to 155 kg $ha^{-1}$ in their field experiments conducted in Alabama in 1986 and 1987.

**Table 4.5 Simulated average (1994-2009) annual nitrogen mass balances (kg N $ha^{-1}$) of the upstream subwatershed under cotton and perennial grasses land uses**

| Land use | Nitrogen (N) inputs | | Nitrogen outputs | | | | | | | Change in soil N |
|---|---|---|---|---|---|---|---|---|---|---|
| | Fertilizer | Rainfall | Runoff | Return flow | Sediment | Leaching | Denitrification | Volatilization | Uptake by harvested portion | |
| Irrigated cotton | 138 | 4.0 | 0.15 (0.11)* | 6.2 (4.4) | 0.25 (0.2) | 18.8 (13.2) | 0.49 (0.3) | 9.36 (6.6) | 38.3 (27.0) | 68.3 (48.1) |
| Dryland cotton | 69 | 4.0 | 0.08 (0.11) | 0.62 (0.8) | 0.18 (0.2) | 1.9 (2.6) | 0.09 (0.1) | 5.32 (7.3) | 18.2 (24.9) | 46.4 (63.5) |
| Irrigated switchgrass | 124 | 4.0 | 0.03 (0.02) | 0.09 (0.1) | 0.001 (0.001) | 0.28 (0.2) | 2.50 (2.0) | 5.98 (4.7) | 122.1 (95.4) | -3.0 (-2.4) |
| Dryland *Miscanthus* | 98 | 4.0 | 0.002 (0.002) | 0.009 (0.004) | 0.004 (0.004) | 0.026 (0.03) | 0.74 (0.7) | 4.57 (4.5) | 58.5 (57.4) | 38.1 (37.4) |

*The numbers in the parentheses indicate the percentages of total nitrogen inputs that were either lost in different pathways or accumulated in soil

### *4.4.3 Biomass and Biofuel Availability from the Changes in Watershed Land Use and Management*

The simulated average annual harvestable biomass under the irrigated switchgrass, dryland *Miscanthus* and honey mesquite scenarios was 17.3, 15.7 and 4.0 Mg $ha^{-1}$, respectively (Table 4.6). The APEX-simulated annual irrigated switchgrass and dryland *Miscanthus* biomass yields in this study were similar to those simulated by the SWAT model (17.5 and 15.6 Mg $ha^{-1}$ biomass of irrigated switchgrass and dryland *Miscanthus*, respectively) in this watershed (Chen et al., 2016a). The predicted annual *Miscanthus* biomass yield under the dryland conditions in this study was also within the range of reported *Miscanthus* biomass yield (9.8 to 17.8 Mg $ha^{-1}$) in the dryland production conditions in the U.K. (Christian, 2008).

The crop database of honey mesquite was adjusted based on the studies of Kiniry (1998) and Ansley et al. (2010) in Texas to match the simulated biomass with the observed biomass in the TRP region (Table 4.2). The simulated total tree biomass of a 30-year old honey mesquite plant in this study was about 40 Mg $ha^{-1}$, which was comparable to the measured biomass of 43 Mg $ha^{-1}$ in a field study in the TRP (Ansley et al., 2010). In addition, the predicted total tree biomass of a nine-year old regrown honey mesquite was the same (28 Mg $ha^{-1}$) as that reported in Ansley et al. (2010). The simulated annual regrowth rate was about 2.4 Mg $ha^{-1}$ for honey mesquite in this study. Ansley et al. (2010) and Wang et al. (2014b) also documented a similar annual production rate of honey mesquite of 2.2 Mg $ha^{-1}$. According to the suggested theoretical ethanol yield (http://www.afdc.energy.gov/fuels/ ethanolfeedstocks.html), the estimated

average annual ethanol that could be produced with the simulated biomass of irrigated switchgrass, dryland *Miscanthus* and honey mesquite was 6,332; 5,746 and 1,246 liters $ha^{-1}$, respectively (Table 4.6).

**Table 4.6 Average (1994-2009) annual biomass and biofuel production of irrigated switchgrass, dryland *Miscanthus* and honey mesquite**

| Annual production | Harvestable biomass (Mg $ha^{-1}$) | Biofuel conversion efficiency (liters ethanol $Mg^{-1}$ biomass)* | Biofuel production (liters ethanol $ha^{-1}$) |
|---|---|---|---|
| Dryland *Miscanthus* | 15.7 | 366 | 5,746 |
| Irrigated switchgrass | 17.3 | 366 | 6,332 |
| Honey mesquite | 4.0 | 309 | 1,246 |

*The theoretical ethanol yield is available from http://www.afdc.energy.gov/fuels/ethanol_feedstocks.html

*4.4.4 Impacts of Biofuel-Induced Land Use Change and Mesquite Harvest on Hydrology*

The average (1994-2009) annual surface runoff from the upstream subwatershed decreased significantly ($p<0.05$) by 88% under the perennial grasses scenario (i.e. irrigated cotton replaced by switchgrass and dryland cotton replaced by *Miscanthus*) compared to the baseline cotton scenario (Table 4.4). The annual percolation increased significantly ($p<0.1$) by approximately 60% under the irrigated switchgrass scenario, and it decreased by approximately 73% under the dryland *Miscanthus* scenario relative to the baseline cotton scenario (Table 4.4). Overall, under the perennial grasses scenario, the average annual percolation in the upstream subwatershed increased by 28% relative to the baseline cotton scenario. However, this trend was not statistically significant at the

$p$<0.1 level. The average annual ET of irrigated switchgrass decreased by approximately 2.6% (not significant at the $p$<0.1 level) when compared to the irrigated cotton. In contrast, the annual ET increased by about 3.6% under the dryland *Miscanthus* scenario compared to that under the baseline dryland cotton scenario. Overall, there was a statistically insignificant small increase in annual ET (0.3%) under the perennial grasses scenario relative to the baseline cotton scenario.

In the case of downstream subwatershed, the simulated average annual ET increased by 8.4% under the post-mesquite-harvest scenario relative to the baseline mesquite scenario (Table 4.7). However, this difference was not statistically significant. Also, a considerable inter-annual variability was found in this trend. For example, under the post-mesquite-harvest scenario, the average annual ET increased by 11% during the normal and wet years (rainfall > 500 mm) and reduced by about 1% during the dry years when compared to the baseline mesquite scenario. The increase in ET in wet years might have been caused by a much higher increase in evaporation when compared to reduction in transpiration after the mesquite harvest. The increase in average annual ET caused a significant ($p$<0.05) decrease in surface runoff by about 98.9% and an insignificant (at $p$<0.1 level) 37.7% reduction in percolation under the post-mesquite-harvest scenario when compared to the baseline mesquite scenario (Table 4.7).

**Table 4.7 The changes in hydrologic and water quality variables due to the harvest of honey mesquite from the downstream watershed for bioenergy purposes**

| Variable | Mesquite (baseline) | Post-mesquite-harvest |
|---|---|---|
| Hydrologic variables | | |
| ET (mm) | 458.0 | 496.3 (8.4)* |
| Surface runoff (mm) | 20.8 | 0.23 (-98.9$^{\#}$) |
| Percolation (mm) | 43.4 | 27.0 (-37.7) |
| Water quality variables | | |
| $NO_3$-N load in surface runoff (kg $ha^{-1}$) | 0.009 | 0.000007 (-99.9$^{\#}$) |
| Organic-N in surface runoff load (kg $ha^{-1}$) | 0.06 | 0.0009 (-99.5$^{\#}$) |
| $NO_3$-N leaching (kg $ha^{-1}$) | 0.12 | 0.18 (56.1) |

* The numbers in the parentheses indicate the percent changes between the post-mesquite-harvest and baseline mesquite scenarios; $^{\#}$ indicates significant differences between the post-mesquite-harvest and baseline mesquite scenarios at $p<0.05$

A hypothetical change in land use from cotton to perennial grasses altered average (1994-2009) monthly ET and soil water content significantly ($p<0.05$) under the irrigated switchgrass and dryland *Miscanthus* scenarios (Figure 4.7a, b, g and h). Monthly ET under the irrigated switchgrass scenario was significantly ($p<0.05$) higher than that under the baseline irrigated cotton scenario in the months of May to July and November (Figure 4.7a). However, it was significantly ($p<0.05$) lower relative to the baseline irrigated cotton scenario in other months. Under the dryland *Miscanthus* scenario, monthly ET increased significantly ($p<0.05$) in April, May and November, but it decreased significantly ($p<0.05$) in months of January, February, July and December compared to the baseline dryland cotton scenario.

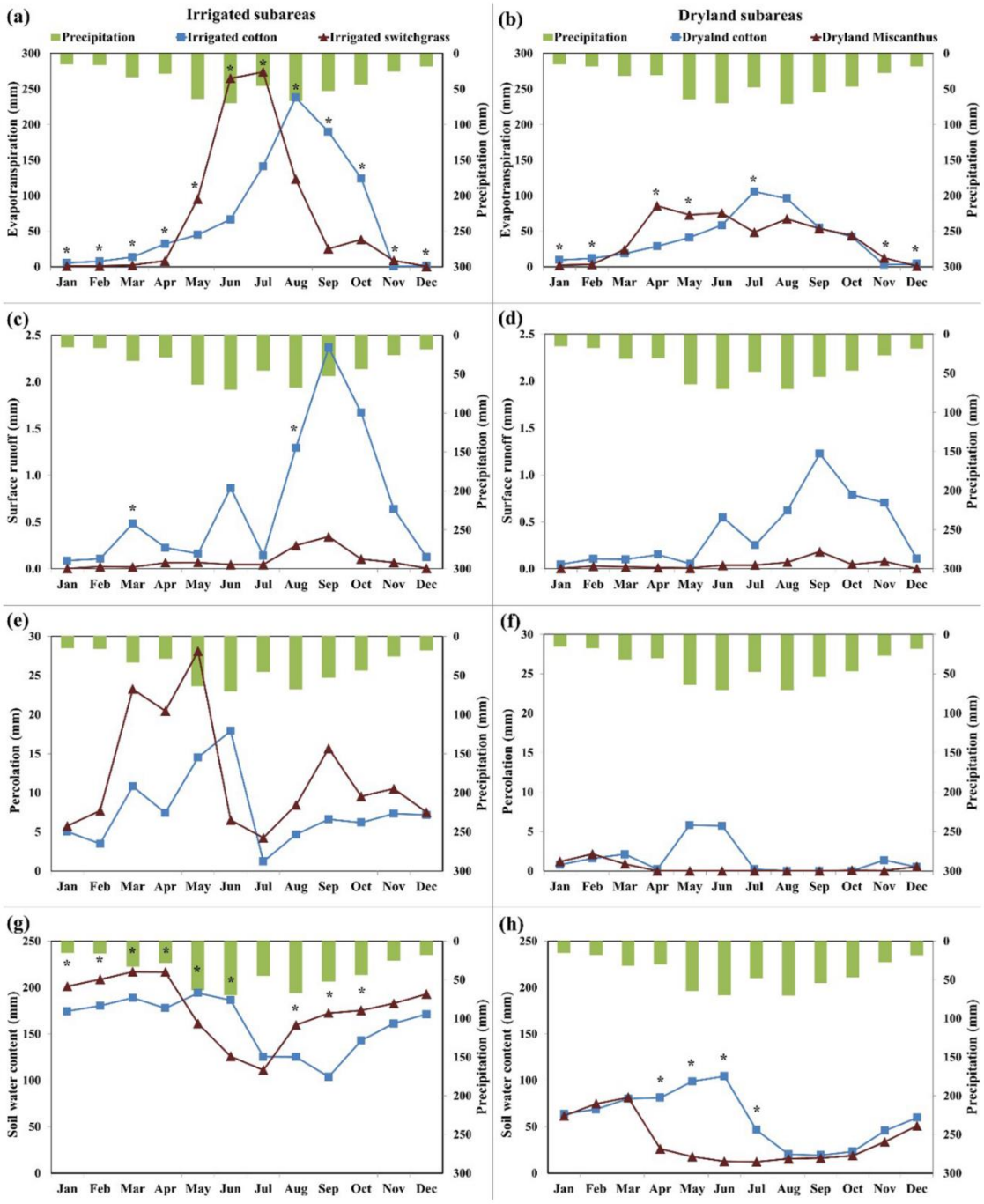


**Figure 4.7 Simulated average (1994-2009) monthly water fluxes in the irrigated and dryland areas under the baseline cotton and hypothetical perennial grass scenarios (* indicates a significant difference at $p<0.05$).**

The simulated soil water content enhanced significantly ($p$<0.05) under the irrigated switchgrass scenario from January to April and from August to October compared to the baseline irrigated cotton scenario. A significant ($p$<0.05) decrease in soil water content was found under the irrigated switchgrass scenario in May and June when the simulated ET was significantly ($p$<0.05) higher under the irrigated switchgrass scenario than the baseline irrigated cotton scenario (Figure 4.7a and g). The soil water content depleted significantly ($p$<0.05) under the dryland *Miscanthus* scenario from April to July relative to the baseline dryland cotton scenario due to the increase in simulated ET during those months. In general, soil water content was enhanced under the irrigated switchgrass scenario relative to the baseline irrigated cotton scenario, while it was reduced under the dryland *Miscanthus* scenario when compared to the dryland cotton scenario.

Negligible surface runoff was generated under the perennial grass scenarios relative to the baseline cotton scenario (Figure 4.7c and d). The surface runoff under the irrigated switchgrass scenario decreased significantly ($p$<0.05) in March and August compared to the baseline irrigated cotton scenario. The percolation under the irrigated switchgrass scenario increased from February to May and from July to November relative to the baseline irrigated cotton scenario (Figure 4.7e). However, this trend was not statistically significant (at the $p$<0.05 level). The percolation was negligible under the dryland *Miscanthus* scenario, and it also corresponded well with the depletion of soil water content under this scenario (Figure 4.7f and h). Even under the baseline dryland

cotton scenario, notable percolation was simulated only in May and June when the precipitation was relatively high and the simulated ET was relatively low.

*4.4.5 Effects of Biofuel-Induced Land Use Change and Mesquite Harvest on N Losses*

The average (1994-2009) annual $NO_3$-N and organic-N loads in the surface runoff and the $NO_3$-N leaching to the groundwater decreased significantly ($p<0.05$) by about 86%, 98% and 100%, respectively, under the perennial grasses scenario compared to the baseline cotton scenario (Table 4.4). The N lost through leaching was much higher compared to that lost through surface runoff (Table 4.4). For example, the $NO_3$-N leaching was about 20 times higher than the N lost through surface runoff under the baseline cotton land use. However, in the case of perennial grasses, $NO_3$-N leaching was only about four times higher than the N lost through surface runoff because of the higher N use efficiency of perennial grasses (Table 4.4).

A close look at the average annual N balances in irrigated conditions indicated that the $NO_3$-N and organic-N losses in surface runoff and $NO_3$-N leaching to groundwater were also significantly ($p<0.05$) lower by about 78%, 100% and 99%, respectively, under the irrigated switchgrass scenario than those under the baseline irrigated cotton scenario (Table 4.4). Although the average annual percolation increased by about 60% under the irrigated switchgrass scenario relative to the baseline irrigated cotton scenario (Table 4.4), the average annual $NO_3$-N leaching reduced by approximately 99% under the irrigated switchgrass scenario due to higher N uptake by harvested switchgrass (95% N uptake for irrigated switchgrass vs. 27% for irrigated cotton) (Table 4.5) and lower amount of N fertilizer application (124 kg N $ha^{-1}$ for

irrigated switchgrass vs. 138 kg N $ha^{-1}$ for irrigated cotton) (Table 4.3). Similar results were found in case of dryland *Miscanthus* scenario. The annual $NO_3$-N load and organic-N load reduced significantly ($p$<0.05) by about 98% and 97%, respectively, under the dryland *Miscanthus* scenario relative to the baseline dryland cotton scenario (Table 4.4). Ng et al. (2010) also predicted that a 50% change in land use from cropland to *Miscanthus* would result in a decrease in $NO_3$-N load in streamflow by about 30% at the watershed outlet in the Salt Creek watershed in Illinois. The average annual $NO_3$-N leaching also decreased significantly ($p$<0.1) by about 100% under the dryland *Miscanthus* scenario compared to the baseline dryland cotton scenario. The N uptake by the dryland *Miscanthus* (167 kg N $ha^{-1}$) was also clearly higher than that of dryland cotton (92 kg N $ha^{-1}$) (Table 4.5).

The average annual $NO_3$-N leaching increased from 0.12 to 0.18 kg $ha^{-1}$ under the post-mesquite-harvest scenario compared to the baseline mesquite scenario (Table 4.7), but these differences were not significant. The $NO_3$-N load and organic-N load through surface runoff were significantly reduced by about 99.9% and 99.5% under the post-mesquite-harvest scenario compared to the baseline mesquite scenario (at $p$<0.05 level). The significant decrease in surface runoff was the key reason for the associated significant reduction in N losses in surface runoff.

The monthly $NO_3$-N and organic-N loads in surface runoff and $NO_3$-N leaching to groundwater were negligible under the perennial grass scenarios when compared to the baseline cotton scenario (Figure 4.8). The $NO_3$-N load in the surface runoff decreased significantly ($p$<0.05) under the irrigated switchgrass scenario in March

(100%), August (89%), September (93%), November (99%) and December (99%) relative to the baseline irrigated cotton scenario. Under the dryland *Miscanthus* scenario, $NO_3$-N load in surface runoff decreased significantly ($p<0.05$) in July (93%) and August (97%) compared to the baseline dryland cotton scenario. Using the APEX model, Feng et al. (2015) also found a significant ($p<0.05$) reduction in N transported by surface water (91%) under the *Miscanthus* production scenario compared to the initial corn/soybean land use in the St. Joseph River watershed in Indiana. Generally, the organic-N load in surface runoff under the perennial grass scenarios was also much lower than that under the baseline cotton scenario (Figure 4.8c and d). However, the differences in organic-N load between the dryland *Miscanthus* and baseline dryland cotton scenarios were not statistically significant (at $p<0.1$ level). In contrast, the organic-N load in surface runoff under the irrigated switchgrass scenario reduced significantly ($p<0.05$) in March (99.5%), August (99%) and December (100%) when compared to the baseline irrigated cotton scenario. The $NO_3$-N leaching to groundwater also decreased significantly ($p<0.05$) under the irrigated switchgrass scenario in January (99.6%), March (99.2%), May (98.9%), June (100%), August (99.8%) and December (99.9%) when compared to the baseline irrigated cotton scenario. When the irrigated cotton land use was changed to irrigated switchgrass, the $NO_3$-N leaching decreased significantly ($p<0.05$) during the high precipitation months such as May, June and August. In this study, when compared to the baseline dryland cotton scenario, $NO_3$-N leaching under the dryland *Miscanthus* scenario decreased significantly ($p<0.05$) by about 100% in June. The highest percolation under the baseline dryland cotton scenario

and the lowest percolation under the dryland *Miscanthus* scenario were both predicted in June (Figure 4.7h) and this might have contributed for the significant ($p$<0.05) reduction in $NO_3$-N leaching under the dryland *Miscanthus* scenario in June compared to the baseline dryland cotton scenario.

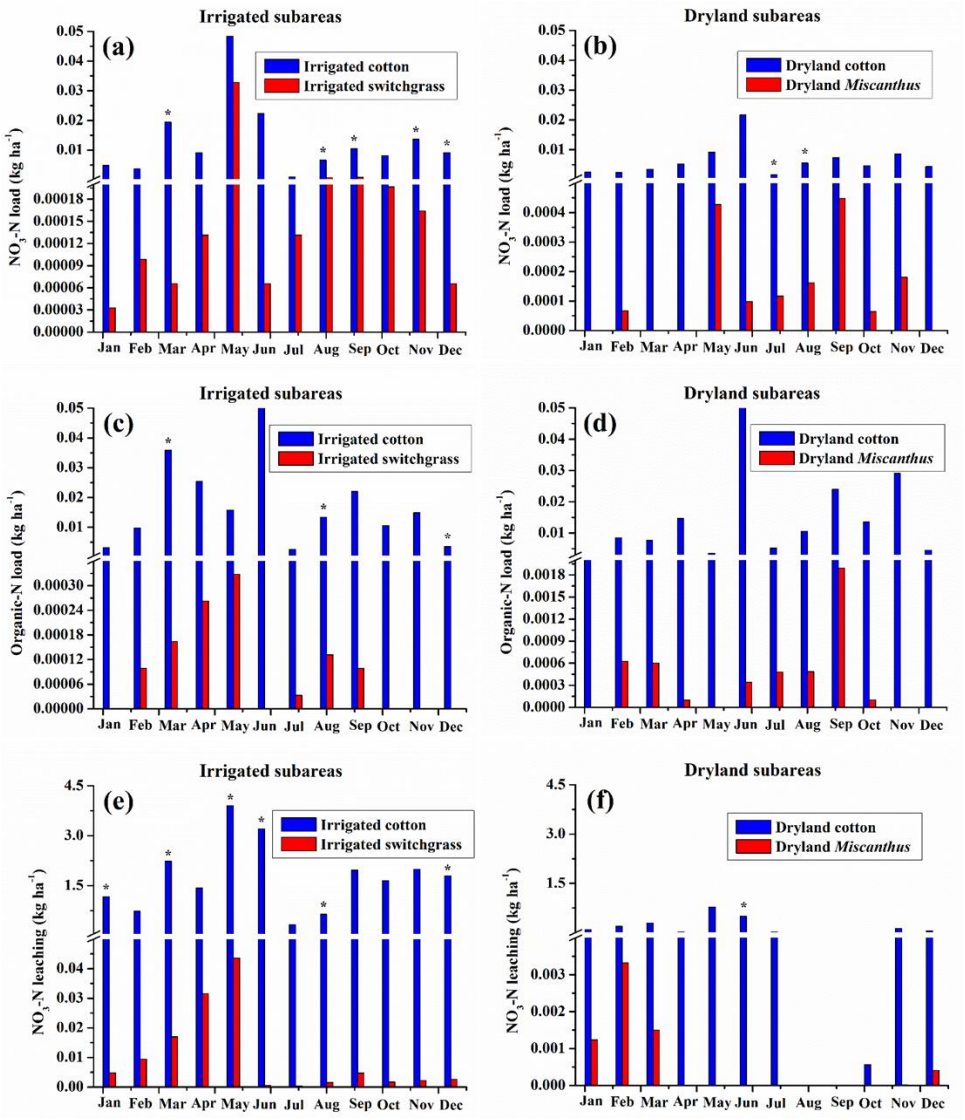


**Figure 4.8 Simulated average (1994-2009) monthly nitrogen loss through surface runoff and leaching under the irrigated and dryland areas under the baseline cotton and hypothetical perennial grass scenarios (* indicates a significant difference at $p$<0.05).**

## 4.5 Discussion

### *4.5.1 Impacts of Biofuel-Induced Changes in Land Use and Management on Water and Nitrogen Balances*

The average (1994-2009) annual surface runoff decreased significantly ($p$<0.05) by 87% under the irrigated switchgrass scenario relative to the baseline irrigated cotton scenario in this study (Table 4.4). Using the SWAT model, Nelson et al. (2006) predicted a 55% decrease in surface runoff in the Delaware basin in northeast Kansas due to the change in land use from the traditional corn-soybean cropping rotation to switchgrass. However, the average annual irrigation water requirement increased by approximately 5% (not significant at the $p$<0.1 level) under the irrigated switchgrass scenario when compared to the baseline irrigated cotton scenario (Table 4.4). It is interesting to find that the net groundwater use (irrigation water minus percolation) decreased by approximately 7.6% under the irrigated switchgrass scenario relative to the baseline irrigated cotton scenario. Monthly ET under the irrigated switchgrass scenario was significantly ($p$<0.05) lower than that under the baseline irrigated cotton scenario in the months of January to April, August to October and December, while it was significantly higher in other months (Figure 4.7a). This was primarily due to the simulated early initiation of regrowth of switchgrass in the study watershed in late April, and its late harvest in mid-November when compared to cotton. Cotton was planted in mid-May and harvested at the end of October. Yimam et al. (2015) also observed that the regrowth of switchgrass occurred around mid-April in a field experiment at Stillwater, Oklahoma. Also, the simulated peak ET occurred earlier in case of irrigated

switchgrass when compared to irrigated cotton (Figure 4.7a). As shown in Figure 4.7a and b, the monthly ET pattern under the perennial grass scenarios shifted two to three months early relative to the baseline cotton scenario. This finding would be helpful in planning appropriate management strategies for growing perennial grasses in the SHP region.

A well-developed root system and better ground cover under the switchgrass scenario enhanced the soil water content significantly ($p<0.05$) from January to April and from August to October compared to the baseline irrigated cotton scenario. However, the soil water content was reduced significantly from April to July under the dryland *Miscanthus* scenario when compared to the dryland cotton scenario. Several studies from the Midwestern U.S. have also reported reductions in soil water content under the *Miscanthus* land use when compared to that of maize (McIsaac et al., 2010; VanLoocke et al., 2010; Le et al., 2011). The large leaf area index of *Miscanthus* (*Miscanthus* vs. switchgrass: 11 vs. 6) resulted in a very high ET which depleted the soil water content.

The average annual N loads though surface runoff decreased significantly ($p<0.05$) by more than 86% under the perennial grasses scenario compared to the baseline cotton scenario (Table 4.4). Using the SWAT model, Sarkar and Miller (2014) also predicted that the N losses through surface runoff under switchgrass were approximately 73% lower than that under cotton in the Black Creek watershed in South Carolina. In another SWAT modeling study in the Arkansas-White-Red River basin, Jager et al. (2015) predicted an 84% reduction in average annual $NO_3$-N load through

surface runoff under the projected future (2022) switchgrass landscape compared to baseline no-cellulosic bioenergy grass scenario. Although the percent reductions in $NO_3$-N losses in above studies were lower, absolute losses in their study were comparable to our results. The reduction in surface runoff and high N use efficiency were the main reasons for substantial reduction in N loads in surface runoff under the perennial grasses scenario when compared to baseline cotton scenario.

The $NO_3$-N leaching to groundwater was reduced by 99.5% under the perennial grasses scenario relative to the baseline cotton scenario (Table 4.4). From a four-year field experiment in central Illinois, McIsaac et al. (2010) also concluded that the average annual $NO_3$-N leaching under maize-soybean land use was much higher (about 40 kg N $ha^{-1}$) when compared to switchgrass (1.4 kg N $ha^{-1}$; 97% reduction) and *Miscanthus* (3 kg N $ha^{-1}$; 93% reduction) land uses. Approximately 95% and 57% of total N inputs (N in fertilizer and rainfall) were taken up by harvested portion of the irrigated switchgrass and dryland *Miscanthus*, respectively, whereas harvested portion of cotton used approximately 27% to 25% of total N inputs (Table 4.5). Powers et al. (2011) also reported that about 87% of the applied N was taken up by the harvested portion of the switchgrass in an APEX modelling study in eastern Iowa. Groundwater contamination by $NO_3$-N is a major concern in the THP region (Chaudhuri and Ale, 2014b), where groundwater is the major source of drinking water for > 95% of rural population (Texas Water Development Board, 2007). Results from this study indicated that the land use change from cotton to perennial grasses could potentially reduce $NO_3$-N leaching to groundwater, and thereby improve groundwater quality in this region in a long run.

It is also interesting to notice that the surface runoff, $NO_3$-N load and organic-N load through surface runoff decreased significantly ($p$<0.05) by about 98.9%, 99.9% and 99.5% under the post-mesquite-harvest scenario compared to the baseline mesquite scenario (Table 4.7). The fast regrowth of the harvested mesquite showed higher simulated ET than the undisturbed mesquite, especially under the wet years. This was a major reason for the reduction in surface runoff and associated N losses. The harvest of honey mesquite could therefore not only benefit the water quality in the study watershed, but also supply biomass for biofuel production.

### *4.5.2 Biomass and Biofuel Production Potential of Irrigated Switchgrass, Dryland Miscanthus and Honey Mesquite*

The land use change from cotton to irrigated switchgrass and dryland *Miscanthus* exhibited superior biomass and ethanol production potential per ha compared to the honey mesquite harvest (Table 4.6). However, the vast extent of honey mesquite acreage in the Southern Great Plains (21 million ha in Texas alone) has the potential to supply abundant quantities of honey mesquite biomass for bioenergy purposes (Ansley et al., 2010; Park et al., 2012). For example, based on an estimated average standing biomass of honey mesquite of 19.4 Mg $ha^{-1}$ reported in Whisenant and Burzlaff (1978) a single harvest of honey mesquite from the entire rangelands of Texas can provide the biomass required for producing 126 million $m^3$ of biofuels, which is approximately equal to 1.6 times the mandated 2022 U.S. biofuel target of 76 million $m^3$ of second generation biofuel. In addition, honey mesquite has a high regrowth potential and it does not require

planting, irrigation and fertilization costs (Park et al., 2012; Wang et al., 2014b). These advantages make honey mesquite an appropriate supplementary bioenergy crop in the downstream subwatershed of this study and other similar areas in the TRP region.

# 5. MODELING THE EFFECTS OF LAND USE CHANGE FROM COTTON (*GOSSYPIUM HIRSUTUM* L.) TO PERENNIAL BIOENERGY GRASSES ON WATERSHED HYDROLOGY AND WATER QUALITY UNDER CHANGING CLIMATE*

## 5.1 Synopsis

Assessing the impacts of climate change on current and potential future biofuel-induced land uses on hydrology, water quality and crop yield is critical for making appropriate decisions on land use change and crop management practices. This study aimed at addressing this research gap by assessing the impacts of climate change on cotton (*Gossypium hirsutum* L.) (current land use) and potential perennial grass land uses in the Double Mountain Fork Brazos watershed in the Texas High Plains (THP) using the Soil and Water Assessment Tool (SWAT) model. While switchgrass (*Panicum virgatum* L.) was assumed to replace cotton in irrigated areas, dryland cotton was replaced by *Miscanthus* × *giganteus* under the hypothetical land use change scenarios. The climate change impacts were simulated based on the Coupled Model Intercomparison Project Phase 5 (CMIP5) climate projections of 19 General Circulation Models (GCMs). Two emission scenarios of Representative Concentration Pathway (RCP) of RCP4.5 and RCP8.5 during two 30-year periods of middle (2040-2069) and end (2070-2099) of the 21$^{st}$ century were considered. Results showed that the simulated median evapotranspiration (ET) and irrigation water use of cotton decreased

* This section is under review in the journal of *BioEnergy Research*. 2016.

substantially within the ranges of 12% to 20% and 41% to 61%, respectively, under all four future climate change scenarios compared to historic period (1994 to 2009). The simulated median annual irrigation water use under the future perennial grass land use scenarios of 2040-2069 RCP4.5, 2040-2069 RCP8.5, 2070-2099 RCP4.5 and 2070-2099 RCP8.5 was reduced by 62%, 69%, 66% and 89%, respectively, than that under respective future cotton land use scenarios according to the 19 GCM projections. In addition, the simulated future median total nitrogen load under perennial grasses land use decreased by approximately 30% when compared to cotton under all four future climate change scenarios. The median yields of irrigated and dryland cotton increased within the ranges of 69% to 91% and 100% to 129%, respectively, under the climate change scenarios compared to the historic period. The median irrigated switchgrass (*Panicum virgatum* L.) biomass yield decreased within a range of 16% to 28%, but the median dryland *Miscanthus* × *giganteus* biomass yield increased within a range of 32% to 38% under the future climate change scenarios.

## 5.2 Introduction

Human population expansion and increased dependence on fossil fuels have considerably raised atmospheric concentrations of greenhouse gases (carbon dioxide-$CO_2$, methane-$CH_4$, nitrous oxide-$N_2O$, etc.), which trap heat and warm the earth system (USEPA, 2015). According to a series of emission scenarios of the Intergovernmental Panel on Climate Change (IPCC), $CO_2$ concentrations are expected to increase from their current level of about 330 parts per million (ppm) to between 530 and 800 ppm by

the end of the 21st century (van Vuuren, 2011). The IPCC emission scenarios also predicted increases in air temperatures and associated changes in the amount, intensity and duration of precipitation due to the increase of greenhouse gas concentrations in the atmosphere (IPCC, 2007). The effects of climate change on water resources and crop production are global concerns (Arnell, 1999; Ye and Grimm, 2013; Williams et al., 2015). Climate change is expected to affect both hydrology (evapotranspiration (ET), surface runoff, etc.) and water quality (sediment and nutrient discharge) at various spatial scales (Zhang et al., 2005; Zierl and Bugmann, 2005; Zhang et al., 2007; Marshall and Randhir, 2008; Ye and Grimm, 2013), and crop yield (Williams et al., 2015).

The effects of climate change vary from a region to region. Most General Circulation Models (GCMs) projected that the Southwest region of the United States, including the Texas High Plains (THP), would become hotter and drier than usual (IPCC, 2007), which could significantly reduce water resources availability in this region (Seager and Vecchi, 2010). Recently, Modala et al. (2016) also predicted an apparent increase in daily temperature by 1.9ºC to 3.2ºC and decrease in precipitation by 30 to 127 mm in the THP in the future (2041-2070). Using Modala et al. (2016) future climate data, Adhikari et al. (2016) simulated a 14%-29% increase in irrigated seed cotton (*Gossypium hirsutum* L.) yield across the THP region under future (2041-2070) climate scenarios relative to the historic period (1971-2000), when atmospheric $CO_2$ concentration was assumed to vary from 493 ppm (in year 2041) to 635 ppm (2070). However, these simulated increases in cotton yield were possible only with increased

irrigation water use in this already groundwater-depleted THP region. Therefore, projected climate change may pose some serious challenges to efficient utilization of water resources and crop production in the semi-arid THP (Barnett et al., 2008; Gober and Kirkwood, 2010), and more studies that investigate climate change effects are needed in this predominantly cotton growing region.

The environmental policies and management strategies aimed at mitigation/adaptation of climate change effects need to be implemented at the watershed/regional scales. Therefore, watershed/regional scale climate change impact assessments are critical for devising and implementing relevant policies and strategies to mitigate negative impacts of climate change (IPCC, 2001; Brekke et al., 2004; Zhang et al., 2007). Some of the watershed-scale climate change mitigation policies and strategies are related to land use change, which has the potential to increase resiliency of the watershed to climate change (IPCC, 2001). Change in land use from conventional row crops, such as cotton, to perennial bioenergy crops could therefore play a significant role in mitigating the effects of climate change (Rose et al., 2012). The effects of biofuel-induced land use change on hydrology and water quality over the historic period were evaluated in several studies (Schilling et al., 2008; Srinivasan et al., 2010; VanLoocke et al., 2010; Zhuang et al., 2013; Chen et al., 2016a and b). However, such evaluations under future climate change scenarios are lacking, especially for the THP, which is one of the important agricultural regions of the United States.

A high variability exists in the future climate projections by different GCMs, and hence their effects on water balances, nutrient discharge and crop yield in the THP

region also would vary considerably from one GCM to the other. In order to better capture these large uncertainties, projected climate data from 19 GCMs were used in this study. The Soil and Water Assessment Tool (SWAT; Arnold et al., 1998) model, which has been widely used for evaluating the climate change and land use change effects on water quantity and quality at the watershed scale (Ficklin et al., 2009; Jha et al., 2006; Wu et al., 2012), was used in this study.

The overall goal of this study was to evaluate the impacts of land use change from cotton to the perennial bioenergy grasses of switchgrass (*Panicum virgatum* L.) and *Miscanthus* × *giganteus* on the water cycle and nitrogen load under the changing climate in the Double Mountain Fork Brazos watershed in the THP. Specific objectives of the study were to: (1) assess the climate sensitivity of the study watershed with regards to water balances, water quality and crop yield under cotton and perennial grass land uses during the historic period (1994-2009); (2) quantify the effects of future climate change on hydrologic fluxes, total nitrogen (TN) load and crop yield under the current cotton land use (baseline scenario) based on 19 GCM projections under two Representative Concentration Pathway (RCP) emission scenarios of RCP4.5 and RCP8.5 during two 30-year periods of middle (2040 to 2069) and end (2070 to 2099) of the 21$^{st}$ century; and (3) assess the impacts of land use change from cotton to perennial grasses on water partitioning, TN load and biomass production potential under the four projected future climate change scenarios (2040-2069 RCP4.5, 2040-2069 RCP8.5, 2070-2099 RCP4.5 and 2070-2099 RCP8.5) compared to respective future cotton land use scenarios.

## 5.3 Materials and Methods

### *5.3.1 Study Watershed*

The Double Mountain Fork Brazos watershed in the THP was selected for this study (Figure 5.1). The average (1994-2009) annual precipitation in the watershed was about 517 mm, and the mean air temperature during the cotton growing season (May to October) was around 24℃. The delineated watershed area is about 6000 $km^2$, and the topography of the watershed is flat. Major land uses in the watershed are cotton (30%), range grass (21%) and range brush (31%). Major soil types are Acuff sandy clay loam (fine-loamy, mixed, superactive, thermic Aridic Paleustolls), Amarillo sandy loam (fine-loamy, mixed, superactive, thermic Aridic Paleustalfs) and Olton clay loam (fine, mixed, superactive, thermic Aridic Paleustolls) (Soil Survey Staff, 2010).

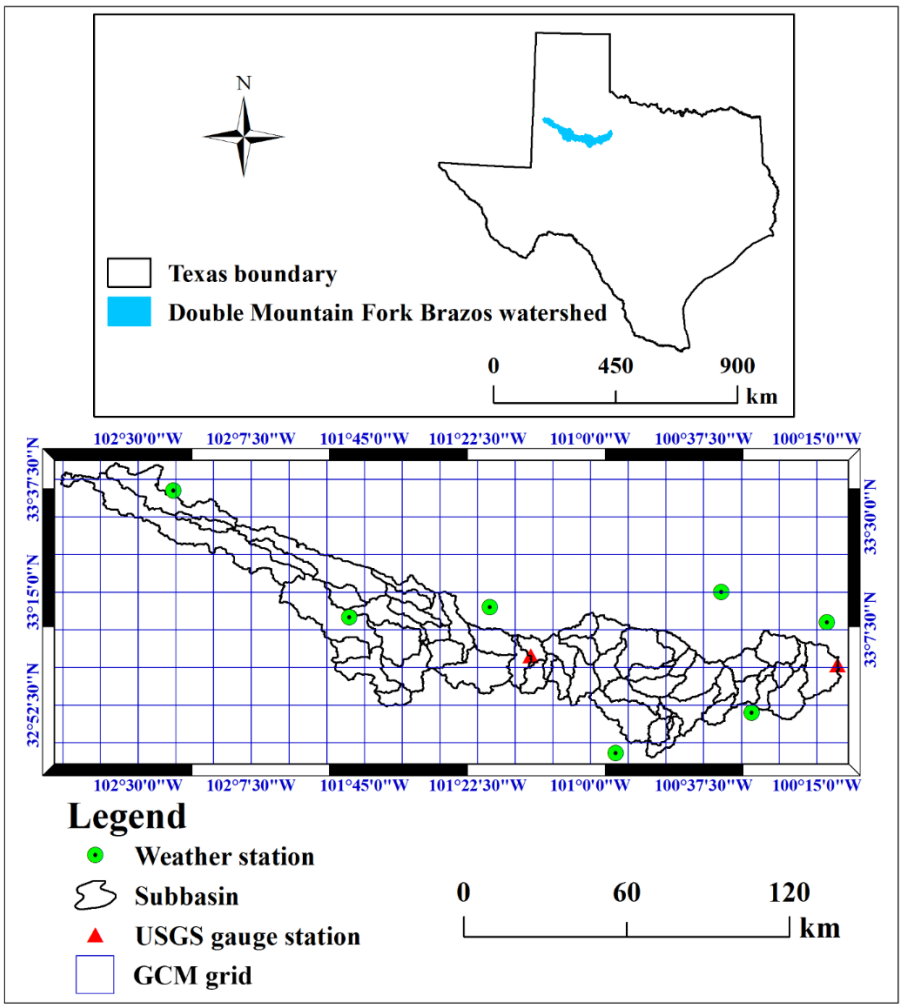


**Figure 5.1 Locations of weather stations, USGS gauge stations and General Circulation Model (GCM) grids in the Double Mountain Fork Brazos watershed in the Texas High Plains.**

### *5.3.2 SWAT Model Inputs and Calibration*

In this study, surface runoff was simulated using the Curve Number method (CN; USDA, 1972) available in the SWAT model, and the potential evapotranspiration (PET) was simulated using the Penman-Monteith method (Penman, 1956; Monteith, 1965). The crop management practices in the model were scheduled by specific dates. More details about the SWAT model inputs and setup for the study watershed are available in Chen et

al. (2016a and c). In this study, the SWAT model (Version 2012.10_2.16 released on 9/9/14) compatible with ArcGIS 10.2.2 platform was used. The Sequential Uncertainty Fitting version-2 (SUFI-2) procedure of SWAT Calibration and Uncertainty Procedures (SWAT-CUP 2012) (Abbaspour et al., 2007) was used for the model sensitivity analysis and calibration of hydrology and water quality related parameters.

The hydrologic and crop yield components of the SWAT model of the study watershed were initially calibrated as a part of our previous study (Chen et al., 2016a). In Chen et al. (2016a) SWAT model, default parameter values were used for range brush, which occupied about 41% of the watershed area. In this study, hydrology and crop yield calibration of the Chen et al. (2016a) SWAT model was further improved by simulating honey mesquite, which is predominant in the range brush land use of the study watershed, in all range brush Hydrologic Response Units (HRUs). The improved SWAT model was then calibrated for water quality predictions using the observed daily TN concentration data (39 samples) at the watershed outlet, which were converted into continuous daily TN load data using the USGS regression model, Load Estimator (LOADEST) (Runkel et al., 2004). A detailed description of the LOADEST model can be found in Jha et al. (2007). The estimated continuous daily TN load data was distributed from 1995 to 2000. The data from 1995 to 1997 and 1998 to 2000 was used for the model calibration and validation, respectively. A five-year warm up period from 1990 to 1994 was adopted for the TN load simulation (Daggupati et al., 2015). The calibrated values of major hydrologic and nutrient related parameters are shown in Table 5.1. The SWAT model performance in prediction of TN load was evaluated on a

monthly basis using three statistical measures: the Nash-Sutcliffe efficiency (*NSE*) (Nash and Sutcliffe, 1970), square of Pearson's product-moment correlation coefficient ($R^2$) (Legates and McCabe, 1999) and percent bias (*PBIAS*).

**Table 5.1 Default and calibrated values of some major hydrology, water quality and crop growth parameters in SWAT**

| No. | Parameter | Description | Default value | Calibrated value | Reference |
|---|---|---|---|---|---|
| Hydrological parameters | | | | | |
| 1 | ESCO | Soil evaporation compensation factor | 0.95 | 0.75 (Gauge I)* 0.80 (Gauge II)# | -- |
| 2 | SOL_AWC | Available soil water capacity (mm $H_2O$ $mm^{-1}$ soil) | 0.1-0.17 | Increased by 10% | -- |
| 3 | CN2 | Curve number for moisture condition II | 39-84 | Decreased by 8% | -- |
| 4 | ALPHA_BF | Base flow recession constant | 0.048 | 0.0765 | -- |
| 5 | GW_REVAP | Groundwater "revap" coefficient | 0.02 | 0.08 (Gauge I) 0.06 (Gauge II)# | |
| Water quality parameters | | | | | |
| 1 | CDN | Denitrification exponential rate coefficient | 1.4 | 0.5 | -- |
| 2 | SDNCO | Denitrification threshold water content | 1.1 | 0.0 | Akhavan et al., 2010 |
| 3 | NPERCO | Nitrogen percolation coefficient | 0.2 | 0.55 | -- |
| 4 | ERORGN | Organic N enrichment ratio | 0 | 5.0 | -- |
| 5 | RS4 | Rate coefficient for organic N settling in the reach at 20 ℃ ($day^{-1}$) | 0.05 | 0.01 | -- |
| 6 | N_UPDIS | Nitrogen uptake distribution parameter | 20 | 15 | -- |
| 7 | BC1 | Rate constant for biological oxidation of $NH_4$ to $NO_2$ in the reach at 20 ℃ in the well-aerated conditions ($day^{-1}$) | 0.55 | 0.1 | -- |
| 8 | BC2 | Rate constant for biological oxidation of $NO_2$ to $NO_3$ in the reach at 20 ℃ in the well-aerated conditions ($day^{-1}$) | 1.1 | 0.2 | -- |
| 9 | BC3 | Rate constant for hydrolysis of organic N to $NH_4$ in the reach at 20 ℃ ($day^{-1}$) | 0.21 | 0.2 | -- |
| 10 | SOL_NO3 | Initial $NO_3$ concentration in the soil layer (mg/kg) | 0 | 28 | -- |

**Table 5.1 Continued**

| No. | Parameter | Description | Default value | Calibrated value | Reference |
|---|---|---|---|---|---|
| Dryand cotton parameters | | | | | |
| 1 | BIO_E | Biomass/energy ratio [(kg $ha^{-1}$)/(MJ $m^{-2}$)] | 15 | 13.6 | Sarkar et al., 2011 |
| 2 | HVSTI | Harvest index [(kg $ha^{-1}$)/(kg $ha^{-1}$)] | 0.5 | 0.49 | Wanjura et al., 2014 |
| 3 | BLAI | Max leaf area index (m2/m2) | 4.0 | 4.7 | Sarkar et al., 2011 |
| 4 | WSYF | Lower limit of harvest index [(kg $ha^{-1}$)/(kg $ha^{-1}$)] | 0.3 | 0.35 | |
| 5 | T_OPT | Optimal temp for plant growth (℃) | 30 | 27.5 | Williams et al., 2015 |
| 6 | T_BASE | Min temp for plant growth (℃) | 15 | 12.5 | Williams et al., 2015 |
| Irrigated cotton parameters | | | | | |
| 1 | BIO_E | Biomass/energy ratio [(kg $ha^{-1}$)/(MJ $m^{-2}$)] | 15 | 13 | Sarkar et al., 2011 |
| 2 | HVSTI | Harvest index [(kg $ha^{-1}$)/(kg $ha^{-1}$)] | 0.50 | 0.48 | Wanjura et al., 2014 |
| 3 | BLAI | Max leaf area index (m2/m2) | 4.0 | 4.5 | Sarkar et al., 2011 |
| 4 | T_OPT | Optimal temp for plant growth (℃) | 30 | 27.5 | Williams et al., 2015 |
| 5 | T_BASE | Min temp for plant growth (℃) | 15 | 12.5 | Williams et al., 2015 |

* Parameter changed for all of the subbasins that discharged to Gauge I
# Parameter changed for the subbasins between Gauge I and Gauge II

### *5.3.3 Scenario Development and Analysis*

#### 5.3.3.1 Climate Sensitivity Analysis

The climate sensitivity analysis was carried out separately for each of three climate variables considered in this study: atmospheric $CO_2$ concentration, precipitation and air temperature. This analysis was conducted over the historic period of 1994 to 2009 and such analysis is useful for better understanding of the impacts of climate change on water balances, water quality and crop yield under different land uses, and

hence vulnerability of the watershed to climate change. The current cotton land use in the watershed was defined as the baseline scenario, during which an average atmospheric $CO_2$ concentration of 330 ppm was assumed (Wu et al., 2012).

**Table 5.2 Scenarios considered in the climate sensitivity and climate change analyses**

| Scenario | $CO_2$ concentration (ppm) | Precipitation change (%) | Temperature increase ($^oC$) |
|---|---|---|---|
| Climate sensitivity scenarios | | | |
| Baseline | 330 | 0 | 0 |
| Run I | 495 | 0 | 0 |
| Run II | 660 | 0 | 0 |
| Run III | 330 | -40% | 0 |
| Run IV | 330 | -30% | 0 |
| Run V | 330 | -20% | 0 |
| Run VI | 330 | -10% | 0 |
| Run VII | 330 | +10% | 0 |
| Run VIII | 330 | +20% | 0 |
| Run IX | 330 | +30% | 0 |
| Run X | 330 | +40% | 0 |
| Run XI | 330 | 0 | +2$^oC$ |
| Run XII | 330 | 0 | +4$^oC$ |
| Run XIII | 330 | 0 | +6$^oC$ |
| Time period | Land use | RCP* | Assumed average $CO_2$ concentration (ppm) |
| Future Climate change scenarios | | | |
| 2040-2069 | Cotton | RCP4.5 | 500 |
| 2040-2069 | Cotton | RCP8.5 | 570 |
| 2040-2069 | Perennial grasses | RCP4.5 | 500 |
| 2040-2069 | Perennial grasses | RCP8.5 | 570 |
| 2070-2099 | Cotton | RCP4.5 | 530 |
| 2070-2099 | Cotton | RCP8.5 | 800 |
| 2070-2099 | Perennial grasses | RCP4.5 | 530 |
| 2070-2099 | Perennial grasses | RCP8.5 | 800 |

* RCP, Representative Concentration Pathway

Thirteen climate sensitivity scenarios were developed by varying one variable at a time (Table 5.2). Specifically, the atmospheric $CO_2$ concentration during the historic

period was increased by 1.5 (495 ppm) and 2 times (660 ppm) relative to the baseline concentration. The measured historic daily precipitation was changed by ±10%, ±20%, ±30% and ±40%, and the daily minimum and maximum temperatures were increased by 2℃, 4℃ and 6℃.

#### 5.3.3.2 The GCM Climate Projections

Bias-Corrected Statistically Downscaled (BCSD) daily future climate data projected by 19 GCMs were obtained from the Downscaled Coupled Model Intercomparison Project Phase 5 (CMIP5) Climate and Hydrology Projections (http://gdo-dcp.ucllnl.org/), and used in the future climate change simulations. Future climate data were obtained for a total of 168 GCM grids that span over the study watershed, and input to the SWAT model for future climate change simulations (Figure 5.1). The GCMs considered in this study include: access1-0, bcc-csm1-1, canesm2, ccsm4, cesm1-bgc, cnrm-cm5, csiro-mk3-6-0, gfdl-esm2g, gfdl-esm2m, inmcm4, ipsl-cm5a-lr, ipsl-cm5a-mr, miroc5, miroc-esm, miroc-esm-chem, mpi-esm-lr, mpi-esm-mr, mri-cgcm3 and noresm1-m. The GCM projections of daily precipitation, maximum temperature and minimum temperature were available for the period from 1950 to 2099. The spatial resolution of the GCM projections is 0.125 degree (~12.5 km×12.5 km).

In this study, GCM climate projections from two RCP emission scenarios of RCP4.5 (moderate) and RCP8.5 (severe) were used. Future climate change projections from these 19 GCMs were obtained for two 30-year periods: 2040 to 2069 (middle of the 21$^{st}$ century) and 2070 to 2099 (end of the 21$^{st}$ century). The four future climate change scenarios simulated in this study are hereafter denoted as 2040-2069 RCP4.5, 2040-2069

RCP8.5, 2070-2099 RCP4.5 and 2070-2099 RCP8.5. The representative $CO_2$ concentrations for 2040-2069 RCP4.5, 2040-2069 RCP8.5, 2070-2099 RCP4.5 and 2070-2099 RCP8.5 scenarios were estimated as 500, 570, 530 and 800 ppm, respectively (Table 5.2) according to Van Vuuren et al. (2011). An R code was used to convert the downloaded future climate data of the study watershed into the format required by the SWAT model.

### *5.3.4 Biofuel-Induced Land Use Change Scenarios under Changing Climate*

For the land use change scenario analysis, two promising perennial bioenergy crops, switchgrass and *Miscanthus* (Kiniry et al., 2008; Kiniry et al., 2012; Kiniry et al., 2013; Wang et al., 2014b; Chen et al., 2016a and b) were selected to replace cotton under both historic and future climate scenarios. Specifically, irrigated cotton was replaced by irrigated switchgrass and dryland cotton was replaced by dryland *Miscanthus* in view of their large biomass production potential and high water use efficiency under different irrigation management practices based on Chen et al. (2016a) study for this study watershed. The management practices implemented for switchgrass and *Miscanthus* simulations were described in detail in Chen et al. (2016a) study.

The simulated annual results for cotton and perennial grass land uses based on each GCM-projected future climate data were averaged for the middle and the end of the 21$^{st}$ century scenarios and compared with the average (1994-2009) annual historic results for cotton land use. Box plots showing the percent changes in simulated variables/parameters/indices under the four future climate change scenarios (2040-2069

RCP4.5, 2040-2069 RCP8.5, 2070-2099 RCP4.5 and 2070-2099 RCP8.5) in comparison to the historic scenario were prepared based on the simulation driven by 19 GCMs. Temperature and water stress days were estimated for each scenario and used to assess the effects of climate change on crop yield/biomass. A day was considered as a temperature/water stress day, if the average air temperature/soil water on that day was different from the specified optimum temperature/soil water (Neitsch et al., 2011).

## 5.4 Results and Discussion

### *5.4.1 Evaluation of the SWAT Model Performance in Predicting Streamflow, Cotton Lint Yield and Total Nitrogen Load*

The predicted monthly streamflow during the calibration (1994-2001) and validation (2002-2009) periods at two USGS gauges closely matched with the observed monthly streamflow (Figures 5.2 and 5.3). The *NSE*, $R^2$ and *PBIAS* values for monthly simulations of streamflow at Gauge I were 0.86, 0.88 and 12.1%, respectively, during the model calibration period, and 0.59, 0.71 and -7.5%, respectively, during the model validation period (Figure 5.2). At Gauge II, the *NSE*, $R^2$ and *PBIAS* for monthly streamflow predictions were 0.62, 0.66 and 14.2%, respectively, during the model calibration period, and 0.61, 0.75 and -12.8%, respectively, during the model validation period (Figure 5.3). The model performance statistics for streamflow prediction were well above satisfactory range according to Moriasi et al. (2007) criteria. The average *PBIAS* in predicting irrigated cotton lint yield over the entire simulation period (1994-2009) was 3.2% (Figure 5.4). In the case of dryland cotton, the average *PBIAS* in cotton lint yield prediction was 2.3%.

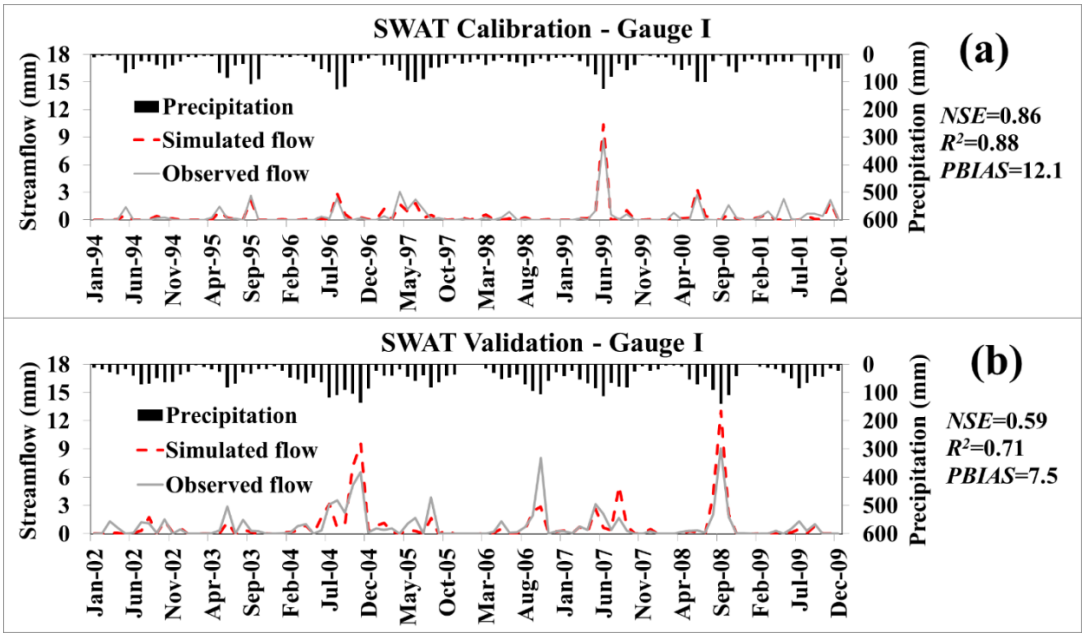


**Figure 5.2 Comparison of observed and simulated monthly streamflow at Gauge I during the model a) calibration and b) validation periods.**

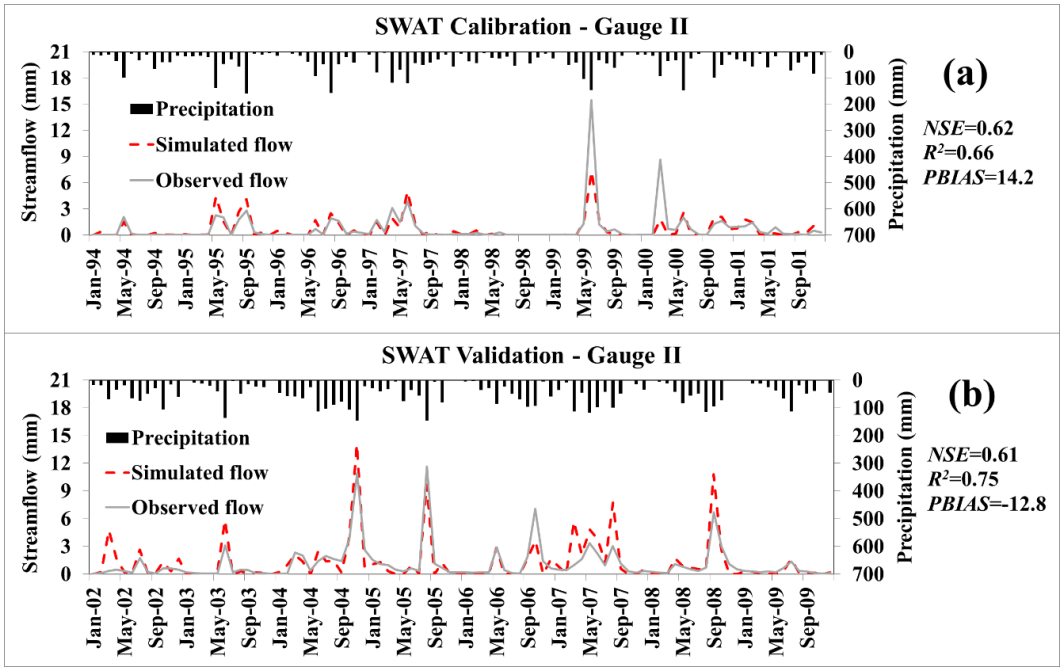


**Figure 5.3 Comparison of observed and simulated monthly streamflow at Gauge II during the model a) calibration and b) validation periods.**

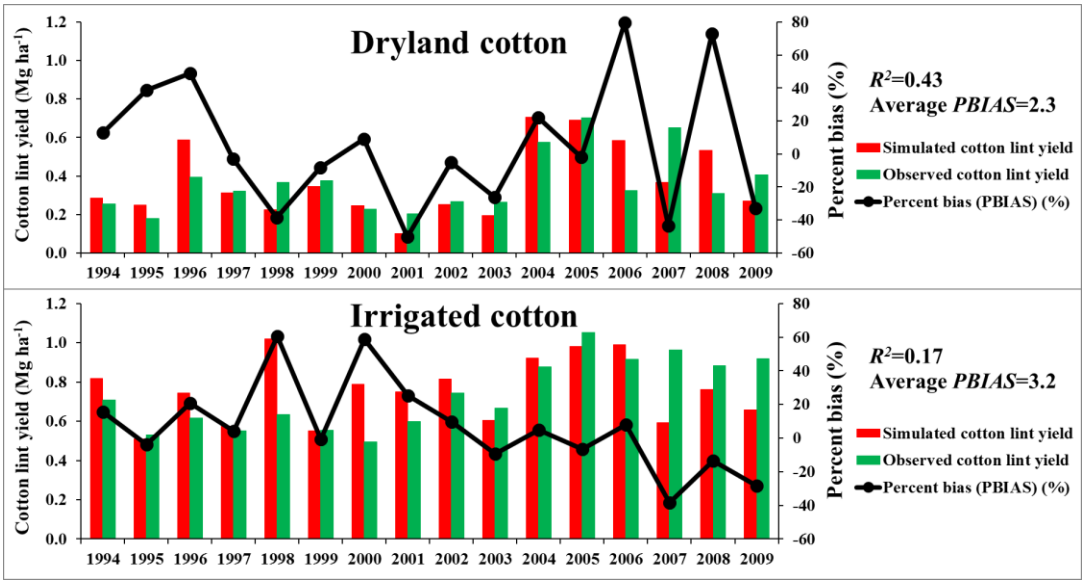


**Figure 5.4 Comparison of simulated and observed cotton lint yield in Lynn County under dryland and irrigated conditions.**

A graphical comparison of monthly simulated TN load with the LOADEST estimated data during the calibration (1995-1997) and validation (1998-2000) periods indicated that they matched fairly well (Figure 5.5). The *NSE* for monthly TN load predictions was 0.75 and 0.71 for the calibration and validation periods, respectively (Table 5.3). The *PBIAS* in predicting TN load was within ±25% during the calibration (-17%) and validation (16.8%) periods. The model performance ratings (*NSE* and *PBIAS)* achieved in this study for monthly TN load predictions during the calibration and validation periods were considered good according to Moriasi et al. (2007) criteria.

**Table 5.3 Model performance statistics during the model calibration and validation for monthly total nitrogen loads**

| Time scale | Calibration (1995-1997) | Validation (1998-2000) |
|---|---|---|
| Total nitrogen loads | | |
| Nash-Sutcliffe efficiency | 0.75 (Very good*) | 0.71 (Good) |
| $R^2$ | 0.81 | 0.86 |
| *PBIAS* (%) | -17.0 (Very good) | 16.8 (Very good) |

* General model performance ratings suggested by Moriasi et al. (2007) for monthly predictions of nitrogen

Observed number of data used in the LOADEST estimation for total nitrogen loads was 39

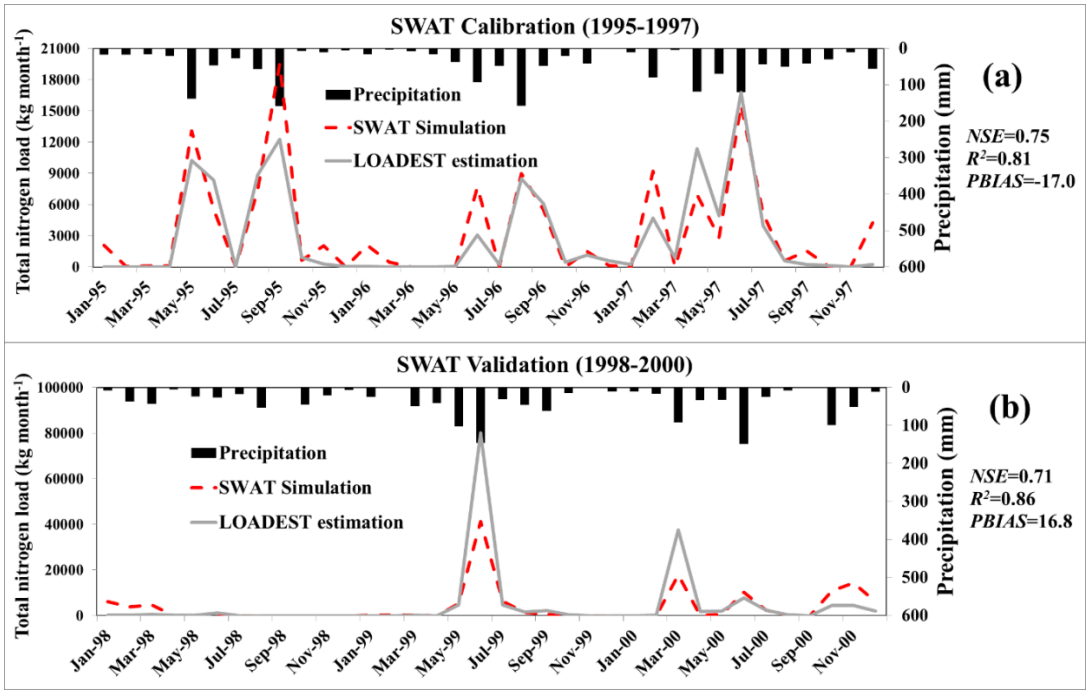


**Figure 5.5 Comparison of the LOADEST estimation and SWAT simulation total nitrogen loads on a monthly basis during a) calibration (1995-1997) and b) validation (1998-2000) periods.**

### *5.4.2 The Sensitivity of Watershed Hydrology, Water Quality and Crop Yield to the Changes in Historic Climate (1994-2009)*

#### 5.4.2.1 Increase in Atmospheric $CO_2$ Concentration

The results showed that the increases in atmospheric $CO_2$ concentration by 50% (run C I) and 100% (run C II) decreased the average (1994-2009) monthly ET of cotton with in the ranges of 2% to 6% and 5% to 12%, respectively, when compared to the baseline $CO_2$ concentration, especially during May to August (Figure 5.6a). The average annual (1994-2009) irrigation water use by cotton reduced by 11% and 26%, respectively, when the $CO_2$ concentration increased by 50% and 100% (Table 5.4). However, the elevated $CO_2$ concentration clearly increased the average monthly surface runoff, soil water content and TN load (Figure 5.6b-d). The average annual cotton lint yield also increased under both the irrigated (31% and 54% increase in yield with 50% and 100% increase in $CO_2$ concentration, respectively) and dryland (39% and 80%) conditions (Table 5.4). The effect of increase in ambient $CO_2$ concentration on the increase of cotton yield was also documented in previous Free Air $CO_2$ Enrichment (FACE: Mauney et al., 1994) and chamber experiments (Reddy et al., 1995 and 1996). The higher concentrations of $CO_2$ resulted in the higher photosynthesis rates and greater water and radiation use efficiencies (Pinter et al., 1994), which led to the yield increase.

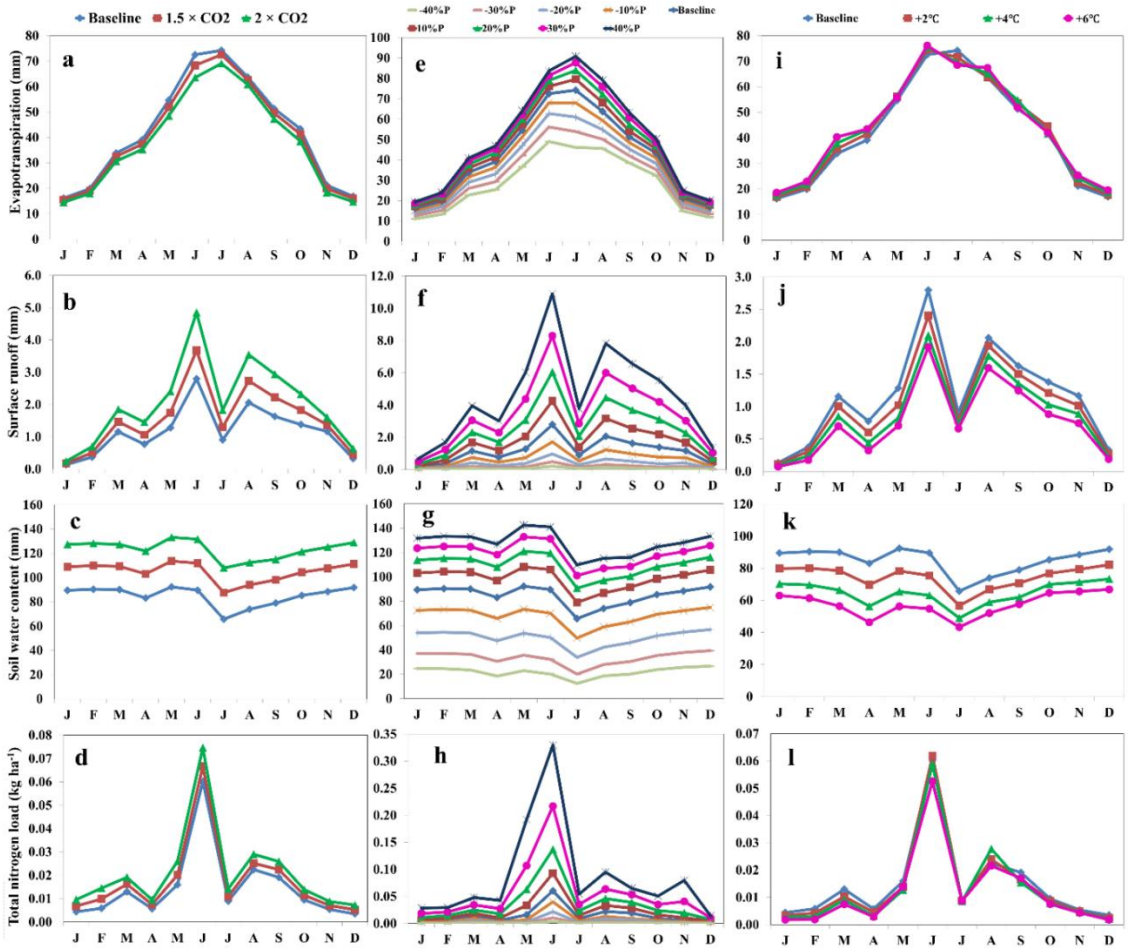


**Figure 5.6 Simulated mean (1994-2009) monthly evapotranspiration, surface runoff, soil water content, and total nitrogen load under different $CO_2$ concentration (a-d), precipitation (e-h), and air temperature (i-l) climate sensitivity analysis scenarios.**

The average annual ET of cotton decreased by 4% and 9%, and the surface runoff increased by 33% and 74% when $CO_2$ concentration was increased by 50% and 100%, respectively (Table 5.4). The stomatal apertures on plant leaves tend to close partially under the increased $CO_2$ concentration (Morison, 1987; Field et al., 1995; Saxe et al., 1998; Wand et al., 1999; Medlyn et al., 2001), and hence inhibit transpiration and thereby reduce ET. The simulated reduction in ET eventually caused an increase in surface runoff (Gedney et al., 2006). It was interesting to note an almost linear increase

in average monthly soil water content under cotton land use in response to the increase in $CO_2$ concentration (Figure 5.6c). The TN load under cotton land use increased approximately by 19% and 45% due to the increase in $CO_2$ concentration by 1.5 and 2 times, respectively, which was mainly due to a corresponding increase in the surface runoff.

**Table 5.4 Simulated average annual changes in water balance and water quality parameters and crop yield under various climate sensitivity analysis scenarios over historic period (1994-2009)**

| ξ Scenario | Climate parameters | Irrigation | ET | Surface runoff | TN load | Irrigated yield | Dryland yield |
|---|---|---|---|---|---|---|---|
| Baseline | Baseline (cotton) | 324.5 mm | 507 mm | 14.0 mm | 0.175 kg ha$^{-1}$ | 0.72 Mg ha$^{-1}$ | 0.37 Mg ha$^{-1}$ |
| Run C I | 1.5 × $CO_2$ | (-10.5)* | (-4.0) | (32.6) | (19.4) | (31.3) | (39.1) |
| Run C II | 2 × $CO_2$ | (-25.9) | (-9.4) | (74.0) | (44.6) | (53.6) | (79.7) |
| Run C III | -40% precipitation | (38.1) | (-31.5) | (-94.1) | (-94.9) | (-1.5) | (-49.3) |
| Run C IV | -30% precipitation | (29.2) | (-22.5) | (-85.2) | (-85.7) | (-1.1) | (-37.7) |
| Run C V | -20% precipitation | (19.1) | (-14.2) | (-68.1) | (-67.4) | (-0.8) | (-26.1) |
| Run C VI | -10% precipitation | (10.1) | (-6.6) | (-40.2) | (-41.7) | (-0.4) | (-13.8) |
| Run C VII | +10% precipitation | (-9.1) | (5.9) | (53.2) | (60.6) | (0.8) | (13.8) |
| Run C VIII | +20% precipitation | (-18.9) | (11.0) | (119.1) | (144.6) | (1.1) | (28.3) |
| Run C IX | +30% precipitation | (-27.1) | (15.7) | (199.5) | (279.4) | (1.9) | (42.0) |
| Run C X | +40% precipitation | (-34.4) | (19.8) | (294.7) | (488.6) | (1.9) | (54.3) |
| Run C XI | +2°C temp | (17.1) | (2.3) | (-12.9) | (-6.9) | (44.5) | (17.4) |
| Run C XII | +4°C temp | (25.4) | (3.9) | (-24.6) | (-10.9) | (47.5) | (4.3) |
| Run C XIII | +6°C temp | (29.6) | (4.9) | (-34.0) | (-18.9) | (17.4) | (-21.0) |
| Run PG I | 1.5 × $CO_2$ | (-15.1) | (-1.2) | (-3.0) | (-44.5) | [6.9] # | [27.9] |
| Run PG II | 2 × $CO_2$ | (-25.2) | (-1.9) | (-2.2) | (-40.7) | [11.7] | [43.5] |
| Run PG III | -40% precipitation | (3.4) | (0.4) | (-3.7) | (-44.4) | [1.1] | [-49.3] |
| Run PG IV | -30% precipitation | (0.1) | (0.1) | (-4.3) | (-48.0) | [0.3] | [-38.2] |
| Run PG V | -20% precipitation | (-1.7) | (-0.1) | (-4.5) | (-49.1) | [0.1] | [-25.4] |
| Run PG VI | -10% precipitation | (-4.9) | (-0.3) | (-4.5) | (-48.0) | [-0.1] | [-12.2] |
| Run PG VII | +10% precipitation | (-8.3) | (-0.9) | (-4.1) | (-54.8) | [0.2] | [10.8] |
| Run PG VIII | +20% precipitation | (-9.1) | (-1.2) | (-3.9) | (-58.6) | [0.5] | [19.3] |
| Run PG IX | +30% precipitation | (-9.7) | (-1.6) | (-4.4) | (-64.5) | [0.9] | [25.6] |
| Run PG X | +40% precipitation | (-13.2) | (-1.9) | (-5.7) | (-71.4) | [1.2] | [30.1] |
| Run PG XI | +2°C temp | (-29.1) | (-2.2) | (-4.4) | (-55.2) | [-18.2] | [-10.3] |
| Run PG XII | +4°C temp | (-33.0) | (-2.6) | (-5.2) | (-60.3) | [-27.4] | [-20.8] |
| Run PG XIII | +6°C temp | (-21.1) | (-1.7) | (-5.8) | (-59.2) | [-30.6] | [-30.4] |

*The number in the parentheses is the percent change of each analysis relative to the baseline

#The number in the brackets is the percent change of each climate sensitivity analysis relative to the land use of switchgrass or *Miscanthus* during the historic period (1994-2009)

ξ Letter C indicates cotton; Letters PG indicate perennial grasses

In comparison to baseline cotton scenario, under perennial grass land use, the elevated atmospheric $CO_2$ concentration reduced average annual irrigation water use (by 15% under PG I and 25% under PG II), ET (1% and 2%), surface runoff (3% and 2%) and TN load (45% and 41%). The increase in $CO_2$ concentration by 1.5 and 2 times increased biomass yield of irrigated switchgrass by 7% and 12%, respectively, and that of dryland *Miscanthus* by 28% and 44%, respectively (Table 5.4). The reduction in water stress days under the dryland conditions due to the increase in $CO_2$ concentration is the major reason for the much higher percent increase in dryland *Miscanthus* biomass yield compared to irrigated switchgrass. However, the simulated increases in irrigated switchgrass and dryland *Miscanthus* biomass yields due to increased $CO_2$ concentration were lower than the increases in cotton lint yields. This was because switchgrass and *Miscanthus*, which are C4 crops, are less sensitive to changes in atmospheric $CO_2$ concentration than cotton, which is a C3 crop (Ghannoum et al., 2000).

**5.4.2.2 Changes in Precipitation**

The increases/decreases in precipitation caused changes in monthly ET, surface runoff, soil water content and TN load under cotton land use in the respective directions (Figure 5.6e-h). For example, the -40%, -30%, -20%, -10%, +10%, +20%, +30% and +40% changes in precipitation (runs C III to C X) caused about -33%, -24%, -15%, -7%, 7%, 12%, 17% and 22% changes in average annual ET (Table 5.4). The simulated changes in cotton ET were substantial during May to September in this study watershed (Figure 5.6e). Surface runoff, soil water content and TN load under cotton land use were also very sensitive to changes in precipitation (Figure 5.6f-h, Table 5.4). For example,

the average annual surface runoff changed by 53% and -40% when annual precipitation was increased and decreased by 10%, respectively (Table 5.4). Similarly, TN load changed within a range of 61% to -42% due to ±10% changes in precipitation (Table 5.4). The simulated percent increase in surface runoff due to increase in precipitation (runs C VII to C X) was much larger than the percent reduction in surface runoff due to reduction in precipitation (runs C III to C VI) (Table 5.4). This result highlighted the high flooding potential of the study watershed during the wet years. Once again, the changes in precipitation caused an almost linear change in average monthly soil water content under cotton land use (Figure 5.6g).

As expected, the average annual irrigation water use by cotton increased within a range of 10% to 38% when precipitation was decreased (runs C III to C VI) and it decreased within a range of 9% to 34% when precipitation increased (runs C VII to C X) (Table 5.4). The requirement for a large amount of irrigation water due to the reduction in precipitation highlighted the risk of drought on cotton yields in this semi-arid watershed. By using BIOME-BGC ecosystem model, Jackson et al. (2001) also predicted an increased occurrence of drought in the northwest Texas of the United States under a future (2061-2090) climate scenario due to reduction in precipitation. The dryland cotton lint yields were also very sensitive to the changes in the precipitation. For example, cotton lint yield decreased by 26% with a 20% reduction in precipitation (Table 5.4).

The changes in precipitation under the perennial grasses land use will primarily decrease the average annual irrigation water use, ET, surface runoff and TN load when

compared to the respective changes in precipitation under the cotton land use (runs PG V to PG X). However, a slightly higher irrigation water use and ET were simulated under perennial grass land uses compared to the cotton land use under the extreme dry conditions (runs PG III and PG IV). The changes in precipitation had much smaller effect (within ±2%) on the simulated irrigated switchgrass biomass yield when compared to dryland *Miscanthus* biomass yield (Table 5.4). The simulated dryland *Miscanthus* biomass yield increased within a range of 11% to 30% when precipitation was increased between 10% and 40%, and decreased within a range of 12% to 39% when precipitation was decreased by 10% to 40% (Table 5.4).

#### 5.4.2.3 Increase in Air Temperature

Both the minimum and maximum temperatures were increased by 2℃, 4℃ and 6℃ in the climate sensitivity analysis. An apparent decrease in the average monthly surface runoff and soil water content under cotton land use were simulated when the air temperature was increased (Figure 5.6j and k). The results also suggested a slight increase in average monthly ET of cotton with the increase in temperature (Figure 5.6i and l). The annual analysis showed that the average ET of cotton increased by 2% to 5% when the air temperature was increased by 2℃ to 6℃ (runs C XI to C XIII) (Table 5.4). The average annual surface runoff decreased within a range of 13% to 34% with the increase in air temperature, mainly due to an increase in ET. The TN load under cotton land use was also reduced by 7%, 11% and 19% when the air temperature was increased by 2℃, 4℃ and 6℃, respectively (Table 5.4). Rind et al. (1990) and Schaake (1990) also reported that the higher temperatures would lead to higher ET, lower surface runoff, and

more frequent occurrence of drought events in the United States. A 30% increase in irrigation water use by cotton was simulated when the air temperature was increased by 6℃ (Table 5.4). The aforementioned results indicated that global warming might cause a serious water shortage in the semi-arid/arid regions.

The simulated cotton lint yield increased under both the irrigated and dryland conditions when the air temperature was increased by 2℃ and 4℃ (Table 5.4). The increase in cotton lint yield was much higher (45% to 48%) under the irrigated conditions when compared to the dryland conditions (4% to 17%). This was due to unlimited supply of irrigation water with the use of "auto-irrigation" option in the SWAT model. However, under practical conditions, application of higher amounts of irrigation water under warmer climatic conditions might not be possible due to reduced irrigation capacities. Interestingly, further increase in temperature by 6℃ reduced average cotton lint yield by 21% under the dryland conditions and caused relatively smaller increase (17%) in yield (compared to 2℃ and 4℃ increase in temperature) under the irrigated conditions. The optimal temperature for cotton growth is 27.5℃ (Hake and Silvertooth, 1990). Under the baseline condition, the mean air temperature of the cotton growing season for the study watershed was about 24℃. The simulated increase in average air temperature by 2℃ and 4℃ therefore provided better growth conditions for cotton than under the baseline conditions. However, a 6℃ increase in average air temperature resulted in non-optimum growing condition, and hence reduced cotton lint yields under the dryland conditions. Previous studies also reported that the optimum growth and yield of cotton occurred when the mean air temperature was about 28℃

(Reddy et al., 2000), and the cotton yield decreased substantially when the daily maximum temperature exceeded 32℃ (Schlenker and Roberts, 2009).

Similar to the effects of increase in $CO_2$ concentration, the increase in temperature decreased the average annual irrigation water use (by 29%, 33% and 21%), ET (2%, 3% and 2%), surface runoff (4%, 5% and 6%) and TN load (55%, 60% and 59%) under perennial grasses land use when compared to cotton land use (runs PG XI and PG XIII). A considerable reduction in the irrigated switchgrass biomass yield of 18%, 27% and 31% was simulated with the increase in the air temperature by 2℃, 4℃ and 6℃, respectively. Similarly, about 10% to 30% reduction in the dryland *Miscanthus* biomass yield was predicted due to the increase in air temperature by 2℃ to 6℃ (Table 5.4).

### *5.4.3 The Impacts of Climate and Land Use Changes on Hydrology, Water Quality and Crop Yield*

#### 5.4.3.1 Projected Changes in Future Climate of the Double Mountain Fork Brazos Watershed

According to the future climate data projected by 19 GCMs, the median annual precipitation would decrease by about 5% under the four future climate change scenarios (2040-2069 RCP4.5, 2040-2069 RCP8.5 and 2070-2099 RCP4.5) when compared to the historic period (Figure 5.7a). However, a slight increase in the precipitation during cotton growing period (May to October) was projected under the future climate change scenarios compared to the historic period. A high variation in annual precipitation was

projected among different GCMs, especially under the 2070-2099 RCP8.5 scenario with the changes ranging from -35% to 28% when compared to the historic period (Figure 5.7a). The median annual maximum air temperature increased by 2.8℃, 3.8℃, 3.5℃ and 5.8℃ under the 2040-2069 RCP4.5, 2040-2069 RCP8.5, 2070-2099 RCP4.5 and 2070-2099 RCP8.5 scenarios, respectively, relative to the historic period (Figure 5.7b). The median annual minimum air temperature also increased by 1.3℃, 2.1℃, 1.7℃ and 3.7℃ under the 2040-2069 RCP4.5, 2040-2069 RCP8.5, 2070-2099 RCP4.5 and 2070-2099 RCP8.5 scenarios, respectively (Figure 5.7c). The projected temperatures during the cotton growing period also showed similar increasing trends. The projected changes in precipitation, and maximum and minimum temperature for the study watershed over the mid-century were comparable to those projected by Modala et al. (2016) for the THP using the CMIP3 data. They predicted an increase in average daily minimum temperature by about 1.9 ºC to 2.9 ºC, increase in average daily maximum temperature by 2.0 ºC to 3.2 ºC, and decrease in precipitation by 30 to 127 mm in the future (2041 to 2070). The projected increase in temperature was the highest under the 2070-2099 RCP8.5 scenario, which had the highest projected $CO_2$ concentration (800 ppm) (Figure 5.7b-c). The projected increase in $CO_2$ concentration in the future is expected to trap heat, and hence warm the earth system (USEPA, 2015).

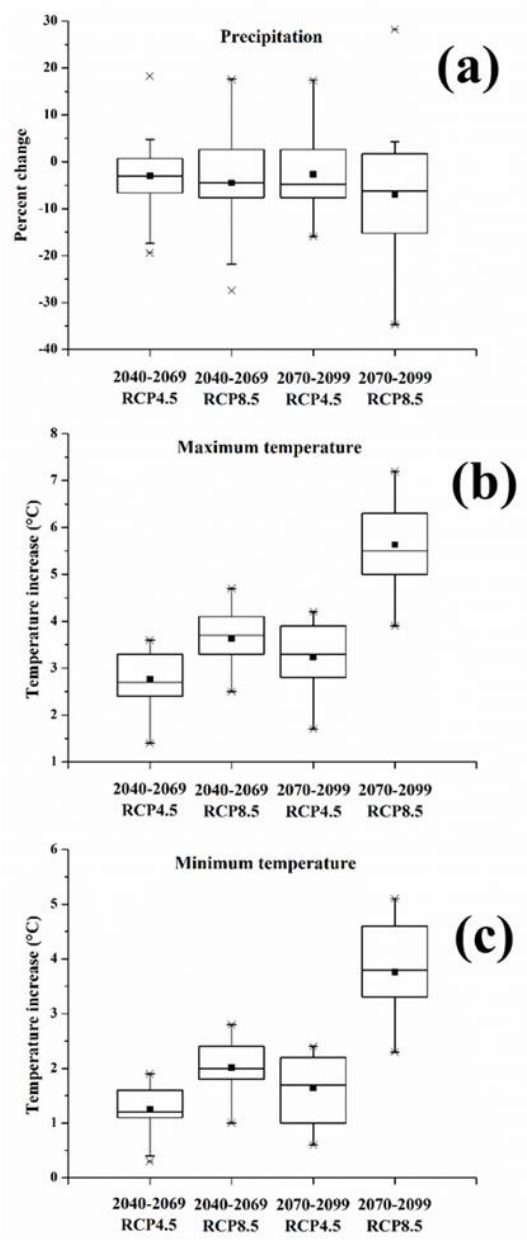


**Figure 5.7 Box plots showing changes in average annual (a) precipitation, (b) maximum air temperature, and (c) minimum air temperature based on 19 GCM projections under RCP4.5 and RCP8.5 scenarios during the 2040 to 2069 and 2070 to2099 time periods with reference to the historic period (1994-2009).**

#### 5.4.3.2 Climate Change Effects on Hydrology, Water Quality and Crop Yield under the Current (Cotton) Land Use

The simulated median annual ET under future cotton land use decreased by 12.1%, 13.9%, 14.2% and 20.2% under the 2040-2069 RCP4.5, 2040-2069 RCP8.5, 2070-2099 RCP4.5 and 2070-2099 RCP8.5 scenarios, respectively, relative to the historic period based on the 19 GCM projections (Figure 5.8a). The increase in $CO_2$ concentration from 330 to 800 ppm under different future climate scenarios was the major reason for this reduction in the simulated future ET under cotton land use. The stomatal apertures close partially under the elevated $CO_2$ concentration (Wand et al., 1999; Medlyn et al., 2001), and hence inhibit transpiration. The reduction in the future median annual ET caused reductions in the annual irrigation water use by cotton. The median annual irrigation water use for future cotton land use reduced by about 41% (ranged from 21% to 65% among different GCM projections), 45% (range: 20% to 76%), 46% (range: 23% to 67%) and 61% (range: 26% to 95%) under the 2040-2069 RCP4.5, 2040-2069 RCP8.5, 2070-2099 RCP4.5 and 2070-2099 RCP8.5 scenarios, respectively, compared to the historic period (Figure 5.8c). The decline in the future irrigation water use by cotton was much higher under the 2070-2099 RCP8.5 scenario when compared to other three future scenarios.

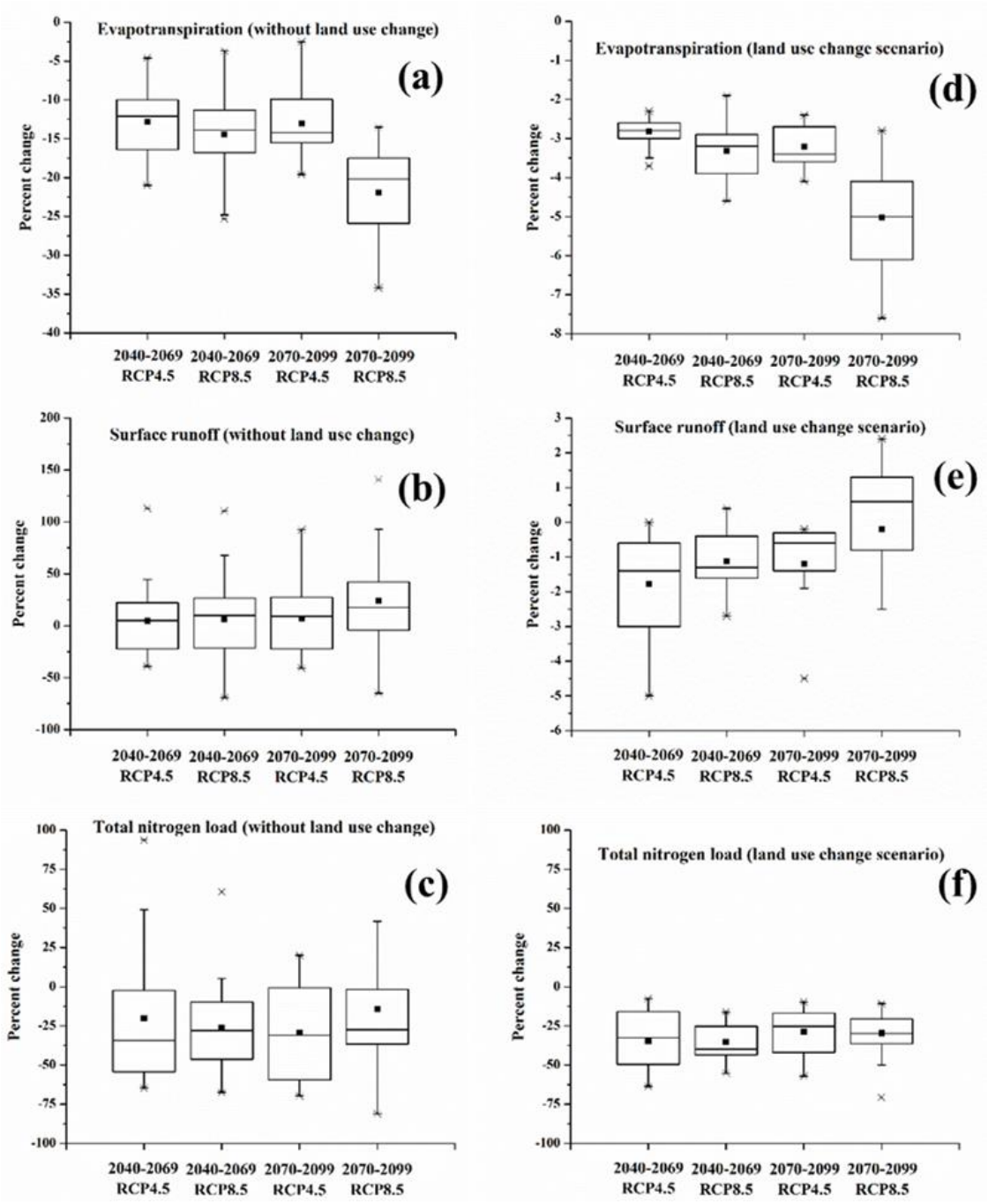


**Figure 5.8 Box plots showing average annual percent changes in evapotranspiration, surface runoff and total nitrogen load (for the entire watershed) based on 19 GCM projections under RCP4.5 and RCP8.5 scenarios during the 2040 to 2069 and 2070 to 2099 time periods compared to the base line cotton scenario over the historic period (1994-2009).**

Interestingly, the median annual surface runoff under cotton land use increased slightly under the four climate change scenarios although the simulated future ET and irrigation water use decreased. However, a large uncertainty existed. For example, under the 2040-2069 RCP4.5 scenario, 11 GCM projections simulated an increase in the surface runoff within a range of 4% to 113% relative to the historic period, while 8 GCMs projected a decrease in the surface runoff by about 1% to 39%. The climate sensitivity analysis also revealed that the surface runoff was very sensitive to the variations of the precipitation (Table 5.4). The large uncertainty in the simulated future surface runoff also emphasized that there was a high variation in the precipitation intensity projected by GCMs. Overall, the simulated future surface runoff under cotton land use ranged from -39% to 113%, -69% to 111%, -41% to 92% and -65% to 141% under the 2040-2069 RCP4.5, 2040-2069 RCP8.5, 2070-2099 RCP4.5 and 2070-2099 RCP8.5 scenarios, respectively, relative to the historic period (Figure 5.8b). The simulated median annual TN loads under cotton land use reduced by about 34%, 28%, 31% and 27% under the four climate change scenarios compared to the historic period. Similar to surface runoff, a large variation in TN load was simulated among different GCMs (Figure 5.8c).

The simulated future cotton lint yields increased under both irrigated (Figure 5.9a) and dryland (Figure 5.10a) conditions based on all 19 GCM projections under the four climate change scenarios. The median irrigated cotton lint yield increased by 69%, 82%, 78% and 91% under the 2040-2069 RCP4.5, 2040-2069 RCP8.5, 2070-2099 RCP4.5 and 2070-2099 RCP8.5 scenarios, respectively, relative to the historic period (Figure

5.9a). Corresponding increases in dryland cotton lint yields under the four climate change scenarios were 100%, 114%, 104% and 129% (Figure 5.10a). The increase in projected future irrigated cotton lint yield was primarily because of the reduction in temperature stress days during May to October (cotton growing period) (Figure 5.9b). However, in case of dryland conditions, both temperature and water stress days reduced during the cotton growing period (Figure 5.10b and c), which resulted in a much higher percent increase in the dryland cotton lint yield as compared to the increases in irrigated cotton lint yield (Figure 5.9a and Figure 5.10a). The optimal temperature for cotton growth is about 27℃ to 28℃ (Reddy et al., 2000). The projected increase in average air temperature by about 3℃ to 5℃ during the cotton growing period would provide better conditions for cotton growth compared to the average air temperature of 24℃ during the historic period. The projected increase in cotton lint yield would lead to an increase in plant nitrogen uptake, which could eventually result in the reduction in TN load through surface runoff.

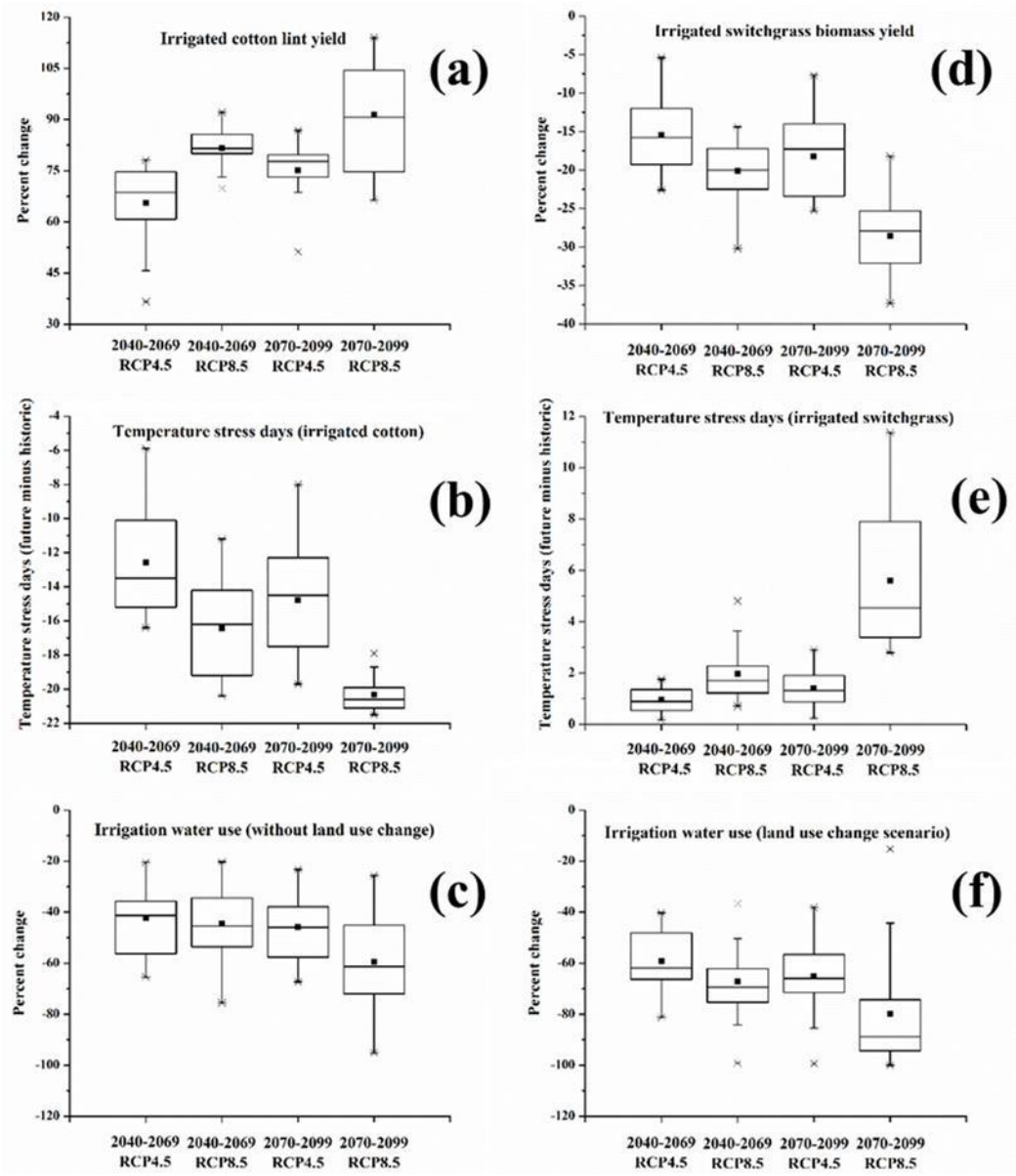


**Figure 5.9 Box plots showing changes in average annual irrigated crop yields, irrigation water use and number of temperature stress days based on 19 GCMs under RCP4.5 and RCP8.5 scenarios during the 2040 to 2069 and 2070 to 2099 time periods compared to the historic period (1994-2009). Irrigation water use under future switchgrass land use was compared to that under the baseline cotton scenario.**

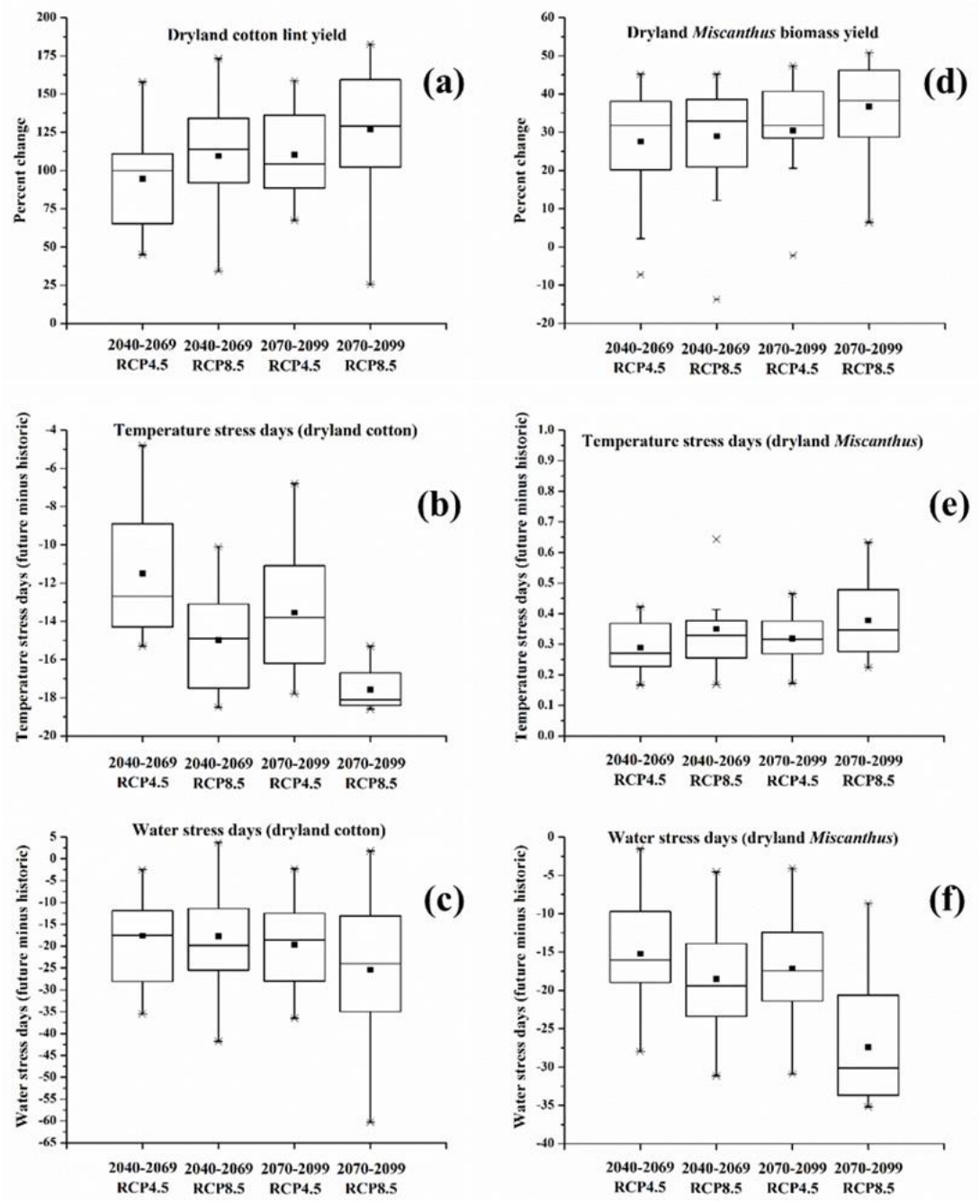


**Figure 5.10 Box plots showing changes in average annual dryland crop yields, and number of temperature and water stress days based on 19 GCM projections under RCP4.5 and RCP8.5 scenarios during the 2040 to 2069 and 2070 to 2099 time periods compared to the historic period (1994-2009).**

#### 5.4.3.3 Combined Effects of Land Use and Climate Changes on Hydrology, Water Quality and Crop Yield

The simulated median annual ET under the future perennial grass land use scenarios of 2040-2069 RCP4.5, 2040-2069 RCP8.5, 2070-2099 RCP4.5 and 2070-2099 RCP8.5 was smaller than that under respective future cotton land use scenarios according to the 19 GCM projections (Figure 5.8d). In addition, the simulated future median irrigation water use of switchgrass was less by 62%, 69%, 66% and 89% than that of cotton under the 2040-2069 RCP4.5, 2040-2069 RCP8.5, 2070-2099 RCP4.5 and 2070-2099 RCP8.5 scenarios, respectively (Figure 5.9f). The decrease in the irrigation water use under the future perennial grass land uses relative to the future cotton land use was simulated in case of all GCM projections.

The simulated future changes in median annual surface runoff under four climate change scenarios were negligible under the perennial grass land uses compared to those under the future cotton land use scenarios (please note the differences in Y-axis scales) (Figure 5.8e). However, the simulated future median annual TN load under the perennial grasses reduced by about 33%, 40%, 25% and 30% under the 2040-2069 RCP4.5, 2040-2069 RCP8.5, 2070-2099 RCP4.5 and 2070-2099 RCP8.5 scenarios, respectively relative to those under the future cotton land use scenarios (Figure 5.8f). Sarkar and Miller (2014) also reported that the SWAT-simulated long-term (15 years) nitrogen losses under the switchgrass land use were approximately 73% lower than those under the cotton land use in the Black Creek watershed in South Carolina. In contrast to surface runoff, large variations in the simulated future TN load were noticed between the

future perennial grass and cotton scenarios. The perennial grasses uptake much higher amounts of nitrogen from the soil compared to cotton (Chen et al., 2016c) and hence lesser quantities of nitrogen are available for the loss via surface runoff.

A decline in the irrigated switchgrass biomass yield, and an increase in the dryland *Miscanthus* biomass yield was simulated under the GCM projections of the four climate change scenarios when compared to respective land use scenarios under the historic period (Figure 5.9d and Figure 5.10d). The primary reason for the decline of irrigated switchgrass biomass yield based on the 19 GCM projections under the four climate change scenarios in this study was the global warming effect (Figure 5.9e). The irrigated switchgrass underwent larger number of temperature stress days during its major growing period (June to September) due to the increase in air temperature under the four climate change scenarios than the historic period (Figure 5.9e). The increase in dryland *Miscanthus* biomass yield was due to the decrease in water stress days during its major growing period (June to September) under the four climate change scenarios (Figure 5.10f). In addition, *Miscanthus* can adapt to wider crop growth temperatures (optimal: 25℃; minimum: 8℃) compared to switchgrass (optimal: 25℃; minimum: 12℃), which resulted in a lower number of temperature stress days in case of *Miscanthus* when compared to switchgrass under climate change scenarios (Figure 5.9e and Figure 5.10e).

## 5.5 Conclusions

The SWAT model was used to investigate the influences of elevated $CO_2$ concentration, increasing temperatures and variations in precipitation on hydrology, water quality and crop yield based on 19 GCM projections under four climate change scenarios in the Double Mountain Fork Brazos watershed of the THP. The climate sensitivity analysis suggested that the water cycle, TN load and crop yield of the study watershed were very sensitive to the changes in climate. For example, a 10% decrease in precipitation is expected to result in a 40% reduction in average (1994-2009) annual surface runoff and a corresponding 42% decrease in TN load. The water balances, TN load and crop yield were also simulated to alter substantially according to the projected climate of 19 GCMs under four climate change scenarios. The simulated median annual TN loads reduced by about 34%, 28%, 31% and 27% under the 2040-2069 RCP4.5, 2040-2069 RCP8.5, 2070-2099 RCP4.5 and 2070-2099 RCP8.5 scenarios, respectively, when compared to the historic cotton land use. The potential land use change from irrigated cotton to irrigated switchgrass in the future was projected to enhance water conservation due to reduction in ET losses and hence groundwater use for irrigation under future climate scenarios. In addition, biofuel-induced land use change from cotton to perennial grasses was found to improve water quality by reducing discharge of the TN load by approximately 30% at the watershed outlet. A considerable increase in median biomass yields within a range of 32% to 38% was also predicted under the dryland *Miscanthus* land use under the four climate change scenarios. The results from this study indicated that the irrigated switchgrass land use would be more suitable for the study

watershed under the current climatic conditions when compared to the irrigated cotton land use. However, under future climate scenarios, irrigated switchgrass yields were projected to reduce within a range of 16% to 28% when compared to historic yields. Under dryland conditions, *Miscanthus* land use was found to be more appropriate under the future climate situations. The elevated $CO_2$ concentrations and reduced water stress days were the major factors for the increase in *Miscanthus* biomass. While the occurrence of future climatic conditions remain indefinite, this study provided an overview of the impacts of climate change and land use change on the orientation and magnitude of water balances, water quality and crop production. This type of studies can provide valuable information regarding the selection of appropriate land uses and the associated best management practices for the study watershed under the changing climate.

# 6. USING EDDY COVARIANCE DATA FOR CALIBRATING HYDROLOGY MODELS FOR ASSESSING LAND USE CHANGE IMPLICATIONS

## 6.1 Synopsis

The semi-arid Texas High Plains (THP) is one of the most important cotton (*Gossypium hirsutum* L.) production regions in the US. This region also holds enormous potential for growing cellulosic bioenergy crops, such as the native grass of Old World bluestem [*Bothriochloa bladhii* (Retz) S.T. Blake] and biomass sorghum [*Sorghum bicolor* (L.) Moench]. A comparison of hydrological responses of potential land use changes from cotton to cellulosic bioenergy crops enables assessment of feasibility for the proposed land use change. The One Hydrologic Response Unit (HRU) method available in the Soil and Water Assessment Tool (SWAT) model was used in this study for assessing the land use change impacts at the field-scale. The model was calibrated and validated using three-years (2013 to 2015) eddy covariance data on daily evapotranspiration (ET) and bi-weekly crop biomass from four field sites in the THP. These fields were planted to dryland cotton, irrigated cotton, biomass sorghum and Old World bluestem (simulated as big bluestem in SWAT). Good match between the simulated and observed daily ET was achieved during the model evaluation for all four land uses with the Nash-Sutcliffe efficiency (*NSE*) of > 0.5 and percent bias (*PBIAS*) within ±25%. Model was also evaluated reasonably well for aboveground biomass prediction at the four sites as indicated by the model performance statistics: *NSE* > 0.5, $R^2$ > 0.6 and *PBIAS* within ±10%. Land use change scenario analysis showed that the

average annual (1994-2015) surface runoff decreased by 86% and 52% under the dryland big bluestem and dryland biomass sorghum scenarios, respectively, relative to the dryland cotton land use. Under the irrigated conditions, the average annual surface runoff reduced by 64% and 19%, respectively, under the big bluestem and biomass sorghum scenarios compared to the irrigated cotton land use. The net groundwater use (irrigation water use minus percolation) was reduced by 11% and 48% under the irrigated biomass sorghum and irrigated big bluestem scenarios, respectively, relative to the irrigated cotton land use. About 2.5, 3.1, 10.7 and 15.8 Mg $ha^{-1}$ of biomass could potentially be produced if cotton was replaced by dryland big bluestem, irrigated big bluestem, dryland biomass sorghum and irrigated biomass sorghum, respectively. Finally, biomass sorghum was found to be an ideal bioenergy crop for the study area due to lower groundwater water use, greater biomass and biofuel production potential and lower surface runoff potential compared to cotton or big bluestem.

## 6.2 Introduction

Hydrologic and water quality (H&WQ) models are widely used for assessing the impacts of land use and climate changes at various spatial scales. These models need to be thoroughly calibrated and validated against the observed data before using them for any application/decision making. In most of the watershed-scale studies, H&WQ models are calibrated using the measured data on streamflow and nitrogen loads at the watershed outlet (Wellen et al., 2015). A very limited number of studies have used field data at multiple locations in the watershed for calibrating the H&WQ models. Based on an

assessment of a sample of 257 process-based watershed modeling papers published between 1992 and 2010, Wellen et al. (2015) found that the models were calibrated for more than one location spatially in only 19% of the studies. They also reported that in about 96% of studies, models were calibrated based on streamflow, and in the remaining 4% of studies, models were calibrated using surface runoff. They have therefore found that none of the studies evaluated the ability of their models to predict any other hydrological parameters. Researchers have cautioned that the watershed-scale model calibration based on measured data on a single hydrologic parameter from only one spatial location in a watershed could lead to incorrect conclusions as errors in the prediction of one hydrologic parameter can be compensated by errors in prediction of another hydrological parameter in the opposite sign (Beven, 2006; Kirchner, 2006). Modelers are therefore emphasizing the need for using other observed hydrological data from multiple sites in the watershed in addition to streamflow for calibrating hydrologic models at the watershed scale. In addition, it is worth noting that the USGS gauges do not exist in a lot of watersheds, especially in the semi-arid THP region, and calibrating H&WQ models for such ungauged watershed watersheds becomes a challenge.

Recently, the eddy covariance method has been widely used around the world for studying the hydrologic cycles of different ecosystems (Yamamoto et al., 2001; Baldocchi, 2003; Dolman et al., 2006; Yu et al., 2006). In the US, the network of AmeriFlux (fluxnetweb.ornl.gov) maintains the flux data from approximately 200 sites and this data is made available to researchers on a collaborative basis. Use of such detailed field-scale data for calibrating the H&WQ models could greatly improve the

model predictions. The eddy covariance method is used to directly measure the exchange of water between the vegetation surface and atmosphere. In the eddy covariance method, latent heat flux or evapotranspiration (ET) is determined as the covariance between vertical wind velocity and water vapor concentration (Goulden et al., 1996; Ham and Heilman, 2003; Rajan et al., 2010). Measurements of wind velocity and water vapor concentration are made using fast-response instruments.

Very few studies have reported the use of eddy covariance flux data from multiple sites in the calibration of the Soil and Water Assessment Tool (SWAT) model (Zhang et al., 2013). The SWAT model divides a watershed into a number of Hydrologic Response Units (HRUs) and aggregates them into subbasins. An HRU is a basic computational unit in the SWAT model and it is assumed to be homogeneous in hydrologic response to changes in land use and management since it contains the same land use, soil type and soil slope. An HRU in the SWAT model therefore makes it a good representation of the field conditions. This modeling structure in the SWAT model enables simulation of hydrologic and water quality responses for a single HRU, and hence making the model useful for field-scale assessments. This emerging One-HRU method in the SWAT model is a very flexible and time-saving method. In this study, the data collected from four eddy covariance flux towers set up in dryland cotton, irrigated cotton, irrigated biomass sorghum [*Sorghum bicolor* (L.) Moench] and dryland Old World bluestem [*Bothriochloa bladhii* (Retz) S.T. Blake] (simulated as big bluestem in SWAT) fields in the study watershed was used for calibrating the SWAT One-HRU

model at the field-scale. The flux data used in this study include the continuous measurements of daily ET and bi-weekly crop biomass from 2013 to 2015.

The overall goal of this study was to calibrate the SWAT One-HRU model using the eddy covariance data and then use it for evaluating the field-scale hydrologic impacts of land use change from cotton to cellulosic bioenergy crops. Specifically, the objectives of this study were to: (1) calibrate the SWAT model against the daily eddy covariance ET and bi-weekly crop biomass data from multiple sites using the One-HRU method, (2) assess the field-scale hydrological responses of land use change from cotton to the perennial crop of big bluestem and annual crop of biomass sorghum, and (3) estimate the biofuel production by replacing cotton with big bluestem and biomass sorghum.

## 6.3 Materials and Methods

### *6.3.1 Study Sites*

Four study sites - dryland cotton, irrigated cotton, irrigated biomass sorghum and dryland Old World bluestem (simulated as big bluestem in the SWAT model) - were used in this study. These sites are located near Plainview, Texas. The long-term (1990-2015) average annual precipitation for this region is about 514 mm, and the long-term average annual maximum and minimum temperatures are 23°C and 8°C, respectively. The topography of the four fields are very flat with slope < 1%. The primary soil type in the study sites is Pullman clay loam (fine, mixed, superactive, thermic Torrertic Paleustoll) (Soil Survey Staff, 2010). The specific planting and harvesting dates of the fields from 2013 to 2015 are listed in Table 6.1. Conventional tillage was used for irrigated cotton,

dryland cotton and biomass sorghum fields before planting. About 137 kg $ha^{-1}$ of anhydrous ammonia and 33.6 kg $ha^{-1}$ phosphorus were applied to the irrigated cotton each year around May 7 (Table 6.2). No fertilizer was applied to dryland cotton and dryland big bluestem. About 384 kg $ha^{-1}$ of urea and 33.6 kg $ha^{-1}$ phosphorus were applied to the biomass sorghum around May 15 (Table 6.2). The center-pivot irrigation system was used to apply water to irrigated cotton and biomass sorghum fields.

**Table 6.1 Planting and harvesting dates of irrigated cotton, dryland cotton, biomass sorghum and big bluestem**

| 2013 | Irrigated cotton | Dryland cotton | Biomass sorghum | Big bluestem |
|---|---|---|---|---|
| Planting date | May 31 | Crop failure | May 20 | 2007 |
| Harvesting date | November 7 | Crop failure | October 8 | November 15 |
| 2014 | | | | |
| Planting date | June 9 | June 1 | May 20 | |
| Harvesting date | November 10 | October 15 | October 14 | November 15 |
| 2015 | | | | |
| Planting date | June 1 | June 1 | June 4 | |
| Harvesting date | November 9 | Without harvesting | October 1 | November 15 |

**Table 6.2 Simulated management practices for cotton, biomass sorghum and big bluestem in SWAT**

| No. | Operations | Description | Input data |
|---|---|---|---|
| Irrigated cotton | | | |
| 1 | Tillage Parameters (Tillage on May 10) | | |
| | TILL_ID | Tillage ID | Generic Fall Plowing[#] |
| 2 | Fertilizer Application Parameters (May 15)* | | |
| | FERT_ID | Fertilizer ID | Anhydrous Ammonia |
| | FRT_KG | Amount of fertilizer applied to HRU | 137 (kg $ha^{-1}$) |
| 3 | Fertilizer Application Parameters (May 15) | | |
| | FERT_ID | Fertilizer ID | Elemental Phosphorus |
| | FRT_KG | Amount of fertilizer applied to HRU | 33.6 (kg $ha^{-1}$) |
| 4 | Begin Growing Season Parameters ( Planting on June 3) | | Default |
| | Heat units to maturity | | 2354℃-day ξ |
| 5 | Auto-irrigation Parameters (Start date: June 3; End date: November 9) | | |
| | WSTRS_ID | Water stress identifier | Plant Water Demand |
| | IRR_SCA | Irrigation source | Shallow Aquifer |
| | AUTO_WSTRS | Water stress threshold | 0.9 |
| | IRR_EFF | Irrigation efficiency | 0.80[#] |
| 6 | Harvest and Kill Parameters (Kill on November 9) | | Default |
| Dryland cotton | | | |
| 1 | Tillage Parameters (Tillage on May 10) | | |
| | TILL_ID | Tillage ID | Generic Fall Plowing[#] |
| 2 | Begin Growing Season Parameters (Planting on June 1) | | Default |
| | Heat units to maturity | | 2354℃-day ξ |
| 3 | Harvest and Kill Parameters (Kill on October 15) | | Default |
| Irrigated biomass sorghum | | | |
| 1 | Tillage Parameters (Tillage on May 10) | | |
| | TILL_ID | Tillage ID | Generic Fall Plowing[#] |
| 2 | Fertilizer Application Parameters (May 18) | | |
| | FERT_ID | Fertilizer ID | Urea |
| | FRT_KG | Amount of fertilizer applied to HRU | 384 (kg $ha^{-1}$) |
| 3 | Fertilizer Application Parameters (May 18) | | |
| | FERT_ID | Fertilizer ID | Elemental Phosphorus |
| | FRT_KG | Amount of fertilizer applied to HRU | 33.6 (kg $ha^{-1}$) |
| 4 | Begin Growing Season Parameters (Planting on May 25) | | Default |
| | Heat units to maturity | | 1295℃-day ξ |
| 5 | Auto-irrigation Parameters (Start date: May 25; End date: October 8) | | |
| | WSTRS_ID | Water stress identifier | Plant water demand |
| | IRR_SCA | Irrigation source | Shallow aquifer |
| | AUTO_WSTRS | Water stress threshold | 0.9 |
| | IRR_EFF | Irrigation efficiency | 0.80 |
| 6 | Harvest and Kill Parameters (Kill on October 8) | | Default |
| Dryland big bluestem | | | |
| 1 | Begin Growing Season Parameters (Planting on May 15) | | Default |
| | Heat units to maturity | | 1800℃-day ξ |
| 2 | Harvest (only) Parameters (Harvest on November 15) | | Default |

*The specific dates of the management practices were assigned based on the average value of the date from 2013 to 2015 in the fields

ξ Heat units to maturity for cotton and winter wheat were estimated using the SWAT-PHU program (http://swat.tamu.edu/software/potential-heat-unit-program/)

### *6.3.2 ET Data Collection and Analysis*

Four eddy covariance flux towers were established in the center of the study fields at the beginning of planting in 2013. The flux tower instruments included a three-dimensional sonic anemometer (CSAT-3D, Campbell Scientific, Logan, UT) for measuring wind and an open-path infrared gas analyzer (IRGA Model LI-7500, LI-COR, Lincoln, NE) for measuring water vapor concentrations in the ambient atmosphere. These instruments were placed on the tower facing into the prevailing wind direction (south-west) at a height of 1.5 m above the top of the canopy. Other meteorological measurements made at the flux tower site included net radiation (Kipp & Zonen NR-Lite net radiometer), global irradiance (LI-190SB pyranometer, LI-COR, Lincoln, NE), air temperature and relative humidity (HMP50, Campbell Scientific, Logan,UT), and precipitation (TE525 rain gauge, Campbell Scientific, Logan, UT). Soil volumetric water content at 4 cm below the surface was measured using time domain reflectometry sensors (CS-616, Campbell Scientific, Logan, UT). Data from the IRGA and sonic anemometer were measured at 10Hz sampling rate and stored in a memory card on a CR3000 data logger for further analysis. Data from the meteorological sensors were measured at 5-sec intervals using the same CR3000 data logger and data were stored as 30-min average values. More detail about the flux tower instruments can be found in Rajan et al. (2013).

The high frequency water vapor and wind velocity data were analyzed using EddyPro 4.0 software (LI-COR Biosciences, Lincoln, NE) to output 30-min average

values of latent heat flux (LE). The 30-min LE data was converted to ET using the following equation:

$$A = \frac{LE}{\rho\lambda}$$

where LE is latent heat flux in J $s^{-1}$, ρ is the density of water (1000 kg $m^{-3}$) and λ is the latent heat of vaporization (2.5 x $10^6$ J $kg^{-1}$).

### *6.3.3 Plant Data*

The aboveground crop biomass data were collected at biweekly intervals during the crop growing season from 2013 to 2015. Plant samples were dried at 65˚C, and the dry weight of plants were obtained in the laboratory.

### *6.3.4 SWAT Model Setup*

#### 6.3.4.1 Topography, Soil and Slope

The 30 m horizontal resolution Digital Elevation Model (DEM) of Hale and Floyd Counties, which contains all four flux tower sites, was downloaded from the U.S. Geological Survey (http://viewer.nationalmap.gov/viewer/#) and input to the SWAT model. The DEM was useful for estimation of watershed topography related parameters for the study sites. The finer-scale soils data from the Soil Survey Geographic Database (SSURGO) (Soil Survey Staff, 2015) was used in this study. Three slope classes were used to classify the study sites according to soil slope: < 0.5%, 0.5%-1% and > 1%. For the HRU definition, thresholds of 0% were used for land use, soil type and slope.

#### 6.3.4.2 Climate Data

Daily climate data (wind velocity, solar radiation, precipitation, maximum temperature and minimum temperature) for each site from 2013 to 2015 was obtained from the onsite gauges on flux towers. The missing climate data for this period was filled with climate data obtained from the National Climatic Data Center (NCDC) (NOAA-NCDC, 2016). Weather data from 1992 to 2012 period were also obtained from the NCDC weather stations that are closest to the study sites, and used in long-term simulations.

### *6.3.5 SWAT Model Calibration*

In this study, ArcSWAT (Version 2012_2.18 released on 9/9/15) for the ArcGIS 10.2.2 platform was used. The model simulation period was from 1992 to 2015. The model warmup period was from 1992 to 1993. The calibration and validation periods were from 01/01/2013 to 12/31/2014 and 01/01/2015 to 12/31/2015, respectively. Before using a model, key parameters and initial state variables need to be determined. One calibration strategy that has been adopted in multiple model assessment and intercomparison projects consists of parameterizing variables based on prior information (e.g. from literature or field experiments) without attempting to extensively calibrate parameters to match observed variables of interest (Schwalm et al., 2010; Srinivasan et al., 2010; Zhang et al., 2015b), and the same strategy was adopted in this study. In this case, model performance is highly dependent on the quality of input data. Therefore, more focus was placed on deriving data-based agroecosystem parameters to characterize

cropping systems across the study sites and using state-of-the-art geospatial data to drive the SWAT model.

**Table 6.3 Literature and calibrated values of some important hydrologic and crop parameters in SWAT**

| No. | Parameter | Description | Literature value* | Calibrated value | Reference |
|---|---|---|---|---|---|
| Hydrologic parameters | | | | | |
| 1 | ESCO | Soil evaporation compensation factor | 0.855 | 0.90 | -- |
| 2 | EPCO | Plant uptake compensation factor | 1.0 (Default) | 0.8 | -- |
| 3 | SOL_AWC | Available soil water capacity (mm $H_2O$ $mm^{-1}$ soil) | 0.18 (Default) | 0.16 | -- |
| 4 | CN2 | Curve number for moisture condition II | Decreased by 9% | Decreased by 10% | -- |
| Dryland cotton parameters | | | | | |
| 1 | BIO_E | Biomass/energy ratio [(kg $ha^{-1}$)/(MJ $m^{-2}$)] | 25 (Default) | 30 | -- |
| 2 | BLAI | Max leaf area index ($m^2/m^2$) | 4 | 2.5 | Sarkar et al., 2011 |
| 3 | EXT_COEF | Light extinction coefficient | 0.65 (Default) | 0.8 | Sarkar et al., 2011 |
| Irrigated cotton parameters | | | | | |
| 1 | BIO_E | Biomass/energy ratio [(kg $ha^{-1}$)/(MJ $m^{-2}$)] | 25 (Default) | 30 | -- |
| 2 | BLAI | Max leaf area index ($m^2/m^2$) | 5.98 | 8.0 | -- |
| 3 | EXT_COEF | Light extinction coefficient | 0.78 | 0.8 | Sarkar et al., 2011 |
| Irrigated biomass sorghum parameters | | | | | |
| 1 | BIO_E | Biomass/energy ratio [(kg $ha^{-1}$)/(MJ $m^{-2}$)] | 35 (Default) | 45 | -- |
| 2 | BLAI | Max leaf area index ($m^2/m^2$) | 5.0 (Default) | 8.0 | -- |
| Dryland big bluestem parameters | | | | | |
| 1 | BIO_E | Biomass/energy ratio [(kg $ha^{-1}$)/(MJ $m^{-2}$)] | 14 (Default) | 10.3 | -- |
| 2 | BLAI | Max leaf area index ($m^2/m^2$) | 2.5 (Default) | 2.3 | -- |

* Chen, Y., Ale, S., Rajan, N., Morgan, C.L.S., Park, J.Y. 2016. Hydrological responses of land use change from cotton (*Gossypium hirsutum* L.) to cellulosic bioenergy crops in the Southern High Plains of Texas, USA. Global Change Biology Bioenergy. 8:981-999.

When available, the data collected at the study sites (e.g. climate data for 2013-2015) were used. The finer-scale SSURGO soils data was also used to accurately parameterize the model. In addition, important parameters and initial state variables were taken from the SWAT model calibrated for the adjacent Double Mountain Fork Brazos

watershed in the THP (Section 2; Chen et al., 2016a). Finally, these parameters and some additional parameters were manually adjusted to get a good fit between the simulated and observed data. The calibrated values of some important hydrologic and crop parameters are listed in Table 6.3.

### *6.3.6 Model Performance Assessment*

The SWAT model performance in predicting daily ET during calibration and validation periods was evaluated using three different statistical measures: percent bias (*PBIAS*), Nash-Sutcliffe efficiency (*NSE*) (Nash and Sutcliffe, 1970) and square of Pearson's product-moment correlation coefficient ($R^2$) (Legates and McCabe, 1999). In this study, we aimed to achieve *NSE*, $R^2$ and *PBIAS* of > 0.5, > 0.6 and within ±15%, respectively, during the model calibration and validation periods. The model's performance in simulations of aboveground crop biomass was also assessed using *NSE*, $R^2$ and *PBIAS* and our goal was to achieve *NSE*, $R^2$ and *PBIAS* of > 0.5, > 0.6 and within ±10%, respectively, during the entire simulation period.

### *6.3.7 Land Use Change Scenario Analysis*

After achieving a satisfactory calibration of the SWAT One-HRU model, hypothetical land use change scenario analysis was conducted. Big bluestem and biomass sorghum were hypothetically selected to replace cotton. The annual impacts of land use change on water balances were evaluated over the period from 1994 to 2015. The impacts were assessed under both dryland and irrigated conditions.

The management practices for big bluestem and biomass sorghum were set up in the SWAT model according to the actual practices followed at the field sites. Big bluestem was planted on May 15 of 1992 and harvested without killing on November 15$^{th}$ of each year for biomass (Table 6.2). Biomass sorghum was planted on May 25 and harvested on October 8 in each year. In the scenarios where big bluestem and biomass sorghum replaced irrigated cotton, they were also assigned the same irrigation management practices as the irrigated cotton. For management of big bluestem as a bioenergy crop, about 270 and 180 kg ha$^{-1}$ of urea was applied to irrigated and dryland big bluestem, respectively (Yimam et al., 2014). About 384 and 192 kg ha$^{-1}$ of urea was applied to irrigated and dryland biomass sorghum, respectively, based on the field observations in this study (Table 6.2). Conventional tillage was used for both irrigated and dryland biomass sorghum. No tillage was simulated for big bluestem.

## 6.4 Results and Discussion

### *6.4.1 Evaluation of the SWAT One-HRU Model for ET Prediction*

#### 6.4.1.1 Cotton

The *NSE*, $R^2$ and *PBIAS* values obtained during the model calibration (2014) and validation (2015) periods for the prediction of daily ET from the dryland cotton field were 0.61 and 0.52, 0.65 and 0.56, 1.0% and -8.6%, respectively (Figure 6.1). Although considered as satisfactory, lower *NSE* value obtained for the dryland cotton field during the validation period was probably due to differences in precipitation data input into the model and the actual precipitation that occurred in the field in April and May of 2015

(Figure 6.1b). The onsite rain gauge was broken during this time, and hence the adjacent rain gauge from the big bluestem field was used for the dryland cotton field.

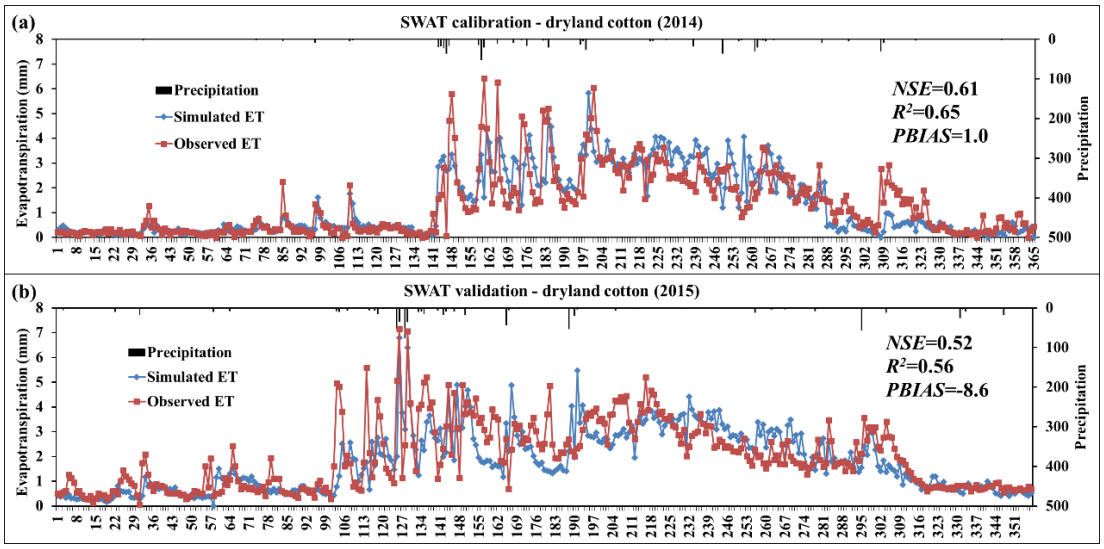


**Figure 6.1 Comparison of observed and simulated daily evapotranspiration at the dryland cotton field during the model a) calibration and b) validation periods.**

For the irrigated cotton field, the model performance statistics fell under satisfactory range during calibration (*NSE*, $R^2$ and *PBIAS*: 0.55. 0.63 and -24.8%) and validation (*NSE*, $R^2$ and *PBIAS*: 0.54. 0.58 and 1.4%) periods (Figure 6.2). The high *PBIAS* during the calibration period was mainly due to under-prediction of ET from June to August of 2014. In the SWAT model, auto-irrigation option was used, which resulted in application of irrigation water until soil moisture reached field capacity. However, producers tend to apply larger amounts of irrigation water in the real situation, which might have causes this discrepancy between the predicted and the observed ET during the major cotton growing period from June to August of 2014.

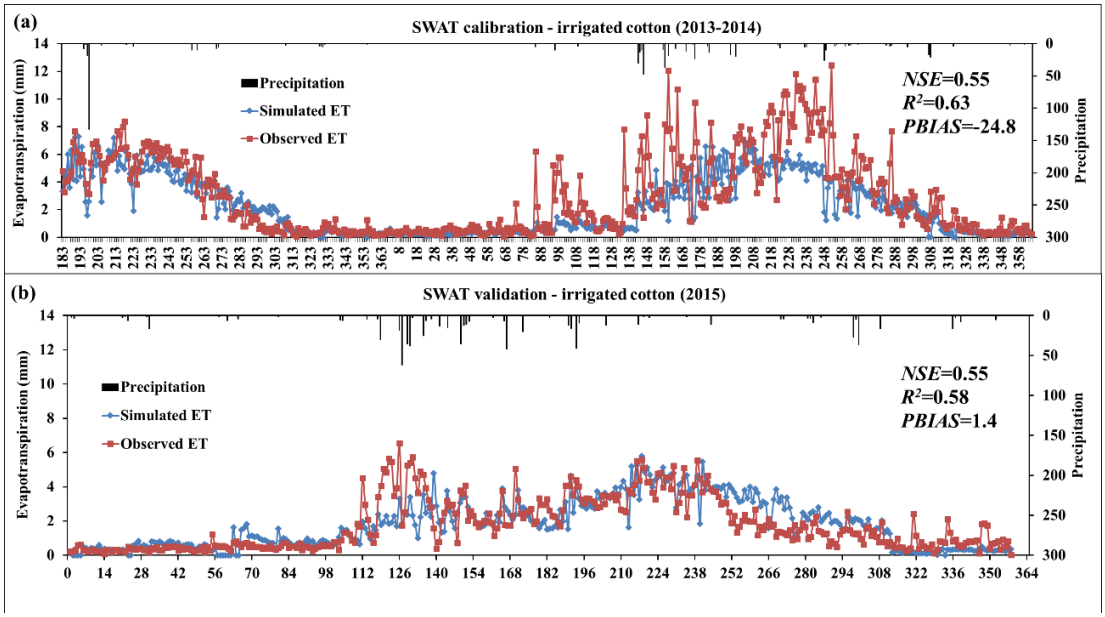


**Figure 6.2 Comparison of observed and simulated daily evapotranspiration at the irrigated cotton field during the model a) calibration and b) validation periods.**

### 6.4.1.2 Irrigated Biomass Sorghum

As shown in Figure 6.3, the predicted daily ET from the irrigated biomass sorghum field fit well with the observed ET during the model calibration period. The *NSE*, $R^2$ and *PBIAS* were 0.67, 0.71, -3.3%, respectively, which represented a good agreement. The *NSE*, $R^2$ and *PBIAS* during the model validation period were 0.54, 0.61 and 4.8%, which also denoted a satisfactory match between the simulated and observed ET.

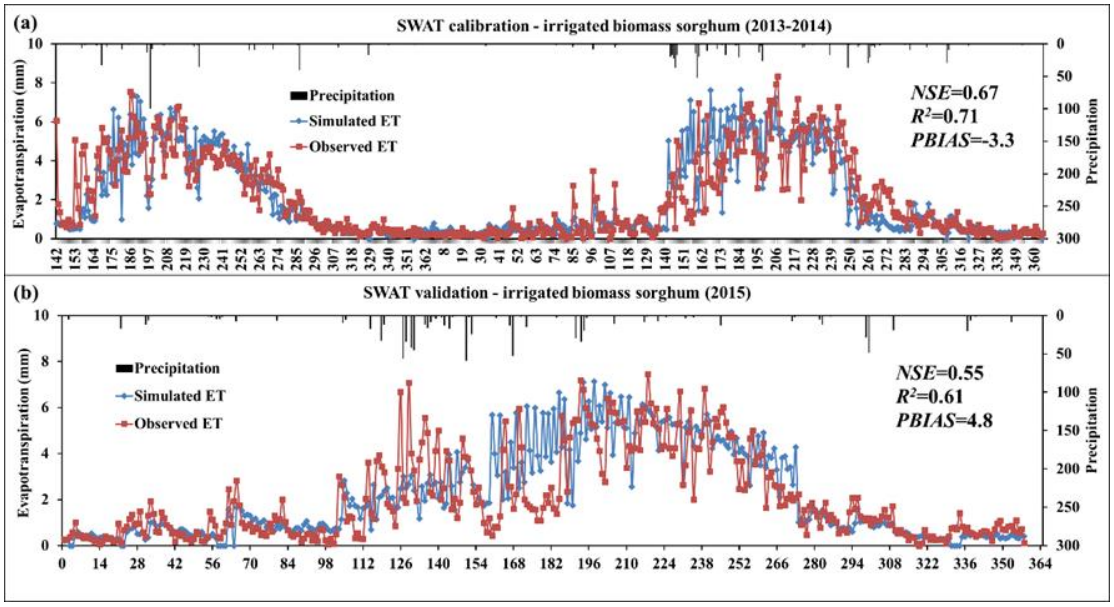


**Figure 6.3 Comparison of observed and simulated daily evapotranspiration at the irrigated biomass sorghum field during the model a) calibration and b) validation periods.**

#### 6.4.1.3 Dryland Big Bluestem

The simulated daily ET from the dryland big bluestem field closely matched with the observed ET during both calibration (2013-2014) and validation (2015) periods (Figure 6.4). The *NSE*, $R^2$ and *PBIAS* for daily predictions of ET during the model calibration period were 0.61, 0.63 and -9.7%, respectively, and they were 0.68, 0.69 and -6.1% during the model validation period. The model performance statistics during the calibration and validation periods demonstrated "good" agreement between the simulated and observed ET according to Moriasi et al. (2007) criteria (Figure 6.4).

Overall, good to satisfactory match between the predicted and the observed ET was achieved during the model calibration and validation periods at all four fields. The SWAT One-HRU method was therefore found to be a reasonably good tool for simulating hydrologic parameters under various land uses and management practices.

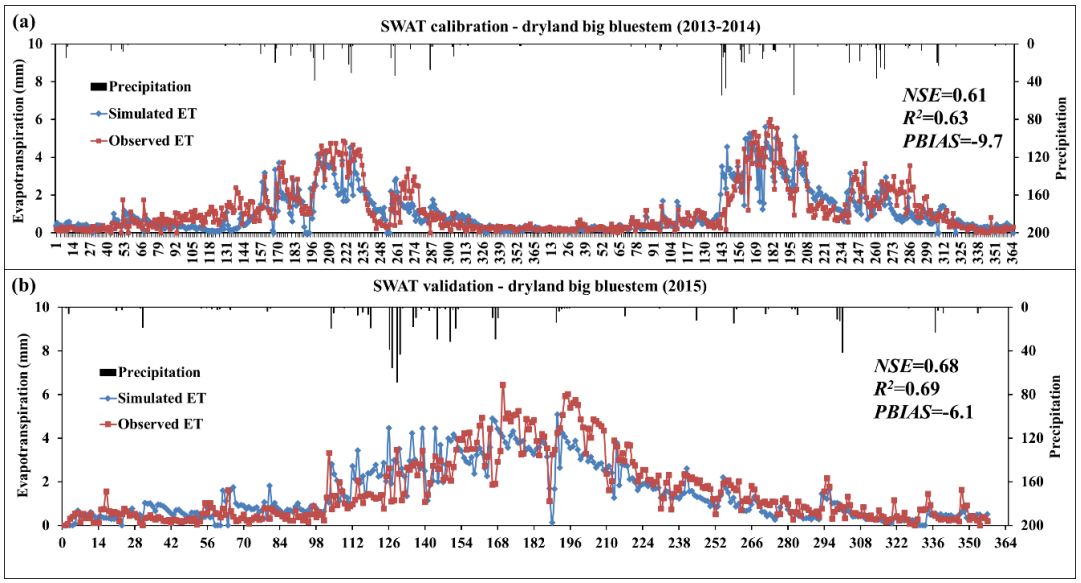


**Figure 6.4 Comparison of observed and simulated daily evapotranspiration at the dryland big bluestem field during the model a) calibration and b) validation periods.**

*6.4.2 Comparison of SWAT Simulated Crop Biomass with the Field Observations*

**6.4.2.1 Cotton**

After calibrating the model for ET simulation, SWAT One-HRU model was further calibrated for crop biomass prediction. The *NSE*, $R^2$ and *PBIAS* values achieved for the prediction of aboveground biomass of dryland cotton from 2014 to 2015, were 0.88, 0.91 and 0.9%, respectively, which represented a very good agreement between the predicted and observed dryland cotton biomasses (Figure 6.5). The simulated aboveground biomass of the irrigated cotton also matched very well with the observed data with the *NSE*, $R^2$ and *PBIAS* values of 0.91, 0.92 and 2.4%, respectively (Figure 6.6).

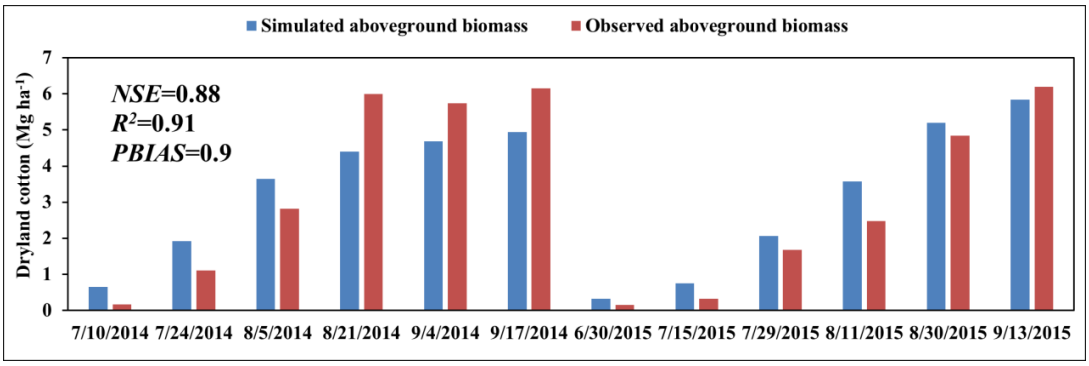


**Figure 6.5 Comparison of observed and simulated crop biomass at the dryland cotton field.**

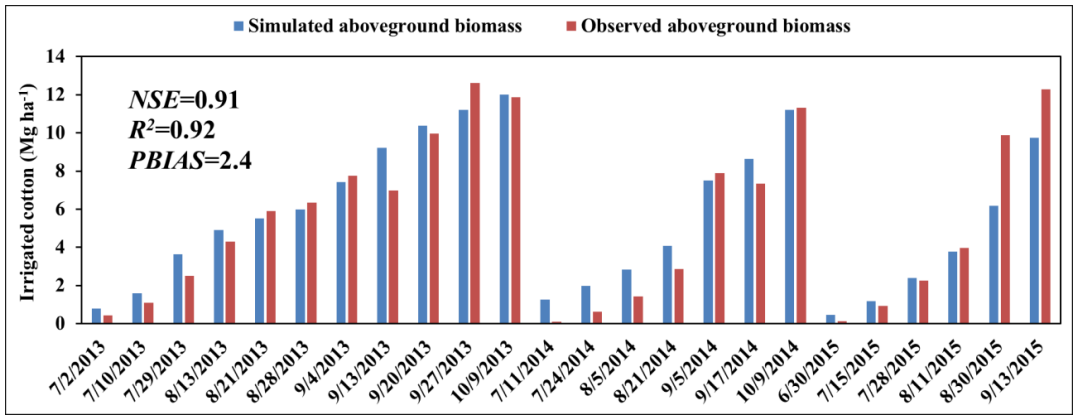


**Figure 6.6 Comparison of observed and simulated crop biomass at the irrigated cotton field.**

### 6.4.2.2 Irrigated Biomass Sorghum and Dryland Big Bluestem

An excellent match was found between the simulated and measured biomass of irrigated biomass sorghum, as indicated by the *NSE*, $R^2$ and *PBIAS* values of 0.94, 0.96 and -6.6%, respectively (Figure 6.7). The *NSE*, $R^2$ and *PBIAS* values in predicting the aboveground biomass of dryland big bluestem over the entire simulation period (2013-2015) were 0.55, 0.71 and 0.2%, respectively, indicating a reasonable match between the simulated and observed big bluestem biomasses under dryland conditions (Figure 6.8). The predictions of crop biomass are also well above satisfactory ranges at four fields.

The evaluation of the SWAT One-HRU model for crop biomass prediction enhanced our confidence to use the calibrated model for predictions of ET and biomass production potential.

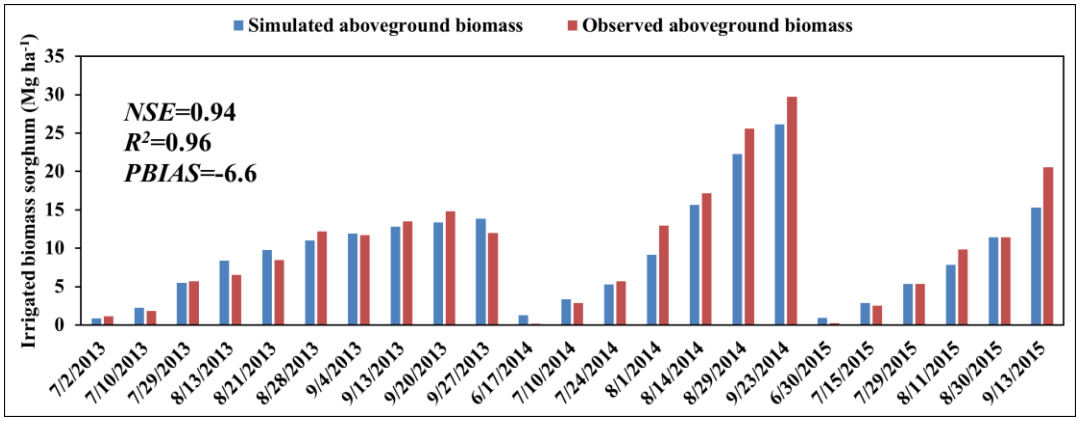


**Figure 6.7 Comparison of observed and simulated crop biomass at the irrigated biomass sorghum field.**

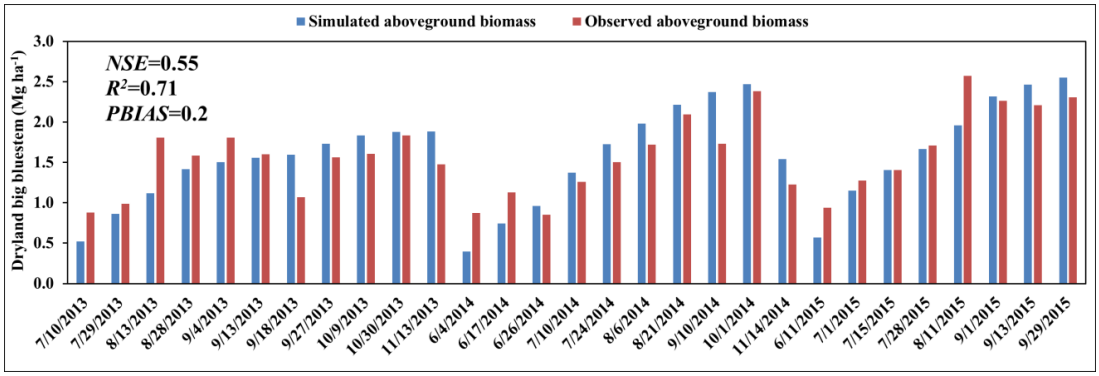


**Figure 6.8 Comparison of observed and simulated crop biomass at the dryland big bluestem field.**

### *6.4.3 Biomass and Biofuel Production Potential from Replacing Cotton with Big Bluestem and Biomass Sorghum*

The highest average annual (1994-2015) biomass was simulated under the irrigated biomass sorghum scenario (15.8 Mg ha$^{-1}$) followed by the dryland biomass sorghum scenario (10.7 Mg ha$^{-1}$) (Table 6.4). The observed average annual (2013-2015)

production of biomass in the irrigated biomass sorghum field in this study was about 16.3 Mg $ha^{-1}$, which was close to the simulated biomass yield under the irrigated biomass sorghum scenario. The simulated biomass under the dryland biomass sorghum scenario (10.7 Mg $ha^{-1}$) was higher than that obtained in the Chen et al. (2016a) SWAT modeling study (7.6 Mg $ha^{-1}$) in the adjacent Double Mountain Fork Brazos watershed. This might have been due to application of higher amount of nitrogen fertilizer application in the study sites. Limited biomasses (2.6 and 3.1 Mg $ha^{-1}$: dryland and irrigated big bluestem) were simulated from irrigated and dryland big bluestem scenarios (Table 6.4). The observed aboveground biomass of the dryland big bluestem at the field site in this study, in which fertilizer was not applied, was about 2.1 Mg $ha^{-1}$. Chen et al. (2016a) SWAT simulations also reported a 2.8 Mg $ha^{-1}$ biomass yield under the dryland big bluestem scenario in the adjacent Double Mountain Fork Brazos watershed in the THP.

**Table 6.4 Average (1994-2015) annual simulated biomass and biofuel production of big bluestem and biomass sorghum under the hypothetical land use change scenarios**

| Big bluestem | Dryland conditions | Irrigated conditions |
|---|---|---|
| Biomass production (Mg $ha^{-1}$) | 2.6 | 3.1 |
| Biofuel production* (liter ethanol $ha^{-1}$) | 933 | 1,131 |
| **Biomass sorghum** | **Dryland conditions** | **Irrigated conditions** |
| Biomass production (Mg $ha^{-1}$ $yr^{-1}$) | 10.7 | 15.8 |
| Biofuel production* (liter ethanol $ha^{-1}$) | 4,556 | 6,776 |

*The theoretical ethanol yield is available from http://www.afdc.energy.gov/fuels/ethanol_feedstocks.html

Based on the estimated theoretical ethanol yield by the US Department of Energy (http://www.afdc.energy.gov/fuels/ethanol_feedstocks.html), the average annual ethanol that could be produced with the simulated biomasses of irrigated and dryland biomass sorghum were 6,776 and 4,556 liters $ha^{-1}$, respectively (Table 6.4). The estimated ethanol production from the biomasses of irrigated and dryland big bluestem were 1,131 and 933 liters $ha^{-1}$, respectively. The biomass sorghum was therefore found to be a promising bioenergy crop for the THP.

### *6.4.4 Simulated Hydrological Fluxes under the Baseline and Hypothetical Land Use Change Scenarios*

A comparison of the simulated water balances at the four field sites from 1994 to 2015 (Table 6.5a) indicated that under the dryland fields of cotton and big bluestem, more than 95% of precipitation was lost by ET. About 80% and 83% of total input water (precipitation + irrigation) was lost due to ET under the irrigated biomass sorghum and irrigated cotton fields (Table 6.5a). Hao et al. (2014) also reported that about 90% of the growing season precipitation was lost as the growing season ET under the biomass sorghum production systems in the THP. The simulated irrigation water use was 8% lower under the irrigated biomass sorghum field compared to the irrigated cotton field. In addition, the net groundwater use (irrigation minus percolation) by the irrigated biomass sorghum was 13% lower relative to the irrigated cotton land use. The surface runoff was 79% lower under the dryland big bluestem field compared to the dryland cotton field (Table 6.5a).

The rainfall amounts received at the field sites were different. Therefore, in order to appropriately compare water dynamics under different land uses, the land use changes from cotton to big bluestem and biomass sorghum were evaluated (Table 6.5b). Results showed that the average (1994-2015) annual surface runoff under the dryland and irrigated big bluestem scenarios decreased by about 86% and 64%, respectively, when compared to the dryland and irrigated cotton land uses (Table 6.5b). The higher plant populations and lower surface runoff potential (calibrated curve number of 57) of the big bluestem compared to cotton (calibrated curve number of 75) led to the decrease in surface runoff. Chen et al. (2016a) also predicted that land use change from cotton to big bluestem decreased the surface runoff by 94% and 93% under the irrigated and dryland conditions, respectively, using the SWAT model in the THP. The simulated average annual surface runoff also reduced by 52% and 19% under the dryland and irrigated biomass sorghum scenarios (Table 6.5b). However, when cotton was replaced by biomass sorghum, average annual percolation decreased by about 100% and 17% under the dryland and irrigated biomass sorghum scenarios, respectively.

The net groundwater use declined by 48% and 11% under the irrigated big bluestem and irrigated biomass sorghum scenarios, respectively, relative to the irrigated cotton land use. Chen et al. (2016a) SWAT simulations also showed that land use change from irrigated cotton to irrigated biomass sorghum and irrigated big bluestem decreased the irrigation water use by 54% and 35%, respectively, in the adjacent Double Mountain Fork Brazos watershed. This is a very useful finding in the light of rapid groundwater depletion in the THP. The ET increased by 3% and 2% under the dryland big bluestem

and dryland biomass sorghum scenarios, respectively, compared to the dryland cotton land use (Table 6.5b). However, the ET under the irrigated big bluestem and irrigated biomass sorghum scenarios was reduced by 13% and 4%, respectively, relative to the irrigated cotton land use.

**Table 6.5 Comparison of the simulated average (1994-2015) annual water balances under the baseline and hypothetical land use change scenarios**

| Unit (mm) | Dryland cotton | Irrigated cotton | Irrigated biomass sorghum | Dryland big bluestem |
|---|---|---|---|---|
| a) Initial land uses | | | | |
| Precipitation | 480.2 | 477.1 | 518.8 | 479.1 |
| Irrigation | 0 | 278.3 | 255.2 [-8.3][#] | 0 |
| Evapotranspiration | 457.9 | 630.0 | 623.5 [-1.0] | 469.9 [2.6] |
| Surface runoff | 15.1 | 35.6 | 49.7 [39.7] | 3.1 [-79] |
| Percolation | 3.8 | 98.5 | 98.7 [0.42] | 3.9 [2.1] |
| b) Land use change (cotton replacement) scenarios | | | | |
| Change percentage (%) | Dryland bluestem | Irrigated bluestem | Dryland sorghum | Irrigated sorghum |
| Precipitation | 480.2 | 477.1 | 480.2 | 477.1 |
| Irrigation | 0 | 234.4 (-15.8) | 0 | 241.3 (-13.3) |
| Evapotranspiration | 470.6 (2.8)* | 551.5 (-12.5) | 468.2 (2.3) | 607.2 (-3.6) |
| Surface runoff | 2.1 (-86) | 12.7 (-64.4) | 7.2 (-52) | 28.9 (-18.7) |
| Percolation | 0.8 (-80) | 140.2 (42.4) | 0 (-100) | 81.7 (-17.0) |

[#] Numbers in square bracket indicate the percent change of irrigated biomass sorghum land use compared to the irrigated cotton land use and dryland big bluestem compared to the dryland cotton land use

* Numbers in parentheses indicate the percent change under land use change scenario relative to the cotton land use in the irrigated and dryland conditions

Among the simulated bioenergy crops, biomass sorghum yielded more biomass than big bluestem (Table 6.4). In addition, biomass sorghum requires less net irrigation water use than irrigated cotton, which is very important in view of depleting groundwater levels in the Ogallala Aquifer in the THP. Furthermore, the biomass sorghum has the potential to decrease surface runoff compared to cotton when they

receive the same amount of water (rainfall and/or irrigation water) (Table 6.5). Due to the lower net groundwater water use, greater biomass and biofuel production potential, and lower surface runoff potential, biomass sorghum was identified as a good bioenergy crop to replace cotton in the THP. Big bluestem could also serve as an alternate crop because of its ability to protect groundwater.

# 7. SUMMARY AND CONCLUSIONS

## 7.1 Summary

Texas High Plains (THP) is one of the important cotton growing regions in the US. Agriculture in the THP faces several challenges from declining groundwater levels in the underlying Ogallala Aquifer, deteriorating groundwater quality and recurring droughts. In addition, climate change studies for this region predict warmer and drier summers. Change in land use from cotton to cellulosic bioenergy crops could not only address the above challenges, but also assist in meeting the national biofuel target. In addition, the THP region holds substantial potential for growing bioenergy crops. Assessment of the impacts of land use change from cotton to cellulosic bioenergy crops on hydrology and water quality enables better understanding of the associated key agroecosystem processes and suggestion of best management practices for sustainable agriculture in the THP. The overall goal of this study is to assess the implications of biofuel-induced land use change (replacing cotton with cellulosic bioenergy crops) on hydrology, water quality and crop yield under current and future climate change scenarios in the Double Mountain Fork Brazos watershed in the THP using multiple models (SWAT, APEX and Integrated APEX-SWAT).

As a first step, the SWAT model was calibrated for the study watershed using observed streamflow data at two USGS gauges. Later, it was calibrated against observed cotton lint yield data. The calibrated model was used to evaluate the impacts of land use change from cotton to cellulosic bioenergy crops on water balances in the study

watershed, and identification of ideal bioenergy crops for the THP region under the irrigated and dryland conditions.

The APEX model was initially set up for the upstream subwatershed and calibrated using the observed streamflow data at Gauge I in the middle of the watershed. It was also calibrated against the observed cotton lint yield data. The calibrated APEX model was initially used to identify marginal cotton-growing lands for replacement with switchgrass. The spatial variability in water use efficiency and water fluxes of ET, percolation, surface runoff and soil water content in both irrigated and dryland subareas under the baseline cotton and hypothetical switchgrass replacement scenarios were then compared and contrasted.

An integrated APEX-SWAT model was developed based on the above calibrated models to take advantage of strengths of these models in simulating certain crops/processes. In addition to calibrating the integrated model based on observed streamflow at two USGS gauges in the study watershed, it was further calibrated against the TN load data at the watershed outlet. The calibrated Integrated APEX-SWAT model was used to compare and contrast the impacts of the proposed changes in land use from cotton to perennial grasses on water and nitrogen balances under both irrigated and dryland conditions. Additionally, the biomass and biofuel production potential of the proposed bioenergy crops were estimated.

Finally, the evaluated SWAT hydrology model was calibrated for water quality predictions at the watershed outlet, and used to assess the combined effects of land use change from cotton to perennial grasses and climate change on watershed hydrology and

water quality. The CMIP5 future climate data projected by 19 GCMs from two RCP emission scenarios of RCP4.5 (moderate) and RCP8.5 (severe) were obtained for two 30-year periods: 2040 to 2069 (middle of the 21$^{st}$ century) and 2070 to 2099 (end of the 21$^{st}$ century), and used in these simulations. The impacts of land use change from cotton to perennial grasses on water balances, TN load and biomass production potential under the historic and projected future climate change (2040-2069 RCP4.5, 2040-2069 RCP8.5, 2070-2099 RCP4.5 and 2070-2099 RCP8.5) scenarios were compared and contrasted with respective historic and future cotton land use scenarios.

## 7.2 Conclusions

The following conclusions were drawn from this study:

1. When compared to the baseline cotton scenario, simulated average annual (1994-2009) surface runoff decreased by about 88% under the perennial grass scenarios, and increased by about 59% under the biomass sorghum scenario.
2. The simulated average annual percolation increased by about 28% under the perennial grass scenarios compared to the baseline cotton scenario. Perennial grass land use change scenarios also suggested an increase in soil water content from August to April.
3. About 27, 17, 4 and 12 Mg ha$^{-1}$ yr$^{-1}$ of biomass could potentially be produced under the irrigated *Miscanthus*, switchgrass, big bluestem and biomass sorghum land uses, respectively. Based on the suggested theoretical ethanol yield by the US Department of Energy, about 4931, 7548, 1170 and 3279 liters ha$^{-1}$ of biofuel

could potentially be produced from irrigated *Miscanthus*, switchgrass, big bluestem and biomass sorghum, respectively.

4. Under the dryland conditions, about 16, 8, 8 and 3 Mg $ha^{-1}$ $yr^{-1}$ of biomass could potentially be produced under the land uses of *Miscanthus*, switchgrass, big bluestem and biomass sorghum, respectively. The estimated biofuel production potential from these land uses is 4398, 2347, 778 and 2143 liters $ha^{-1}$.
5. *Miscanthus* and switchgrass were found to be ideal bioenergy crops for the dryland and irrigated conditions in the study watershed, respectively due to their higher water use efficiency, better potential for water conservation, greater biomass and biofuel production potential, and minimum crop management.
6. Surface runoff to cotton yield ratio was found to be a good criterion for identifying/mapping marginal cotton-growing areas in the watershed for potential replacement with switchgrass.
7. The average annual $NO_3$-N load in surface runoff and $NO_3$-N leaching to groundwater were reduced by 86% and 100%, respectively, under the perennial grass scenarios relative to the baseline cotton scenario. High percentage of nitrogen uptake by perennial grasses was the main reason for the reduced nitrogen losses through surface runoff and leaching.
8. The simulated annual irrigation water use under the future perennial grass land use scenarios of 2040-2069 RCP4.5, 2040-2069 RCP8.5, 2070-2099 RCP4.5 and 2070-2099 RCP8.5 was reduced by 62%, 69%, 66% and 89%, respectively, than

that under respective future cotton land use scenarios according to the 19 GCM projections.

9. The biofuel-induced land use change from cotton to perennial grasses showed the potential to improve water quality by reducing the median discharge of the TN load at the watershed outlet by about 30% based on 19 GCM projections under the future climate change scenarios.
10. A substantial increase in dryland *Miscanthus* biomass yield by about 35% could be achieved under the future climate change scenarios based on 19 GCM projections. However, the simulated irrigated switchgrass biomass yield was projected to decline by 16% under the future climate change scenarios. The elevated $CO_2$ concentrations, reduced water stress days and the changes in temperature stress days under the future climate change scenarios were the primary reasons for the differences in future biomass yields of perennial grasses.
11. The One-HRU method in the SWAT model demonstrated potential to simulate the hydrologic impacts of biofuel-induced land use change at the field-scale.

## 7.3 Future Work

Some suggestions for future work include: i) determining the environmental impacts of growing perennial bioenergy crops in the "marginal lands" and "riparian buffers" of the study watershed only instead of replacing row crops from agricultural lands, and ii) studying carbon dynamics associated with the land use change from cotton to perennial grasses by calibrating the models using observed daily net ecosystem

exchange (NEE) data collected from the eddy covariance flux towers in the Texas High Plains.

## REFERENCES


Abbaspour, K.C., Vejdani, M., Haghighat, S. 2007. SWAT-CUP calibration and uncertainty programs for SWAT. In Proc. Intl. Congress on Modelling and Simulation (MODSIM'07), 1603-1609. L. Oxley and D. Kulasiri, eds. Melbourne, Australia: Modelling and Simulation Society of Australia and New Zealand.

Adati, S., Shiotani, I. 1962. The cytotaxonomy of the genus *Miscanthus* and its phylogenetic status. Bull Fac Agric Mie Univ. 25:1-24.

Adhikari, P., Ale, S., Bordovsky, J.P., Thorp, K.R., Modala, N.R., Rajan, N., Barnes, E.M. 2016. Simulating future climate change impacts on seed cotton yield in the Texas High Plains using the CSM-CROPGRO-Cotton model. Agricultural Water Management. 164:317-330.

Agricultural Resources and Environmental Indicators (1996-97) U.S. Department of Agriculture, Economic Research Service, Natural Resources and Environment Division. Agricultural Handbook No. 712

Akhavan, S., Abedi-Koupai, J., Mousavi, S.F., Afyuni, M., Eslamian, S.S., Abbaspour, K.C. 2010. Application of SWAT model to investigate nitrate leaching in Hamadan-Bahar Watershed, Iran. Agriculture, Ecosystems and Environment. 139:675-688.

Ale, S., Bowling, L.C., Brouder, S.M., Frankenberger, J.R., Youssef, M.A. 2009. Simulated effect of drainage water management operational strategy on hydrology and crop yield for Drummer soil in the Midwestern United States. Agricultural Water Management. 96:653-665.

Ansley, R.J., Mirik, M., Castellano, M.J. 2010. Structural biomass partitioning in regrowth and undisturbed mesquite (*Prosopis glandulosa*): implications for bioenergy uses. Global Change Biology Bioenergy. 2:26-36.

Arnell, N.W. 1999. Climate change and global water resources. Global Environmental Change. 9:S31-S49.

Arnold, J.G., Allen, P.M. 1999. Automated methods for estimating baseflow and ground water recharge from streamflow records. Journal of the American Water Resources Association. 35:411-424.

Arnold, J.G., Allen, P.M., Muttiah, R., Bernhardt, G. 1995. Automated base flow separation and recession analysis techniques. Ground Water. 33:1010-1018.

Arnold, J.G., Moriasi, D.N., Gassman, P.W., Abbaspour, K.C., White, M.J., Srinivasan, R., Santhi, C., Harmel, R.D., van Griensven, A., Van Liew, M.W., Kannan, N., Jha,

M.K. 2012. SWAT: model use, calibration, and validation. Transactions of the ASABE. 55:1491-1508.

Arnold, J.G., Srinivasan, R., Muttiah, R.S., Williams, J.R. 1998. Large-area hydrologic modeling and assessment: Part I. Model development. Journal of the American Water Resources Association. 34:73-89.

Asner, G.P., Archer, S.R., Hughes, R.F., Ansley, R.J., Wessman, C.A. 2003. Net changes in regional woody vegetation cover and carbon storage in Texas drylands, 1937-1999. Global Change Biology. 9:316-335.

Ávila-Carrasco, J.R., Dávila, F.M., Moriasi, D.N., et al. 2012. Calibration of SWAT 2009 using crop biomass, evapotranspiration, and deep recharge: Calera watershed in Zacatecas, Mexico case study. Journal of Water Resource and Protection. 4:439-450.

Ayre, M. 2007. "Will biofuel leave the poor hungry?". BBC News. Available online at http://news.bbc.co.uk/2/hi/business/7026105.stm (accessed 4 August 2015).

Baier, W., Robertson, G.W. 1965. Estimation of latent evaporation from simple weather observations. Canadian Journal of Plant Science. 45:276-284.

Baldocchi, D.D. 2003. Assessing the eddy covariance technique for evaluating carbon dioxide exchange rates of ecosystems: Past, present and future. Global Change Biology. 9:479-492.

Barnett, T.P., Pierce, D.W., Hidalgo, H.G., Bonfils, C., Santer, B.D., Das, T., Bala, G., Wood, A.W., Nozawa, T., Mirin, A.A., Cayan, D.R., Dettinger, M.D. 2008. Human-induced changes in the hydrology of the Western United States. Science. 319:1080-1083.

Behrman, K.D., Keitt, T.H., Kiniry, J.R. 2014. Modeling differential growth in switchgrass cultivars across the central and Southern Great Plains. BioEnergy Research. 7:1165-1173.

Beven, K., Binley, A. 1992. The future of distributed models-model calibration and uncertainty prediction. Hydrological Processes. 6:279-298.

Beven, K. 2006. A manifesto for the equifinality thesis. Journal of Hydrology. 320(1-2):18-36.

Bos, M.G. 1980. Irrigation efficiencies at crop production level. ICID Bull. 29:18-25, 60

Brekke, L.D., Miller, N.L., Bashford, K.E., Quinn, N.W.T., Dracup, J.A. 2004. Climate change impacts uncertainty for water resources in the San Joaquin River basin, California. Journal of the American Water Resources Association. 40:149-164.

Bruton, B.D., Fish, W.W., Subbarao, K.V., Isakeit, T. 2007. First report of Verticillium wilt of watermelon in the Texas High Plains. Plant Disease. 91:8.

Cai, X.M., Zhang, X., Wang, D.B. 2011. Land Availability for Biofuel Production. Environmental Science & Technology. 45:334-339.

Campbell, J.E., Lobell, D.B., Genova, R.C., Field, C.B. 2008. The global potential of bioenergy on abandoned agriculture lands. Environmental Science & Technology. 42:5791-5794.

Chandra, P., Patel, P.L., Porey, P.D., Gupta, I.D. 2014. Estimation of sediment yield using SWAT model for Upper Tapi basin. ISH Journal of Hydraulic Engineering. 20:291-300.

Chaudhuri, S., Ale, S. 2014a. Long-term (1930-2010) trends in groundwater levels in Texas: influences of soils, landcover and water use. Science of the Total Environment. 490:379-390.

Chaudhuri, S., Ale, S. 2014b. Long-term (1960-2010) trends in groundwater contamination and salinization in the Ogallala aquifer in Texas, USA. Journal of Hydrology. 513:376-390.

Chen, Y., Ale, S., Rajan, N., Morgan, C.L.S., Park, J.Y. 2016a. Hydrological responses of land use change from cotton (*Gossypium hirsutum* L.) to cellulosic bioenergy crops in the Southern High Plains of Texas, USA. Global Change Biology Bioenergy. 8:981-999.

Chen, Y., Ale, S., Rajan, N. 2016b. Spatial variability of biofuel production potential and hydrologic fluxes of land use change from cotton (*Gossypium hirsutum* L.) to Alamo switchgrass (*Panicum virgatum* L.) in the Texas High Plains. BioEnergy Research. doi: 10.1007/s12155-016-9758-7

Chen, Y., Ale, S., Rajan, N., Munster, C. 2016c. Assessing the hydrologic and water quality impacts of biofuel-induced changes in land use and management. Global Change Biology Bioenergy. Under review.

Christakopoulos, P., Li, L.W., Kekos, D., Macris, B.J. 1993. Direct conversion of sorghum carbohydrates to ethanol by a mixed microbial culture. Bioresource Technology. 45:89-92.

Christian, D., Riche, A., Yates, N. 2008. Growth, yield and mineral content of *Miscanthus* × *giganteus* grown as a biofuel for 14 successive harvests. Industrial Crops and Products. 28: 320-732.

Cibin, R., Trybula, E., Chaubey, I., Brouder, S., Volenec, J.J. 2016. Watershed scale impacts of bioenergy crops on hydrology and water quality using improved SWAT model. Global Change Biology Bioenergy. 8:837-848.

Clifton-Brown, J.C., Lewandowski, I., Andersson, B., et al. 2001. Performance of 15 genotypes at five sites in Europe. Agronomy Journal. 93:1013-1019.

Cosentino, S.L., Patanè, C., Sanzone, E., Copani, V., Foti, S. 2007. Effects of soil water content and nitrogen supply on the productivity of *Miscanthus* × *giganteus* Greef et Deu. in a Mediterranean environment. Industrial Crops and Products. 25:75-88.

Daggupati, P., Pai, N., Ale, S., Douglas-Mankin, K.R., Zeckoski, R.W., Jeong, J., Parajuli, P.B., Saraswat, D., Youssef, M.A. 2015. A recommended calibration and validation strategy for hydrologic and water quality models. Transactions of the ASABE. 58:1705-1719.

Daloğlu, I., Cho, K.H., Scavia, D. 2012. Evaluating causes of trends in long-term dissolved reactive phosphorus loads to Lake Erie. Environmental Science & Technology. 46:10660-10666.

Danalatos, N.G., Archontoulis, S.V., Mitsios, I. 2007. Potential growth and biomass productivity of *Miscanthus*×*giganteus* as affected by plant density and N-fertilization in central Greece. Biomass and Bioenergy. 31:145-152.

Demissie, Y., Yan, E., Wu, M. 2012. Assessing regional hydrology and water quality implications of large-scale biofuel feedstock production in the Upper Mississippi River Basin. Environmental Science & Technology. 46:9174-9182.

Diggs, G.M., Lipscomb, B.L., O'Kennon, R.J. 1999. Shinner's and Mahler's illustrated flora of north central Texas. Botanical Research Institute of Texas, Fort Worth, Texas, USA.

Dolman, A.J., Tolk, L., Ronda, R., Noilhan, J., Sarrat, C., Brut, A., et al. 2006. The CarboEurope Regional Experiment Strategy Bulletin of the American Meteorological Society 87:1367-1379.

EISA (Energy Independence and Security Act) of 2007 Public Law 110-140. 2007. http://www.gpo.gov/fdsys/pkg/PLAW-110publ140/pdf/PLAW-110publ140.pdf (accessed 3 September 2015).

Faramarzi, M., Abbaspour, K.C., Schulin, R., Yang, H. 2009. Modeling blue and green water resources availability in Iran. Hydrological Processes. 23:486-501.

Faramarzi, M., Yang, H., Schulin, R., Abbaspour, K.C. 2010. Modeling wheat yield and crop water productivity in Iran: implications of agricultural water management for wheat production. Agricultural Water Management. 97:1861-1875.

Fargione, J., Plevin, R.J., Hill, J.D. 2010. The ecological impact of biofuels. Annual Review of Ecology, Evolution, and Systematics. 41:351-377.

Feng, Q.Y., Chaubey, I., Gu Her, Y., Cibin, R., Engel, B., Volenec, J., Wang, X.Y. 2015. Hydrologic and water quality impacts and biomass production potential on marginal land. Environmental Modeling & Software. 72:230-238.

Ficklin, D.L., Luo, Y.Z., Luedeling, E., Zhang, M.H. 2009. Climate change sensitivity assessment of a highly agricultural watershed using SWAT. Journal of Hydrology. 374:16-29.

Field, C., Jackson, R., Mooney, H. 1995. Stomatal responses to increased $CO_2$: implications from the plant to the global-scale. Plant, Cell & Environment. 18:1214-1255.

Foley, J.A., Ramankutty, N., Brauman, K.A., et al. 2011. Solutions for a cultivated planet. Nature. 478:337-342.

Garen, D.C., Moore, D.S. 2005. Curve number hydrology in water quality modeling: uses, abuses, and future directions. JAWRA Journal of the American Water Resources Association. 41:377-388.

Gassman, P.W., Sadeghi, A.M., Srinivasan, R. 2014. Applications of the SWAT model special section: overview and insights. Journal of Environmental Quality. 43:1-8.

Gassman, P.W., Williams, J.R., Wang, X., Saleh, A., Osei, E., Hauck, L.M., Izaurralde, R.C., Flowers, J.D. 2010. The Agricultural Policy/Environmental Extender (APEX) model: An emerging tool for landscape and watershed environmental analyses. Transactions of the ASABE. 53:711-740.

Gedney, N., Cox, P.M., Betts, R.A., Boucher, O., Huntingford, C., Stott, P.A. 2006. Detection of a direct carbon dioxide effect in continental river runoff records. Nature. 439:835-838.

Ghaffari, G., Keesstra, S., Ghodousi, J., Ahmadi, H. 2010. SWAT-simulated hydrological impact of land-use change in the Zanjanrood Basin, Northwest Iran. Hydrological Processes. 24:892-903.

Ghannoum, O., von Caemmerer, S., Ziska, L.H., Conroy, J.P. 2000. The growth response of C4 plants to rising atmospheric $CO_2$ partial pressure: a reassessment. Plant, Cell & Environment. 23:931-942.

Gober, P., Kirkwood, C.W. 2010. Vulnerability assessment of climate-induced water shortage in Phoenix. PNAS. 107:21295-21299.

Golmohammadi, G., Prasher, S., Madani, A., Rudra, R. 2014. Evaluating three hydrological distributed watershed models: MIKE-SHE, APEX, SWAT. Hydrology. 1:20-39.

Gould, F.W., Shaw R.B. 1983. Grass systematics. 2nd ed. Texas A&M University Press, College Station, TX.

Goulden, M.L., Munger, J.W., Fan, S.M., Daube, B.C. Wofsy, S.C. 1996. Measurements of carbon sequestration by long-term eddy covariance: methods and a critical evaluation of accuracy. Global Change Biology. 2:169-182.

Gowda, P.H., Mulla, D.J., Desmond, E.D., Ward, A.D., Moriasi, D.N. 2012. ADAPT: Model use calibration, and validation. Transactions of the ASABE. 55:1345-1352.

Graham, R.L. 1994. An analysis of the potential land base for energy crops in the conterminous United States. Biomass and Bioenergy. 6:175-189.

Green, W.H., Ampt, G.A. 1911. Studies on soil physics: 1. Flow of air and water through soils. Journal of Agricultural Science. 4:1-24.

Griffith, A.P., Haque, M., Epplin, F.M. 2014. Cost to produce and deliver cellulosic feedstock to a biorefinery: Switchgrass and forage sorghum. Applied Energy. 127:44-54.

Hake, K., Silvertooth, J. 1990. High temperature effects on cotton. Physiology Today, Available at: https://www.cotton.org/tech/physiology/cpt/plantphysiology/upload/CPT-July90-REPOP.pdf (accessed May 2016).

Ham, J.M., Heilman, J.L. 2003. Experimental test of density and energy-balance corrections on carbon dioxide flux as measured using open-path eddy covariance. Agronomy Journal. 95:1393-1403.

Hao, B.Z., Xue, Q.W., Bean, B.W., Rooney, W.L., Becker, J.D. 2014. Biomass production, water and nitrogen use efficiency in photoperiod-sensitive sorghum in the Texas High Plains. Biomass and Bioenergy. 62:108-116.

Hargreaves, G.H., Samani, Z.A. 1985. Reference crop evapotranspiration from temperature. Applied Engineering in Agriculture. 1:96-99.

Harmel, R.D., Smith, P.K., Migliaccio, K.W., Chaubey, I., Douglas-Mankin, K.R., Benham, B., Shukla, S., Muñoz-Carpena, R., Robson, B.J. 2014. Evaluating,

interpreting, and communicating performance of hydrologic/water quality models considering intended use: A review and recommendations. Environmental Modelling & Software. 57:40-51.

Heaton, E., Voigt, T., Long, S.P. 2004. A quantitative review comparing the yields of two candidate C-4 perennial biomass crops in relation to nitrogen, temperature and water. Biomass and Bioenergy. 27:21-30.

Heaton, E.A., Dohleman, F.G., Long, S.P. 2008. Meeting US biofuel goals with less land: The potential of *Miscanthus*. Global Change Biology. 14:2000-2014.

Hill, J., Nelson, E., Tilman, D., Polasky, S., Tiffany, D. 2006. Environmental, economic, and energetic costs and benefits of biodiesel and ethanol biofuels. PNAS. 103:11206-11210.

Hornbeck, R., Keskin, P. 2012. The historically evolving impact of the Ogallala Aquifer: agricultural adaptation to groundwater and drought. Discussion Paper 2012-39, Cambridge, Mass.: Harvard Environmental Economics Program.

Howell, T.A. 2001. Enhancing water use efficiency in irrigated agriculture. Agronomy Journal. 93:281-289.

HPUWCD (High Plains Underground Water Conservation District) 2015. Rule 5 Recording and Reporting Requirements. Available at: http://static1.squarespace.com/static/53286fe5e4b0bbf6a4535d75/t/54db8326e4b09b0ec42ee61d/1423672102940/%28RuleExplanationRevised.pdf (accessed 18 July 2015).

Hu, X., McIsaac, G.F., David, M.B., Louwers, C.A.L. 2007. Modeling Riverine Nitrate Export from an East-Central Illinois Watershed Using SWAT. Journal of Environmental Quality. 36:996-1005.

Hudiburg, T.W., Davis, S.C., Parton, W., Delucia, E.H. 2015. Bioenergy crop greenhouse gas mitigation potential under a range of management practices. Global Change Biology Bioenergy. 7:366-374.

Intergovernmental Panel on Climate Change (IPCC) 2001. Climate Change 2001: Impacts, Adaptation, and Vulnerability Contribution of Working Group II to the Third Assessment Report of the Intergovernmental Panel on Climate Change. Cambridge University Press, Cambridge, United Kingdom and New York, NY, USA.

Intergovernmental Panel on Climate Change (IPCC) 2007. Climate Change 2007: The Physical Science Basis. Contribution of Working Group I to the Fourth Assessment Report of the Intergovernmental Panel on Climate Change. Cambridge University Press, Cambridge, United Kingdom and New York, NY, USA.

Jackson, R.B., Carpenter, S.R., Dahm, C.N., et al. 2001. Water in a changing world. Ecological Applications. 11:1027-1045.

Jager, H.I., Baskaran, L.M., Schweizer, P.E., Turhollow, A.F., Brandt, C.C., Srinivasan, R. 2015. Forecasting changes in water quality in rivers associated with growing biofuels in the Arkansas-White-Red river drainage, USA. Global Change Biology Bioenergy. 7:774-784.

Jain, A.K., Khanna, M., Erickson, M., Huang, H.X. 2010. An integrated biogeochemical and economic analysis of bioenergy crops in the Midwestern United States. Global Change Biology Bioenergy. 2:217-234.

Jha, M., Arnold, J.G., Gassman, P.W., Giorgi, F., Gu, R.R. 2006. Climate change sensitivity assessment on Upper Mississippi River Basin streamflows using SWAT. Journal of the American Water Resources Association. 42:997-1015.

Jha, M.K., Gassman, P.W., Arnold, J.G. 2007. Water quality modeling for the Raccoon River watershed using SWAT. Transactions of the ASABE. 50:479-493.

Jung, C.G., Park, J.Y., Kim, S.J., Park, G.A. 2014. The SRI (system of rice intensification) water management evaluation by SWAPP (SWAT-APEX Program) modeling in an agricultural watershed of South Korea. Paddy and Water Environment. 12:251-261.

Kindred, D., Sylvester-Bradley, R., Garstang, J., Weightman, R., Kilpatrick, J. 2008. Anticipated and potential improvements in land productivity and increased agricultural inputs with intensification. A study commissioned by AEA Technology as part of the Gallagher biofuels review for Renewable Fuels Agency, Department for Transport. Cambs, UK: ADAS UK Ltd; p. 59.

Kiniry, J.R., Anderson, L.C., Johnson, M.V.V., et al. 2013. Perennial biomass grasses and the Mason-Dixon line: comparative productivity across latitudes in the Southern Great Plains. BioEnergy Research. 6:276-291.

Kiniry, J.R., Johnson, M.V.V., Bruckerhoff, S.B., Kaiser, J.U., Cordsiemon, R.S., Harmel, R.D. 2012. Clash of the Titans: comparing productivity via radiation use efficiency for two grass giants of the biofuel field. BioEnergy Research. 5:41-48.

Kiniry, J.R., Lynd, L., Greene, N., Johnson, M.V.V., Casler, M., Laser, M.S. 2008. Biofuels and Water Use: Comparison of Maize and Switchgrass and General Perspectives. New Research on Biofuels. Nova Science Publ., New York.

Kiniry, J.R., Sanderson, M.A., Williams, J.R., Tischler, C.R., Hussey, M.A., Ocumpaugh, W.R., Read, J.C., Van Esbroeck, G., Reed, R.L. 1996. Simulating Alamo Switchgrass with the ALMANAC Model. Agronomy Journal. 88:602-606.

Kirchner, J. W. Getting the right answers for the right reasons: Linking measurements, analyses, and models to advance the science of hydrology. Water Resources Research. 42:W03S04.

Knapp, A.K., Briggs, J.M., Hartnett, D.C., Collins, S.L. 1998. Grassland dynamics: long-term ecological research in tallgrass prairie: Oxford University Press New York.

Knisel, W.G. 1980. CREAMS: A field-scale model for chemicals, runoff, and erosion from agricultural management systems. Conservation Research Report No. 26. Washington, D.C.: USDA National Resources Conservation Service.

Ko, J.H., Piccinni, G., Steglich, E. 2009. Using EPIC model to manage irrigated cotton and maize. Agricultural Water Management. 96:1323-1331.

Le, P.V.V., Kumar, P., Drewry, D.T. 2011. Implications for the hydrologic cycle under climate change due to the expansion of bioenergy crops in the Midwestern United States. PNAS. 108:15085-15090.

Legates, D.R., McCabe Jr, G.J. 1999. Evaluating the use of ‘‘goodness-of-fit’’ measures in hydrologic and hydroclimatic model validation. Water Resources Research. 35:233-241.

Leonard, R.A., Knisel, W.G., Still, D.A. 1987. GLEAMS: Groundwater loading effects on agricultural management systems. Transactions of the ASABE. 30:1403-1418.

Lewandowski, I., Clifton-Brown, J., Scurlock, J., Huisman, W. 2000. *Miscanthus*: European experience with a novel energy crop. Biomass and Bioenergy. 19:209-227.

Lewandowski, I., Schmidt, U. 2006. Nitrogen, energy and land use efficiencies of miscanthus, reed canary grass and triticale as determined by the boundary line approach. Biomass and Bioenergy. 112:335-346.

Li, H., Lascano, R.J. 2011. Deficit irrigation for enhancing sustainable water use: Comparison of cotton nitrogen uptake and prediction of lint yield in a multivariate autoregressive state-space model. Environmental and Experimental Botany. 71:224-231.

Love, B.J., Nejadhashemi, A.P. 2011. Water quality impact assessment of large-scale biofuel crops expansion in agricultural regions of Michigan. Biomass and Bioenergy. 35:2200-2216.

Lynd, L.R., Laser, M.S., Bransby, D., Dale, B.E., Davison, B., Hamilton, R., Himmel, M., Keller, M., Mcmillan, J.D., Sheehan, J. 2008. How biotech can transform biofuels. Nature Biotechnology. 26:169-172.

Marshall, E., Randhir, T. 2008. Effect of climate change on watershed system: a regional analysis. Climatic Change. 89:263-280.

Marshall, L., Nott, D., Sharma, A. 2004. A comparative study of Markov chain Monte Carlo methods for conceptual rainfall-runoff modeling. Water Resources Research. 40:W02501.

Mauney, J.R., Kimball, B.A., Pinter Jr, P.J., et al. 1994. Growth and yield of cotton in response to a free-air carbon dioxide enrichment (FACE) environment. Agricultural and Forest Meteorology. 70:49-67.

Maupin, M.A., Barber, N.L. 2005. Estimated Withdrawals from Principal Aquifers in the United States, 2000. Survey Circular 1279 (US Geological Survey, Reston, VA).

McIsaac, G.F., David, M.B., Mitchell, C.A. 2010. *Miscanthus* and switchgrass production in central Illinois: impacts on hydrology and inorganic nitrogen leaching. Journal of Environmental Quality. 39:1790-1799.

McLaughlin, S.B., Adams, K.L. 2005. Development of switchgrass (*Panicum virgatum*) as a bioenergy feedstock in the United States. Biomass and Bioenergy. 28:515-35.

Medlyn, B.E., Barton, C.V.M., Broadmeadow, M.S.J., et al. 2001. Stomatal conductance of forest species after long-term exposure to elevated $CO_2$ concentration: a synthesis. New Phytologist. 149:247-64.

Mednick, A.C. 2010. Does soil data resolution matter? State soil geographic database versus soil survey geographic database in rainfall-runoff modeling across Wisconsin. Journal of Soil and Water Conservation. 65:190-199.

Mittelstet, A.R., Storm, D.E., Stoecker, A.L. 2015. Using SWAT and an empirical relationship to simulate crop yields and salinity levels in the North Fork River Basin. International Journal of Agricultural and Biological Engineering. 8:110-124.

Modala, N.R., Ale, S., Goldberg, D., Olivares, M., Munster, C., Rajan, N., Feagin, R. 2016. Climate change projections for the Texas High Plains and Rolling Plains. Theoretical and Applied Climatology. doi: 10.1007/s00704-016-1773-2

Monteith, J.L. 1965. Evaporation and environment. Symposia of the Society for Experimental Biology. 19:205-234.

Moriasi, D.N., Arnold, J.G., Van Liew, M.W., Binger, R.L., Harmel, R.D., Veith, T. 2007. Model evaluation guidelines for systematic quantification of accuracy in watershed simulations. Transactions of the ASABE. 50:885-900.

Morison, J.I.L. 1987. Intercellular $CO_2$ concentration and stomatal response to $CO_2$.

Stanford, USA: Stanford University Press.

Mullins, G.L., Burmester, C.H. 1990. Dry matter, nitrogen, phosphorus, and potassium accumulation by four cotton varieties. Agronomy Journal. 82:729-736.

Musick, J.T., Jones, O.R., Stewart, B.A., Dusek, D.A. 1994. Water-yield relationships for irrigated and dryland wheat in the U.S. Southern Plains. Agronomy Journal. 86:980-986.

Nair, S., Maas, S., Wang, C., Mauget, S. 2013. Optimal field partitioning for center-pivot-irrigated cotton in the Texas High Plains. Agronomy Journal. 105:124-133.

Nair, S.S., King, K.W., Witter, J.D., Sohngen, B.L., Fausey, N.R. 2011. Importance of crop yield in calibrating watershed water quality simulation tools. Journal of the American Water Resources Association. 47:1285-1297.

Nash, J.E., Sutcliffe, J.V. 1970. River flow forecasting through conceptual models, Part I-a discussion of principles. Journal of Hydrology. 10:282-290.

NASS (National Agricultural Statistics Service NASS) quick stats of cotton planting area. 2014. http://www.nass.usda.gov/Quick_Stats/Lite/#E0B0B59C-D3B5-38B3-B2DB-D7875C90B937 (accessed August 2014).

Neitsch, S.L., Arnold, J.G., Kiniry, J.R., Williams, J.R. 2011. Soil and Water Assessment Tool Theoretical Documentation Version 2009; Texas Water Resources Institute: College Station, TX; http://swat.tamu.edu/media/99192/swat2009-theory.pdf

Nelson, R.G., Ascough II, J.C., Langemeier, M.R. 2006. Environmental and economic analysis of switchgrass production for water quality improvement in northeast Kansas. Journal of Environmental Management. 79:336-347.

Ng, T.Z., Eheart, J.W., Cai, X., Miguez, F. 2010. Modeling *miscanthus* in the soil and water assessment tool (SWAT) to simulate its water quality effects as a bioenergy crop. Environmental Science & Technology. 44:7138-7144.

NOAA-NCDC (National Oceanic and Atmospheric Administration-National Climatic Data Center) 2014. Weather Data. Available online: http://gis.ncdc.noaa.gov/map/viewer/#app=cdo&cfg=cdo&theme=daily&layers=111&node=gis (accessed 2 September 2015).

Ocumpaugh, W., Hussey, M., Read, J., Muir, J., Jones, R., Hons, F., Evers, G., Phillips, M., Cassida, K., Kee, D., Venuto, B. 1998. Evaluation of switchgrass cultivars and cultural methods for biomass production in the south central US Annual Report 1998.

Ohwi, J. 1964. Flora of Japan. Smithsonian Inst, Washington, DC.

Oikawa, P.Y., Jenerette, G.D., Grantz, D.A. 2015. Offsetting high water demands with high productivity: Sorghum as a biofuel crop in a high irradiance arid ecosystem. Global Change Biology Bioenergy. 7:974-983.

Padron, E., Navarro, R.M. 2004. Estimation of above-ground biomass in naturally occurring populations of *Prosopis pallida* (H. & B. ex. Willd.) H.B.K. in the north of Peru. Journal of Arid Environments. 56:283-292.

Park, J.Y. Ale, S., Teague, W.R., Dowhower, S.L. 2015. Modeling hydrologic responses to alternate grazing management practices at the ranch and watershed scales. Journal of Soil and Water Conservation. In Press.

Park, S.C., Ansley, R.J., Mirik, M., Maindrault, M.A. 2012. Delivered biomass costs of honey mesquite (*prosopis glandulosa*) for bioenergy uses in the South Central USA. BioEnergy Research. 5:989-1001.

Penman, H.L. 1948. Natural evaporation from open water, bare soil, and grass. Proc. Royal Soc. London A. 193:120-145.

Penman, H.L. 1956. Evaporation: an introductory survey. Netherlands Journal of Agricultural Science. 1, 9-29, 89-97, 151-153.

Pinter Jr, P.J., Kimball, B.A., Mauncy, J.R., et al. 1994. Effects of free-air carbon dioxide enrichment on PAR absorption and conversion efficiency by cotton. Agricultural and Forest Meteorology. 70:209-230.

Powelson, D., Riche, A., Shield, I. 2005. Biofuels and other approaches for decreasing fossil fuel emissions from agriculture. Annals of Applied Biology. 146:193-201.

Powers, S.E., Ascough II, J.C., Nelson, R.G., Larocque, G.R. 2011. Modeling water and soil quality environmental impacts associated with bioenergy crop production and biomass removal in the Midwest USA. Ecological Modelling. 222:2430-2447.

Priestley, C.H.B., Taylor, R.J. 1972. On the assessment of surface heat flux and evaporation using large-scale parameters. Monthly Weather Review. 100:81-92.

Qin, Z.C., Zhuang, Q.L., Cai, X.M. 2015. Bioenergy crop productivity and potential climate change mitigation from marginal lands in the United States: An ecosystem modeling perspective. Global Change Biology Bioenergy. 7:1211-1221.

Qin, Z.C., Zhuang, Q.L., Zhu, X.D., Cai, X.M., Zhang, X. 2011. Carbon consequences and agricultural implications of growing biofuel crops on marginal agricultural lands in China. Environmental Science & Technology. 45:10765-10772.

Rajan, N., Maas, S.J., Cui, S. 2013. Extreme drought effects on carbon dynamics of a semiarid pasture. Agronomy Journal. 105:1749-1760.

Rajan, N., Maas, S., Cui, S. 2015a. Extreme drought effects on evapotranspiration and energy balance of a pasture in the Southern Great High Plains. Ecohydrology. 8:1194-1204.

Rajan, N., Maas, S., Kellison, R., Dollar, M., Cui, S., Sharma, S., Attia, A. 2015b. Emitter uniformity and application efficiency for center-pivot irrigation systems. Irrigation and Drainage. 64:353-361.

Rao, M.N., Yang, Z.M. 2010. Groundwater impacts due to conservation reserve program in Texas County, Oklahoma. Applied Geography. 30:317-328.

Rathjens, H., Oppelt, N., Bosch, D.D., Arnold, J.G., Volk, M. 2015. Development of a grid-based version of the SWAT landscape model. Hydrological Processes. 29:900-914.

Reddy, K., Hodges, H., McKinion, J. 1995. Carbon dioxide and temperature effects on pima cotton growth. Agriculture, Ecosystems & Environment. 54:17-29.

Reddy, K., Hodges, H., McKinion, J. 1996. Can cotton crops be sustained in future climates? In: Beltwide Cotton Conferences (USA), 1996.

Reddy, K.R., Hodges, H.F., Kimball, B.A. 2000. Crop ecosystem responses to global climate change: cotton. In: Reddy KR, Hodges HF (eds) Climate change and global crop productivity. CAB International, Wallingford, pp 162-187.

Refsgaard, J.C., Storm, B. 1995. MIKE SHE, In Computer Models of Watershed Hydrology; Singh, V.P., Ed.; Water Resources Publications: Highlands Ranch, CO, USA; pp. 809-846.

Rind, D., Goldberg, R., Hansen, J., Rosenzweig, C., Ruedy, R. 1990. Potential evapotranspiration and the likelihood of future drought. Journal of Geophysical Research: Atmospheres. 95:9983-10004.

Rockström, J.W., Steffen, K., Noone, Å. 2009. Planetary boundaries: exploring the safe operating space for humanity. Ecology and Society. 14:32.

Rooney, W.L., Blumenthal, J., Bean, B., Mullet, J.E. 2007. Designing sorghum as a dedicated bioenergy feedstock. Biofuels, Bioproducts and Biorefining. 1:147-157.

Rose, S.K., Ahammad, H., Eickhout, B., Fisher, B., Kurosawa, A., Rao, S., Riahi, K., van Vuuren, D.P. 2012. Land-based mitigation in climate stabilization. Energy Economics. 34:365-380.

Rosenberg, N.J., Epstein, D.J., Wang, D., Vail, L., Srinivasan, R., Arnold, J.G. 1999. Possible impacts of global warming on the hydrology of the Ogallala Aquifer region. Climatic Change. 42:677-692.

Runkel, R.L., Crawford, C.G., Cohn, T.A. 2004. Load Estimator (LOADEST): A FORTRAN program for estimating constituent loads in streams and rivers. USGS Techniques and Methods Book 4, Chapter A5. Reston, Va.: U.S. Geological Survey. Available at: http://pubs.er.usgs.gov/publication/tm4A5 (accessed May 2016).

Saleh, A., Gallego, O. 2007. Application of SWAT and APEX using the SWAPP (SWAT-APEX Program) for the upper North Bosque River watershed in Texas. Transactions of the ASABE. 50:1177-1187.

Santhi, C., Kannan, N., White, M., Di Luzio, M. Arnold, J.G., Wang, X., Williams, J.R. 2014. An integrated modeling approach for estimating the water quality benefits of conservation practices at river basin scale. Journal of Environmental Quality. 43:177-198.

Sarkar, S., Miller, S.A. 2014. Water quality impacts of converting intensively-managed agricultural lands to switchgrass. Biomass and Bioenergy. 68:32-43.

Sarkar, S., Miller, S.A., Frederick, J.R., Chamberlain, J.F. 2011. Modeling nitrogen loss from switchgrass agricultural systems. Biomass and Bioenergy. 35:4381-4389.

Saxe, H., Ellsworth, D.S., Heath, J. 1998. Tree and forest functioning in an enriched $CO_2$ atmosphere. New Phytologist. 139:395-436.

Scherer, L., Venkatesh, A., Karuppiah, R., Pfister, S. 2015. Large-scale hydrological modeling for calculating water stress indices: implications of improved spatiotemporal resolution, surface-groundwater differentiation, and uncertainty characterization. Environmental Science & Technology. 49:4971-4979.

Schilling, K.E., Jha, M.K., Zhang, Y.K., Gassman, P.W., Wolter, C.F. 2008. Impact of land use and land cover change on the water balance of a large agricultural watershed: Historical effects and future directions. Water Resources Research. 44:W00A09.

Schwalm, C.R., Williams, C.A., Schaefer, K., et al. 2010. A model-data intercomparison of CO2 exchange across North America: results from the North American carbon program site synthesis. Journal of Geophysical Research. 115: G00H05.

SCS, 1988. Texas brush inventory. United States Department of Agriculture, Soil Conservation Service Misc. Report, Temple, TX.

Seager, R., Vecchi, G.A. 2010. Greenhouse warming and the 21st century hydroclimate

of Southwestern North America. PNAS. 107:21277-21282.

Searchinger, T., Heimlich, R., Houghton, R.A., et al. 2008. Use of US croplands for biofuels increases greenhouse gases through emissions from land-use change. Science. 319:1238-1240.

Singh, G., Mutha, S., Bala, N. 2007. Effect of tree density on productivity of a *Prosopis cineraria* agroforestry system in north western India. Journal of Arid Environments. 70:152-163.

Skaggs, R.W., Youssef, M.A., Chescheir, G.M. 2012. DRAINMOD: model use, calibration, and validation. Transactions of the ASABE. 55:1509-1522.

Soil Survey Staff, 2010. Keys to Soil Taxonomy, 11th ed. USDA-Natural Resources Conservation Service, Washington, DC.

Soil Survey Staff, 2015. Natural Resources Conservation Service, United States Department of Agriculture. Soil Survey Geographic (SSURGO) Database for [Survey Area, State]. Available online at http://www.arcgis.com/apps/OnePane/basicviewer/index.html?appid=a23eb436f6ec4ad6982000dbaddea5ea (accessed 6 September 2015).

Srinivasan, R., Zhang, X., Arnold, J.G. 2010. SWAT ungauged: hydrological budget and crop yield predictions in the upper Mississippi river basin. Transactions of the ASABE. 53:1533-1546.

Teague, W.R., Dowhower, S.L. 2003. Patch dynamics under rotational and continuous grazing management in large, heterogeneous paddocks. Journal of Arid Environments. 53:211-229.

Tenenbaum, D.J. 2008. Food vs. fuel: diversion of crops could cause more hunger. Environmental Health Perspectives. 116:254-257.

Texas Water Development Board, 2005. Volumetric Survey of Alan Henry reservoir. Available online at http://www.twdb.texas.gov/hydro_survey/alanhenry/ 2005-07/AlanHenry2005_FinalReport.pdf (accessed 8 July 2015).

Ton, P. 2004. Cotton and climate change in west Africa. The Impact of Climate Change on Drylands Environment & Policy Volume 39, pp 97-115

Trybula, E.M., Cibin, R., Burks, J.L., Chaubey, I., Brouder, S.M., Volenec, J.J. 2015. Perennial rhizomatous grasses as bioenergy feedstock in SWAT: parameter development and model improvement. Global Change Biology Bioenergy. 7:1185-1202.

Tuppad, P., Santhi, C., Wang, X., Williams, J.R., Srinivasan, R., Gowda, P.H. 2010. Simulation of conservation practices using the APEX model. Transactions of the ASABE. 26:779-794.

Tuppad, P., Winchell, M.F., Wang, X., Srinivasan, R., Williams, J.R. 2009. ArcAPEX: ArcGIS interface for Agricultural Policy Environmental Extender (APEX) hydrology/water quality model. International Agricultural Engineering Journal. 18:59-71.

Turhollow, A.F., Webb, E.G., Downing, M.E. 2010. Review of sorghum production practices: applications for bioenergy. Environmental Sciences Division.

USDA, 1972. National Engineering Handbook: Hydrology. In: Agriculture. U.S. Government Print Office, Washington D.C.

USDA, 2010. A USDA Regional roadmap to meeting the biofuels goals of the Renewable Fuels Standard by 2022. Biofuels strategic production report. USDA, Washington, D.C. Available online at http://www.usda.gov/documents/USDA_Biofuels_Report_6232010.pdf (accessed 3 September 2015).

USDA-NRCS, 1986. Urban hydrology for small watersheds. Technical Release 55. Washington, D.C.: USDA National Resource Conservation Service. Available online at: www.hydrocad.net/pdf/TR-55%20Manual.pdf (accessed 3 September 2015).

USDA-NRCS, 2004. Chapter 10: Estimation of direct runoff from storm rainfall. In NRCS National Engineering Handbook, Part 630: Hydrology, 10.1-10.22. Washington, D.C.: USDA National Resource Conservation Service. Available online at: http://directives.sc.egov.usda.gov/viewerFS.aspx?hid=21422 (accessed 4 September 2015).

USEPA Climate Change: Basic Information. Available at: http://www.epa.gov/climatechange/basics/ (accessed May 2016).

Vaghefi, S.A., Mousavi, S.J., Abbaspour, K.C., Srinivasan, R., Yang, H. 2014. Analyses of the impact of climate change on water resources components, drought and wheat yield in semiarid regions: Karkheh River Basin in Iran. Hydrological Processes. 28:2018-2032.

Van Griensven, A., Meixner, T. 2006. Methods to quantify and identify the sources of uncertainty for river basin water quality models. Water Science and Technology. 53:51-59.

Van Vuuren, D.P., Stehfest, E., den Elzen, M.G.J. et al. 2011. RCP2.6: Exploring the possibility to keep global mean temperature increase below 2°C. Climatic Change.

109:95-116.

VanLoocke, A., Bernacchi, C.J., Twine, T.E. 2010. The impacts of *Miscanthus×giganteus* production on the Midwest US hydrologic cycle. Global Change Biology Bioenergy. 2:180-191.

Veith, T.L., Van Liew, M.W., Bosch, D.D., Arnold, J.G. 2010. Parameter sensitivity and uncertainty in SWAT: a comparison across five USDA-ARS watersheds. Transactions of the ASABE. 53:1477-1486.

Wand, S.J.E., Midgley, G.F., Jones, M.H., Curtis, P.S. 1999. Responses of wild C4 and C3 grass (Poaceae) species to elevated atmospheric $CO_2$ concentration: a meta-analytic test of current theories and perceptions. Global Change Biology. 5:723-741.

Wang, T., Park, S., Ansley, R.J., Amosson, S.H. 2014. Economic and greenhouse gas efficiency of honey mesquite relative to other energy feedstocks for bioenergy uses in the Southern Great Plains. BioEnergy Research. 7:1493-1505.

Wang, X., Kannan, N., Santhi, C., Potter, S.R., Williams, J.R., Arnold, J.G. 2011. Integrating APEX output for cultivated cropland with SWAT simulation for regional modeling. Transactions of the ASABE. 54:1281-1298.

Wang, X., Williams, J.R., Gassman, P.W., Baffaut, C., Izaurralde, R.C., Jeong, J., Kiniry, J.R. 2012. EPIC and APEX: Model use, calibration, and validation. Transactions of the ASABE. 55:1447-1462.

Wang, X., Yen, H., Liu, Q., Liu, J. 2014a. An auto-calibration tool for the Agricultural Policy Environmental Extender (APEX) model. Transactions of the ASABE. 57:1-12.

Wang, T., Park, S., Ansley, R.J., Amosson, S.H. 2014b. Economic and greenhouse gas efficiency of honey mesquite relative to other energy feedstocks for bioenergy uses in the Southern Great Plains. BioEnergy Research. 7:1493-1505.

Wanjura, J.D., Barnes, E.M., Kelley, M.S., Holt, G.A., Pelletier, M.G. 2014. Quantification and characterization of cotton crop biomass residue. Industrial Crops and Products. 56:94-104.

Webb, W.P. 1931. The Great Plains. Ginn and Co., New York, NY.

Wellen, C., Kamran-Disfani, A., Arhonditsis, G.B. 2015. Evaluation of the current state of distributed watershed nutrient water quality modeling. Environmental Science & Technology. 49(6):3278-3290.

White, M., Storm, D., Busteed, P., Stoodley, S., Phillips, S. 2009. Evaluating nonpoint-source critical source area contributions at the watershed scale. Journal of Environmental Quality. 38:1654-1663.

Williams, A., White, N., Mushtaq, S., Cockfield, G., Power, B., Kouadio, L. 2015. Quantifying the response of cotton production in eastern Australia to climate change. Climatic Change. 129:183-196.

Williams, J.R. 1995. The EPIC Model, In Computer Models of Watershed Hydrology; Singh, V.P., Ed.; Water Resources Publications: Highlands Ranch, CO, USA; pp. 909-1000.

Williams, J.R., Arnold, J.G., Kiniry, J.R., Gassman, P.W., Green, C.H. 2008. History of model development at Temple, Texas. Hydrological Sciences Journal. 53:948-960.

Williams, J.R., Izaurralde, R.C. 2006. The APEX model. In Watershed Models, 437-482. V. P. Singh and D. K. Frevert, eds. Boca Raton, Fla.: CRC Press.

Williams, J.R., Jones, C.A., Kiniry, J.R., Spanel, D.A. 1989. The EPIC crop growth model. Transactions of the ASABE. 32:497-511.

Willmott, C.J. 1981. On the validation of models. Physical geography. 2:184-194.

Wright, L. 2007. Historical perspective on how and why switchgrass was selected as a "model" high-potential energy crop. ORNL/TM-2007/109 Oak Ridge, TN: Bioenergy Resources and Engineering Systems.

Wu, Y.P., Liu, S.G. 2012. Impacts of biofuels production alternatives on water quantity and quality in the Iowa River Basin. Biomass and Bioenergy. 36:182-191.

Wu, Y.P., Liu, S.G., Gallant, A.L. 2012. Predicting impacts of increased $CO_2$ and climate change on the water cycle and water quality in the semiarid James River Basin of the Midwestern USA. Science of the Total Environment. 430:150-160.

Yamamoto, S., Saigusa, N., Ohtani, Y., Fujinuma, Y., Inoue, G., Hirano, T., Fukushima Y. 2001. Present status of Asia Flux Network and a view toward the future. In: Abstracts, AGU Fall Meeting, San Francisco. 10-14 Dec. 2001. Vol. 1. American Geophysical Union, Washington, DC. Abstract B41A-03.

Ye, L., Grimm, N.B. 2013. Modelling potential impacts of climate change on water and nitrate export from a mid-sized, semiarid watershed in the US Southwest. Climatic Change. 120:419-431.

Yimam, Y.T., Ochsner, T.E., Kakani, V.G. 2015. Evapotranspiration partitioning and water use efficiency of switchgrass and biomass sorghum managed for biofuel. Agricultural Water Management. 155:40-47.

Yimam, Y.T., Ochsner, T.E., Kakani, V.G., Warren, J.G. 2014. Soil moisture dynamics and evapotranspiration under annual and perennial bioenergy crops. Soil Science Society of America Journal. 78:1584-1592.

Youssef, M.A., Skaggs, R.W., Chescheir, G.M., Gilliam, J.W. 2005. The nitrogen simulation model, DRAINMOD-N II. Transactions of the ASAE. 48:1-16.

Yu, G.R., Wen, X.F., Sun, X.M., Tanner, B.D., Lee, X., Chen, J.Y. 2006. Overview of ChinaFLUX and evaluation of its eddy covariance measurement. Agricultural and Forest Meteorology. 137:125-137.

Zatta, A., Clifton-brown, J., Robson, P., Hastings, A., Monti, A. 2014. Land use change from C3 grassland to C4 *Miscanthus*: effects on soil carbon content and estimated mitigation benefit after six years. Global Change Biology Bioenergy. 6:360-370.

Zhang, G.H., Nearing, M.A., Liu, B.Y. 2005. Potential effects of climate change on rainfall erosivity in the Yellow River basin of China. Transactions of the ASABE. 48:511-517.

Zhang, K., Johnson, L., Prasad, P.V.V., Pei, Z.J., Yuan, W.Q., Wang, D.H. 2015a. Comparison of big bluestem with other native grasses: Chemical composition and biofuel yield. Energy. 83:358-365.

Zhang, X., Sahajpal, R., Manowitz, D.H., Zhao, K., LeDuc, S.D., Xu, M., Xiong, W., Zhang, A., Izaurralde, R.C., Thomson, A.M. 2014. Multi-scale geospatial agroecosystem modeling: a case study on the influence of soil data resolution on carbon budget estimates. Science of the Total Environment. 479:138-150.

Zhang, X., Srinivasan, R., Hao, F. 2007. Predicting hydrologic response to climate change in the Luohe River basin using the SWAT model. Transactions of the ASABE. 50:901-910.

Zhang, X.S., Izaurralde, R.C., Arnold, J.G., Williams, J.R., Srinivasan, R. 2013. Modifying the soil and water assessment tool to simulate cropland carbon flux: model development and initial evaluation. Science of the Total Environment. 463:810-822.

Zhang, X.S., Izaurralde, R.C., Manowitz, D.H., Sahajpal, R., West, T.O., Thomson, A.M., Xu, M., Zhao, K.G., LeDuc, S.D., Williams, J.R. 2015b. Regional scale cropland carbon budgets: Evaluating a geospatial agricultural modeling system using inventory data. Environmental Modelling & Software. 63:199-216.

Zhuang, Q.L., Qin, Z.C., Chen, M. 2013. Biofuel, land and water: maize, switchgrass or *Miscanthus*? Environmental Research Letters. 8:015020.

Zierl, B., Bugmann, H. 2005. Global change impacts on hydrological processes in Alpine catchments. Water Resource Research. 41:W02028.